A Systems Approach to Assessing the Sustainability of Hybrid Community Energy Systems

By

Kevork Hacatoglu

A Thesis Submitted in Partial Fulfillment
of the Requirements for the Degree of

Doctor of Philosophy

in

Mechanical Engineering

Faculty of Engineering and Applied Science

University of Ontario Institute of Technology

September 2014

Abstract

The goal to achieve a sustainable society that will endure over the long term is generally regarded as a positive evolutionary course. One of the challenges with this goal is developing a quantitative assessment of the sustainability of a system. Despite the different measures available in the literature, a standard and universally accepted index for assessing sustainability does not yet exist. This thesis develops a novel Integrated Sustainability Index (ISI) for energy systems that considers critical multidimensional sustainability criteria. The originality of this new index is that it incorporates fundamental thermodynamic, economic, and environmental constraints to combine indicators from multiple dimensions into a single-score evaluation of sustainability. The index is therefore unique because it can assess sustainability relative to an ideal reference state instead of being limited to ranking systems via relative assessments.

The ISI of an energy system is determined by normalization, weighting, and aggregation of sustainability indicators. Indicators are normalized relative to sustainable threshold values and weighted based on time, space, and receptor (i.e., human or ecosystem impacts) criteria. Aggregation yields an ISI between zero and one, where one represents a sustainable system. The ISI is calculated for several different case studies spanning a range of fossil- and renewable-based energy systems. Each is designed as a stand-alone system to meet the energy needs of a small community in Southern Ontario. The analysis shows that of the various alternatives, a solar-photovoltaic-hydrogen system has the best ISI, which ranges from 0.65-0.90 and is a 4-25% improvement over the reference, gas-fired system. For the solar-photovoltaic-hydrogen system and many others, climate change and ozone layer depletion indicators have the strongest effect on ISI. Affordability, commercial viability, and land area indicators are also critical for other energy systems. The ISI is expected to prove useful as a high-level, multi-criteria decision analysis tool for understanding and fostering sustainable energy systems, alone or in concert with other approaches.

Keywords: Energy system; Index; Life-cycle assessment; Sustainability; Weighting factor

Acknowledgements

I must thank my supervisor Dr. Ibrahim Dincer and co-supervisor Dr. Marc Rosen for their invaluable assistance and support over the course of my studies. The decision to pursue a PhD is not to be taken lightly but the opportunity to learn directly from leaders in my field of interest was too good to pass up. It feels like only yesterday (May 3, 2007 to be exact) as a graduate student at Queen's University I downloaded an article, "Exergy as a Driver for Achieving Sustainability" by I. Dincer and M.A. Rosen, published in the inaugural issue of the International Journal of Green Energy. As luck would have it, I ended up working with both of them and publishing our own articles that might someday inspire others.

My experience at UOIT was made all the more memorable by the amazing faculty and staff. They are some of the friendliest and most helpful people I've ever met. The same goes for my fellow graduate students in the Mechanical Engineering department and across all other departments and faculties.

Finally, thanks to my wonderful family and to J.J. and A.K. for extending my sustainability time scale and teaching me about intergenerational equity without so much as a word.

Table of Contents

List of Tables

List of Figures

Nomenclature

α	Azimuth angle, °
A	Dimensional sustainability indicator
AFR	Air-fuel ratio
B	Non-dimensional sustainability indicator
$BGCF$	Biogas conversion factor
BVS	Biodegradable volatile solids
c	Scale parameter, m s^{-1}
Cn	Clearness number
COP	Coefficient of performance
C_P	Power coefficient
CR	Concentration ratio
$\dot{E}$	Energy rate, kW
ex	Specific exergy, kJ kg^{-1}
$\dot{E}x$	Exergy rate, kW
f	Fate factor
h	Specific enthalpy, kJ kg^{-1}
HLR	Heat loss ratio
k	Shape parameter
k_C	Local extinction coefficient
$\dot{m}$	Mass flow rate, kg s^{-1}
$MATAI$	Median after-tax annual income, $ yr^{-1}
MC	Moisture content
MH	Mixing height, m
$OFMSW$	Organic fraction of MSW
P	Pressure, kPa
Pop	Population
PR	Pressure ratio
$\dot{Q}$	Heat rate, kW

R	Recoverable reserves, kg
RR	Rotor radius, m
s	Specific entropy, kJ kg^{-1} K^{-1}
$\dot{S}$	Entropy rate, kW K^{-1}
t	Time, year
T	Temperature, K
U_L	Overall thermal loss coefficient, W m^{-2} K^{-1}
UR	Utilization ratio
V	Specific volume, m^3 kg^{-1}
VS	Volatile solids fraction
W	Weighting factor
$\dot{W}$	Work rate, kW
WS	Wind speed, m s^{-1}

Greek Letters

α	Adjustment factor
β	Collector tilt angle, °
ε	Effectiveness
η	Energy efficiency
θ	Elevation angle, °
Γ	Absorbance factor
ρ	Density, kg m^{-3}
τ	Residence time, hr
ϕ	Incidence angle, °
ψ	Exergy efficiency

Subscripts

0	Reference environment
Abs	Absorber
act	Activation
amb	Ambient

ARC	Absorption refrigeration cycle
BOM	Biodegradable organic material
C	Compressor
CC	Combustion chamber
ch	Chemical
Col	Collector
Comb	Combustion
conc	Concentration
Cond	Condenser
CT	Cold tank
D	Destruction
ETR	Extraterrestrial radiation
EV	Expansion valve
Evap	Evaporator
Exp	Expansion turbine
G	Generation
Gen	Generator
GF	Geofluid
GT	Gas turbine
HT	Hot tank
i	Sub-indicator
j	Category indicator
m	Number of sub-indicators
Mech	Mechanical
n	Number of category indicators
ohm	Ohmic
ORC	Organic Rankine cycle
P	Pump
ph	Physical

PTC	Parabolic trough collector
Q	Thermal
R	Receiver
Reg	Regenerator
rev	Reversible
ST	Steam turbine
Sust	Sustainability
T	Target
WT	Wind turbine

Abbreviations

AD	Anaerobic Digestion
ADP	Abiotic Depletion Potential
AF	Affordability
APP	Air Pollution Potential
CFC	Chlorofluorocarbon
CV	Commercial Viability
DCB	Dichlorobenzene
DHW	Domestic Hot Water
EES	Engineering Equation Solver
EF	Economic Factor
EIA	Energy Information Administration
EnER	Energy Efficiency Ratio
EP	Eutrophication Potential
EPA	Environmental Protection Agency
ER	Efficiency Ratio
ESI	Environmental Sustainability Index
ExER	Exergy Efficiency Ratio
FAETP	Freshwater Aquatic Ecotoxicity Potential
GDP	Gross Domestic Product

GEIP	Global Environmental Impact Potential
GHG	Greenhouse Gas
GWP	Global Warming Potential
HHV	Higher Heating Value
HTF	Heat Transfer Fluid
IAEA	International Atomic Energy Agency
IPCC	Intergovernmental Panel on Climate Change
ISI	Integrated Sustainability Index
LCA	Life-Cycle Assessment
LHV	Lower Heating Value
MAETP	Marine Aquatic Ecotoxicity Potential
MSW	Municipal Solid Waste
NRC	National Research Council
OEE	Office of Energy Efficiency
PM	Particulate Matter
PV	Photovoltaic
RCP	Representative Concentration Pathway
SF	Size Factor
SODP	Stratospheric Ozone Depletion Potential
UV	Ultraviolet
WCED	World Commission on Environment and Development
WPP	Water Pollution Potential

Chemical Compounds

CH_4	Methane
CO	Carbon monoxide
CO_2	Carbon dioxide
H_2	Hydrogen
H_2O	Water
N_2	Nitrogen

N_2O	Nitrous oxide
NH_3	Ammonia
NO_2	Nitrogen dioxide
O_2	Oxygen
O_3	Ozone
Pb	Lead
PO_4^{3-}	Phosphate
Sb	Antimony
SO_2	Sulphur dioxide

Chapter 1 : Introduction

This chapter presents the motivation and objectives of the thesis as well as an outline of its contents.

1.1 Energy and Sustainability

The struggle to achieve a sustainable society is not unique to the modern age. Sustainability has been a goal since the earliest human civilizations. Ever since the Neolithic Revolution approximately 10,000 years ago, when human beings transitioned from mobile hunter-gatherers to agriculture and settlements, the sustainability of the local lifestyle has been essential to avoid societal collapse.

A classic example of how an unsustainable lifestyle can lead to societal collapse is that of the Polynesians on Easter Island. The inhabitants of Easter Island exhausted the resources of their remote habitat to the point where they could no longer feed themselves or even build canoes to escape. The ecological destruction of Easter Island led to a catastrophic societal collapse that decimated its population (Tainter, 1988).

Another notable illustration of societal collapse is the decline of the Western Roman Empire which, unlike the circumstances of Easter Island, occurred without environmental destruction (Tainter, 1988). Although diminishing returns from natural resource production played a role in the decline, there were also contributing social factors – highlighting the multidimensional nature of sustainability.

The dominant energy paradigm in modern capitalist economies is based on centralized energy generation with fossil fuels that deliver heat, power, and transportation services. The hydrocarbon economy has led to many positive economic and social developments. Despite its many benefits, the repercussions of the hydrocarbon economy are beginning to emerge. There are growing concerns related to accelerated rates of climate change, the human health effect of pollution, and access to adequate, affordable, and reliable energy supplies. These are intra- and intergenerational concerns.

1.2 Motivation

One of the most ambitious goals of a society is to achieve sustainability. Making sustainability operational as opposed to a grand but ambiguous idea is a challenge. For example, various definitions of sustainability exist, none of which applies to all circumstances. Even after selecting a definition, there is no universal method of measuring sustainability, which makes it extremely difficult to track progress towards sustainability.

There is an inherent difficulty in measuring the various dimensions of sustainability. For example, although standard of living is often defined as gross domestic product (GDP) per capita, quality of life is a more important albeit elusive measure of human well-being and happiness. Furthermore, although it is well known that greenhouse gas (GHG) emissions and ozone-depleting substances are harmful, quantifying the economic and social impacts is very difficult.

1.3 Objectives

The overall objective of this thesis is to develop an index to assess the sustainability of community energy systems. There are many other objectives and sub-objectives that were met before successful completion of the thesis:

I. Identify sustainability indicators
    a. Collect the appropriate data to calculate sustainability indicators.
    b. Determine target values based on thermodynamic, economic, and environmental threshold values.

II. Estimate weighting factors
    a. Develop a method to determine intra- and inter-category weighting factors.
    b. Differentiate between importance and trade-off coefficients.
    c. Identify the different perspectives and how they affect weighting factor estimation.

III. Develop hybrid community energy systems
    a. Identify the inputs to the system.

b. Identify the operating principles of the system (e.g., when is storage required, which parts of the system are activated at certain times of the day, year, etc.).
c. Conduct thermodynamic, cost, and life-cycle emission assessments.

IV. Apply the methodology

a. Assess the sustainability of the various case studies.
b. Study the parameters that influence the sustainability index.
c. Perform a comparative analysis of the different case studies.
d. Investigate ways of improving the sustainability index of an energy system.

The original contribution of this thesis is the development of a novel sustainability assessment index for energy systems that considers several critical multidimensional sustainability criteria such as exergy efficiency, affordability, land area, greenhouse gas emissions, stratospheric ozone depletion, air pollution, and water pollution. This new, Integrated Sustainability Index (ISI) incorporates fundamental thermodynamic, economic, and environmental constraints to combine indicators from multiple dimensions into an overall composite index. The index is therefore unique because it can assess the sustainability of a system relative to an ideal reference state. Other approaches are limited to relative assessments between systems that are useful for ranking purposes but provide little insight with respect to overall sustainability.

Consequently, the ISI can provide important insight on the attributes of an energy system that positively or negatively affect sustainability. The disaggregated components of the index inform the sustainability analyst of the criteria that need further improvement to enhance the sustainability of the system. Furthermore, the ISI has value as a high-level, quantitative preliminary assessment of sustainability that can be easily communicated to policy makers and may prove useful as a tool to assist in the decision-making process.

1.4 Outline of Thesis

This thesis is organized as follows. Chapter 1 identifies the motivation for the thesis and its objectives. Chapter 2 is a literature review of sustainability assessment methodologies. Chapter 3 provides background information. Chapter 4 presents a general framework for sustainability assessment. Chapter 5 introduces the methodological approach to assess the sustainability of energy systems. Chapter 6 describes the case studies. Chapter 7 presents results and discussion related to the case studies. Chapter 8 includes concluding remarks and recommendations for future work.

Chapter 2 : Literature Review

This chapter presents a review of the existing literature on sustainability assessment. Generic approaches to sustainability assessment and those that focus on energy systems are reviewed.

2.1 Generic Sustainability Assessment

There have been many attempts at measuring sustainability but a universal approach has not yet been developed. Parris and Kates (2003) identified over 500 attempts at developing quantitative indicators of sustainable development in the literature. However, although the conflicting objectives to both “sustain” and “develop" are often acknowledged, the indicators developed are mostly one-dimensional, focusing only on economic development or environmental sustainability. Their review of twelve popular methods of measuring sustainable development concluded that there are no indicator sets that are universally accepted. One of the twelve methodologies analyzed was the Environmental Sustainability Index (ESI), which ranks nations according to an aggregation of several environmental indicators. An analysis by Morse and Fraser (2005) concluded that the ESI is misleading and biased towards Western countries, resulting in overly simplistic ideas correlating economic growth to environmental sustainability.

A common sustainability assessment methodology is to attach monetary values to social and environmental capital. However, the valuation of non-market goods and services is controversial and not well developed. Furthermore, our limited understanding of ecosystems and the unknown services they provide normally leads to improper financial valuations.

Biophysical-based assessment approaches are more appropriate for assessing environmental sustainability. Applying scientific principles such as the laws of thermodynamics and mass and energy balances allow for more quantitative assessments of sustainability. Although biophysical models are appropriate for quantifying resource use and environmental impact, they are inadequate in addressing social issues and some economic aspects of sustainability

In one of the earliest studies on sustainability assessment methodologies, Daly (1990) developed operational principles of sustainable development for renewable resources and quasi-sustainable use of non-renewable resources. Daly's assessment approach followed the strong sustainability paradigm, where the substitutability between capital and natural resources is limited.

Another early treatment analyzed indicators based on both weak and strong sustainability. Rennings and Wiggering (1997) proposed indicators measuring sustainable development that link ecological (physical) and economic (monetary) approaches. They argued that economic approaches can be used to develop strong sustainability indicators as long as they are supplemented by physical indicators that consider threshold values of critical ecological functions.

Ness et al. (2007) reviewed an umbrella of sustainability assessment tools discussed in the literature. The first umbrella is comprised of sustainability indicators and indices. Indicators were defined as simple quantitative proxies that measure economic, social, and environmental factors. An aggregate of indicators forms an index. Non-integrated indicators measure a single aspect of sustainability while integrated indicators combine different nature-society dimensions. Although it follows a reductionist approach, integrated indicators offer a more holistic perspective on complex human-environmental systems.

The second umbrella consists of product-related assessment tools built on evaluating flows in connection with production and consumption of a good or service. Well-known tools such as life-cycle assessment (LCA) focus on resource use and environmental impact while others may integrate the economic and environmental dimensions (e.g. life-cycle costing).

The third umbrella includes integrated assessment tools used as decision-support methods for managing complex issues. Tools based on systems analysis approaches such as multi-criteria analysis, risk analysis, vulnerability analysis, and cost-benefit analysis can be extended across disciplinary boundaries and used in sustainability assessment.

A comprehensive review of sustainability assessment methodologies was conducted by Singh et al. (2009). They discovered that only a few of the methodologies had an integral approach that considered economic, social, and environmental aspects of sustainability. Furthermore, they found that the construction of composite indicators involved subjective decisions in data normalization, weighting, and aggregation methods. There are numerous indices that aggregate sustainability indicators to provide a one-dimensional metric of valuation. According to Böhringer and Jochem (2007), policy makers demand an aggregate sustainability index that can be easily interpreted and communicated to the general public. Their analysis of eleven prominent sustainability indices revealed that scientific rules for normalization, weighting, and aggregation towards composite indices were not taken into account. Since the indices also failed to adequately represent the different dimensions of sustainability, they concluded that sustainability indices currently employed in policy making were ineffective and misleading.

Gasparatos et al. (2008) reviewed reductionist methodologies in measuring progress towards sustainability. Although the reductionist paradigm simplifies the task of sustainability assessment, they were critical of some of its other characteristics such as single-variable measurements of dimensions of sustainability. Another criticism was the loss of useful information that occurs when aggregating sustainability indicators from different dimensions into a single composite index. They also consider money- and biophysical-based approaches to sustainability assessment. Money-based approaches attach monetary values to social and environmental capital. However, the valuation of non-market goods and services is controversial and not well developed. Biophysical approaches such as emergy, exergy, and ecological footprint analysis apply a natural science perspective to sustainability assessment. Although biophysical models do a good job of quantifying resource use and environmental impact, they are inadequate in addressing social issues and some economic aspects of sustainability.

Bossel (2001) applied a systems approach to develop comprehensive indicators of sustainable development. He identified seven basic orientors essential for system

viability and sustainability: existence, effectiveness, freedom of action, security, adaptability, coexistence, and psychological needs. Reed et al. (2005) extended the work of Bossel (2001) by integrating reductionist and participatory approaches to measure progress towards sustainable development. They identified reductionist and participatory approaches as the primary methodological paradigms in the literature on developing sustainability indicators. They argue that participatory approaches are essential to engage communities in sustainability assessment.

2.2 Energy Sustainability Assessment

The literature on energy sustainability assessment varies. Some studies comment on the sustainability of an energy system from a thermodynamic (Dewulf et al., 2000; Ferrari et al., 2001) or greenhouse gas (Zvolinschi et al., 2007) perspective. Others focus on the role of social indicators in sustainability assessment (Carrera and Mack, 2010). More comprehensive approaches that consider different aspects of sustainability but rank indicators without normalization with respect to sustainability target values are better suited to relative assessments of energy systems (Evans et al., 2009; Gnanapragasam et al., 2010). Other studies develop quantitative sustainability assessment tools that address technical, economic, social, and environmental criteria (Afgan et al. 2000, Afgan and Carvalho, 2002; Afgan, 2010; Frangopoulos and Keramioti, 2010). However, sustainability indicators are not normalized with respect to a reference state that represents limits on, for example, emissions of pollutants.

Afgan et al. (2000) developed a set of sustainability indicators related to resource, economic, social, and environment criteria. Resource indicators measured the fuel, carbon steel, copper, and aluminum intensity of energy services. Economic indicators measured the efficiency, capital investment, and local economic impact. Social indicators measured impacts on job creation, standard of living, and energy diversification. Environment indicators assessed carbon dioxide (CO_2), nitrogen oxide (NO_x), and sulphur dioxide (SO_2) emissions as well as waste generation. Future works by Afgan and Carvalho (2002) and Afgan (2010) employed a multi-criteria evaluation to

create a general index of sustainability based on aggregation of a selected number of energy indicators.

Vera and Langlois (2007) summarized the efforts of an international partnership initiative led by the International Atomic Energy Agency (IAEA) to identify indicators for sustainable energy development (IAEA, 2005). The project identified 30 energy indicators within the economic, social, and environmental spheres. Economic energy indicators were related to patterns of energy use, supply efficiency, diversification of supply, price, and security. Social energy indicators included concerns over equity and accessibility, affordability and disparities, and health and safety. Environmental energy indicators were mostly concerned with air and water emissions, deforestation, and waste production. Due to an uneven distribution across the various spheres, an index for sustainable energy development was not generated by aggregating indicators.

Evans et al. (2009) assessed renewable electricity generation technologies against a range of indicators and ranked their relative sustainability. The indicators used in their study were price of electricity generation, GHG emissions, availability of technology, energy conversion efficiency, land use requirements, water consumption, and social impacts. Each indicator was then ranked on a scale of 1-4 for photovoltaic, wind, hydro, and geothermal energy, where lower numbers indicated better performance.

Genoud and Lesourd (2009) developed a decision-support method for selecting power generation technologies based on sustainable development criteria. The criteria for assessing technologies were based on economic, social, and environmental considerations. Economic criteria were exergy efficiency, renewability, storability, flexibility, growth potential, and production cost. Social criteria included non-rivalry in the consumption of a primary energy source (i.e., similar to a public good), land area requirements, energy payback ratio, job creation, supply risk, and local energy resources. Environmental criteria were related to life-cycle emissions of several pollutants such as CO_2, SO_2, NO_x, particulate matter, biochemical oxygen demand, cadmium, methane (CH_4), and radioactivity as well as noise pollution.

Gnanapragasam et al. (2010) derived an energy system assessment methodology by considering indicators within the technological, sociological, and ecological dimensions of sustainability. Dimensions contained ten indicators each, which were assigned performance values between 0 and 1. The usefulness of this methodology is to compare alternative energy systems based on their final numerical score. Measuring the approach of an energy system to sustainability is only possible by comparing system performance to actual reference values.

Neves and Leal (2010) developed local energy sustainability indicators for municipalities based on a review of existing sets of sustainability indicators. They built a core set of eight local energy sustainability indicators and a complementary set of 18 indicators. Case studies of municipalities employing sustainability indicators revealed that very few local authorities were using indicators as decision criteria.

Brent and Rogers (2010) performed a sustainability assessment of a stand-alone renewable energy system in a rural village in Africa. Their sustainability assessment model was based on the principles of sustainability science: transdisciplinarity, resilience, complexity, adaptive management, and adaptive capacity. A systems approach to sustainability assessment decomposed the overall system into technological, economic, ecological, institutional, and social subsystems. The integrated renewable energy system was not viable for a number of reasons such as the high-cost of electricity and lack of resilience of the technological subsystem.

Some of the studies in the literature relate sustainability to entropy generation and the second law of thermodynamics. Dewulf et al. (2000) and Ferrari et al. (2001) quantified the sustainability of a technological process by its degree of irreversibility. Both studies developed an exergy-based sustainability coefficient. They each concluded that a process can only be sustainable if driven exclusively by renewable resources. Dewulf and Van Langenhove (2005) then used second-law approaches integrated with industrial ecology principles to evaluate environmental sustainability. Production pathways were assessed according to five exergy-based indicators: renewability of resources, toxicity of emissions, input of used materials, recoverability of products, and

process efficiency. Zvolinschi et al. (2007) calculated exergy-based sustainability indicators to compare gas- and hydrogen-fired combined-cycle power plants. The indicators were exergy renewability, environmental compatibility, and exergy efficiency. The analysis revealed that there is often a trade-off between exergy renewability and exergy efficiency. Jørgensen (2010) measures ecosystem services in terms of eco-exergy, which is an estimate of the work capacity of an ecosystem. Frangopoulos and Keramioti (2010) implemented a multi-criteria approach to determine a composite sustainability index of energy systems. The index was determined by aggregating technical, economic, social, and environmental sustainability indicators. Exergy efficiency indicators consisted of half of the technical indicators.

2.3 Summary

A review of sustainability assessment methodologies reveals that only a few of the approaches consider the economy, society, and environment. Methodologies based on weak sustainability tend to concentrate on economic considerations while neglecting the biophysical aspects of sustainability. However, biophysical approaches are mostly concerned with environmental sustainability while neglecting socio-economic dimensions.

A review of the literature on sustainability assessment revealed a number of shortcomings with existing methodologies. As shown by Singh et al. (2009), very few of the methodologies follow an integral approach and the construction of composite indicators is often done incorrectly. Even when aggregation of indicators is done correctly, there is an inevitable loss of information since the resulting composite index does not identify where the system under investigation needs improvement.

Another difficulty with some of the existing approaches is when indicators are ranked on a specified scale to estimate the approach to sustainability. This method is only useful when comparing different systems and does not indicate sustainability. To measure sustainability, there need to be sustainability reference values for indicators and systems have to be compared to those reference values.

Policy makers usually prefer an aggregate sustainability index that can be easily interpreted and communicated to the general public. Construction of composite indicators requires data normalization, weighting, and aggregation, which are not always done correctly. Although a single-value measure of sustainability that a composite index provides is attractive from a communication perspective, there is a loss of useful information during aggregation. Sustainability is a multidimensional concept and a single-value measurement can be misleading as it masks details, such as the strengths and weaknesses of the subject under investigation.

Chapter 3 : Background

This chapter provides background information helpful in understanding the rest of the thesis. Topics covered include hybrid energy systems, life-cycle analysis, exergy analysis, and sustainability.

3.1 Hybrid Energy Systems

The decentralized generation paradigm is manifested in community energy systems. The increase in interest is due to concerns about energy supply and the environment while the liberalization of electricity markets makes distributed systems more practical to implement (Pepermans et al., 2005). On-site power plants have the added benefit of multi-generation for combined production of heat, power, and other energy products (Chicco and Mancarella, 2009). Thus, the energy needs of a community can be met by a well-designed decentralized energy system without extensive long-distance transmission and distribution.

3.1.1 Energy Resources

3.1.1.1 Solar

Solar-thermal technologies use the sun's thermal energy to supply heating or electrical services. Solar-thermal collectors are basic heat exchangers that convert solar energy to heat. Non-concentrating solar-thermal technologies, where the collector and absorber areas are equal, are appropriate for space heating and domestic hot water applications (Reddy et al., 2007). Examples of non-concentrating collectors are flat-plate and evacuated-tube collectors (Evans, 2007).

Power generation techniques require more advanced solar-thermal collectors. A conventional Rankine cycle using steam as a working fluid can generate solar-thermal-based electricity. However, concentrating collectors are required to provide thermal energy at temperatures greater than 100°C. The geometric concentration ratio of a solar-thermal collector is defined as the area of the collecting aperture divided by the area of the absorbing/receiving aperture (Kreith and Kreider, 2011). Non-concentrating

technologies have a concentration ratio of approximately one while the ratio is larger for concentrating collectors.

There are four major optical concentration technologies available for solar-thermal power plants – parabolic trough collectors, linear Fresnel systems, power towers, and dish/engine systems (Romero-Alvarez and Zarza, 2007). Parabolic trough collectors and linear Fresnel systems can heat a thermal fluid up to 393°C by concentrating solar radiation 30-80 times. Power towers have concentration factors between 200 and 1000 and working fluid temperatures vary between 300°C and 1000°C. Dish/engine systems have very high concentration ratios (1000-4000) but unit sizes are less than 25 kW.

Systems that generate a higher temperature working fluid are usually more efficient as well. For example, dish/engine systems have a peak efficiency of 29% compared to 21% for parabolic trough collectors and linear Fresnel systems. On the other hand, parabolic trough collectors and linear Fresnel systems are demonstrated technologies while power towers and dish/engine systems are still at the pilot scale (Romero-Alvarez and Zarza, 2007). A parabolic-trough-based power plant developed by the Luz Corporation in Southern California achieved an overall solar-to-electricity conversion efficiency of 15% (Kreith and Kreider, 2011).

Solar-thermal power plants exhibit high capacity factors (up to 60%) when combined with thermal energy storage systems (Evans, 2007). A number of commercial solar-thermal power plants were built from 1984 to 1991 in the Mojave Desert in California (Kreith and Kreider, 2011). The most commercialized solar thermal technology is a parabolic trough collector, which concentrates direct radiation 30-80 times (Romero-Alvarez and Zarza, 2007).

Thermal storage technologies such as single- and two-tank systems can improve the reliability of solar-thermal systems (Hacatoglu et al., 2013a). In the two-tank system, fluid is divided into hot and cold tanks. The two-tank direct system uses the same fluid in the solar circuit and in storage whereas the two-tank indirect system uses different fluids. Single-tank systems have a temperature gradient from hot to cold that can cool a hot fluid (charging) or heat a cold fluid (discharging).

The photovoltaic (PV) effect is when a photon of light is absorbed by a valence electron of an atom, which causes it to jump into the conduction band where it can move freely (Kreith and Kreider, 2011). Solar-PV devices can convert up to 20% of sunlight directly to electricity (Scheirmeier, 2008). As a modular technology, solar-PV panels can provide electricity for a single household or be linked together in an array for larger purposes.

Solar radiation is an intermittent source of energy that varies over the course of a day and seasonally. The availability of solar energy is best during the day and summer while the intensity of solar radiation is weaker during the winter and unavailable at night. However, solar energy is also affected by other factors such as cloud cover. Consequently, the capacity factor of a solar-PV system is approximately 15% (Evans, 2007). Integrating solar-PV technologies with electrical energy storage systems can improve reliability and deliver a continuous supply of power. Energy storage of PV-based power is an important component of designing a stand-alone energy system.

3.1.1.2 Wind

Wind power is generated by converting the kinetic energy of wind into electricity. Since kinetic energy is proportional to the square of velocity, wind speed is a determining factor of the power output from a wind turbine. Most wind turbine configurations are classified as horizontal- or vertical-axis wind turbine. The majority of manufacturers produce horizontal-axis wind turbines partly because horizontal-axis wind turbines can be placed on tall towers to access higher wind speeds (Berg, 2007). Wind turbines range in size from 3-15 kW for a single home to 1-5 MW for large commercial wind turbines (Kreith and Kreidel, 2011).

The movement of wind is random, which makes wind energy an intermittent source of power. An individual wind turbine has a capacity factor of approximately 25% (Evans, 2007). In other words, a wind turbine designed for a peak capacity of 1 MW will only operate at that level about 25% of the time. Integration with electrical energy storage

technologies can improve the reliability of wind power, which is an important factor when designing a stand-alone energy system.

Wind power is estimated to be one of the least expensive sources of renewable energy. Berg (2007) presents a total cost of electricity between 4.3-5.6 cents kWh^{-1} for turbine ratings of 750 kW to 5.0 MW. The minimum cost of electricity was calculated for a wind turbine with a rating of 1.5 MW while the wind turbine rated at 5.0 MW was the most expensive.

Some communities near wind turbines have raised concerns about noise issues. The noise level of modern commercial wind turbines is approximately 35-45 decibels (dB) from 200-300 m away, which is less than the noise emanating from the average home (Kreith and Kreidel, 2011). It is possible for small wind turbines to have higher noise levels due to higher rates of rotation.

3.1.1.3 Geothermal

Geothermal-based energy systems use high-temperature heat from the earth's interior to provide heating or power generation (Evans, 2007). The best geothermal sites contain localized high-temperature, high-flux heat due to the movement of magma into the earth's crust (Kitz, 2007). High-temperature geothermal resources with high heat fluxes can be integrated in power generation cycles for the production of electricity. However, there are a limited number of geothermal sites where the rate of heat flow from the earth's core is high enough to sustain electricity production (Schiermeier et al., 2008).

Enhanced geothermal systems for power generation could exploit geothermal sites without naturally occurring localized heating. Enhanced geothermal technologies attempt to drill up to a depth of approximately 1000 m into the earth and pump hot water through two interconnected pipes (Kreith and Kreider, 2011). High-pressure cold water is pumped down an injection well through a fracture zone where it gradually heats up. Hot water then comes back up through a production well, where it could then

be used directly or in a heat exchanger to generate steam to drive a conventional turbine.

Unlike solar and wind energy, geothermal resources are not intermittent sources of power and can generate base load power for a community. The capacity factor for geothermal power plants is about 75%, which is high compared to other renewable energy technologies (Kitz, 2007). Geothermal energy could therefore play an important role in designing reliable sustainable community energy systems. Although the number of geothermal sites for conventional power generation is limited, enhanced geothermal systems can be developed anywhere. Despite their potential, enhanced geothermal systems have not yet been commercialized (Kreith and Kreider, 2011).

3.1.2 Storage

A key technical challenge associated with renewable energy is intermittency. The availability of solar and wind energy fluctuates but integration with storage technologies diminishes variability and improves the reliability of supply. Another method of improving the reliability of renewable energy systems is through hybridization. Combining several technologies into a hybrid system improves the chances that at least one of the energy sources will be available at a given time.

Community energy systems are usually driven by renewable resources combined with storage technologies or back-up fossil generators. A stand-alone community energy system will usually be a hybrid system composed of more than one source of energy generation. The general layout of a self-sufficient hybrid renewable energy system is shown in Figure 3.1.

Flows of renewable energy sources are converted to thermal or electrical energy in renewable energy subsystems. Thermal or electrical energy is then delivered to a load, where it meets the energy demand of a community. Surplus energy production charges thermal and electrical storage subsystems. The intermittency of certain renewable energy sources means that occasionally the load will be supplied by discharging stored

thermal and electrical energy. This is a general layout as there are many alternative hybrid community energy system designs in the literature.

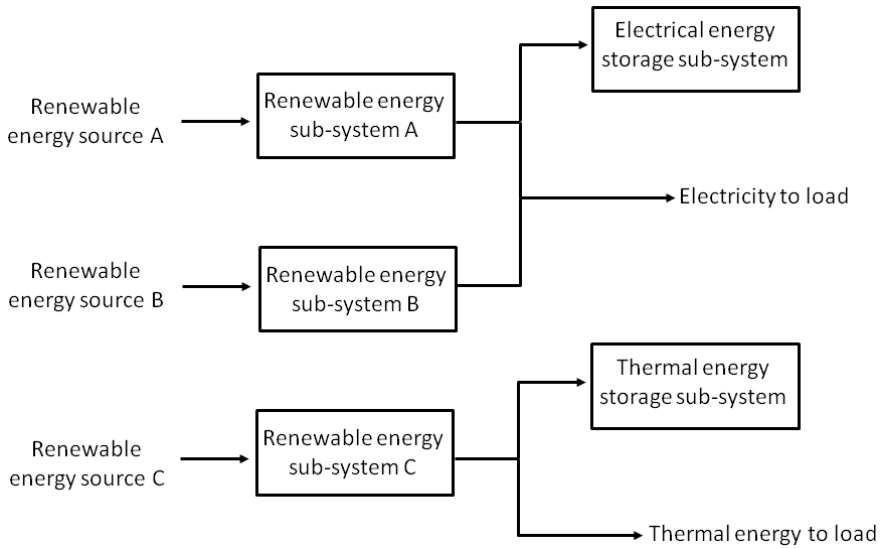

Figure 3.1: General layout of a hybrid renewable energy system.

Isherwood et al. (2000) performed an analytical optimization of a remote power system for an Alaskan village that imports diesel as its primary fuel. Heavy transportation costs and adverse environmental impacts associated with diesel make remote Alaskan communities especially attractive for self-sufficient hybrid energy systems. They constructed three hybrid energy scenarios and compared them to the existing diesel-only base case. The first scenario was a wind-diesel system, where surplus wind power provided heating for homes backed up by diesel generators/furnaces. The second scenario was a wind-hydrogen-diesel system, where surplus electricity generated hydrogen for later use. This scenario still required a back-up diesel subsystem but to a smaller extent compared to the first scenario. The third scenario was a wind-zinc-diesel system, where surplus wind power produced zinc pellets for later use in a zinc-air fuel cell. Their analysis revealed that as much as 75% of existing diesel fuel consumption can be displaced with 30-40% cost savings.

Carta and González (2001) designed a self-sufficient wind-diesel power system to meet the energy and potable water requirements of a small isolated fishing village in

the Canary Islands. Diesel-only generation resulted in the lowest cost of energy (40 cents kWh^{-1}) while combined wind-diesel systems were more expensive (49-52 cents kWh^{-1}) with fewer GHG emissions.

Bernal-Agustín et al. (2006) designed and performed a multi-objective optimization of an isolated hybrid photovoltaic-wind-diesel system with battery storage. The objective functions to be minimized were the total net present cost and GHG emissions. Applying a Multi-Objective Evolutionary Algorithm resulted in a Pareto-optimal solution set, with trade-offs between cost and emissions.

Neto et al. (2010) developed a biogas/photovoltaic hybrid power system with battery and biogas storage to supply energy to rural areas of Brazil. Biogas and a fertilizer-quality digestate are generated through an anaerobic digestion (AD) process fed by goat manure. The proposed system aids in agricultural land management, improves and reduces the strain on forest biomass resources. Less use of forest biomass slows the spread of deforestation and improves health by reducing the effects of firewood smoke on humans.

Bekele and Palm (2010) proposed a stand-alone solar-wind hybrid system with battery storage to supply electricity to a remotely located 1000-person community in Ethiopia. Due to the variability of solar and wind power, a back-up diesel generator is also suggested. The proposed system could significantly reduce food insecurity and drought events, which have been linked to the heavy reliance on biomass fuels. The levelized cost of electricity was calculated to be 38 and 46 cents kWh^{-1} for systems with 51% and 81% utilization of renewable resources, respectively.

Østergaard et al. (2010) developed a geothermal-wind-biomass system to meet Aalborg Municipality's energy needs without fossil fuels. Low-temperature geothermal heat is intended for district heating systems while wind and biomass resources supply power and transportation fuels. Unlike most community energy system designs, Østergaard et al. (2010) designed a system to meet heat, power, and transportation demand. Their analysis revealed that electricity would have to be imported at times for assistance in terms of power balancing.

Pérez-Navarro et al. (2010) proposed a hybrid wind-biomass power plant combined with a syngas storage system to provide a predictable source of electricity from a Spanish wind park. A reliable wind-based energy system requires storage to compensate for the variability of wind. Gasification of dry woody and herbaceous biomass generates a syngas that can be stored for when wind energy is unavailable. Modelling showed that year-round demand can be met with a pay-back period of about 4 years.

Community energy systems that generate surplus electricity are often integrated with a hydrogen storage subsystem. Conventional battery storage can be prohibitive for renewable energy systems that require large storage capacity due to their low energy density. Although the process of storing electrical energy as hydrogen is more complex, it can be more practical for community-scale projects. A basic renewable-energy-hydrogen integration is presented in Figure 3.2.

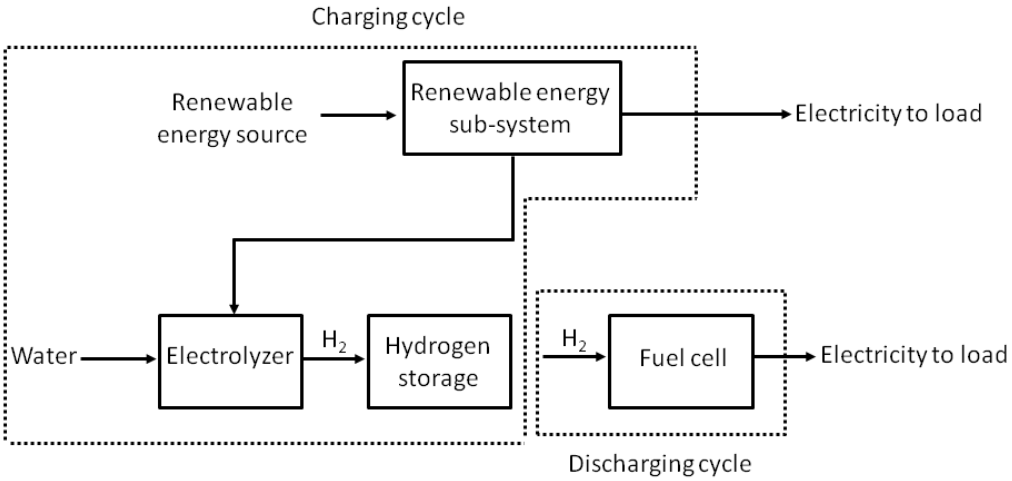

Figure 3.2: General layout of a renewable energy subsystem integrated with hydrogen storage.

The overall system operates on a charging and discharging cycle depending on the availability of renewable energy. When a source of renewable energy is on-line, electricity is delivered to the load while the remainder powers an electrolytic water-splitting process. The generated hydrogen then charges one of the various types of storage mediums (i.e. compressed gas, cryogenic liquid, metal hydrides, carbon structures, etc.). When the availability of renewable energy is insufficient to meet

demand, hydrogen is discharged from storage to generate electricity in a fuel cell. There are many hybrid systems in the literature that use hydrogen storage technologies.

Khan and Iqbal (2005) modelled a small hybrid wind-hydrogen energy system for off-grid power generation in remote communities. Fluctuating output from a wind turbine was reduced by integrating with an electrolyzer to generate hydrogen for later use. Stored hydrogen was then fed to a proton exchange membrane fuel cell to generate power. Their analysis revealed that a reliable supply of energy could be delivered without any conventional battery storage.

Shakya et al. (2005) assessed the feasibility of a stand-alone hybrid wind-photovoltaic system integrated with compressed hydrogen gas storage for Cooma, Australia. The levelized cost of electricity was determined to be 250 cents kWh^{-1}. More than 50% of total project costs were due to the electrolyzer.

Zoulias and Lymberopoulos (2007) performed a techno-economic analysis on integrating hydrogen technologies into stand-alone systems. Substituting with hydrogen storage was predicted to be technologically feasible but economic feasibility was dependent on significant reductions in the cost of electrolyzers and hydrogen tanks.

The high energy and economic costs of hydrogen compression and liquefaction have generated interest in solid-state storage in metal hydrides or carbon structures. The advantage of activated carbon as a storage medium is its high surface area and density of adsorbed hydrogen although low operating temperatures are still required. Zini et al. (2010) developed a hybrid photovoltaic-hydrogen system with activated carbon storage while Zini and Tartarini (2010) developed a similar system based on wind energy. An exergy analysis of a hybrid solar-hydrogen system with activated carbon storage was performed by Hacatoglu et al. (2011).

3.2 Life-Cycle Assessment

Life-cycle assessment is the quantification and evaluation of the inputs, outputs, and potential environmental impacts of a product (Guinée, 2002). It is commonly applied as

a tool to compare and evaluate the life-cycle emissions of similar-purpose products (Hacatoglu et al., 2012).

Inventory analysis and impact assessment are key stages of a life-cycle assessment. An inventory analysis is a collection of the materials and energy used in a system and released to the environment. The inventory results are then translated into potential environmental impacts in an impact assessment (Azapagic, 2007). There are two main types of impact assessment approaches – midpoint and endpoint. Midpoint approaches link environmental emissions from the inventory analysis to an intermediate position between the point of release and the damage incurred. Endpoint approaches are damage-oriented methods that model the actual damage inflicted by environmental emissions on areas of protection (e.g., human health and biodiversity) (Guinée, 2002).

The potential environmental impacts of emissions can be classified according to several common impact categories. In the midpoint method, characterization factors are used to convert the potential environmental impact of an emission into a reference substance. Table 3.1 lists the various impact categories and their reference substances.

Table 3.1: Common impact categories and reference substances in life-cycle impact assessment.

Impact category	Reference substance
Abiotic Depletion Potential	Antimony (Sb)
Acidification Potential	Sulphur dioxide (SO_2)
Eutrophication Potential	Phosphate (PO_4^{3-})
Freshwater Aquatic Ecotoxicity Potential	1,4-dichlorobenzene ($C_6H_4Cl_2$)
Global Warming Potential	Carbon dioxide (CO_2)
Marine Aquatic Ecotoxicity Potential	1,4-dichlorobenzene ($C_6H_4Cl_2$)
Photochemical Oxidant Creation Potential	Ozone (O_3)
Stratospheric Ozone Depletion Potential	Trichlorofluoromethane (CCl_3F or CFC-11)

The most well-known characterization factors are global warming and stratospheric ozone depletion potentials. For example, the 100-year global warming potential of methane (CH_4) and nitrous oxide (N_2O) is 34 and 310, respectively. Moreover, N_2O has recently been identified as an ozone-depleting substance with an ozone depletion potential of 0.017 (Ravishankara et al., 2009). The ozone depletion potential of N_2O is

low relative to more conventional chlorofluorocarbons but as a by-product of agricultural production its global emissions are significant. The characterization factor of a reference substance is by definition equal to one.

3.3 Exergy Analysis

Efficient use of energy resources requires a clear understanding of not just quantity but also quality of energy. Traditional energy analysis based on the first law of thermodynamics should be augmented by a second-law-based exergy approach that also considers quality (Rosen and Dincer, 1997). Linkages between exergy and increasingly important areas such as the environment and sustainable development have expanded the potential benefits of exergy analysis (Dincer and Rosen, 2013).

The overall specific exergy (*ex*) of a substance is the sum of its physical (ex_{ph}) and chemical (ex_{ch}) specific exergies. The chemical exergy of a substance needs to be considered when calculating exergy changes of chemical reactions. The chemical exergy for various molecules is provided by Morris and Szargut (1986). The specific physical exergy of a flowing stream of matter is based on its specific enthalpy (*h*) and entropy (*s*) and the reference environment conditions. As a result,

$$ex = ex_{ph} + ex_{ch} \tag{3.1}$$

$$ex_{ph} = h - h_0 - T_0(s - s_0) \tag{3.2}$$

where h_0, s_0, and T_0 are the specific enthalpy, specific entropy, and temperature of the reference environment, respectively.

The exergy flow rate ($\dot{E}x_Q$) associated with a heat transfer rate ($\dot{Q}$) at a temperature *T* is usually defined as the heat transfer rate multiplied by the Carnot factor. This leads to,

$$\dot{E}x_Q = \dot{Q}\left(1 - \frac{T_0}{T}\right) \tag{3.3}$$

The first law of thermodynamics states that energy cannot be created or destroyed but exergy is based on the first and second laws. It is therefore possible for irreversibilities in a system to destroy exergy. The exergy balance for a steady-state process is therefore,

$$\dot{E}x_{In} = \dot{E}x_{Out} + \dot{E}x_{D} \quad (3.4)$$

where $\dot{E}x_D$ is the exergy destruction rate of the process. A study of the exergy destruction rates of various components in a system can identify the main sources of irreversibilities and potential areas of improvement.

3.4 Sustainability

A literal interpretation of sustainability such as "to endure in perpetuity" is correct but not very helpful. Ehrenfeld (2004) defines sustainability as, "the possibility that human and other forms of life will flourish on the planet forever," which incorporates elements of society and the environment although the time scale is unworkable. Almost everything can be sustained over the short term while nothing can be sustained forever.

Sustainability can be defined from a more scientific perspective in terms of carrying capacity, which is the maximum number of people that can be supported in a given area. The carrying capacity for any given area is a function of the demand and supply of natural resources. However, sustainability cannot be defined exclusively from an environmental perspective and is usually viewed as having three dimensions – economic, social, and environmental (Figure 3.3).

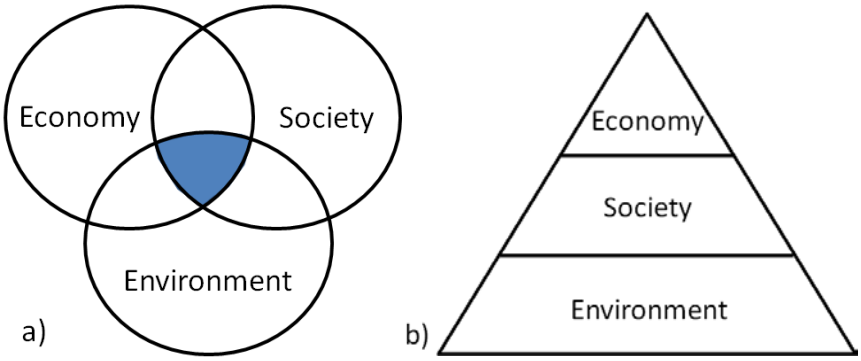

Figure 3.3: Illustrations of a) sustainability as the intersection of economic, societal, and environmental spheres and b) the hierarchy of the dimensions of sustainability (adapted from Hart (1999)).

Sustainability can be represented as the region of intersection of three partially overlapping circles that represent the economy, society, and environment (Figure 3.3a). The benefit of this model is the extension of sustainability from beyond carrying capacity to include socio-economic factors. A multidimensional model of sustainability coincides well with our understanding of societal collapse, which is influenced by several factors. The three dimensions of sustainability can be alternatively depicted in a hierarchal structure, where the economy is a subsystem of society, both of which are embedded in the environment (Figure 3.3b). These models illustrate the interconnectedness of the economy, society, and environment and their effect on the sustainability of a system. Progress towards sustainability is often viewed as a "systems problem," where the overall interaction between subsystems needs to combine to generate a sustainable system.

3.4.1 Economy

A vibrant economy that supports many well-paying jobs and facilitates a good standard of living for people is an essential part of a sustainable society. Modern capitalist economies are dependent on economic growth to expand job opportunities and absorb displaced workers from other sectors (Homer-Dixon, 2007). However, a growing economy is not necessarily sustainable over long periods of time since the economy is a subsystem of a finite planet (Daly, 2005). A sustainable society needs long-term economic development as opposed to economic growth.

At some point the global economy will need to stop growing and be replaced by a zero-growth, steady-state economy. Daly (2008) argues that economic growth, as measured by a rise in GDP, is desirable as a means of increasing well-being in poor countries. However, rich countries need to develop instead of grow their economies to free up resources and waste-assimilation capacity.

3.4.2 Society

Much of the early literature on sustainability was differentiated into extremes of economic development or environmental sustainability. Recently, there has been a greater emphasis on human development (Kates et al., 2005). There is no universal agreement on what comprises social sustainability but two major branches include health and equity.

Health and human well-being is an important component of social sustainability. People need access to clean drinking water, safe disposal of waste, and an environment free of exposure to toxic chemicals that can induce acute or chronic diseases. Other important measures of human well-being are infant mortality and life expectancy, which Smil (2003) identifies as two of the best measures of the development of a country.

The concept of sustainability is directly related to intergenerational equity, which is about equity between present and future generations. A sustainability time scale of 50 years envisions the economic, social, and environmental conditions two generations into the future (Graedel and Allenby, 2010). At the most basic level, sustainability is about ensuring that human beings in future generations have the means to attain a decent quality of life that may parallel but may not necessarily be identical to preceding generations. For example, future generations of North Americans may live in smaller houses in high-density neighbourhoods with fewer material goods and less travel. It is possible that the standard of living as measured by GDP per capita of future generations will be lower but the quality of life could exceed modern standards.

One of the primary reasons a sustainable society may require the standard of living in modern capitalist economies to decline is resource constraints when striving for intra-generational equity, which is about equity between people of the same generation. A more balanced distribution of wealth would require a sizable shift in resources between rich and poor economies and within nations (Homer-Dixon, 2007).

3.4.3 Environment

The economy and society are subsystems of the environment, which is the source and sink of all material and energy transformations on Earth. Ensuring the sustainability of the human species means ensuring the ability of the planet to perform life-supporting functions. Human economies and populations have grown to such an extent that anthropogenic activities have global effects and far-reaching consequences that can impair the ability of the planet to support life (Kemp, 2004). Two of the most important environmental sustainability issues are climate change and stratospheric ozone layer depletion.

One of the greatest challenges of the 21st century is to stabilize the concentration of greenhouse gases in the atmosphere to prevent the harmful effects of global warming. Greenhouse gases such as CO_2, CH_4, and N_2O in the lower atmosphere absorb outgoing infrared radiation emitted by the earth's surface, which causes a "greenhouse effect" that warms the planet (vanLoon and Duffy, 2003). Primary sources of anthropogenic greenhouse gas emissions include combustion of fossil fuels, nitrogen use in agriculture, and enteric fermentation in ruminant animals (Steinfeld et al., 2006).

Since 1990, the Intergovernmental Panel on Climate Change (IPCC) has published comprehensive assessment reports reviewing the latest climate science and updating its predictions on future warming trends. The fourth assessment report was released in 2007 and upgraded warming trends from "likely" to "very likely" due to anthropogenic activities. As climate models have become more advanced, the predicted amount of warming and its potential impacts grow. Positive feedback cycles in the climate system such as greater absorption of solar radiation as a result of the loss of reflecting surfaces such as ice exacerbate warming and increase the risk of climate destabilization (Homer-Dixon, 2007).

Higher up in the atmosphere is a thin layer of stratospheric ozone (O_3) that moderates the transmission of solar radiation to the earth's surface. The stratospheric ozone absorbs shorter wavelength ultraviolet (UV) radiation, specifically UV-B, which can be harmful to both plant and animal species (vanLoon and Duffy, 2003). In the early 1980s,

noticeable declines in ozone levels above Antarctica were observed. Chlorinated fluorocarbons (CFCs), which were originally developed in the 1930s for use as refrigerants, were discovered to be ozone-depleting substances and the source of the "hole" in the ozone layer. CFC molecules dissociate in the stratosphere and release chlorine radicals that participate in numerous ozone-destroying reactions over their lifetime (Goedkoop and Spriensma, 2000). The Montreal Protocol of 1989 produced legislation to phase out the use of CFCs although they are still used in low-income countries and their long residence time in the atmosphere means that the ozone layer will recover slowly over many decades (IPCC, 2005).

There are many other environmental concerns that affect sustainability. Air pollutants released by heavy industry, coal-fired power plants, and internal combustion engine vehicles have an adverse effect on air quality and human health. Industrial wastewater emissions and runoff from agricultural fields can lead to eutrophication of bodies of water or bioaccumulation of toxic compounds in the fat cells of aquatic animals. Deforestation and development cause habitat destruction and force animals to migrate from well-adapted areas. Conserving biodiversity in a world of economic growth and development is a challenge and a threat to sustainability as economic and human systems continue expanding.

3.4.4 Sustainable Development

The terms "sustainability" and "sustainable development" are often used interchangeably despite their differences. Since "develop" can mean "to bring gradually to a better state," sustainable development can be thought of as a "continuous and sustained improvement" of a system. Development is a qualitative improvement in a system not to be confused with growth, which is a quantitative increase in physical scale (Daly, 1990). The distinction between sustainable development and sustainability is that the former is a course of action that improves the quality of life of human beings and can endure into the future. On the other hand, sustainability is a state that can be maintained into the future.

The concept of sustainable development was popularized by the World Commission on Environment and Development (WCED) of the United Nations and its 1987 report, "Our Common Future" (WCED, 1987). The report defines sustainable development as "meeting the needs of the present without compromising the ability of future generations to meet their own needs." The subsequent United Nations Conference on Environment and Development in 1992 produced an international environmental treaty known as the United Nations Framework Convention on Climate Change based on the first assessment report of the IPCC. This eventually led to the adoption of the legally binding Kyoto Protocol in 1997. The purpose of the treaty and the protocol is to stabilize greenhouse gas concentrations in the atmosphere at a level that avoids dangerous anthropogenic climate change.

Sustainable development can also be defined in terms of what is to be sustained and what is to be developed. The Board on Sustainable Development of the U.S. National Research Council proposes that nature, life-support systems, and communities are to be sustained while people, the economy, and society are to be developed (NRC, 1999). This approach to defining sustainable development can be seen in Figure 3.4.

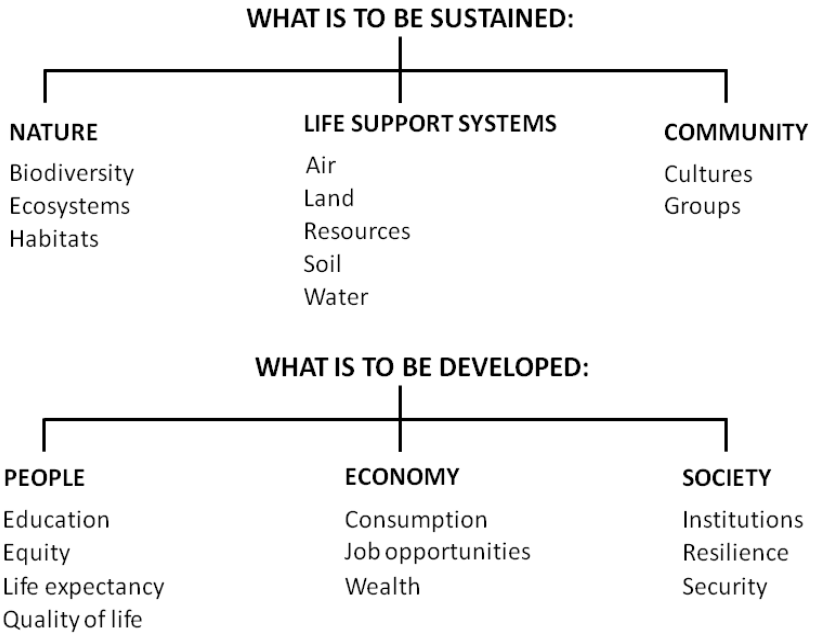

Figure 3.4: A two-faceted approach to defining sustainable development (adapted from NRC (1999)).

The earth and its embedded ecosystems provide natural resources as well as ecosystem services such as air and water purification, pollination, and a stable climate. These resources and services in turn allow human communities to flourish and endure into the future. Therefore, it is essential to sustain the earth and other lower-level systems to sustain the services of nature human beings have adapted to and depend on.

Human-made economic and social systems are not perfect and can be improved through development. Education, more equitable distribution of wealth, and less reliance on non-renewable resources can improve the quality of life of millions of residents of developing countries and create a more equitable society.

There is an ongoing debate between advocates of weak and strong sustainability, which is centred upon the substitutability of human-made versus natural capital (Ayres, 2007). Adherents of weak sustainability (usually economists) argue that sustainability is equivalent to non-decreasing total capital stock, which is the sum of manufactured and natural capital. Advocates of strong sustainability (usually natural scientists) hold that natural capital provides essential non-substitutable ecosystem services. Adherence to the precautionary principle favours the strong sustainability perspective due to our incomplete knowledge of how ecosystems function, the unknown services they provide, and our inability to provide those services ourselves.

Chapter 4 : Framework Development

Sustainability is a multidimensional concept that links the economy, society, and environment. A sustainability analyst must combine results from disparate fields to make an assessment on the sustainability of a system. The field of multi-criteria decision analysis is therefore very applicable to sustainability assessment.

This chapter develops a general framework for sustainability assessment that consists of normalization, weighting, and aggregation steps. However, the methodology imposed on the sustainability analyst at each step is a function of the type of assessment (i.e., compensatory or non-compensatory).

4.1 Normalization

Normalization transforms a sustainability indicator into a non-dimensional value between zero and one through a comparison to a sustainable reference level. Normalization is a necessary precursor to weighting and aggregation procedures when performing a compensatory multi-criteria decision analysis. However, normalization is not essential in non-compensatory approaches that only rank systems based on their relative performance.

Non-dimensional sustainability sub-indicators ($B_{i,j}$) between zero (undesired) and one (desired) are derived by comparing actual sustainability sub-indicators ($A_{i,j}$) to smaller target values ($A_{i,j,T}$). In special cases where an actual sub-indicator is less than its target value, the non-dimensional sub-indicator is adjusted to one. A non-dimensional sub-indicator is therefore calculated by,

$$B_{i,j} = \begin{cases} \dfrac{A_{i,j,T}}{A_{i,j}}, A_{i,j} > A_{i,j,T} \\ 1, A_{i,j} \le A_{i,j,T} \end{cases} \tag{4.1}$$

where $A_{i,j}$ represents sub-indicator i for category j and $A_{i,j,T}$ is the associated target value with the same units as $A_{i,j}$. The piecewise function described in Equation (4.1) is illustrated graphically in Figure 4.1 for an arbitrary target value (i.e., $A_{i,j,T}$) equal to one.

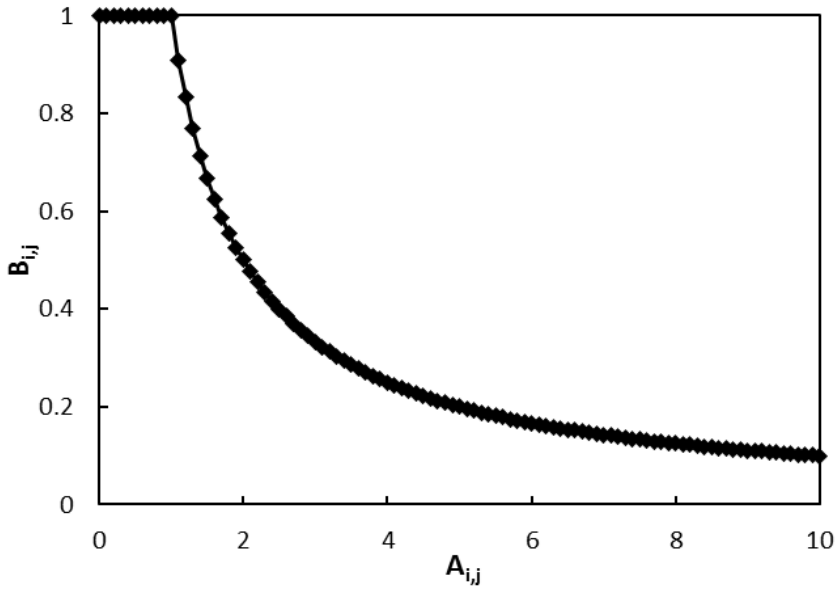

Figure 4.1: Graphical illustration of the change in the non-dimensional sustainability sub-indicator ($B_{i,j}$) with respect to the dimensional sustainability sub-indicator ($A_{i,j}$) when the target value is equal to one.

The value of $B_{i,j}$ decreases rapidly when $A_{i,j}$ first increases past the target value. For example, when $A_{i,j}$ is twice as large as $A_{i,j,T}$ (i.e., twice as large as the sustainable threshold), $B_{i,j}$ is equal to 0.50. However, $A_{i,j}$ has to increase to ten times more than $A_{i,j,T}$ for $B_{i,j}$ to be equal to 0.10.

The selection of $A_{i,j,T}$ is of critical importance to the sustainability assessment. For a given sub-indicator, $A_{i,j,T}$ represents the threshold beyond which a system may exhibit negative impacts from an economic, social, or environmental perspective. The selection of $A_{i,j,T}$ often depends on local characteristics but may also be of a global nature. For example, a sub-indicator related to freshwater consumption is strongly linked to the local context and its sustainable target value will vary across geographic regions. On the other hand, climate change has a global impact and international carbon budgets have been proposed to limit the rise in global average surface temperatures below certain levels. A sustainable target value for GHG emissions should therefore exhibit less variability although the method of allocating a carbon budget has a strong effect on local target values.

4.2 Weighting

Determining the weighting factors of indicators is an essential but often controversial step in a sustainability assessment. Many sustainability assessments circumvent the pitfalls associated with weighting by assuming equivalent weighting factors for all indicators or by not assigning weights at all, which is analogous to the equivalency assumption (Rowley et al., 2012).

There are many different approaches to determine weighting factors, all of which have advantages and drawbacks. One popular approach is the panel method, where a panel of experts and stakeholders are asked to weight the importance of various criteria. A typical approach in life-cycle impact assessment for deriving weighting factors is the distance-to-target method (Guinée, 2002), where weights are derived based on political or other targets. Monetary valuation methods are another class of weighting approaches. The relative importance of criteria in monetary valuation methods are assessed depending on market prices, willingness to pay, or avoidance costs (Ahlroth et al., 2011). However, there are well-known challenges associated with ecosystem valuation.

The exact meaning of a weight depends on whether a compensatory or non-compensatory aggregation method is being implemented (Rowley et al., 2012). Weights used with compensatory approaches represent trade-off factors or substitution rates. They describe the capacity for trade-offs between indicators. Weights used with non-compensatory approaches represent importance coefficients that describe the relative importance of an indicator in comparison to others.

4.2.1 Importance Coefficients

Eliciting the relative importance of an indicator or its trade-off with respect to other indicators is a subjective, inexact science. One possibility is to use the relative importance of an indicator to then determine trade-offs with respect to other indicators. Relative importance coefficients can then be utilized in non-compensatory

sustainability assessments while trade-off factors can be utilized in compensatory approaches.

The suggested approach for evaluating the relative importance of sustainability indicators is based on time, space, and receptor criteria. The time and physical scales of an indicator are important characteristics of sustainability, which are related to intergenerational and intragenerational equity, respectively. The receptor criterion is related to the extent of the indicator's impact on human or ecosystem receptors.

The importance of a sustainability indicator is evaluated on a scale of 1-5 ("very unimportant" to "very important") with respect to each of the aforementioned criteria. This type of rating scale is similar to Likert responding formats, which are commonly used in questionnaires across many different fields (Carifio and Perla, 2007). These Likert-type rating scales provide the most benefit when respondents are presented with 5-7 response categories (Neuman, 2010). Questionnaires with less than five categories do not provide much range to differentiate between responses whereas more than seven is confusing to respondents. In addition, response formats that feature an odd number of response categories (equal number of "positive" and "negative" responses plus a "neutral" middle option) provide the most balance (Neuman, 2010). The uncertainty associated with evaluating the importance of sustainability sub-indicators led to the decision to adopt a five-point rating scale, which is easier to manage and within the recommended range.

The relative importance of a sustainability indicator is calculated by dividing the overall score of an indicator by the overall scores of all indicators in the category. A sample calculation presented in Table 4.1 shows that Y is the most important indicator followed by X then Z. Variables X, Y, and Z can be sub-indicators in a category or category indicators as part of an overall assessment. This implies that 0.31, 0.52, and 0.17 can be intra-category or inter-category weighting factors.

The score assigned by a sustainability analyst to an indicator with respect to time, space, and receptor criteria is a function of the perspective of the decision maker. A

summary of the different archetypes and how they relate to the weighting factor criteria is presented in Table 4.2.

Table 4.1: Determining the relative importance of sustainability indicators with respect to time, space, and receptor criteria (1 – very unimportant; 2 – unimportant; 3 – neutral; 4 – important; 5 – very important).

Criteria	Sustainability indicator		
	X	Y	Z
Time	3	5	3
Space	3	5	1
Receptor	3	5	1
Sum	9	15	5
Relative importance	**0.31**	**0.52**	**0.17**

Table 4.2: Summary of the different archetypes for scoring and evaluating weighting factors.

Archetype	Time	Space	Receptor
Individualist	Short	Local	Humans
Egalitarian	Long	Global	Ecosystems
Hierarchist	Medium	Regional	Both

The individualist perspective is self-seeking and uninterested in inter- and intragenerational equity. Consequently, the evaluation of indicators is of a short-term and local perspective. The individualist view of nature is as resilient and plentiful, which translates into concerns regarding human as opposed to ecosystem receptors.

The egalitarian perspective is concerned with inter- and intragenerational equity and thus exhibits a long-term and global perspective. The egalitarian view of nature as fragile leads to concerns with respect to ecosystem receptors.

The hierarchist perspective is more moderate, believing that nature and natural resources can be managed within certain limits. It leads to a balanced approach to decision making, predicated on negotiation and compromise.

Real-world decision makers and stakeholders cannot be classified as individualist, egalitarian, or hierarchist. It is however a useful abstraction that demonstrates how a certain group with vested interests may favour one particular system over another.

4.2.2 Trade-Off Factors

The Analytic Hierarchy Process is a methodology to extract trade-off factors from a set of indicators by pair-wise comparisons (Nardo et al., 2008). Trade-off represents the willingness to forego a given indicator in exchange for another indicator. Using the Analytic Hierarchy Process, pair-wise comparisons (i.e., determining the trade-offs between pairs of indicators) can be transformed into overall trade-off factors for a set of any number of indicators. The minimum number of pair-wise comparisons needed for a system of x indicators is $x(x\text{-}1)/2$.

The key step in the Analytic Hierarchy Process is performing the pair-wise comparisons. However, a pair-wise comparison is a subjective exercise that strongly depends on the perspective of the decision maker. For example, the trade-off between the cost of a product or service and its life-cycle GHG emissions is affected by a decision maker's time horizon, spatial considerations, and concern for human or ecosystem receptors.

A possible approach for performing pair-wise comparisons and eliciting trade-off factors is to utilize the methodology for deriving importance coefficients. Sustainability indicators are first scored with respect to time, space, and receptor criteria. The trade-offs between indicators are then evaluated by a series of pair-wise comparisons according to the procedure described in Table 4.3.

A pair of indicators with the same overall score based on time, space, and receptor criteria are equally weighted and therefore have a trade-off factor equal to 1. This scenario corresponds to columns 5 and 6 in row 4 of Table 4.3 (i.e., 0 and 1). The next row down represents a situation where the overall score of indicator A is one point greater than the overall score of indicator B (i.e., +1). The trade-off for this scenario is 2. The reverse situation is where the overall score of indicator A is one point less than the

overall score of indicator B (i.e., -1). The trade-off for this scenario is 0.50, which is the reciprocal of the "+1" scenario. This trend continues until the largest possible difference, which is ±12 given that the minimum and maximum overall scores for a single indicator are 3 and 15, respectively.

Table 4.3: Pair-wise comparison procedure to determine the trade-off of indicator A with respect to indicator B based on the difference (A−B) of their overall scores for time, space, and receptor criteria.

A−B	Trade-off	A−B	Trade-off	A−B	Trade-off	A−B	Trade-off	A−B	Trade-off
-12	0.077	-7	0.125	-2	0.33	+3	4	+8	9
-11	0.083	-6	0.143	-1	0.50	+4	5	+9	10
-10	0.091	-5	0.167	0	1	+5	6	+10	11
-9	0.100	-4	0.200	+1	2	+6	7	+11	12
-8	0.111	-3	0.250	+2	3	+7	8	+12	13

Referring to Table 4.1, the overall score for indicator X (i.e., 9) minus the overall score for indicator Y (i.e., 15) is equal to -6. Based on the conversions listed in Table 4.3, the trade-off of X with respect to Y is 0.143. The trade-off of X with respect to Z is 5 because the difference between the overall scores is equal to +4. Finally, the trade-off of Y with respect to Z is 11 because the difference between the overall scores is equal to +10. The results of the pair-wise comparisons are compiled in a comparison matrix shown in Table 4.4.

Table 4.4: Comparison matrix for the X-Y-Z set of indicators illustrating the trade-offs between each indicator.

Sustainability indicator	X	Y	Z
X	1	0.14	5
Y	7	1	11
Z	0.2	0.09	1
Sum	8.2	1.2	17

The trade-offs shaded in grey flow directly from the overall scores in Table 4.1 and the procedure illustrated in Table 4.3. Only three comparisons are required for a three-indicator system. Each entry in the diagonal is always equal to one while the remaining

cells are equal to the reciprocal of their counterpart. For example, the trade-off of Y with respect to X (row 3, column 2) is equal to the reciprocal of the trade-off of X with respect to Y (row 2, column 3). The overall trade-off factors for each indicator are determined in an evaluation matrix as in Table 4.5.

Table 4.5: Evaluation matrix for the X-Y-Z set of indicators to determine overall trade-off factors.

Sustainability indicator	X	Y	Z	Trade-off factor
X	0.122	0.116	0.294	**0.177**
Y	0.854	0.811	0.647	**0.770**
Z	0.024	0.074	0.059	**0.052**

The values in columns X, Y, and Z are obtained by dividing each entry in Table 4.4 by the sum of the entries in the column. For example, the value in row 2, column 2 of Table 4.5 (i.e., 0.122) is equal to the value in row 2, column 2 of Table 4.4 (i.e., 1) divided by the sum of the entries in column 2 (i.e., 8.2). The trade-off factor for each sustainability indicator (i.e., column 5 in Table 4.5) is then calculated by evaluating the mean of each row.

4.3 Aggregation

Aggregation of sustainability indicators into a single-value composite index is attractive to decision and policy makers because it is simple and can be easily communicated to stakeholders and the general public. The various aggregation procedures can be defined as compensatory or non-compensatory.

4.3.1 Compensatory

Compensatory aggregation methods allow for the possibility of offsetting a disadvantage on some indicators by a sufficiently large advantage on other indicators (Rowley et al., 2012). Since trade-offs may occur between indicators, compensatory methods are compatible with the "weak" sustainability perspective, where human capital and natural capital are assumed to be interchangeable.

Compensatory aggregation procedures combine sub-indicators into a composite index. Non-dimensional sub-indicators are aggregated into a category indicator (B_j) through the use of intra-category weighting factors implemented in either a linear (4.2) or geometric (4.3) aggregation procedure. Consequently,

$$B_j = \sum_{i=1}^{m} \left(B_{i,j} \times W_{i,j} \right) \tag{4.2}$$

$$\sum_{i=1}^{m} W_{i,j} = 1$$

$$B_j = \prod_{i=1}^{m} B_{i,j}^{W_{i,j}} \tag{4.3}$$

where m represents the number of sub-indicators in a category and $W_{i,j}$ represents the weight associated with sub-indicator i in category j. The sum of the intra-category weights is equal to one irrespective of the aggregation procedure.

Overall sustainability is represented by the Integrated Sustainability Index (ISI), which is determined by aggregating category indicators and their respective weights by linear (4.4) or geometric (4.5) aggregation techniques. This leads to,

$$ISI = \sum_{j=1}^{n} \left(B_j \times W_j \right) \tag{4.4}$$

$$\sum_{j=1}^{n} W_j = 1$$

$$ISI = \prod_{j=1}^{n} B_j^{W_j} \tag{4.5}$$

where n represents the number of categories in an assessment and W_j represents the weight associated with category j. The sum of the inter-category weights is equal to one irrespective of the aggregation procedure.

Linear aggregation procedures assume perfect substitutability and compensability among sub-indicators (Juwana et al., 2012). This implies that a very low value of an indicator can be compensated by a very high value in another indicator. The overall composite index is therefore insensitive to extreme values in sub-indicators. Perfect substitutability is demonstrated by the horizontal line in Figure 4.2, where ISI based on

linear aggregation is independent of the difference between sub-indicators (i.e., B_1–B_2). In all cases, assuming equivalent weights and that the summation of B_1 and B_2 is equal to one, the ISI is always equal to 0.50.

Unlike linear techniques, geometric aggregation procedures only assume partial substitutability and compensability among sub-indicators. This implies that a larger difference between sub-indicators is penalized through a lower composite index. Partial substitutability and compensability is illustrated by the geometric aggregation function in Figure 4.2, where the value of ISI increases to a maximum of 0.50 as the absolute value of the difference between B_1 and B_2 decreases to zero.

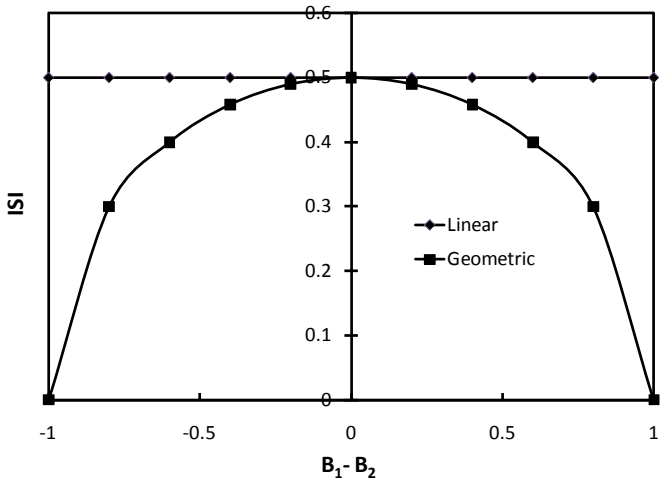

Figure 4.2: Variation of ISI with respect to two non-dimensional sub-indicators using linear and geometric aggregation procedures.

The linear weighted-sum approach described in Equations (4.2) and (4.4) is the most common aggregation method (Juwana et al., 2012). However, it is susceptible to double counting if indicators are not independent (Rowley et al., 2012). Each indicator is intended to measure a unique dimension of the aggregate but there will almost always be some positive correlation and dependence between different indicators (Nardo et al., 2008).

4.3.2 Non-Compensatory

Non-compensatory aggregation methods do not allow for the possibility of offsetting a disadvantage on some indicators by a sufficiently large advantage on other indicators. The absence of substitutability between indicators implies that non-compensatory approaches are more aligned with the concept of strong as opposed to weak sustainability. Consequently, the weighting factors utilized in non-compensatory multi-criteria decision analysis are interpreted as importance coefficients as opposed to trade-off factors or substitution rates.

The methodology of non-compensatory sustainability assessment can best be described through an example consisting of the aforementioned indicators X, Y, and Z. Four different options (A, B, C, and D) are compared on the basis of their relative X, Y, and Z indicator values to assess which option is more sustainable. The first step is to construct an impact matrix that contains the values of all the indicators (Table 4.6). The relative importance of each indicator is drawn from Table 4.1.

Table 4.6: Impact matrix of indicators X, Y, and Z for options A, B, C, and D, with relative importance values from Table 4.1.

Sustainability indicator	Option				Relative importance
	A	B	C	D	
X	100	50	75	20	0.31
Y	20	30	25	50	0.52
Z	65	45	70	10	0.17

The impact matrix uses the actual, non-adjusted (i.e., non-normalized) values of each indicator. Similar to Equation (4.1), smaller indicator values are preferred (e.g., GHG emissions). For example, option A has the poorest score with respect to indicator X but the best score with respect to Y. Normalization is unnecessary for non-compensatory aggregation because comparisons are done on the basis of which indicator is higher or lower. The advantage of this approach is that non-numerical indicators can also be implemented into the analysis. The impact matrix leads directly to the outranking matrix (Table 4.7), which compares the indicators of the different options.

Table 4.7: Outranking matrix to compare and select from options A, B, C, and D.

Option	Option				Sum
	A	B	C	D	
A	0	0.52	0.69	0.52	**1.73**
B	0.48	0	0.31	0.52	**1.31**
C	0.31	0.69	0	0.52	**1.52**
D	0.48	0.48	0.48	0	**1.44**

Each cell in the outranking matrix compares one option to another taking into consideration the relative importance of each indicator. In a comparison, higher indicator values are scored as zero while lower values are scored as the relative importance of the indicator. For example, the entry in row “A” and column “B” is a comparison of option A with respect to B from the perspective of option A. For indicator X, 100 is greater than 50 (Table 4.6), which leads to a value of 0 in row “A”, column “B”. For indicator Y, 20 is less than 30, which leads to a value of 0.52 in row “A”, column “B”. Lastly, 65 is greater than 45, which leads to a value of 0 in row “A”, column “B”. The sum of these three values is 0.52. Conversely, the entry in row “B” and column “A” is from the perspective of option B and should be equal to one minus the entry in row “A”, column “B”.

The sum of the scores in each row leads to the overall score for each option. The highest overall score is the preferred option. The final ranking is therefore A-C-D-B. Unlike compensatory aggregation, the degree to which one indicator is smaller/larger than another indicator is not taken into account. The only consideration is whether an indicator is better or worse than its counterpart. This eliminates the possibility of compensating for a disadvantage in several areas by a large advantage in a few areas. The drawback of non-compensatory approaches is that they are limited to relative assessments between different options.

Chapter 5 : Assessment Methodology

This chapter builds on the general framework described in Chapter 4 to develop a methodology to assess the sustainability of energy systems.

Sustainability is a multidimensional concept that transcends conventional disciplines and ways of thinking (Kates et al., 2005). An overview of some of the critical factors that comprise sustainability is presented in Figure 5.1.

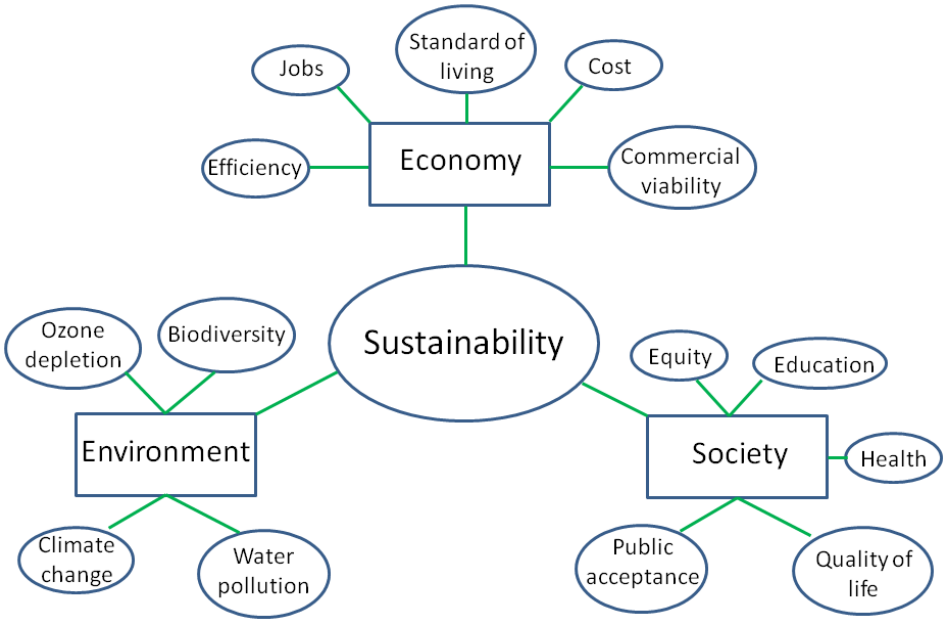

Figure 5.1: Overview of some of the critical factors that affect sustainability.

The three-pillar approach to sustainability (i.e., economy, society, and environment) is a common organizational structure when dealing with sustainability issues. Each pillar is associated with other key areas of sustainability. Any of the criteria in Figure 5.1 can be part of a sustainability assessment and even more criteria can be developed.

The Integrated Sustainability Index developed in this thesis does not consider all of the factors identified in Figure 5.1. The scope of the assessment is limited to several key indicators and sub-indicators shown in Figure 5.2. A more comprehensive assessment can include additional indicators that relate directly do the system under investigation. This is addressed in Section 5.3 of this chapter.

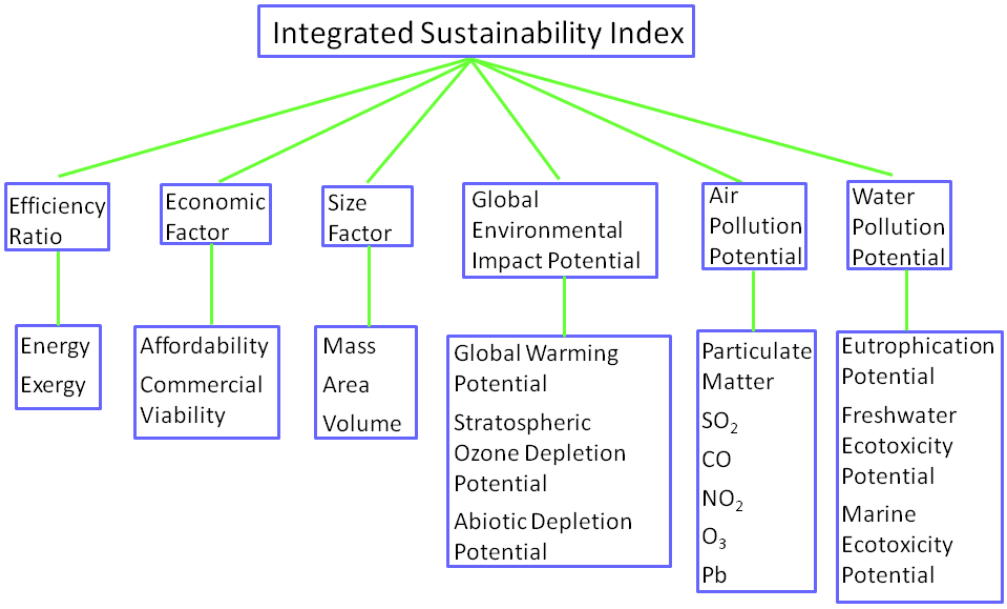

Figure 5.2: Components of the ISI.

5.1 Methodology

A detailed methodology to assess the sustainability of energy systems is presented here. The approach is illustrated using linear aggregation techniques although geometric procedures are also viable.

5.1.1 Efficiency Ratio (ER)

The efficiency of an energy system is a measure of its ability to convert inputs into products. The ER category indicator (B_{ER}) is comprised of energy- and exergy-based sub-indicators. Therefore,

$$B_{ER} = B_{ER,En} \times W_{ER,En} + B_{ER,Ex} \times W_{ER,Ex} \quad (5.1)$$

where $B_{ER,En}$ and $B_{ER,Ex}$ represent the non-dimensional sub-indicators and $W_{ER,En}$ and $W_{ER,Ex}$ represent the weights of energy and exergy efficiency ratios, respectively. Both the energy and exergy efficiency ratio terms compare actual efficiency to the upper (i.e., reversible) thermodynamic limit.

5.1.1.1 Energy Efficiency Ratio (EnER)

The energy efficiency of a system is defined as the ratio of useful energy products to energy inputs and is calculated using a traditional energy analysis based on the first law of thermodynamics. All energy transformations contain irreversibilities that reduce the actual efficiency relative to the upper limit (i.e., reversible) thermodynamic efficiency. Consequently, the actual efficiency of an energy system is always less than the reversible efficiency.

The implicit assumption in Equation (4.1) is that the target value is less than the indicator (e.g., minimizing pollution). However, unlike pollution-related criteria, the target efficiency is greater than the actual efficiency. The non-dimensional EnER sub-indicator is therefore calculated as,

$$B_{ER,En} = \frac{1 - A_{ER,En,T}}{1 - A_{ER,En}} \tag{5.2}$$

where $A_{ER,En}$ is the energy efficiency and $A_{ER,En,T}$ is the reversible (or target) energy efficiency of the system. The term $(1 - A_{ER,En})$ represents the actual amount of incoming energy not utilized while $(1 - A_{ER,En,T})$ represents the minimum amount of unavailable energy.

5.1.1.2 Exergy Efficiency Ratio (ExER)

More efficient use of energy resources requires a better understanding of not just quantity but also quality of energy. In that respect, traditional energy analysis should be augmented by a second-law, exergy-based approach that also considers the quality of energy.

Exergy analysis identifies the locations of energy degradation in a process and provides a superior measure of the useful work that can be extracted from a system (Dincer and Rosen, 2013). The non-dimensional ExER sub-indicator ($B_{ER,Ex}$) is calculated similarly to the energy-based sub-indicator from Equation (5.2). Therefore,

$$B_{ER,Ex} = \frac{1 - A_{ER,Ex,T}}{1 - A_{ER,Ex}} \tag{5.3}$$

where $A_{ER,Ex}$ is the exergy efficiency and $A_{ER,Ex,T}$ is the reversible (or target) exergy efficiency of the system.

5.1.2 Economic Factor (EF)

Economic considerations are one of the main pillars of sustainable development (Kates et al., 2005). The cost and commercial viability of an energy technology will affect its adoption by communities. Hence, we can write:

$$B_{EF} = B_{EF,AF} \times W_{EF,AF} + B_{EF,CV} \times W_{EF,CV} \quad (5.4)$$

where $B_{EF,AF}$ and $B_{EF,CV}$ represent the non-dimensional sub-indicators and $W_{EF,AF}$ and $W_{EF,CV}$ represent the weights of Affordability and Commercial Viability, respectively.

5.1.2.1 Affordability (AF)

Access to affordable energy services is critical for households with limited financial resources. The cost of energy should be evaluated relative to a household's ability to pay. This leads to,

$$B_{EF,AF} = \frac{A_{EF,AF,T}}{A_{EF,AF}} \quad (5.5)$$

where $A_{EF,AF}$ is the annual cost of energy per household and $A_{EF,AF,T}$ is the cost of energy a household can afford. The cost of energy delivered by the system should be compared to the median after-tax income in a region. The amount that a household can afford is therefore,

$$A_{EF,AF,T} = MATAI \times \alpha_{AF} \quad (5.6)$$

where *MATAI* is the median after-tax annual income in Ontario in 2010 ($69,300 per household; Statistics Canada, 2012) and α_{AF} is an adjustment factor that takes into consideration the fraction of household expenditures that can be dedicated to energy (10%; Fankhauser and Tepic, 2007). Adjustment factors are prevalent in the methodology as they account for the fact that individual or household financial, GHG, or resource "budgets" cannot be entirely allocated towards a single service or product (e.g., electricity).

5.1.2.2 Commercial Viability (CV)

The CV of a technology over the time scale for considering sustainability is another important consideration, where mature, commercialized technologies receive a better score than non-commercialized technologies. The indicator of CV ($B_{EF,CV}$) can be set to zero or one, where one indicates a commercially viable technology and zero a non-commercially viable technology.

5.1.3 Size Factor (SF)

The size of the energy system can be a limiting factor depending on the application. The actual size of the system should be compared to the limiting size factor, which can be either mass, area, or volume. The size factor category indicator (B_{SF}) is therefore,

$$B_{SF} = B_{SF,Mass} \times W_{SF,Mass} + B_{SF,Area} \times W_{SF,Area} + B_{SF,Volume} \times W_{SF,Volume} \quad (5.7)$$

where $B_{SF,Mass}$, $B_{SF,Area}$, and $B_{SF,Volume}$ are the non-dimensional sub-indicators and $W_{SF,Mass}$, $W_{SF,Area}$, and $W_{SF,Volume}$ are the weights for mass, area, and volume, respectively.

5.1.3.1 Mass

The mass of an energy system can be a limiting factor in certain applications such as mobile energy production systems. Thus, we can write:

$$B_{SF,Mass} = \frac{A_{SF,Mass,T}}{A_{SF,Mass}} \quad (5.8)$$

where $A_{SF,Mass}$ is the mass of the system and $A_{SF,Mass,T}$ is the target mass of the system.

5.1.3.2 Area

Land area has traditionally been an important aspect of sustainability analysis as demonstrated through concepts such as carrying capacity and ecological footprint. The land area occupied by an energy system is an important sustainability criterion in various applications. Therefore,

$$B_{SF,Area} = \frac{A_{SF,Area,T}}{A_{SF,Area}} \tag{5.9}$$

where $A_{SF,Area}$ is the area occupied by the system and $A_{SF,Area,T}$ is the target area of the system. For stationary applications within a bounded region, the target area may be estimated by determining the total area available per person then multiplying by a region-specific area factor that yields the total area available per person for residential energy production. For example,

$$A_{SF,Area,T} = \frac{Area_{S,ON}}{Pop_{S,ON}} \times \alpha_{Area} \tag{5.10}$$

where $Area_{S,ON}$ and $Pop_{S,ON}$ represent the land area and population of Southern Ontario, respectively. The region-specific factor is a function of numerous considerations such as agricultural, industrial, and commercial land use. The factor is assumed to be 5% in this study.

5.1.3.3 Volume

The volume of an energy system can be a limiting factor in certain applications such as mobile energy production systems. In this case,

$$B_{SF,Volume} = \frac{A_{SF,Volume,T}}{A_{SF,Volume}} \tag{5.11}$$

where $A_{SF,Volume}$ is the volume of the system and $A_{SF,Volume,T}$ is the target volume of the system.

5.1.4 Global Environmental Impact Potential (GEIP)

Environmental impacts range in terms of their spatial and temporal magnitude. Long-term environmental impacts that affect the entire planet are of greatest concern to humanity. The potential negative impact of global warming, stratospheric ozone depletion, and abiotic depletion are considered here. The GEIP category indicator (B_{GEIP}) is therefore,

$$B_{GEIP} = B_{GEIP,GWP} \times W_{GEIP,GWP} + B_{GEIP,SODP} \times W_{GEIP,SODP} + B_{GEIP,ADP} \times W_{GEIP,ADP} \tag{5.12}$$

where $B_{GEIP,GWP}$, $B_{GEIP,SODP}$, and $B_{GEIP,ADP}$ are the non-dimensional sub-indicators and $W_{GEIP,GWP}$, $W_{GEIP,SODP}$, and $W_{GEIP,ADP}$ are the weights for Global Warming Potential, Stratospheric Ozone Depletion Potential, and Abiotic Depletion Potential, respectively.

5.1.4.1 Global Warming Potential (GWP)

Anthropogenic GHG emissions are linked to accelerated rates of climate change and global warming. The most common GHGs are carbon dioxide (CO_2), methane (CH_4), and nitrous oxide (N_2O) amongst several others. Total GHG emissions can be estimated in CO_2 equivalents (CO_2e) by considering the 100-year warming potential of all life-cycle GHG emissions. Thus, the GWP sub-indicator is

$$B_{GEIP,GWP} = \frac{A_{GEIP,GWP,T}}{A_{GEIP,GWP}} \tag{5.13}$$

where $A_{GEIP,GWP}$ represents annual life-cycle GHG emissions per capita and $A_{GEIP,GWP,T}$ is the limit of annual emissions per capita.

The most recent IPCC report proposes representative concentration pathways (RCPs) that describe four possible climate futures. The most ambitious is RCP2.6, which restricts radiative forcing to 2.6 W m^{-2} above 1750 levels by the year 2100 and limits the predicted increase in global average surface temperature to 0.3-1.7°C (IPCC, 2013). On the other hand, the business-as-usual pathway (RCP8.5) is predicted to increase global average surface temperatures by 2.6-4.8°C by 2100. The threshold for energy-related GHG emissions is therefore,

$$A_{GEIP,GWP,T} = \frac{GHG}{Pop_{World}} \times \alpha_{GWP} \tag{5.14}$$

where *GHG* represents the annual carbon budget associated with the lower (5.8 Gt CO_2e yr^{-1}) or upper (17 Gt CO_2e yr^{-1}) limit of RCP2.6, Pop_{World} is the global population (7 billion), and α_{GWP} is the fraction of energy-related GHG emissions that can be attributed to residential energy production (20%; OEE, 2013).

5.1.4.2 Stratospheric Ozone Depletion Potential (SODP)

Ozone molecules in the stratosphere filter high-energy ultraviolet radiation from the sun that can otherwise have adverse human health and environmental impacts. Releases of halogenated hydrocarbons such as trichlorofluoromethane (also known as CFC-11 and Freon-11) that contain chlorine or bromine atoms engage in ozone-depleting chemical reactions upon entering the stratosphere.

Although the Montreal Protocol banned the production of CFC-11 and other chlorofluorocarbons, emissions from old stocks of equipment and their long residence time in the atmosphere means that the ozone layer will recover slowly over many decades (IPCC, 2005). Moreover, future ozone layer depletion is expected to be driven by N_2O, which is an unregulated ozone-depleting substance (Ravishankara, 2009). Overall life-cycle emissions of ozone-depleting substances can be described in terms of CFC-11 equivalents by utilizing ozone depletion potentials. The SODP sub-indicator can be calculated as

$$B_{GEIP,SODP} = \frac{A_{GEIP,SODP,T}}{A_{GEIP,SODP}} \tag{5.15}$$

where $A_{GEIP,SODP}$ represents annual life-cycle CFC-11 equivalent emissions per capita and $A_{GEIP,SODP,T}$ is the limit of emissions per capita.

Identifying the limit of CFC-11 equivalent emissions is a challenge since the objective of the Montreal Protocol is a complete ban on the production and use of ozone-depleting substances. The target value in the sustainability assessment then becomes zero, which is not a practical option. Instead, we can define an acceptable amount of ozone depletion (ΔO_3) over the time scale for considering sustainability. This leads to,

$$A_{GEIP,SODP,T} = \frac{\Delta O_3}{k_{Cl-O_3} \times f_{CFC-11} \times n_{Cl} \times Pop_{World} \times t_{Sust}} \alpha_{SODP} \tag{5.16}$$

where k_{Cl-O_3} is the relationship between stratospheric chlorine concentration and ozone depletion, f_{CFC-11} is the fate factor of CFC-11 when emitted from the surface of the earth, n_{Cl} is the number of chlorine atoms in a molecule of CFC-11, and t_{Sust} is the time scale for considering sustainability (Goedkoop and Spriensma, 2000).

SimaPro is used as the life-cycle assessment software to estimate life-cycle emissions and impacts of pollutants. Version 7.3.2 of the software does not characterize N_2O as an ozone-depleting substance. Post-processing of the output is required to incorporate the effect of N_2O by multiplying N_2O emissions (obtained from the inventory analysis) by its ozone-depletion potential (Ravishankara et al., 2009).

The time scale for considering sustainability can range from less than five years to infinity. However, Equation (5.16) demonstrates that an infinite time scale yields a target value equal to zero, which implies no tolerance for stratospheric ozone depletion. A more appropriate time frame for evaluating sustainability is 50 years (Table 5.1). The disadvantage of choosing a 50-year time horizon is that it may encourage pollution or profligate use of scarce resources and may not leave a sizable margin of error if a specific resource is unexpectedly needed in the future (Graedel and Allenby, 2010).

Table 5.1: Input data to sustainability assessment.

Parameter	Value
$Area_{S,ON}$	97,281 km^2
ΔO_3	2%
$f_{CFC\text{-}11}$	2.8×10^{-9}
GHG	5.8 Gt CO_2e yr^{-1}
k_{Cl-O_3}	0.02
MATAI	\$69,300 yr^{-1}
n_{Cl}	3
ODP	0.017
Population (S. Ontario)	12 million
Population (World)	7 billion
R_{Sb}	4.63×10^{15} kg
t_{Sust}	50 yr

5.1.4.3 Abiotic Depletion Potential (ADP)

A life-cycle impact assessment can reveal the ADP of a system, which is a measure of its use of non-renewable resources. The non-dimensional sub-indicator ($B_{GEIP,ADP}$) can be represented by:

$$B_{GEIP,ADP} = \frac{A_{GEIP,ADP,T}}{A_{GEIP,ADP}} \tag{5.17}$$

where $A_{GEIP,ADP}$ represents life-cycle use of antimony equivalents per capita per year and $A_{GEIP,ADP,T}$ represents the annual sustainable allotment of antimony. The target value is a function of the time scale for considering sustainability. Therefore,

$$A_{GEIP,ADP,T} = \frac{R_{Sb}}{Pop_{World} \times t_{Sust}} \times \alpha_{ADP} \tag{5.18}$$

where R_{Sb} represents the recoverable reserves of antimony.

5.1.5 Air Pollution Potential (APP)

Air pollution is the source of a number of environmental concerns such as acid rain and ground-level ozone formation as well as impacts on human health. Although there are thousands of contaminants that can cause air pollution, the US Environmental Protection Agency (EPA) has identified six criteria air contaminants to be monitored as part of its National Ambient Air Quality Standards (EPA, 2011). This leads to,

$$\begin{aligned} B_{APP} = {} & B_{APP,PM_{2.5}} \times W_{APP,PM_{2.5}} + B_{APP,PM_{10}} \times W_{APP,PM_{10}} + B_{APP,SO_2} \times W_{APP,SO_2} \\ & + B_{APP,CO} \times W_{APP,CO} + B_{APP,NO_2} \times W_{APP,NO_2} + B_{APP,O_3} \times W_{APP,O_3} + B_{APP,Pb} \times W_{APP,Pb} \end{aligned} \tag{5.19}$$

where $B_{APP,PM_{2.5}}$, $B_{APP,PM_{10}}$, B_{APP,SO_2}, $B_{APP,CO}$, B_{APP,NO_2}, B_{APP,O_3}, and $B_{APP,Pb}$ are the non-dimensional sub-indicators and $W_{APP,PM_{2.5}}$, $W_{APP,PM_{10}}$, W_{APP,SO_2}, $W_{APP,CO}$, W_{APP,NO_2}, W_{APP,O_3}, and $W_{APP,Pb}$ are the weighting factors for the Fine Particulate Matter, Coarse Particulate Matter, Sulphur Dioxide, Carbon Monoxide, Nitrogen Dioxide, Ground-Level Ozone, and Lead sub-indicators, respectively.

Evaluating sustainability sub-indicators for the APP category requires data on the background level, threshold concentration, and residence time of each air contaminant. The required data is available in Table 5.2.

5.1.5.1 Fine Particulate Matter ($PM_{2.5}$)

The presence of particulate matter in the troposphere is largely a human health concern. Particulate matter smaller than 2.5 μm in diameter ($PM_{2.5}$) penetrate into the gas-exchange regions of the lung and cause respiratory problems in humans. Moreover, since the settling velocity of particulate matter is proportional to size, the residence

time of fine particulate matter (i.e., $PM_{2.5}$) is longer than that of coarse particulate matter (i.e., PM_{10}). Thus,

$$B_{APP,PM_{2.5}} = \frac{A_{APP,PM_{2.5},T}}{A_{APP,PM_{2.5}}} \tag{5.20}$$

where $A_{APP,PM_{2.5}}$ represents the concentration of $PM_{2.5}$ in the local environment and $A_{APP,PM_{2.5},T}$ is the ambient air quality standard of 12 μg m^{-3} (EPA, 2011). The box model of air pollution dispersion is applied to determine the total concentration of a contaminant in the atmosphere.

Table 5.2: Data required on criteria air contaminants to evaluate APP sub-indicators.

Air contaminant	Background (μg m^{-3})	Threshold (μg m^{-3})	Residence time (hr)
Particulate matter (≤2.5 μm)	10	35	24
Particulate matter (≤10 μm)	15	50	12
Sulphur dioxide	55	194	24
Carbon monoxide	600	10,000	840
Nitrogen dioxide	30	100	24
Ground-level ozone	70	150	1
Lead	0.02	0.15	72

Life-cycle emissions of a pollutant are distributed evenly over the lifetime of a project and divided by the product of area and mixing height. The concentration is therefore calculated by

$$A_{APP,PM_{2.5}} = PM_{2.5,0} + \frac{PM_{2.5}}{Area_{S,ON} \times MH_{PM_{2.5}}} \times \frac{\tau_{PM_{2.5}}}{8760} \times \frac{Pop_{S,ON}}{N} \tag{5.21}$$

where $PM_{2.5,0}$ is the background concentration in the atmosphere, $PM_{2.5}$ is the annualized life-cycle emissions, and N is the number of people in the community. Winds are assumed to evenly distribute a pollutant over the land area. However, vertical mixing heights lengthen for longer residence times (Evans et al., 2002). Therefore,

$$MH_i = 30.088(\tau_i)^{0.61} \tag{5.22}$$

where τ_i and MH_i are the residence time and vertical mixing height of air contaminant i measured in years and km, respectively.

5.1.5.2 Coarse Particulate Matter (PM_{10})

Particulate matter smaller than 10 μm in diameter (PM_{10}) penetrate into the deepest part of the lungs and cause respiratory problems in humans. Consequently, we can write,

$$B_{APP,PM_{10}} = \frac{A_{APP,PM_{10},T}}{A_{APP,PM_{10}}} \tag{5.23}$$

where $A_{APP,PM_{10}}$ represents the concentration of coarse particulate matter in the local environment and $A_{APP,PM_{10},T}$ is the ambient air quality standard of 150 μg m^{-3} (EPA, 2011). The concentration is calculated by,

$$A_{APP,PM_{10}} = PM_{10,0} + \frac{PM_{10}}{Area_{S,ON} \times MH_{PM_{10}}} \times \frac{\tau_{PM_{10}}}{8760} \times \frac{Pop_{S,ON}}{N} \tag{5.24}$$

where $PM_{10,0}$, $PM_{2.5}$, $\tau_{PM_{10}}$, and $MH_{PM_{10}}$ represent the background concentration, annualized life-cycle emissions, residence time, and vertical mixing height of coarse particulate matter, respectively.

5.1.5.3 Sulphur Dioxide (SO_2)

Combustion of fuels that contain sulphur compounds such as coal and petroleum generates sulphur dioxide (SO_2), which is a precursor to acid rain. Modern coal-fired power plants limit the release of SO_2 to the environment through flue-gas desulphurization and low-sulphur transportation fuels are ubiquitous in the developed world. However, SO_2 emissions still occur. We can write for this sub-indicator,

$$B_{APP,SO_2} = \frac{A_{APP,SO_2,T}}{A_{APP,SO_2}} \tag{5.25}$$

where A_{APP,SO_2} represents the concentration of SO_2 in the local environment and $A_{APP,SO_2,T}$ is the ambient air quality standard of 190 μg m^{-3} (EPA, 2011). The concentration is calculated by,

$$A_{APP,SO_2} = SO_{2,0} + \frac{SO_2}{Area_{S,ON} \times MH_{SO_2}} \times \frac{\tau_{SO_2}}{8760} \times \frac{Pop_{S,ON}}{N} \tag{5.26}$$

where $SO_{2,0}$, SO_2, τ_{SO_2}, and MH_{SO_2} represent the background concentration, annualized life-cycle emissions, residence time, and vertical mixing height of SO_2, respectively.

5.1.5.4 Carbon Monoxide (CO)

The primary source of carbon monoxide emissions is incomplete combustion of fossil fuels within internal combustion engines. CO is a precursor to ground-level ozone formation and photochemical smog. Unlike CO_2, which has a residence time measured in years, CO is more reactive and has a residence time in the troposphere of 65 days. The CO sub-indicator is therefore,

$$B_{APP,CO} = \frac{A_{APP,CO,T}}{A_{APP,CO}} \tag{5.27}$$

where $A_{APP,CO}$ represents the concentration of CO in the local environment and $A_{APP,CO,T}$ is the ambient air quality standard of 10 mg m^{-3} (EPA, 2011). The concentration is calculated by,

$$A_{APP,CO} = CO_0 + \frac{CO}{Area_{S,ON} \times MH_{CO}} \times \frac{\tau_{CO}}{8760} \times \frac{Pop_{S,ON}}{N} \tag{5.28}$$

where CO_0, CO, τ_{CO}, and MH_{CO} represent the background concentration, annualized life-cycle emissions, residence time, and vertical mixing height of CO, respectively.

5.1.5.5 Nitrogen Dioxide (NO_2)

High-temperature combustion of fossil fuels in nitrogen-containing air leads to the formation of nitrogen dioxide, which is a precursor to acid rain and ground-level ozone. NO_2 is an oxidizing agent and has a short residence time in the troposphere of 24 hr. Consequently, the NO_2 sub-indicator can be calculated as,

$$B_{APP,NO_2} = \frac{A_{APP,NO_2,T}}{A_{APP,NO_2}} \tag{5.29}$$

where A_{APP,NO_2} represents the concentration of NO_2 in the local environment and $A_{APP,NO_2,T}$ is the ambient air quality standard of 100 μg m^{-3} (EPA, 2011). The concentration is calculated by,

$$A_{APP,NO_2} = NO_{2,0} + \frac{NO_2}{Area_{S,ON} \times MH_{NO_2}} \times \frac{\tau_{NO_2}}{8760} \times \frac{Pop_{S,ON}}{N} \quad (5.30)$$

where $NO_{2,0}$, NO_2, τ_{NO_2}, and MH_{NO_2} represent the background concentration, annualized life-cycle emissions, residence time, and vertical mixing height of NO_2, respectively.

5.1.5.6 Ground-Level Ozone (O_3)

Although ozone molecules in the stratosphere perform essential life-supporting services by filtering high-energy ultraviolet radiation, ozone in the troposphere (or ground-level ozone) has an adverse impact on human health. The residence time of ozone in the troposphere is one hour. The ground-level O_3 sub-indicator is therefore,

$$B_{APP,O_3} = \frac{A_{APP,O_3,T}}{A_{APP,O_3}} \quad (5.31)$$

where A_{APP,O_3} represents the concentration of ground-level O_3 and $A_{APP,O_3,T}$ is the ambient air quality standard of 150 μg m^{-3} (EPA, 2011). The concentration is calculated by,

$$A_{APP,O_3} = O_{3,0} + \frac{O_3}{Area_{S,ON} \times MH_{O_3}} \times \frac{\tau_{O_3}}{8760} \times \frac{Pop_{S,ON}}{N} \quad (5.32)$$

where $O_{3,0}$, O_3, τ_{O_3}, and MH_{O_3} represent the background concentration, annualized life-cycle emissions, residence time, and vertical mixing height of O_3, respectively.

5.1.5.7 Lead (Pb)

There are several toxic air pollutants emitted by industrial processes that have adverse effects on human health. The EPA identifies lead as a criteria air contaminant that should be closely monitored. There are no significant chemical processes that accelerate the removal of atmospheric lead. For lead particles with a mass size distribution of 0.1–1.0 μm, the mean residence time in the troposphere is approximately three days (Niisoe et al., 2010). In this case,

$$B_{APP,Pb} = \frac{A_{APP,Pb,T}}{A_{APP,Pb}} \quad (5.33)$$

where $A_{APP,Pb}$ represents life-cycle emissions of lead and $A_{APP,Pb,T}$ is the ambient air quality standard of 0.15 μg m^{-3} (EPA, 2011). The concentration is calculated by,

$$A_{APP,Pb} = Pb_0 + \frac{Pb}{Area_{S,ON} \times MH_{Pb}} \times \frac{\tau_{Pb}}{8760} \times \frac{Pop_{S,ON}}{N} \quad (5.34)$$

where Pb_0, Pb, τ_{Pb}, and MH_{Pb} represent the background concentration, annualized life-cycle emissions, residence time, and vertical mixing height of Pb, respectively.

5.1.6 Water Pollution Potential (WPP)

Water ecosystems are an integral part of the environment and are also utilized by humans for drinking water, food, and leisure. Industrial effluents and agricultural runoff are sources of water pollution that can disrupt aquatic ecosystems. Taking these factors into account leads to,

$$B_{WPP} = B_{WPP,EP} \times W_{WPP,EP} + B_{WPP,FAETP} \times W_{WPP,FAETP} + B_{WPP,MAETP} \times W_{WPP,MAETP} \quad (5.35)$$

where $B_{WPP,EP}$, $B_{WPP,FAETP}$, and $B_{WPP,FAET}$ are the non-dimensional sub-indicators and $W_{WPP,EP}$, $W_{WPP,FAETP}$, and $W_{WPP,MAETP}$ are the weighting factors for Eutrophication Potential, Freshwater Aquatic Ecotoxicity Potential, and Marine Aquatic Ecotoxicity Potential, respectively.

5.1.6.1 Eutrophication Potential (EP)

Eutrophication in aquatic ecosystems is due to excess nutrient loads. Phosphorus is often a limiting nutrient in eutrophic systems. Hence, eutrophication is characterized in terms of phosphate (PO_4^{3-}) equivalents in life-cycle impact assessment. The EP sub-indicator can be written as,

$$B_{WPP,EP} = \frac{A_{WPP,EP,T}}{A_{WPP,EP}} \quad (5.36)$$

where $A_{WPP,EP}$ and $A_{WPP,EP,T}$ represent life-cycle and target emissions of PO_4^{3-} per capita per year, respectively. The threshold value of PO_4^{3-} can be calculated as,

$$A_{WPP,EP,T} = EP_{ref} \times \alpha_{EP} \quad (5.37)$$

where EP_{ref} represents global annual per capita PO_4^{3-} emissions and α_{EP} represents the adjustment factor.

5.1.6.2 Freshwater Aquatic Ecotoxicity Potential (FAETP)

Water emissions may contain harmful substances that are toxic to aquatic organisms. The ecotoxicity of emissions can be converted to common units of 1,4-dichlorobenzene (1,4-DCB) based on equivalency factors. Consequently,

$$B_{WPP,FAETP} = \frac{A_{WPP,FAETP,T}}{A_{WPP,FAETP}} \tag{5.38}$$

where $A_{WPP,FAETP}$ and $A_{WPP,FAETP,T}$ represent life-cycle and target emissions of 1,4-DCB to freshwater systems per capita per year, respectively. The threshold value of 1,4-DCB can be calculated as,

$$A_{WPP,FAETP,T} = FAETP_{ref} \times \alpha_{FAETP} \tag{5.39}$$

where $FAETP_{ref}$ represents global annual per capita 1,4-DCB emissions to freshwater systems and α_{FAETP} represents the adjustment factor.

5.1.6.3 Marine Aquatic Ecotoxicity Potential (MAETP)

Liquid wastes are also discharged to marine aquatic ecosystems. Marine emissions can also be converted to common units of 1,4-DCB based on equivalency factors. Consequently,

$$B_{WPP,MAETP} = \frac{A_{WPP,MAETP,T}}{A_{WPP,MAETP}} \tag{5.40}$$

where $A_{WPP,MAETP}$ and $A_{WPP,MAETP,T}$ represent life-cycle and target emissions of 1,4-DCB to marine aquatic systems per capita per year, respectively. The threshold value of 1,4-DCB can be calculated as,

$$B_{WPP,MAETP,T} = MAETP_{ref} \times \alpha_{MAETP} \tag{5.41}$$

where $MAETP_{ref}$ represents global annual per capita 1,4-DCB emissions to marine systems and α_{MAETP} represents the adjustment factor.

5.1.7 Other Indicators

There are many other indicators that can be included in a sustainability assessment that are not explored in detail in this study. Some of these indicators are presented here. As with any set of indicators, there may be overlaps within this set of indicators or with those identified in Sections 5.1.1-5.1.6.

5.1.7.1 Health and Safety

Health and safety are related concepts that are important aspects of social sustainability. Health and safety concerns can be seen from two different perspectives: occupational and public health and safety.

Occupational health and safety is regulated by legislation such as the province of Ontario's Occupational Health and Safety Act. The purpose of the Act is to set out the rights and duties of all parties in the workplace and establish procedures for dealing with workplace hazards (Ministry of Labour, 2012). An indicator to assess occupational health and safety may therefore not be necessary.

An indicator related to public health and safety might have more relevance. One common metric for assessing health and safety issues is disability-adjusted life years (Blanc et al., 2008). However, it is important to note that an indicator that measures impacts on health and safety is an endpoint indicator. Combining this endpoint indicator with a midpoint indicator such as APP, which indirectly measures human health effects, will lead to double-counting problems.

5.1.7.2 Technology Use

The viability of a technology to meet the energy needs of a community is site-specific. Communities will have different levels of knowledge, experience, and comfort with technology, all of which needs to be considered to ensure broad public acceptance. There are technical considerations such as the availability of local resources, expertise, and integration with existing infrastructure. Also important are social factors such as job creation, past experiences, and political support. Finally, environmental considerations

are also critical such as existing environmental challenges and the new technology's ability to improve or worsen the current situation.

5.1.7.3 Water Availability

Water availability can be an important determinant in the selection of energy system. Thermal generating stations in particular (e.g., coal, natural gas, nuclear, central solar) consume significant quantities of water. Once-through cooling systems withdraw from a direct water source then release the water back to its original source at a temperature 5-10°C higher (McMahon and Price, 2011). This can lead to thermal pollution and negative environmental impacts on aquatic ecosystems (Kemp, 2004). Closed-loop cooling systems withdraw less water and enable electricity to be produced in arid regions but evaporate losses increase overall water consumption (McMahon and Price, 2011). Dry-cooling systems are less water-intensive alternatives but also less efficient compared to water-cooled systems.

The availability of cooling water to ensure efficient and safe operation of a thermal generation station is therefore a useful potential sustainability indicator. Target values need to be set based on the maximum temperature of released water that limits environmental impact for once-through cooling systems or the acceptable amount of evaporative water losses for closed-loop cooling systems.

5.2 Benefits

There are three advantages of this new approach to sustainability assessment. The first is that the assessment considers a diverse range of factors that contribute to sustainability. The approach goes beyond traditional thermodynamic, carbon footprint, or life-cycle analysis to address important criteria of sustainability such as land area (related to carrying capacity), affordability, global environmental emissions, and air quality standards.

The second advantage is that the method employs a life-cycle perspective when estimating environmental impacts. The inventory analysis and impact assessment stages

of a life-cycle assessment provide a comprehensive summary of the resources used in an energy system and their associated environmental impacts, respectively. Identifying the full-scale environmental impact of an energy system without life-cycle-based techniques is a challenge.

The third advantage is that the approach establishes normalization references through sustainability-based threshold values. All sub-indicators are compared and normalized with respect to a reference state that represents the sustainable threshold. Thus, actual system efficiencies are compared to upper limit thermodynamic efficiencies while economic costs are compared to available household income. Similar thresholds are established for environmental emissions. Normalization references in traditional life-cycle analysis are usually based on regional or global per capita emissions (Bare et al., 2006; Guinée, 2002; Kim et al., 2012; Stranddorf et al., 2005). However, the current approach establishes environmental threshold values based on research and science-based policies of organizations such as the IPCC and US EPA.

The combination of these three features produces a novel multi-criteria decision analysis tool that can be used for quantitative sustainability assessments. In addition, aggregation of indicators into an easily understood, single-score Integrated Sustainability Index can assist in the decision-making process. Nevertheless, users and decision makers need to be aware that there is an inevitable loss of information when aggregating indicators (Bell and Morse, 2008) and considering only the Integrated Sustainability Index can lead to an incomplete assessment of the system.

5.3 Limitations

There are also limitations with the sustainability assessment methodology developed in this study. One issue is double counting in life-cycle analysis. Double-counting problems are common in life-cycle analysis, especially where there is overlap of products and processes in an overall system (Lenzen, 2008). For example, life-cycle inventory data may exist for two separate subsystems in an overall network. After integration, the sum of the life-cycle emissions from both subsystems is greater than the

actual emissions due to overlap of select pieces of equipment. This type of double counting can be avoided by knowing exactly the type of equipment accounted for in each subsystem or by generating the inventory analysis using only individual pieces of equipment. Unfortunately life-cycle data is not always desegregated in this manner.

Another life-cycle assessment double-counting issue to be aware of is mixing midpoint and endpoint indicators within a single assessment. The developed sustainability assessment approach relies on midpoint indicators (e.g., GHG emissions) to estimate potential environmental impacts and set threshold target values. This implies that including endpoint indicators that assess actual impacts and changes in the environment (e.g., temperature, sea level, etc.) could lead to double-counting problems. For example, a potentially useful sustainability indicator is eco-exergy, which is an estimate of the work capacity of an organism (or a network of organisms in an ecosystem) based on the information embodied in its genome and its biomass concentration (Jørgensen et al., 2010). Tracking eco-exergy therefore provides a measure on the state of an ecosystem and its development path (Coscieme et al., 2013). Although it provides valuable insight, double counting can occur when combining an endpoint indicator such as eco-exergy with midpoint indicators that track emissions into the environment.

Double-counting problems can also occur when indicators are not independent. As stated earlier, linear aggregation procedures are particularly sensitive to double counting when indicators are correlated and not independent (Rowley et al. 2012). For example, there is expected to be a certain degree of correlation between GWP and SODP. Both sub-indicators measure different dimensions of sustainability but share common sources. Table 5.3 lists the ozone-depletion potential and global-warming potential of common refrigerants.

An increase in ozone-depleting substances emissions inevitably leads to a rise in GHG emissions. The GWP sub-indicator is therefore partially dependent on the SODP sub-indicator. However, the reverse does not necessarily apply because of the most common GHGs (i.e, CO_2, CH_4, and N_2O), only N_2O has a non-zero ozone-depletion potential. This implies that emissions of substances that have both ozone-depletion and

global-warming potential are double counted. This is an acceptable case of double counting because two unique environmental impacts are being measured.

Table 5.3: Ozone-depletion potential and global-warming potential of common refrigerants (Critchley, 2011).

Refrigerant	Ozone-depletion potential	Global-warming potential
Halon 1301	16	7140
CFC-11	1	4000
CFC-12	1	2400
HCFC-22	0.05	1700
HFC-134a	0	1300

There are cases where the proposed sustainability assessment methodology is inappropriate. For example, the APP category includes critical air contaminants identified by the US EPA. However, there are several other harmful air pollutants not taken into consideration. For example, incineration of municipal solid waste or other refuse-derived fuel can lead to the formation of dioxins and furans, which can be human carcinogens (McKay, 2002; Rivera-Austrui et al., 2011). The assessment methodology does not have a sub-indicator to account for dioxin and furan emissions, which would therefore go unnoticed.

There is a special case that exposes a limitation with respect to the methodology used to estimate APP sub-indicators. Recall that air emissions over the life cycle of an energy system are combined with background levels to predict the local ambient air concentration of a pollutant. However, it is possible for the background concentration of a contaminant to be greater than the ambient air quality criteria threshold. Such cases inevitably result in a B-value of one for the sub-indicator in question irrespective of the amount of emissions generated by the energy system. For example, benzene is a known human carcinogen found in gasoline-powered motor vehicle exhaust (EPA, 2012). The ambient concentration of benzene is monitored by Environment Canada as part of the National Air Pollution Surveillance program. The annual average ambient air quality criterion for benzene is 0.45 $\mu g\ m^{-3}$ (Ministry of the Environment, 2011). However, several monitoring stations in Ontario exceeded the annual average threshold in 2012 –

the most recent year for which data is available. Stations in Kitchener (0.48 μg m^{-3}), Brampton (0.54 μg m^{-3}), Toronto (0.62 μg m^{-3}), and Hamilton (0.98 μg m^{-3}) all report annual average ambient concentrations that exceed the threshold (Environment Canada, 2013). A benzene sub-indicator for any of these regions would automatically be equal to the maximum value of one.

Another limitation of the assessment methodology is related to resource depletion. The existing approach has an ADP sub-indicator that flows directly from the life-cycle impact assessment. The reference substance for the ADP impact category is antimony (Sb). All the resources that show up in the life-cycle inventory analysis are multiplied by a characterization factor that converts relative depletion rates into units of kg Sb-equivalents. The drawback of this aggregate approach is that the rapid depletion of a particular compound might be too small to have an appreciable effect on the overall depletion rate and will go unnoticed by the sustainability analyst. For example, lithium production has increased significantly in recent years in part due to its importance in next-generation batteries. However, there are concerns with respect to global lithium availability and the sustainability of current production levels (Gruber et al., 2011; Kushnir and Sandén, 2012).

Fortunately, there are solutions to these types of problems. Improvised sustainability assessment approaches can be developed for specific energy systems if there is prior knowledge about the potential economic, social, or environmental impacts. For the waste incineration example, sub-indicators that relate to dioxin and furan emissions can be incorporated into the APP category using the same template that exists for other air pollutants. For the resource depletion example, an additional sub-indicator can be added to the assessment that deals specifically with lithium. An important aspect of these modified assessments is awareness of key considerations of an energy system prior to the assessment.

Chapter 6 : Case Studies

The sustainability assessment methodology developed in Chapter 5 is applied to several different case studies. This chapter describes and analyzes the various systems from a mass, energy, entropy, and exergy perspective.

6.1 Demand Profile

The case studies are designed to meet the heat, cold, and electrical energy needs of a 50-household community in Southern Ontario. The daily average electricity demand of a household is predicted based on a measurement campaign to record the electrical demands of a sample of 12 houses in Southern Ontario at one-minute intervals for one year (Saldanha and Beausoleil-Morrison, 2012). The demand-side input variables are therefore, 1) electricity (non-HVAC), 2) air conditioning, 3) domestic hot water, and 4) ambient temperature. The space heating needs of a household ($\dot{Q}_{Heat}$) are therefore,

$$\dot{Q}_{Heat} = \dot{Q}_{Heat,ref} \times Area_{Indoor} \times \left(T_{Indoor} - T_{amb}\right) \tag{6.1}$$

where $\dot{Q}_{Heat,ref}$ is an empirical parameter (Sørensen, 2011) that represents the heat rate required per m^2 of liveable floor space ($Area_{Indoor}$) and per °C temperature difference between the indoor (T_{Indoor}) and outdoor (T_{amb}) environment.

Combining the four input variables along with Equation (6.1) yields the energy demand of a household over the course of a year, as illustrated in Figures 6.1 and 6.2. Each of the case studies presented in this chapter are designed to meet these daily demand profiles.

Electricity demand is separated from air conditioning because some of the proposed case studies supply cooling through an absorption refrigeration cycle driven by thermal energy, as opposed to electrical. The required heat removal rate, which represents the duty of the absorption refrigeration cycle, is calculated from air conditioning data (Saldanha and Beausoleil-Morrison, 2012) using an average coefficient of performance (COP) of four for central air conditioners.

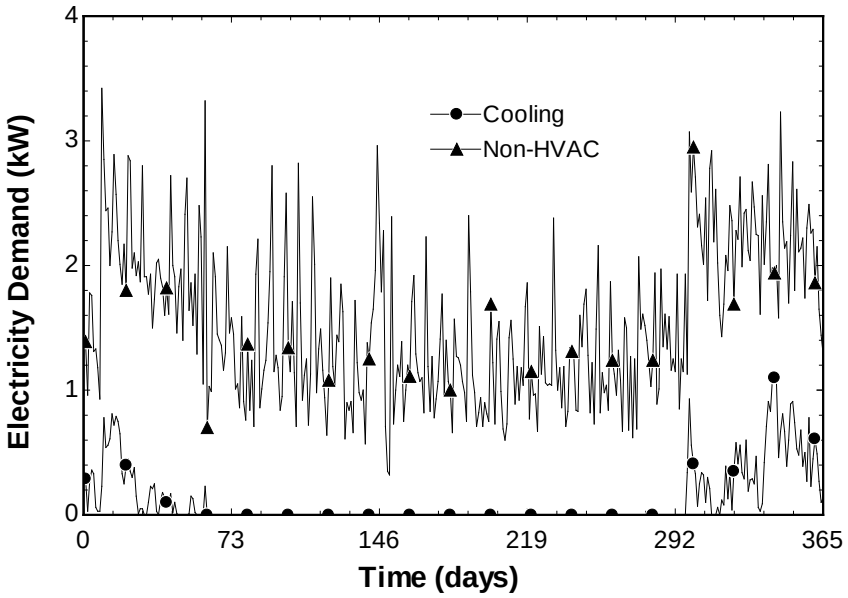

Figure 6.1: Cooling and non-HVAC electricity demand over one year for a typical household in Ontario (day "1" corresponds to August 1, 2009).

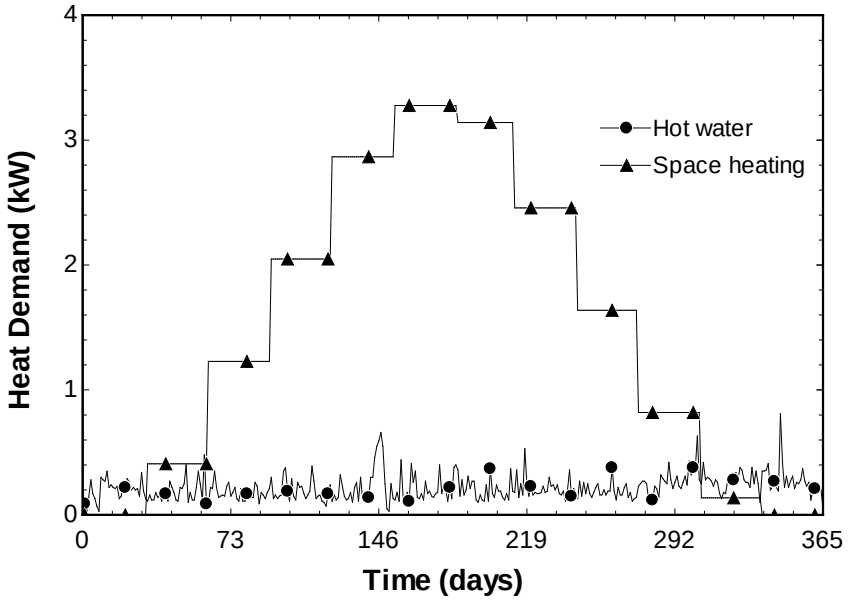

Figure 6.2: Daily average domestic hot water and space heating demand over one year for a typical household in Ontario (day "1" corresponds to August 1, 2009).

6.2 Reference System

The first case study is a traditional fossil-fired energy system. A gas-turbine power plant with regeneration serves as the reference case to meet the heat, cold, and

electrical energy needs of a 50-household community in Ontario. A thermodynamic model of the system was developed using the Engineering Equation Solver (EES) software. The model was run for 365 days with the input variables identified in Section 6.1.

6.2.1 System Description

The exothermic thermal energy generated by complete combustion of natural gas can potentially meet the energy needs of a community. The general layout of a gas-turbine power plant with regeneration is shown in Figure 6.3. The system is assumed to be driven by methane, which makes up approximately 95% of natural gas by volume.

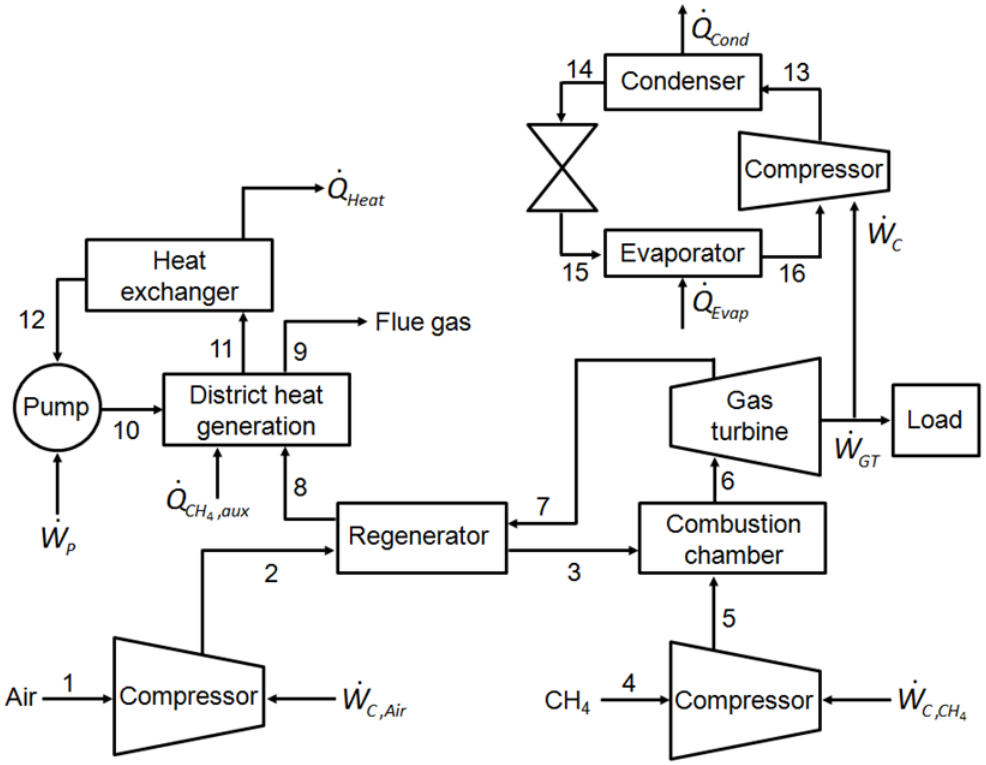

Figure 6.3: General layout of a gas-turbine power plant with regeneration, district heating, and a refrigeration cycle.

The temperature and pressure of air at state 1 increase from environmental conditions to state 2 in an electrically-driven compressor. The temperature of air then increases to state 3 through contact with hot exhaust gases in an isobaric regenerator.

An air-methane mixture is then ignited in the combustion chamber, generating hot combustion products at state 6. The high-temperature gas then expands in a gas turbine, which produces mechanical work followed by electricity using a generator. Electricity is required to meet the electrical energy needs of the community and to run the compressor in the vapour-compression refrigeration cycle (states 13-16). The combustion products then pass through a regenerator to preheat incoming air. The exhaust gas then generates pressurized hot water for the district heating system before finally being exhausted to the environment at state 9. Make-up gas is provided to the district heating network as a supplementary fuel when required.

6.2.2 Analysis

The size and technical performance of the gas-turbine power plant is assessed by constructing a thermodynamic model of the system using the EES software. Mass, energy, entropy, and exergy balance equations for each component of the system are entered into the equation solver along with input variables, parameters, and any necessary programming logic. The parameters that apply to all case studies are presented in Table 6.1. The parameters that specifically apply to the reference system are presented in Table 6.2. The following assumptions apply to the system:

- Natural gas consists entirely of methane.
- Compressors, pumps, and turbines are modelled as partially isentropic devices.
- Methane undergoes complete combustion in the combustion chamber.
- Fugitive emissions of refrigerant (R-410A) are negligible.

<u>Air compressor</u>

Air enters the compressor at state 1 and leaves at a higher temperature and pressure at state 2. The conditions at state 2 are determined by making use of a compressor isentropic efficiency (η_C) and a pressure ratio (*PR*).

$$\dot{m}_1 = \dot{m}_2 \tag{6.2}$$

$$\dot{m}_1 h_1 + \dot{W}_{C,Air} = \dot{m}_2 h_2 \tag{6.3}$$

$$\dot{m}_1 h_1 + \dot{W}_{C,Air,rev} = \dot{m}_2 h_{2,rev} \tag{6.4}$$

$$\eta_C = \frac{\dot{W}_{C,Air,rev}}{\dot{W}_{C,Air}} \tag{6.5}$$

$$PR = \frac{P_2}{P_1} \tag{6.6}$$

$$\dot{m}_1 s_1 + \dot{S}_{G,C,Air} = \dot{m}_2 s_2 \tag{6.7}$$

$$s_1 = s_{2,rev} \tag{6.8}$$

$$\dot{m}_1 ex_1 + \dot{W}_{C,Air} = \dot{m}_2 ex_2 + \dot{E}x_{D,C,Air} \tag{6.9}$$

Regenerator

Air enters the regenerator at state 2 and leaves at a higher temperature at state 3. Hot exhaust gases enter the regenerator at state 7 and exit at a lower temperature at state 8. The effectiveness of the regenerator (ε) determines the amount of heat transferred to the incoming air.

$$\dot{m}_2 = \dot{m}_3 \tag{6.10}$$

$$\dot{m}_7 = \dot{m}_8 \tag{6.11}$$

$$\dot{m}_2 h_2 + \dot{m}_7 h_7 = \dot{m}_3 h_3 + \dot{m}_8 h_8 \tag{6.12}$$

$$\varepsilon = \frac{h_3 - h_2}{h_{3,Max} - h_2} \tag{6.13}$$

$$\dot{m}_2 s_2 + \dot{m}_7 s_7 + \dot{S}_{G,Reg} = \dot{m}_3 s_3 + \dot{m}_8 s_8 \tag{6.14}$$

$$\dot{m}_2 ex_2 + \dot{m}_7 ex_7 = \dot{m}_3 ex_3 + \dot{m}_8 ex_8 + \dot{E}x_{D,Reg} \tag{6.15}$$

Methane compressor

Methane enters the compressor at state 4 and leaves at a higher temperature and pressure at state 5. The conditions at state 5 are determined by making use of a compressor isentropic efficiency.

$$\dot{m}_4 = \dot{m}_5 \tag{6.16}$$

$$\dot{m}_4 h_4 + \dot{W}_{C,CH_4} = \dot{m}_5 h_5 \tag{6.17}$$

$$\dot{m}_4 h_4 + \dot{W}_{C,CH_4,rev} = \dot{m}_5 h_{5,rev} \tag{6.18}$$

$$\eta_C = \frac{\dot{W}_{C,CH_4,rev}}{\dot{W}_{C,CH_4}} \tag{6.19}$$

$$\dot{m}_4 s_4 + \dot{S}_{G,C,CH_4} = \dot{m}_5 s_5 \tag{6.20}$$

$$s_4 = s_{5,rev} \tag{6.21}$$

$$\dot{m}_4 ex_4 + \dot{W}_{C,CH_4} = \dot{m}_5 ex_5 + \dot{E}x_{D,C,CH_4} \tag{6.22}$$

Combustion chamber

Air and methane react in the combustion chamber, which leads to hot exhaust gases at state 6. The balanced chemical reaction equation is,

$$CH_4 + 2(O_2 + 3.76N_2) \rightarrow CO_2 + 2H_2O + 7.52N_2 \tag{6.23}$$

The above chemical reaction generally occurs in excess air to ensure complete combustion of the fuel. The stoichiometric air-fuel ratio (AFR) of this reaction is approximately 17 while the actual AFR is closer to 50 (Cengel and Boles, 2010).

$$\dot{m}_3 + \dot{m}_5 = \dot{m}_6 \tag{6.24}$$

$$AFR = \frac{\dot{m}_3}{\dot{m}_5} \tag{6.25}$$

$$\dot{m}_3 h_3 + \dot{m}_5 h_5 = \dot{m}_6 h_6 + \dot{Q}_{Loss} \tag{6.26}$$

$$\dot{m}_3 s_3 + \dot{m}_5 s_5 + \dot{S}_{G,CC} = \dot{m}_6 s_6 + \frac{\dot{Q}_{Loss}}{T_{amb}} \tag{6.27}$$

$$\dot{m}_3 ex_3 + \dot{m}_5 ex_5 = \dot{m}_6 ex_6 + \dot{E}x_{Q,Loss} + \dot{E}x_{D,CC} \tag{6.28}$$

$$\dot{E}x_{Q,Loss} = \dot{Q}_{Loss}\left(1 - \frac{T_0}{T_{amb}}\right) \tag{6.29}$$

Gas turbine

High-temperate exhaust gas at state 6 enters the gas turbine and leaves at a lower temperature and pressure at state 7. The conditions at state 7 are determined by making use of a gas turbine isentropic efficiency (η_{GT}).

$$\dot{m}_6 = \dot{m}_7 \tag{6.30}$$

$$\dot{m}_6 h_6 = \dot{m}_7 h_7 + \dot{W}_{GT} \tag{6.31}$$

$$\dot{m}_6 h_6 = \dot{m}_7 h_{7,rev} + \dot{W}_{GT,rev} \tag{6.32}$$

$$\eta_{GT} = \frac{\dot{W}_{GT}}{\dot{W}_{GT,rev}} \tag{6.33}$$

$$PR = \frac{P_6}{P_7} \tag{6.34}$$

$$\dot{m}_6 s_6 + \dot{S}_{G,GT} = \dot{m}_7 s_7 \tag{6.35}$$

$$s_6 = s_{7,rev} \tag{6.36}$$

$$\dot{m}_6 ex_6 = \dot{m}_7 ex_7 + \dot{W}_{GT} + \dot{E}x_{D,GT} \tag{6.37}$$

District heat generation

The thermal energy in exhaust gas can be recovered to generate pressurized hot water for the district heating system.

$$\dot{m}_8 = \dot{m}_9 \tag{6.38}$$

$$\dot{m}_{10} = \dot{m}_{11} \tag{6.39}$$

$$\dot{m}_8 h_8 + \dot{m}_{10} h_{10} + \dot{Q}_{CH_4,aux} = \dot{m}_9 h_9 + \dot{m}_{11} h_{11} \tag{6.40}$$

$$\dot{Q}_{CH_4,aux} = \dot{m}_{CH_4,aux} HHV_{CH_4} \tag{6.41}$$

$$\dot{m}_8 s_8 + \dot{m}_{10} s_{10} + \frac{\dot{Q}_{CH_4,aux}}{T_{CH_4}} + \dot{S}_{G,DHG} = \dot{m}_9 s_9 + \dot{m}_{11} s_{11} \tag{6.42}$$

$$\dot{m}_8 ex_8 + \dot{m}_{10} ex_{10} + \dot{E}x_{Q,CH_4,aux} = \dot{m}_9 ex_9 + \dot{m}_{11} ex_{11} + \dot{E}x_{D,DHG} \tag{6.43}$$

$$\dot{E}x_{Q,CH_4,aux} = \dot{Q}_{CH_4,aux}\left(1 - \frac{T_0}{T_{CH_4,aux}}\right) \tag{6.44}$$

Heat exchanger

Hot pressurized water is distributed to meet the space heating needs of the community. Heat is extracted from hot water via on-site heat exchangers.

$$\dot{m}_{11} = \dot{m}_{12} \tag{6.45}$$

$$\dot{m}_{11} h_{11} = \dot{m}_{12} h_{12} + \dot{Q}_{Heat} \tag{6.46}$$

$$\dot{m}_{11} s_{11} + \dot{S}_{G,HXGR} = \dot{m}_{12} s_{12} + \frac{\dot{Q}_{Heat}}{T_{Indoor}} \tag{6.47}$$

$$\dot{m}_{11} ex_{11} = \dot{m}_{12} ex_{12} + \dot{E}x_{Q,Heat} + \dot{E}x_{D,HXGR} \tag{6.48}$$

$$\dot{E}x_{Q,Heat} = \dot{Q}_{Heat}\left(1 - \frac{T_0}{T_{Indoor}}\right) \tag{6.49}$$

Circulating pump

A circulating pump is required to restore the pressure of the working fluid due to pressure drops across the heat exchangers.

$$\dot{m}_{12} h_{12} + \dot{W}_P = \dot{m}_{10} h_{10} \tag{6.50}$$

$$\dot{m}_{12} h_{12} + \dot{W}_{P,rev} = \dot{m}_{10} h_{10,rev} \tag{6.51}$$

$$\eta_P = \frac{\dot{W}_{P,rev}}{\dot{W}_P} \tag{6.52}$$

$$\dot{m}_{12} s_{12} + \dot{S}_{G,P} = \dot{m}_{10} s_{10} \tag{6.53}$$

$$s_{12} = s_{10,rev} \tag{6.54}$$

$$\dot{m}_{12} ex_{12} + \dot{W}_P = \dot{m}_{10} ex_{10} + \dot{E}x_{D,P} \tag{6.55}$$

Condenser

In a refrigeration cycle, the working fluid rejects heat to the ambient high-temperature reservoir via a condenser.

$$\dot{m}_{13} = \dot{m}_{14} \tag{6.56}$$

$$\dot{m}_{13} h_{13} = \dot{m}_{14} h_{14} + \dot{Q}_{Cond} \tag{6.57}$$

$$\dot{m}_{13} s_{13} + \dot{S}_{G,Cond} = \dot{m}_{14} s_{14} + \frac{\dot{Q}_{Cond}}{T_{amb}} \tag{6.58}$$

$$\dot{m}_{13} ex_{13} = \dot{m}_{14} ex_{14} + \dot{E}x_{Q,Cond} + \dot{E}x_{D,Cond} \tag{6.59}$$

$$\dot{E}x_{Q,Cond} = \dot{Q}_{Cond}\left(1 - \frac{T_0}{T_{amb}}\right) \tag{6.60}$$

Expansion valve

The expansion valve is modelled as an isenthalpic process, where the compressed working fluid flashes to a liquid-vapour mixture.

$$\dot{m}_{14} = \dot{m}_{15} \tag{6.61}$$

$$\dot{m}_{14} h_{14} = \dot{m}_{15} h_{15} \tag{6.62}$$

$$\dot{m}_{14} s_{14} + \dot{S}_{G,EV} = \dot{m}_{15} s_{15} \tag{6.63}$$

$$\dot{m}_{14} ex_{14} = \dot{m}_{15} ex_{15} + \dot{E}x_{D,EV} \tag{6.64}$$

Evaporator

In a refrigeration cycle, the working fluid absorbs heat from the low-temperature reservoir via an evaporator. The amount of heat that needs to be absorbed is estimated by the air conditioning demand of a household.

$$\dot{m}_{15} = \dot{m}_{16} \tag{6.65}$$

$$\dot{m}_{15} h_{15} + \dot{Q}_{Evap} = \dot{m}_{16} h_{16} \tag{6.66}$$

$$\dot{Q}_{Evap} = \dot{W}_{AC} COP_{Avg} N_{Households} \tag{6.67}$$

$$\dot{m}_{15} s_{15} + \frac{\dot{Q}_{Evap}}{T_{Indoor}} + \dot{S}_{G,Evap} = \dot{m}_{16} s_{16} \tag{6.68}$$

$$\dot{m}_{15} ex_{15} = \dot{m}_{16} ex_{16} + \dot{E}x_{Q,Evap} + \dot{E}x_{D,Evap} \tag{6.69}$$

$$\dot{E}x_{Q,Evap} = \dot{Q}_{Evap} \left(1 - \frac{T_0}{T_{Indoor}} \right) \tag{6.70}$$

Compressor

A compressor is required in a vapour-compression refrigeration cycle to recompress the working fluid.

$$\dot{m}_{16} h_{16} + \dot{W}_{C,R410A} = \dot{m}_{13} h_{13} \tag{6.71}$$

$$\dot{m}_{16} h_{16} + \dot{W}_{C,R410A,rev} = \dot{m}_{13} h_{13,rev} \tag{6.72}$$

$$\eta_C = \frac{\dot{W}_{C,R410A,rev}}{\dot{W}_{C,R410A}} \tag{6.73}$$

$$\dot{m}_{16} s_{16} + \dot{S}_{G,C,R410A} = \dot{m}_{13} s_{13} \tag{6.74}$$

$$s_{16} = s_{13,rev} \tag{6.75}$$

$$\dot{m}_{16} ex_{16} + \dot{W}_{C,R410A} = \dot{m}_{13} ex_{13} + \dot{E}x_{D,C,R410A} \tag{6.76}$$

The first-law (energy) efficiency for this system is defined as the energy outputs divided by the higher heating value (HHV) of the fuel:

$$\eta = \frac{\dot{W}_{Load} + \dot{Q}_{Cold} + \dot{Q}_{Heat} + \dot{Q}_{DHW}}{\left(\dot{m}HHV\right)_{CH_4}} \tag{6.77}$$

where $\dot{W}_{Load}$ is the non-HVAC demand and $\dot{Q}_{Cold}$, $\dot{Q}_{Heat}$, and $\dot{Q}_{DHW}$ are the cooling, heating, and domestic hot water demand, respectively. Moreover, $\dot{m}$ and HHV are the mass flow rate and higher heating value of CH_4, respectively.

The second-law (exergy) efficiency for this system is defined as the exergy outputs divided by the chemical exergy (ex_{ch,CH_4}) of the fuel:

$$\psi = \frac{\dot{W}_{Load} + \dot{E}x_{Q,Cold} + \dot{E}x_{Q,Heat} + \dot{E}x_{Q,DHW}}{\left(\dot{m}ex_{ch}\right)_{CH_4}} \tag{6.78}$$

where $\dot{E}x_{Q,Cold}$, $\dot{E}x_{Q,Heat}$, and $\dot{E}x_{Q,DHW}$ are the thermal exergies of cold, heat, and domestic hot water, respectively.

Table 6.1: Modelling parameters that apply to all case studies.

Parameter	Value	Reference
Liveable floor space	195 m^2	Saldanha and Beausoleil-Morrison (2012)
Coefficient of performance of an average central air conditioning system	4	Sandler (1999)
Effectiveness of regenerator	0.75	Cengel and Boles (2010)
Efficiency of combustion	0.85	Sandler (1999)
Electric generator efficiency	0.92	Zini and Tartarini (2010)
Isentropic efficiency of a compressor	0.75	Cengel and Boles (2010)
Isentropic efficiency of a gas turbine	0.75	Cengel and Boles (2010)
Isentropic efficiency of a pump	0.75	Cengel and Boles (2010)
Number of people per household	4	Saldanha and Beausoleil-Morrison (2012)
Space heating factor	0.7 W m^{-2} K^{-1}	Sørensen (2011)
Temperature of domestic hot water	60 °C	Sandler (1999)
Temperature of household	18 °C	Saldanha and Beausoleil-Morrison (2012)

Table 6.2: Modelling parameters that apply to the reference system.

Parameter	Value	Reference
Air-fuel ratio	50	Cengel and Boles (2010)
Chemical exergy (methane)	51,978 kJ kg^{-1}	Morris and Szargut (1986)
Higher heating value (methane)	55,512 kJ kg^{-1}	Sandler (1999)
Pressure ratio	8	Cengel and Boles (2010)

6.3 Wind-Diesel System

A wind-diesel system integrates an intermittent source with fossil-based storage to meet the heat, cold, and electricity needs of a 50-household community in Ontario. The wind turbine and diesel generator produce electricity, which is then used to meet the load of the community as well as heat and cold demand via a heat pump. The refrigerant used in the heat pump is R-410A, which does not contribute to stratospheric ozone depletion but has a 100-year global warming potential of 1725 (Critchley, 2011).

6.3.1 System Description

A wind turbine that converts the kinetic energy of wind to electricity is proposed to meet the energy needs of a 50-household community in Ontario. The wind turbine is integrated with a diesel generator (Figure 6.4) to ensure the community has a reliable supply of energy during periods of low wind activity.

6.3.2 Analysis

A thermodynamic model of the system developed through EES was run for 365 days with the input variables identified in Section 6.1 as well as an additional input variable for wind speed. The modelling parameters that specifically apply to the wind-diesel system are presented in Table 6.3. The following assumptions apply to the system:

- Air-standard assumption for the diesel-fired gas-turbine subsystem.
- Diesel combustion occurs externally.
- Compressors, pumps, and turbines are modelled as partially isentropic devices.
- Coefficient of performance of the wind turbine is constant.

- Fugitive emissions of refrigerant (R-410A) are negligible.

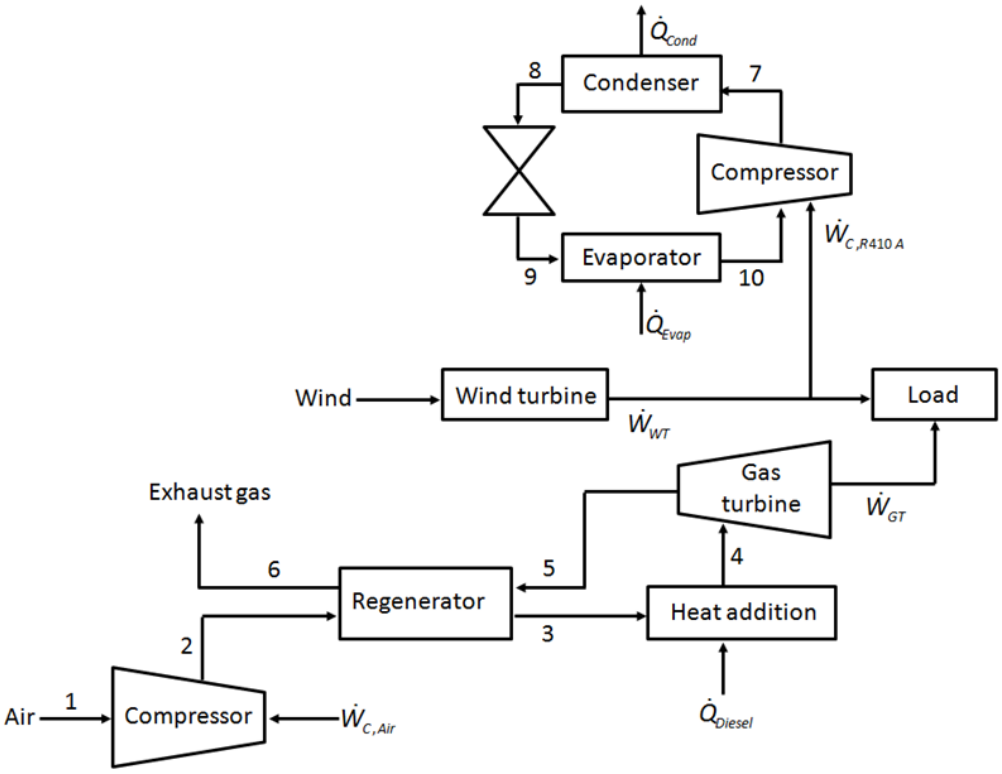

Figure 6.4: General layout of a wind-diesel system with an air-source heat pump.

Wind turbine

The wind speed (*WS*) profile of an average site can be modelled based on a Weibull probability density function with a shape parameter (*k*) between 1.5 and 2.5 (dimensionless) and a scale parameter (*c*) between 5 and 10 m s^{-1} (Zini and Tartarini, 2010). For the probability function we can write,

$$f(WS) = \frac{k}{c}\left(\frac{WS}{c}\right)^{k-1} \exp\left[-\left(\frac{WS}{c}\right)^{k}\right] \tag{6.79}$$

The daily average wind speed for Southern Ontario is shown in Figure 6.5. The wind speed profile was developed using a Weibull probability density function with shape and scale parameters of 2.0 and 7.5 m s^{-1}, respectively.

Wind speed significantly fluctuates over the course of the year, which highlights the need for energy storage. Storage is also needed during periods of low- and high-wind activity because the turbine does not generate electricity below the cut-in speed of 5 m s^{-1} or above the cut-out speed of 23 m s^{-1} (Berg, 2007). The rated wind speed is approximately 15 m s^{-1}, above which the turbine generates a constant power output (Berg, 2007).

The kinetic energy of wind ($\dot{E}_{Wind}$) is directly proportional to the swept area of the turbine blades and to the cube of wind speed (Zini and Tartarini, 2010). This leads to

$$\dot{E}_{Wind} = \frac{1}{2}\rho\pi(RR)^2(WS)^3 \tag{6.80}$$

where ρ is the density of air and RR is the rotor radius. The actual power generated by the wind turbine ($\dot{W}_{WT}$) depends on the power coefficient (C_P), mechanical efficiency (η_{Mech}), and the efficiency of the electric generator (η_{Gen}). Therefore,

$$\dot{W}_{WT} = C_P\eta_{Mech}\eta_{Gen}\frac{1}{2}\rho\pi(RR)^2(WS)^3 \tag{6.81}$$

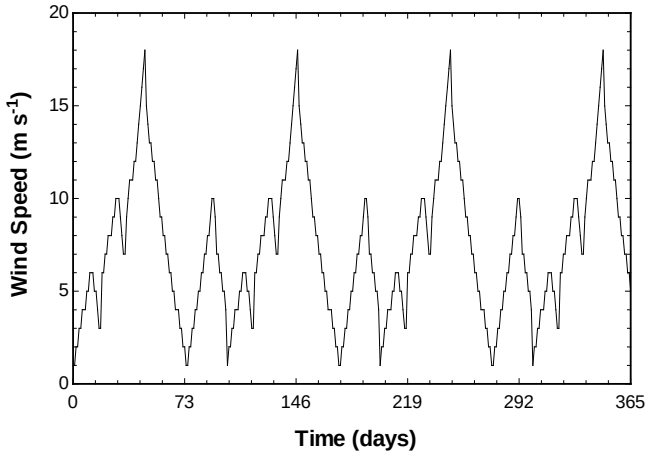

Figure 6.5: Daily average wind speed for Southern Ontario over the course of one year (day "1" corresponds to August 1, 2009).

Air compressor

Air enters the compressor at state 1 and leaves at a higher temperature and pressure at state 2.

$$\dot{m}_1 = \dot{m}_2 \tag{6.82}$$

$$\dot{m}_1 h_1 + \dot{W}_C = \dot{m}_2 h_2 \tag{6.83}$$

$$\dot{m}_1 h_1 + \dot{W}_{C,rev} = \dot{m}_2 h_{2,rev} \tag{6.84}$$

$$\eta_C = \frac{\dot{W}_{C,rev}}{\dot{W}_C} \tag{6.85}$$

$$PR = \frac{P_2}{P_1} \tag{6.86}$$

$$\dot{m}_1 s_1 + \dot{S}_{G,C} = \dot{m}_2 s_2 \tag{6.87}$$

$$s_1 = s_{2,rev} \tag{6.88}$$

$$\dot{m}_1 ex_1 + \dot{W}_C = \dot{m}_2 ex_2 + \dot{E}x_{D,C,Air} \tag{6.89}$$

Regenerator

Air enters the regenerator at state 2 and leaves at a higher temperature at state 3. Hot exhaust gases (modelled as air) enter the regenerator at state 5 and exit at a lower temperature at state 6.

$$\dot{m}_2 = \dot{m}_3 \tag{6.90}$$

$$\dot{m}_5 = \dot{m}_6 \tag{6.91}$$

$$\dot{m}_2 h_2 + \dot{m}_5 h_5 = \dot{m}_3 h_3 + \dot{m}_6 h_6 \tag{6.92}$$

$$\varepsilon = \frac{h_3 - h_2}{h_5 - h_2} \tag{6.93}$$

$$\dot{m}_2 s_2 + \dot{m}_5 s_5 + \dot{S}_{G,Reg} = \dot{m}_3 s_3 + \dot{m}_6 s_6 \tag{6.94}$$

$$\dot{m}_2 ex_2 + \dot{m}_5 ex_5 = \dot{m}_3 ex_3 + \dot{m}_6 ex_6 + \dot{E}x_{D,Reg} \tag{6.95}$$

Heat addition

Heat addition by diesel fuel combustion increases the temperature of the working fluid (i.e., air) from state 3 to state 4.

$$\dot{m}_3 + \dot{m}_{Diesel} = \dot{m}_4 \tag{6.96}$$

$$AFR = \frac{\dot{m}_3}{\dot{m}_{Diesel}} \tag{6.97}$$

$$\dot{m}_3 h_3 + \dot{Q}_{Diesel} = \dot{m}_4 h_4 + \dot{Q}_{Loss} \tag{6.98}$$

$$\dot{m}_3 s_3 + \frac{\dot{Q}_{Diesel}}{T_{Diesel}} + \dot{S}_{G,Heating} = \dot{m}_4 s_4 + \frac{\dot{Q}_{Loss}}{T_{amb}} \tag{6.99}$$

$$\dot{m}_3 ex_3 + \dot{E}x_{Q,Diesel} = \dot{m}_4 ex_4 + \dot{E}x_{Q,Loss} + \dot{E}x_{D,Heating} \tag{6.100}$$

$$\dot{E}x_{Q,Diesel} = \dot{Q}_{Diesel}\left(1 - \frac{T_0}{T_{Diesel}}\right) \tag{6.101}$$

$$\dot{E}x_{Q,Loss} = \dot{Q}_{Loss}\left(1 - \frac{T_0}{T_{amb}}\right) \tag{6.102}$$

Gas turbine

High-temperate air at state 5 enters the gas turbine and leaves at a lower temperature and pressure at state 6.

$$\dot{m}_4 = \dot{m}_5 \tag{6.103}$$

$$\dot{m}_4 h_4 = \dot{m}_5 h_5 + \dot{W}_{GT} \tag{6.104}$$

$$\dot{m}_4 h_4 = \dot{m}_5 h_{5,rev} + \dot{W}_{GT,rev} \tag{6.105}$$

$$\eta_{GT} = \frac{\dot{W}_{GT}}{\dot{W}_{GT,rev}} \tag{6.106}$$

$$PR = \frac{P_4}{P_5} \tag{6.107}$$

$$\dot{m}_4 s_4 + \dot{S}_{G,GT} = \dot{m}_5 s_5 \tag{6.108}$$

$$s_4 = s_{5,rev} \tag{6.109}$$

$$\dot{m}_4 ex_4 = \dot{m}_5 ex_5 + \dot{W}_{GT} + \dot{E}x_{D,GT} \tag{6.110}$$

The first-law (energy) efficiency for this system is defined as the energy outputs divided by the energy inputs (i.e., kinetic energy of wind and diesel fuel). Therefore,

$$\eta = \frac{\dot{W}_{Load} + \dot{Q}_{Cold} + \dot{Q}_{Heat} + \dot{Q}_{DHW}}{\dot{E}_{Wind} + \dot{m}_{Diesel} HHV_{Diesel}} \tag{6.111}$$

where $\dot{W}_{Load}$ is the non-HVAC demand and $\dot{Q}_{Cold}$, $\dot{Q}_{Heat}$, and $\dot{Q}_{DHW}$ are the cooling, heating, and domestic hot water demand, respectively. Moreover, $\dot{m}$ and *HHV* are the mass flow rate and higher heating value of CH_4, respectively.

The second-law (exergy) efficiency for this system is defined as the exergy outputs divided by the exergy of wind and the chemical exergy (ex_{ch,CH_4}) of the fuel. Therefore,

$$\psi = \frac{\dot{W}_{Load} + \dot{E}x_{Q,Cold} + \dot{E}x_{Q,Heat} + \dot{E}x_{Q,DHW}}{\dot{E}x_{Wind} + \dot{m}_{Diesel} ex_{ch,Diesel}} \tag{6.112}$$

where $\dot{E}x_{Q,Cold}$, $\dot{E}x_{Q,Heat}$, and $\dot{E}x_{Q,DHW}$ are the thermal exergies of cold, heat, and domestic hot water, respectively.

Table 6.3: Modelling parameters that apply to the wind-diesel system.

Parameter	Value	Reference
Air-fuel ratio	50	Cengel and Boles (2010)
Chemical exergy (diesel)	42,700 kJ kg^{-1}	Morris and Szargut (1986)
Cut-in wind speed	5 m s^{-1}	Berg (2007)
Cut-out wind speed	23 m s^{-1}	Berg (2007)
Lower heating value (diesel)	42,000 kJ kg^{-1}	Sandler (1999)
Mechanical efficiency of a wind turbine	0.60	Zini and Tartarini (2010)
Power coefficient of a wind turbine	0.45	Zini and Tartarini (2010)
Pressure ratio	8	Cengel and Boles (2010)
Rated wind speed	15 m s^{-1}	Berg (2007)

6.4 Wind-Battery System

A wind-battery system is entirely free of fossil fuels during operation. The absence of a fossil-based back-up system means that a very large storage system is required to reliably meet the energy needs of a community. This case study implements a lead-acid battery as the electrical energy storage medium.

6.4.1 System Description

A wind turbine that converts the kinetic energy of wind to electricity is proposed to meet the energy needs of a 50-household community in Ontario. The wind turbine is

integrated with a lead-acid battery and heat pump (Figure 6.6) to ensure the community has a reliable supply of energy during periods of low wind activity.

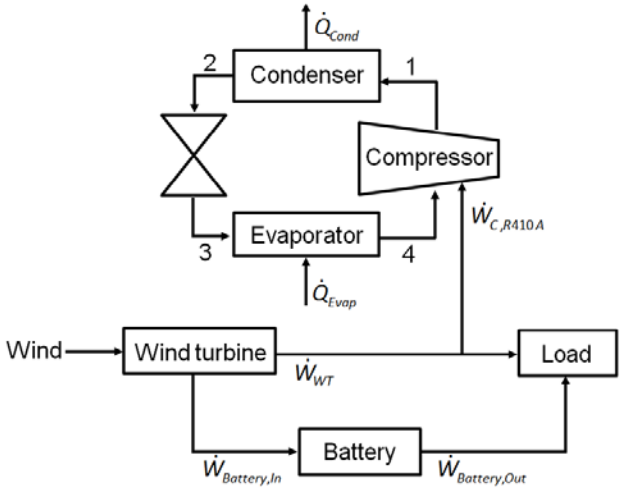

Figure 6.6: General layout of a wind-battery system with an air-source heat pump.

When the power delivered by the wind turbine exceeds the load the battery enters a charging mode. When there is unmet demand the battery discharges. The size of the wind turbine is selected such that the year-end net charge of the battery is positive.

6.4.2 Analysis

A thermodynamic model of the system developed through EES was run for 365 days with the input variables identified in Section 6.1 as well as an additional input variable for wind speed. The modelling parameters that specifically apply to the wind-battery system are presented in Table 6.4 while wind turbine parameters are available in Table 6.3. The following assumptions apply to the system:

- Compressors, pumps, and turbines are modelled as partially isentropic devices.
- Coefficient of performance of the wind turbine is constant.
- Charging and discharging efficiencies of the lead-acid battery are constant.
- Fugitive emissions of refrigerant (R-410A) are negligible.

Battery

The rate of electrical energy flowing into or out of the battery is proportional to the difference between the supply of the wind turbine and the demand of the community. When the battery is in charging mode the energy entering the battery is determined by,

$$\dot{W}_{Battery} = \left(\dot{W}_{WT} - \dot{W}_{Load}\right)\eta_{Battery} \tag{6.113}$$

$$\left(\dot{W}_{WT} - \dot{W}_{Load}\right)\left(1 - \eta_{Battery}\right) = \dot{E}x_{D,Battery} \tag{6.114}$$

where $\dot{W}_{Battery}$ is the flow of energy into the battery and $\eta_{Battery}$ is the charging/ discharging efficiency of a lead-acid battery. When in discharging mode,

$$\dot{W}_{Battery} = \frac{\dot{W}_{WT} - \dot{W}_{Load}}{\eta_{Battery}} \tag{6.115}$$

$$\left(\dot{W}_{Load} - \dot{W}_{WT}\right)\left(\frac{1}{\eta_{Battery}} - 1\right) = \dot{E}x_{D,Battery} \tag{6.116}$$

where $\dot{W}_{Battery}$ is less than zero. The summation of work flows into and out of the battery over 365 days has to be net positive.

The energy (η) and exergy (ψ) efficiency of the system is the ratio of products to inputs. Included as a product is the net work added to the battery. Therefore,

$$\eta = \frac{\dot{W}_{Load} + \dot{Q}_{Cold} + \dot{Q}_{Heat} + \dot{Q}_{DHW} + \dot{W}_{Battery}}{\dot{E}_{Wind}} \tag{6.117}$$

$$\psi = \frac{\dot{W}_{Load} + \dot{E}x_{Q,Cold} + \dot{E}x_{Q,Heat} + \dot{E}x_{Q,DHW} + \dot{W}_{Battery}}{\dot{E}x_{Wind}} \tag{6.118}$$

where $\dot{W}_{Load}$ denotes the community electrical power demand, $\dot{W}_{Battery}$ the net work added to the battery, and $\dot{E}x_{Wind}$ the exergy of wind.

Table 6.4: Modelling parameters that apply to the wind-battery system (Soloveichik, 2011).

Parameter	Value
Charging efficiency of the battery	0.80
Discharging efficiency of the battery	0.80
Specific energy of the battery	0.040 kWh kg^{-1}
Volumetric energy of the battery	70 Wh m^{-3}

6.5 Wind-Hydrogen System

An alternative to the battery storage system described in the previous section is a hydrogen-based storage system.

6.5.1 System Description

A wind turbine that converts the kinetic energy of wind to electricity is proposed to meet the energy needs of a 50-household community in Ontario. The wind turbine is integrated with a hydrogen storage subsystem and heat pump (Figure 6.7) to ensure the community has a reliable supply of energy during periods of low wind activity.

When the power delivered by the wind turbine is greater than the load the electrolyzer is activated to charge the hydrogen storage tanks. When there is unmet demand hydrogen is discharged to the fuel cell. The size of the wind turbine is selected such that the year-end net change of hydrogen in the storage tanks is positive.

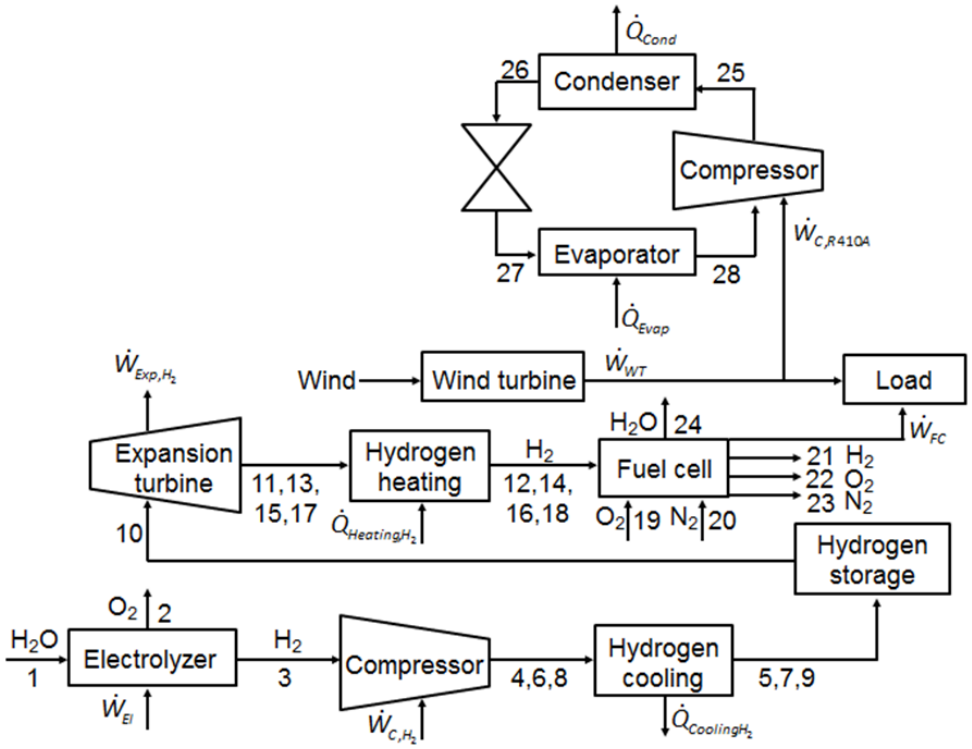

Figure 6.7: General layout of a wind-hydrogen system with an air-source heat pump.

6.5.2 Analysis

A thermodynamic model of the system developed through EES was run for 365 days with the input variables identified in Section 6.1 in addition to wind speed. The modelling parameters that specifically apply to the wind-hydrogen system are presented in Table 6.5 while wind turbine parameters are available in Table 6.3. The following assumptions apply to the system:

- Compressors, pumps, and turbines are modelled as partially isentropic devices.
- Coefficient of performance of the wind turbine is constant.
- Electrolyzer operates at a constant energy efficiency.
- Fugitive emissions of refrigerant (R-410A) are negligible.

Electrolyzer

If the work generated by the wind turbine is greater than the demand of the community, then the surplus work can be used to produce hydrogen in an electrolyzer. Water-based electrolytic hydrogen production undergoes the following endothermic chemical reaction:

$H_2O \rightarrow H_2 + 0.5O_2$ (6.119)

$$\dot{m}_1 = \dot{m}_2 + \dot{m}_3 \quad (6.120)$$

$$\dot{m}_2 = \dot{m}_1 \times \frac{1}{2}\left(\frac{MW_{O_2}}{MW_{H_2O}}\right) \quad (6.121)$$

$$\dot{m}_1 h_1 + \dot{W}_{El} = \dot{m}_2 h_2 + \dot{m}_3 h_3 + \dot{Q}_{El} \quad (6.122)$$

$$\eta_{El} = \frac{\dot{m}_3 HHV_{H_2}}{\dot{W}_{El}} \quad (6.123)$$

$$\dot{m}_1 s_1 + \dot{S}_{G,El} = \dot{m}_2 s_2 + \dot{m}_3 s_3 + \frac{\dot{Q}_{El}}{T_{amb}} \quad (6.124)$$

$$\dot{m}_1 ex_1 + \dot{W}_{El} = \dot{m}_2 ex_2 + \dot{m}_3 ex_3 + \dot{E}x_{Q,El} + \dot{E}x_{D,El} \quad (6.125)$$

$$\dot{E}x_{Q,El} = \dot{Q}_{El}\left(1 - \frac{T_0}{T_{amb}}\right) \quad (6.126)$$

$$ex_1 = h_1 - h_{0,H_2O} - T_0\left(s_1 - s_{0,H_2O}\right) + ex_{ch,H_2O} \quad (6.127)$$

$$ex_2 = h_2 - h_{0,O_2} - T_0\left(s_2 - s_{0,O_2}\right) + ex_{ch,O_2} \tag{6.128}$$

$$ex_3 = h_3 - h_{0,H_2} - T_0\left(s_3 - s_{0,H_2}\right) + ex_{ch,H_2} \tag{6.129}$$

Compressor (stage 1)

Hydrogen gas is compressed to increase its volumetric energy density and improve the feasibility of storage. The autoignition temperature of hydrogen is approximately 500-600°C, which suggests inter-stage cooling between compression operations.

$$\dot{m}_3 = \dot{m}_4 \tag{6.130}$$

$$\dot{m}_3 h_3 + \dot{W}_{C,H_2,1} = \dot{m}_4 h_4 \tag{6.131}$$

$$\dot{m}_3 h_3 + \dot{W}_{C,H_2,1,rev} = \dot{m}_4 h_{4,rev} \tag{6.132}$$

$$\eta_C = \frac{\dot{W}_{C,H_2,1,rev}}{\dot{W}_{C,H_2,1}} \tag{6.133}$$

$$\dot{m}_3 s_3 + \dot{S}_{G,C,H_2,1} = \dot{m}_4 s_4 \tag{6.134}$$

$$\dot{m}_3 ex_3 + \dot{W}_{C,H_2,1} = \dot{m}_4 ex_4 + \dot{E}x_{D,C,H_2,1} \tag{6.135}$$

Cooling (stage 1)

The temperature of hydrogen gas is reduced to ambient conditions following compression through interstage cooling.

$$\dot{m}_4 = \dot{m}_5 \tag{6.136}$$

$$\dot{m}_4 h_4 = \dot{m}_5 h_5 + \dot{Q}_{Cooling,H_2,1} \tag{6.137}$$

$$\dot{m}_4 s_4 + \dot{S}_{G,Cooling,H_2,1} = \dot{m}_5 s_5 + \frac{\dot{Q}_{Cooling,H_2,1}}{T_{amb}} \tag{6.138}$$

$$\dot{m}_4 ex_4 = \dot{m}_5 ex_5 + \dot{E}x_{Q,Cooling,H_2,1} + \dot{E}x_{D,Cooling,H_2,1} \tag{6.139}$$

Expansion turbine (stage 1)

Hydrogen gas is expanded prior to use in a fuel cell. The expansion work done by the gas is partially recovered by an expansion turbine. Multi-stage expansion with inter-stage heating increases the amount of work recovered.

$$\dot{m}_{10} = \dot{m}_{11} \tag{6.140}$$

$$\dot{m}_{10}h_{10} = \dot{m}_{11}h_{11} + \dot{W}_{Exp,H_2,1} \tag{6.141}$$

$$\dot{m}_{10}h_{10} = \dot{m}_{11}h_{11,rev} + \dot{W}_{Exp,H_2,1,rev} \tag{6.142}$$

$$\eta_{Exp} = \frac{\dot{W}_{Exp,H_2,1}}{\dot{W}_{Exp,H_2,1,rev}} \tag{6.143}$$

$$\dot{m}_{10}s_{10} + \dot{S}_{G,Exp,H_2,1} = \dot{m}_{11}s_{11} \tag{6.144}$$

$$\dot{m}_{10}ex_{10} = \dot{m}_{11}ex_{11} + \dot{W}_{Exp,H_2,1} + \dot{E}x_{D,Exp,H_2,1} \tag{6.145}$$

Heating (stage 1)

The temperature of hydrogen gas is increased to ambient conditions following expansion through interstage heating.

$$\dot{m}_{11} = \dot{m}_{12} \tag{6.146}$$

$$\dot{m}_{11}h_{11} + \dot{Q}_{Heating,H_2,1} = \dot{m}_{12}h_{12} \tag{6.147}$$

$$\dot{m}_{11}s_{11} + \frac{\dot{Q}_{Heating,H_2,1}}{T_{amb}} + \dot{S}_{G,Heating,H_2,1} = \dot{m}_{12}s_{12} \tag{6.148}$$

$$\dot{m}_{11}ex_{11} + \dot{E}x_{Q,Heating,H_2,1} = \dot{m}_{12}ex_{12} + \dot{E}x_{D,Heating,H_2,1} \tag{6.149}$$

$$\dot{E}x_{Q,Heating,H_2,1} = \dot{Q}_{Heating,H_2,1}\left(1 - \frac{T_0}{T_{amb}}\right) \tag{6.150}$$

Fuel cell

If the work generated by the wind turbine is less than the demand of the community, then the unmet demand can be addressed by utilizing stored hydrogen in a fuel cell. Hydrogen and oxygen react in a fuel cell to yield the following exothermic chemical reaction:

$$H_2 + 0.5O_2 \rightarrow H_2O \tag{6.151}$$

Ay et al. (2006) developed a thermodynamic model of a proton exchange membrane fuel cell, which is applied in this analysis. The net output voltage delivered by the fuel cell is equivalent to the reversible cell potential minus the sum of the individual overpotentials. The net output voltage is therefore,

$$V = V_{rev} - \left(V_{act} + V_{ohm} + V_{conc}\right) \tag{6.152}$$

The reversible voltage is a function of the temperature of the fuel cell and the partial pressure of hydrogen and oxygen. Consequently,

$$V_{rev} = 1.229 - 8.5\times10^{-4}\left(T_{FC} - 298\right) + 4.3085\times10^{-5}T_{FC}\left[\ln\left(\frac{P_{H_2}}{100}\right) + \frac{1}{2}\ln\left(\frac{P_{O_2}}{100}\right)\right] \tag{6.153}$$

$$P_{H_2} = x_{H_2}P_{Anode} \tag{6.154}$$

$$P_{O_2} = x_{O_2}P_{Cathode} \tag{6.155}$$

$$x_{H_2} = \frac{1 - x_{H_2O,Anode}}{1 + \frac{1}{2}x_{Anode}\left(1 + \frac{Z_{Anode}}{Z_{Anode} - 1}\right)} \tag{6.156}$$

$$x_{O_2} = \frac{1 - x_{H_2O,Cathode}}{1 + \frac{1}{2}x_{Cathode}\left(1 + \frac{Z_{Cathode}}{Z_{Cathode} - 1}\right)} \tag{6.157}$$

$$x_{H_2O,Anode} = \frac{P_{Sat}}{P_{Anode}} \tag{6.158}$$

$$x_{H_2O,Cathode} = \frac{P_{Sat}}{P_{Cathode}} \tag{6.159}$$

$$\log\left(\frac{P_{Sat}}{100}\right) = -2.1794 + 0.02953T_{FC} - 9.1837\times10^{-5}\left(T_{FC}\right)^2 + 1.4454\times10^{-7}\left(T_{FC}\right)^3 \tag{6.160}$$

$$P_{Anode} = P_{FC} \tag{6.161}$$

$$P_{Cathode} = P_{FC} \tag{6.162}$$

The activation overpotential is the difference between the potential at the anode and the potential at the cathode. Therefore,

$$V_{act} = V_{act,Anode} - V_{act,Cathode} \tag{6.163}$$

$$V_{act,Anode} = \frac{RT_{FC}}{\alpha_{Anode}n_{H_2}F}\ln\left(\frac{i}{i_0}\right) \tag{6.164}$$

$$V_{act,Cathode} = \frac{RT_{FC}}{\alpha_{Cathode}n_{H_2}F}\ln\left(\frac{i}{i_0}\right) \tag{6.165}$$

The ohmic overpotential is due to resistance in the electrolyte. It is proportional to the current density and cell resistance. The cell resistance is proportional to the membrane thickness and inversely proportional to membrane conductivity. This leads to,

$$V_{ohm} = iR_{ohm} \tag{6.166}$$

$$R_{ohm} = \frac{t_{mem}}{\sigma_{mem}} \tag{6.167}$$

$$\sigma_{mem} = (0.005139\lambda_{mem} - 0.00326)\exp\left[1268\left(\frac{1}{303} - \frac{1}{T_{FC}}\right)\right] \tag{6.168}$$

$$\lambda_{mem} = 0.043 + 17.81a - 39.85a^2 + 39.85a^3 \tag{6.169}$$

$$a = x_{H_2O,Cathode}\frac{P_{FC}}{P_{Sat}} \tag{6.170}$$

The concentration overpotential is due to increased loss of electrons at high current density. As a result,

$$V_{conc} = i\left(\beta_1 \frac{i}{i_{Max}}\right)^{\beta_2} \tag{6.171}$$

$$\beta_1 = \left(8.66 \times 10^{-5} T_{FC} - 0.068\right)b - 1.60 \times 10^{-4} T_{FC} + 0.54 \tag{6.172}$$

$$b = 8.5\frac{P_{O_2}}{100} + \frac{P_{Sat}}{100} \tag{6.173}$$

The inputs to the fuel cell are H_2, O_2, and N_2 while the outputs are unreacted H_2, O_2, and N_2 as well as water.

$$\dot{m}_{18} + \dot{m}_{19} + \dot{m}_{20} = \dot{m}_{21} + \dot{m}_{22} + \dot{m}_{23} + \dot{m}_{24} \tag{6.174}$$

$$\dot{m}_{18} = \frac{\frac{i}{n_{H_2}F}Area_{FC}MW_{H_2}}{UR_{H_2}} \tag{6.175}$$

$$\dot{m}_{19} = \frac{\frac{1}{2}\frac{i}{n_{H_2}F}Area_{FC}MW_{O_2}}{UR_{O_2}} \tag{6.176}$$

$$\dot{m}_{20} = 3.76\dot{m}_{19}\frac{MW_{N_2}}{MW_{O_2}} \tag{6.177}$$

$$\dot{m}_{21} = \dot{m}_{18}\left(1 - UR_{H_2}\right) \tag{6.178}$$

$$\dot{m}_{22} = \dot{m}_{19}\left(1 - UR_{O_2}\right) \tag{6.179}$$

$$\dot{m}_{23} = \dot{m}_{20} \tag{6.180}$$

The work done by the fuel cell is equal to the product of the net voltage, current density, and surface area:

$$\dot{m}_{18}h_{18} + \dot{m}_{19}h_{19} + \dot{m}_{20}h_{20} = \dot{m}_{21}h_{21} + \dot{m}_{22}h_{22} + \dot{m}_{23}h_{23} + \dot{m}_{24}h_{24} + \dot{W}_{FC} + \dot{Q}_{FC} + \dot{Q}_{Loss,FC} \tag{6.181}$$

$$\dot{W}_{FC} = ViArea_{FC} \tag{6.182}$$

$$\dot{Q}_{Loss,FC} = \dot{Q}_{FC}\frac{HLR}{1 - HLR} \tag{6.183}$$

$$\dot{m}_{18}s_{18} + \dot{m}_{19}s_{19} + \dot{m}_{20}s_{20} + \dot{S}_{Gen,FC} = \dot{m}_{21}s_{21} + \dot{m}_{22}s_{22} + \dot{m}_{23}s_{23} + \dot{m}_{24}s_{24} + \frac{\dot{Q}_{FC}}{T_{FC}} + \frac{\dot{Q}_{Loss,FC}}{T_{amb}} \tag{6.184}$$

$$\dot{m}_{18}ex_{18} + \dot{m}_{19}ex_{19} + \dot{m}_{20}ex_{20} = \dot{m}_{21}ex_{21} + \dot{m}_{22}ex_{22} + \dot{m}_{23}ex_{23} + \dot{m}_{24}ex_{24} + \dot{W}_{FC} + \dot{E}x_{Q,FC} + \dot{E}x_{Q,Loss,FC} + +\dot{E}x_{D,FC} \tag{6.185}$$

$$ex_{18} = h_{18} - h_{0,H_2} - T_0\left(s_{18} - s_{0,H_2}\right) + ex_{ch,H_2} \tag{6.186}$$

$$ex_{19} = h_{19} - h_{0,O_2} - T_0\left(s_{19} - s_{0,O_2}\right) + ex_{ch,O_2} \tag{6.187}$$

$$ex_{20} = h_{20} - h_{0,N_2} - T_0\left(s_{20} - s_{0,N_2}\right) + ex_{ch,N_2} \tag{6.188}$$

$$ex_{21} = h_{21} - h_{0,H_2} - T_0\left(s_{21} - s_{0,H_2}\right) + ex_{ch,H_2} \tag{6.189}$$

$$ex_{22} = h_{22} - h_{0,O_2} - T_0\left(s_{22} - s_{0,O_2}\right) + ex_{ch,O_2} \tag{6.190}$$

$$ex_{23} = h_{23} - h_{0,N_2} - T_0\left(s_{23} - s_{0,N_2}\right) + ex_{ch,N_2} \tag{6.191}$$

$$ex_{24} = h_{24} - h_{0,H_2O} - T_0\left(s_{24} - s_{0,H_2O}\right) + ex_{ch,H_2O} \tag{6.192}$$

The energy and exergy efficiency of the system is the ratio of products to inputs. Included as a product is the net hydrogen production:

$$\eta = \frac{\dot{W}_{Load} + \dot{Q}_{Cold} + \dot{Q}_{Heat} + \dot{Q}_{DHW} + \dot{m}_{H_2}HHV_{H_2}}{\dot{E}_{Wind}} \tag{6.193}$$

$$\psi = \frac{\dot{W}_{Load} + \dot{E}x_{Q,Cold} + \dot{E}x_{Q,Heat} + \dot{E}x_{Q,DHW} + \dot{m}_{H_2}ex_{ch,H_2}}{\dot{E}x_{Wind}} \tag{6.194}$$

where $\dot{W}_{Load}$ denotes the community electrical power demand, $\dot{W}_{Battery}$ the net work added to the battery, and $\dot{E}x_{Wind}$ the exergy of wind.

Table 6.5: Modelling parameters that apply to the wind-hydrogen system.

Parameter	Value	Reference
Anode dry gas mole fraction	0	Ay et al. (2006)
Anode stoichiometry	1.5	Ay et al. (2006)
Anode transfer coefficient	0.5	Ay et al. (2006)
Cathode dry gas mole fraction	3.76	Ay et al. (2006)
Cathode stoichiometry	3	Ay et al. (2006)
Cathode transfer coefficient	1	Ay et al. (2006)
Chemical exergy of hydrogen	118,050 kJ kg^{-1}	Morris and Szargut (1986)
Current density	2 Coulomb cm^{-2} s^{-1}	Ay et al. (2006)
Electrolyzer efficiency	0.75	Harrison and Levene (2008)
Membrane thickness	0.018 cm	Ay et al. (2006)
Operating pressure of fuel cell	300 kPa	Ay et al. (2006)
Radiation heat loss ratio	0.20	Ay et al. (2006)
Temperature of the fuel cell	80°C	Ay et al. (2006)
Utilization ratio of hydrogen	0.8	Ay et al. (2006)
Utilization ratio of oxygen	0.5	Ay et al. (2006)

6.6 Solar-PV-Battery System

A solar-PV-battery system is entirely free of fossil fuels during operation. Much like the wind-battery system, the absence of a fossil-based back-up system means that a very large storage system is required to reliably meet the energy needs of a community. This case study implements a lead-acid battery as the electrical energy storage medium.

6.6.1 System Description

Solar-PV panels that convert direct and indirect solar radiation to electricity are proposed to meet the energy needs of a 50-household community in Ontario. The panels are integrated with a lead-acid battery and heat pump (Figure 6.8) to ensure the community has a reliable supply of energy during periods of low solar activity.

When the power delivered by the PV panels is greater than the load the battery enters a charging mode. When there is unmet demand the battery discharges. The area of the PV system is selected such that the year-end net charge of the battery is positive.

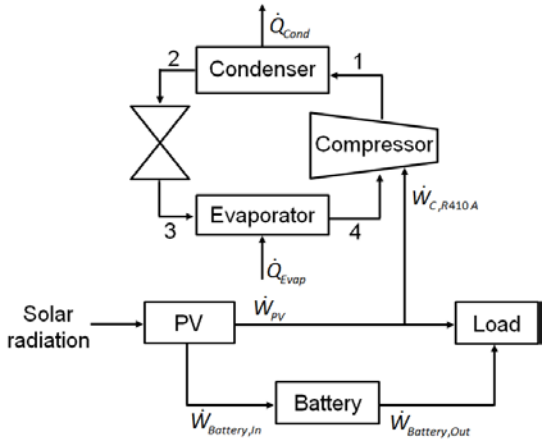

Figure 6.8: General layout of a solar-PV-battery system with an air-source heat pump.

6.6.2 Analysis

A thermodynamic model of the system developed through EES was run for 365 days with the input variables identified in Section 6.1 as well as an additional input variable for solar irradiance. The solar irradiance rate varies over the course of a year as shown in Figure 6.9. The modelling parameters that specifically apply to the solar-PV-battery system are presented in Table 6.7 while lead-acid battery parameters are available in Table 6.4. The following assumptions apply to the system:

- Energy efficiency of a PV cell is constant.
- Charging and discharging efficiencies of the lead-acid battery are constant.
- Fugitive emissions of refrigerant (R-410A) are negligible.

Solar-PV

The solar irradiance available to the city of Toronto can be approximated by a semi-empirical model (Kreith and Kreider, 2011). The direct solar irradiance ($\dot{Q}_{Solar}$) on a tilted plane is a function of the extraterrestrial solar irradiance ($\dot{Q}_{ETR}$), clearness number (Cn), local extinction coefficient (k_c), elevation angle (θ), and incidence angle (ϕ). Thus,

$$\dot{Q}_{Solar} = \dot{Q}_{ETR} Cn \exp(-k_c \sin\theta)\cos\phi \tag{6.195}$$

The angle of incidence is a function of the elevation angle, solar azimuth angle (a_{Solar}), collector azimuth angle (a_{Col}), and collector tilt angle (β). Consequently,

$$\cos\phi = \cos\theta\cos(a_{Solar} - a_{Col})\sin\beta + \sin\theta\cos\beta \tag{6.196}$$

Elevation and solar azimuth angles can be determined from the day of the year, latitude, and longitude of the location. The parameters used to calculate direct solar irradiance and the average monthly ambient temperature in Toronto can be found in Table 6.4. The solar-PV system can be modelled by,

$$\dot{Q}_{Solar} Area_{PV} = \dot{W}_{PV} + \dot{Q}_{Loss,PV} \tag{6.197}$$

$$\eta_{PV} = \frac{\dot{W}_{PV}}{\dot{Q}_{Solar} Area_{PV}} \tag{6.198}$$

$$\frac{\dot{Q}_{Solar}}{T_{Sun}} Area_{PV} + \dot{S}_{G,PV} = \frac{\dot{Q}_{Loss,PV}}{T_{amb}} \tag{6.199}$$

$$\dot{E}x_{Q,Solar} = \dot{W}_{PV} + \dot{E}x_{Q,Loss,PV} + \dot{E}x_{D,PV} \tag{6.200}$$

$$\dot{E}x_{Q,Loss,PV} = \dot{Q}_{Loss,PV}\left(1 - \frac{T_0}{T_{amb}}\right) \tag{6.201}$$

$$\dot{E}x_{Q,Solar} = \dot{Q}_{Solar} Area_{PV}\left[1 - \frac{4}{3}\left(\frac{T_0}{T_{Sun}}\right) + \frac{1}{3}\left(\frac{T_0}{T_{Sun}}\right)^4\right] \tag{6.202}$$

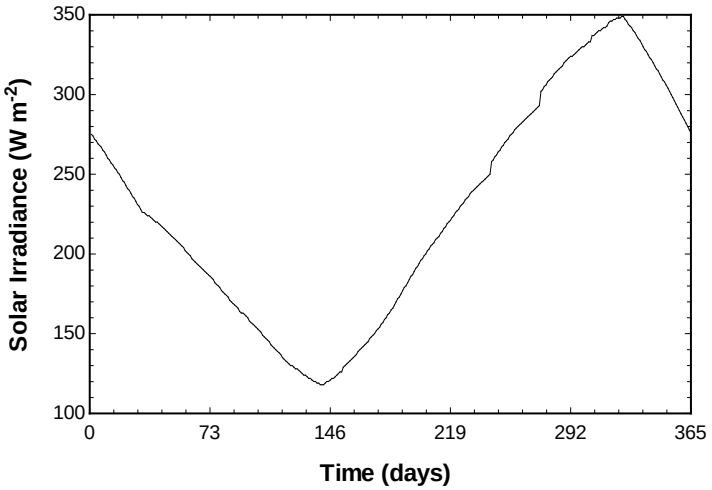

Figure 6.9: Daily average solar irradiance (direct plus diffuse) in Southern Ontario over one year (day "1" corresponds to August 1, 2009).

Table 6.6: Modelling parameters that apply to direct solar irradiance for Toronto, Ontario, Canada.

Month	k_c	Cn	β (°)	a_{Col} (°)	T_{amb} (°C)
January	0.142	0.85	70	0	-6
February	0.144	0.85	60	0	-5
March	0.156	0.85	50	0	0
April	0.180	0.85	30	0	6
May	0.196	0.85	20	0	12
June	0.205	0.85	20	0	17
July	0.207	0.85	20	0	20
August	0.201	0.85	30	0	19
September	0.177	0.85	40	0	15
October	0.160	0.85	60	0	9
November	0.149	0.85	70	0	3
December	0.142	0.85	70	0	-3

Table 6.7: Modelling parameters that apply to the solar-PV-battery system.

Parameter	Value	Reference
Efficiency of a photovoltaic cell	0.15	Kreith and Kreider (2011)
Latitude (Toronto)	43.7°N	Weather Network (2014)
Longitude (Toronto)	79.4°W	Weather Network (2014)
Solar constant	1353 W m^{-2}	Kreith and Kreider (2011)
Solar noon	720 min	Kreith and Kreider (2011)
Temperature of the sun	5778 K	Badescu (2008)
Time zone (eastern)	75°W	Kreith and Kreider (2011)

6.7 Solar-PV-Hydrogen System

An alternative to the battery storage system described in the previous section is a hydrogen-based storage system.

6.7.1 System Description

Solar PV panels that convert solar energy to electricity are proposed to meet the energy needs of a 50-household community in Ontario. The panels are integrated with a hydrogen storage subsystem and heat pump (Figure 6.10) to ensure the community has a reliable supply of energy during periods of low solar activity.

When the power delivered by solar panels is greater than the load, the electrolyzer is activated to charge the hydrogen storage tanks. When there is unmet demand, hydrogen is discharged from storage to the fuel cell. The panel area is selected such that at the end of one year the net change of hydrogen in the storage tanks is positive and the community does not need to import external electrical energy.

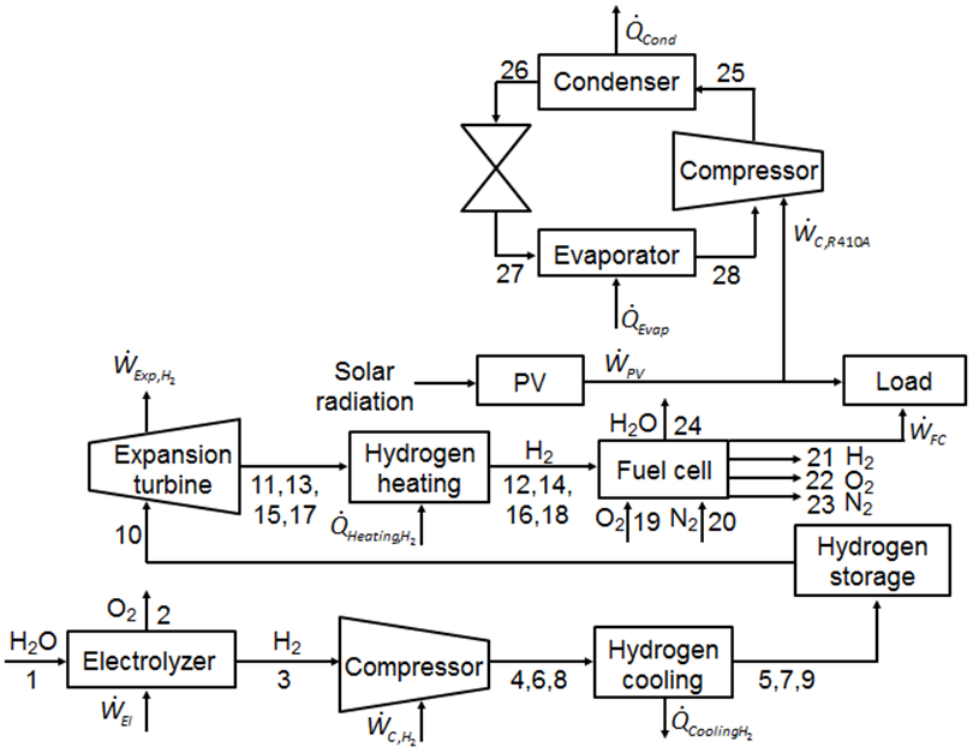

Figure 6.10: General layout of a solar-PV-hydrogen system with an air-source heat pump.

6.7.2 Analysis

A thermodynamic model of the system developed through EES was run for 365 days with the input variables identified in Section 6.1 in addition to solar irradiance. The solar-PV subsystem was described in Section 6.6.2 while the hydrogen storage subsystem was described in Section 6.5.2. The modelling parameters for the hydrogen and solar-PV subsystems are described in Tables 6.5 and 6.7, respectively.

6.8 Solar-PV-Wind-Biomass System

A stand-alone energy system reliant on only one renewable energy source will require a large storage capacity whereas a hybrid system could provide a more reliable supply of energy and mitigate storage requirements. The following case study is a hybrid system that integrates solar, wind, and biomass resources with storage.

6.8.1 System Description

Solar-PV panels, a wind turbine, and anaerobic digestion of biomass are integrated into a hybrid system to meet the heat, cold, and electrical energy needs of a community. The sources are integrated with a hydrogen storage subsystem and a ground-source heat pump (Figure 6.11) to ensure the community has a reliable supply of energy.

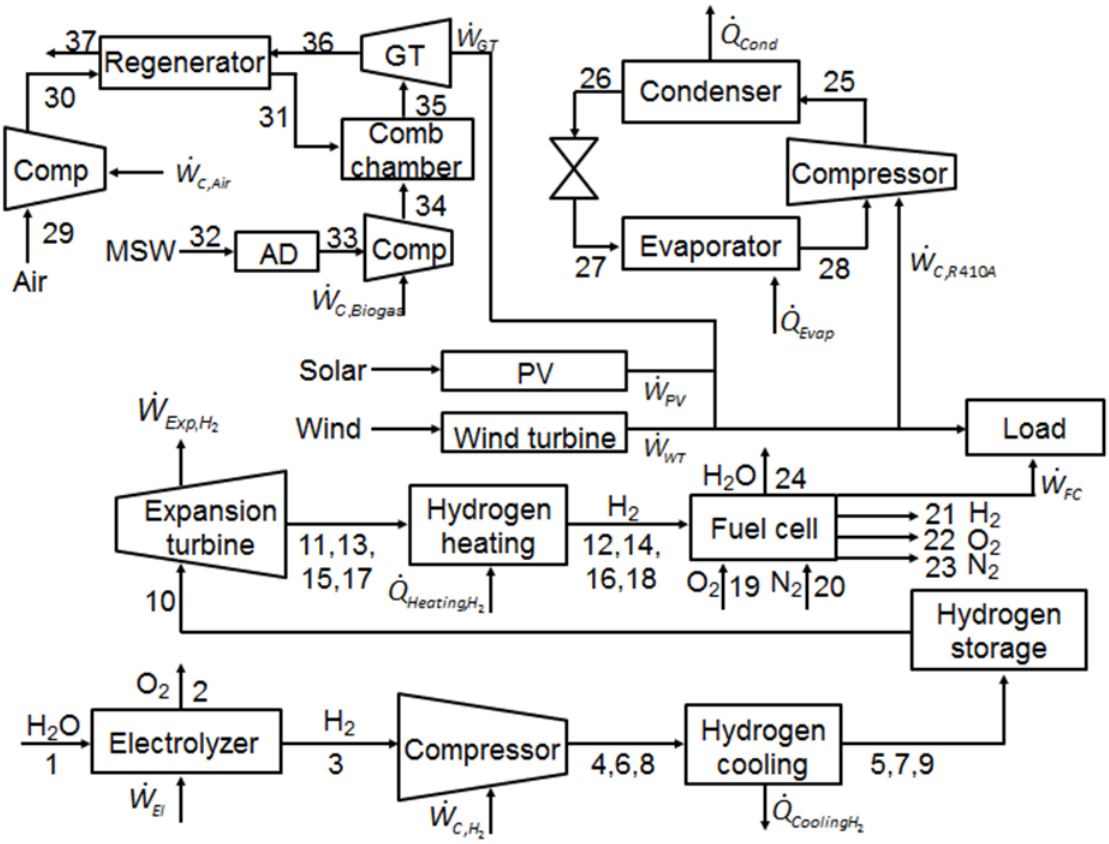

Figure 6.11: General layout of a solar-PV-wind-biomass system with hydrogen-based storage and a ground-source heat pump.

Where there is a surplus of electrical energy available through the contributions of the solar-PV panels, wind turbine, and AD/biogas power generation cycle, the electrolyzer is activated and hydrogen is produced. The hydrogen is then compressed and stored until there is unmet demand, when hydrogen is discharged from storage to produce electricity through a fuel cell.

The ground-source heat pump provides heating and cooling for the community. The advantage to a ground-source heat pump is a smaller temperature difference between the hot and cold reservoirs. In the winter, heat is pumped from the ground and into buildings while the process is reversed in the summer.

Waste biomass is consistently available throughout the year locally as the average person in Ontario produces approximately 1 kg day^{-1} of municipal solid waste (MSW) (Jackson, 1999). Anaerobic digestion of MSW generates a methane-rich biogas and digestate that can be converted to a marketable high-quality humus material via aerobic composting (Kayhanian et al., 2007). The biogas can generate power in an open Brayton cycle with air/exhaust gas as the working fluid. Combustion of biogas generates hot exhaust gases that expand in a gas turbine producing mechanical work. The temperature of the gas at the outlet of the turbine is high enough to preheat fresh incoming compressed air in a regenerator.

6.8.2 Analysis

A thermodynamic model of the system was developed using the input variables described in Section 6.1.2 as well as additional input variables for solar irradiance and wind speed. The components of these systems were described in previous sections.

Most of the material in MSW cannot be converted to biogas. Only the organic fraction of MSW (*OFMSW*) can be converted, exclusive of moisture content (*MC*). Furthermore, it is the biodegradable volatile solids (*BVS*) component of the volatile solids fraction (*VS*) of the dry organic material that can be converted to biogas. A biogas conversion factor (*BGCF*) represents the fraction of biodegradable organic material that forms biogas ($\dot{m}_{BOM}$). This leads to

$$\dot{m}_{BOM} = \dot{m}_{MSW} \times OFMSW \times (1 - MC) \times VS \times BVS \times BGCF \quad (6.203)$$

Biodegradable organic material can be represented chemically by $C_{60}H_{95}O_{38}N$, which can be used to calculate the amount of methane and carbon dioxide produced by anaerobic digestion:

$$C_{60}H_{95}O_{38}N + 18H_2O \rightarrow 32CH_4 + 28CO_2 + NH_3 \quad (6.204)$$

The modelling parameters for wind, hydrogen, and solar-PV subsystems are described in Tables 6.3, 6.5, and 6.7, respectively. The modelling parameters for anaerobic digestion of municipal solid waste are presented in Table 6.8.

Table 6.8: Modelling parameters for anaerobic digestion of MSW.

Parameter	Value	Reference
Biogas conversion factor	0.90	Kayhanian et al. (2007)
Biodegradable volatile solids fraction	0.75	Kayhanian et al. (2007)
Moisture content of MSW	0.20	Kayhanian et al. (2007)
MSW production	1 kg cap^{-1} day^{-1}	Jackson (1999)
Organic fraction of MSW	0.78	Kayhanian et al. (2007)
Volatile solids fraction of MSW	0.835	Kayhanian et al. (2007)

6.9 Solar-Thermal-Wind-Biomass System

The next case study implements an alternative solar energy harvesting technology, which also affects the design of the storage subsystem. It is a hybrid system that integrates solar, wind, and biomass resources with thermal and electrical energy storage technologies.

6.9.1 System Description

Many components comprise the considered solar-thermal-wind-biomass system (Figure 6.12). Solar and wind energy are converted to heat, cold, and electricity to meet the energy demands of the community. MSW from local households is converted to a methane-rich biogas through anaerobic digestion. Variability is managed using thermal and electrical storage technologies. The system will be either in charging or discharging modes depending on the balance between energy demand and supply. Excess supply

from the solar-thermal system charges thermal storage tanks while surplus electricity charges electrical storages.

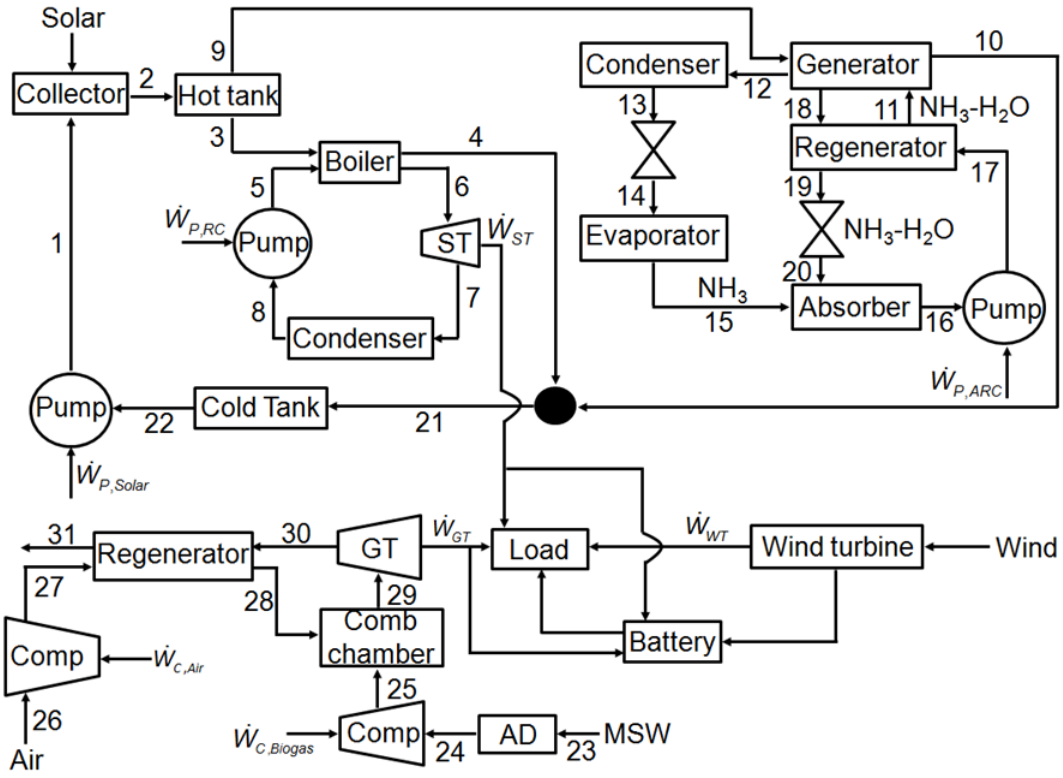

Figure 6.12: General layout of a solar-thermal-wind-biomass system with thermal and electrical energy storage and an absorption chiller.

Direct solar radiation is reflected by parabolic trough collectors to a heat transfer fluid (HTF) circulating through a receiver. The HTF is modelled as Therminol, which has been used in solar-thermal power plants in the past (Kreith and Kreider, 2011). The HTF in a solar-thermal system should be kept in a liquid state, which means that pressurization is required for temperatures above Therminol's normal boiling point of 257°C. Concentration of radiation allows for the temperature of the HTF to increase up to approximately 350°C. The hot HTF can then be used in four ways: 1) space heating, 2) absorption refrigeration, 3) electricity generation, or 4) storage.

The solar-thermal system is the primary source of space heating and cooling for the community. Hot HTF from the receiver or the hot storage tank passes through heat

exchangers to directly provide domestic space heating in the winter or to vaporize and separate the refrigerant (ammonia or NH_3) from the transport medium (water or H_2O) in the generator of an absorption refrigeration cycle in the summer. The NH_3-rich vapour then condenses and flashes via a thermal expansion valve and then evaporates due to the heat collected from households in the community. The weak solution (low in NH_3) leaving the generator preheats the incoming strong solution and flashes via a thermal expansion valve. The NH_3-rich vapour and weak solution recombine to form a strong solution that is pumped and preheated in a heat exchanger.

A power-generating Rankine cycle is only activated when the supply of electricity is insufficient. Hot HTF enters through a steam-generating heat exchanger. The superheated steam drives a turbine that produces mechanical work followed by electricity via an electric generator. The low-pressure steam is condensed and pumped back into the steam generator.

A two-tank direct thermal storage system manages the effects of fluctuations in solar availability. When solar-thermal energy is plentiful, a portion of the circulating HTF is diverted to charge a high-temperature storage tank maintained at 350°C. Charging the hot tank simultaneously discharges the low-temperature tank (250°C). During periods of high demand or low solar and wind availability, hot HTF is discharged from storage, which in turn charges the cold tank.

6.9.2 Analysis

A thermodynamic model of the hybrid system was developed using the EES software. The model was run for 365 days with six different input variables: 1) electricity demand per household (excluding air conditioning), 2) air conditioning demand per household, 3) domestic hot water demand, 4) direct solar irradiance, 5) wind speed, and 6) ambient temperature (Hacatoglu et al., 2013b). The parameters that specifically apply to the solar-thermal system are presented in Table 6.9. The following assumptions apply to the system:

- Compressors, pumps, and turbines are modelled as partially isentropic devices.

- Thermal storage tanks are well insulated with negligible heat loss.
- The temperature of the receiver tube (important for estimating heat loss) is the average of the hot and cold tank temperatures.
- There is some pressure drop across receiver tubes and heat exchangers.
- Specific heat capacity and density of the heat transfer fluid is constant.

Parabolic trough collector and receiver

Direct solar radiation is absorbed by the parabolic trough collector and reflected on to the receiver tubes. The temperature of the heat transfer fluid increases from state 1 to state 2 after leaving the receiver.

$$\dot{m}_1 = \dot{m}_2 \tag{6.205}$$

$$\dot{Q}_{Solar} Area_{PTC} \Gamma - \dot{Q}_{Loss} = \dot{m}_1 C_{P,HTF} \left(T_2 - T_1\right) + V_{HTF} \left(P_2 - P_1\right) \tag{6.206}$$

$$\dot{Q}_{Loss} = U_L Area_R \left(T_R - T_{amb}\right) \tag{6.207}$$

$$U_L = 1.43 - 0.0057\left(T_R - T_{amb}\right) + 0.000046\left(T_R - T_{amb}\right)^2 \tag{6.208}$$

$$CR = \frac{Area_{PTC}}{Area_R} \tag{6.209}$$

$$\frac{\dot{Q}_{Solar} Area_{PTC} \Gamma}{T_{Sun}} + \dot{S}_{G,PTC} = \frac{\dot{Q}_{Loss}}{T_{amb}} + \dot{m}_1 C_{P,HTF} \ln\left(\frac{T_2}{T_1}\right) \tag{6.210}$$

$$\dot{m}_1 ex_1 + \dot{E}x_{Q,Solar} = \dot{m}_2 ex_2 + \dot{E}x_{Q,Loss} + \dot{E}x_{D,PTC} \tag{6.211}$$

$$\dot{E}x_{Q,Solar} = \dot{Q}_{Solar} Area_{PTC} \Gamma \left[1 - \frac{4}{3}\left(\frac{T_0}{T_{Sun}}\right) + \frac{1}{3}\left(\frac{T_0}{T_{Sun}}\right)^4\right] \tag{6.212}$$

$$\dot{E}x_{Q,Loss} = \dot{Q}_{Loss}\left(1 - \frac{T_0}{T_{amb}}\right) \tag{6.213}$$

$$ex_1 = V_{HTF}\left(P_1 - P_0\right) + C_P\left[\left(T_1 - T_0\right) - T_0 \ln\left(\frac{T_1}{T_0}\right)\right] \tag{6.214}$$

$$ex_2 = V_{HTF}\left(P_2 - P_0\right) + C_P\left[\left(T_2 - T_0\right) - T_0 \ln\left(\frac{T_2}{T_0}\right)\right] \tag{6.215}$$

Hot tank

High-temperature HTF from the receiver enters a hot thermal storage tank where it is stored, diverted to a power-generating Rankine cycle, or diverted to an absorption refrigeration cycle.

$$\dot{m}_2 = \dot{m}_3 + \dot{m}_9 + \dot{m}_{HT} \tag{6.216}$$

Boiler

When there is demand for electricity, high-temperature HTF can be used to provide the necessary heat to generate steam in a boiler.

$$\dot{m}_3 = \dot{m}_4 \tag{6.217}$$

$$\dot{m}_5 = \dot{m}_6 \tag{6.218}$$

$$\dot{m}_3 h_3 + \dot{m}_5 h_5 = \dot{m}_4 h_4 + \dot{m}_6 h_6 \tag{6.219}$$

$$\dot{m}_3 s_3 + \dot{m}_5 s_5 + \dot{S}_{G,Boiler} = \dot{m}_4 s_4 + \dot{m}_6 s_6 \tag{6.220}$$

$$\dot{m}_3 ex_3 + \dot{m}_5 ex_5 = \dot{m}_4 ex_4 + \dot{m}_6 ex_6 + \dot{E}x_{D,Boiler} \tag{6.221}$$

$$ex_3 = V_{HTF}\left(P_3 - P_0\right) + C_P\left[\left(T_3 - T_0\right) - T_0 \ln\left(\frac{T_3}{T_0}\right)\right] \tag{6.222}$$

$$ex_4 = V_{HTF}\left(P_4 - P_0\right) + C_P\left[\left(T_4 - T_0\right) - T_0 \ln\left(\frac{T_4}{T_0}\right)\right] \tag{6.223}$$

$$ex_5 = h_5 - h_{0,H_2O} - T_0\left(s_5 - s_{0,H_2O}\right) \tag{6.224}$$

$$ex_6 = h_6 - h_{0,H_2O} - T_0\left(s_6 - s_{0,H_2O}\right) \tag{6.225}$$

Steam turbine

A steam turbine generates work by expanding steam from state 6 to state 7 via a partially isentropic process.

$$\dot{m}_6 = \dot{m}_7 \tag{6.226}$$

$$\dot{m}_6 h_6 = \dot{m}_7 h_7 + \dot{W}_{ST} \tag{6.227}$$

$$\dot{m}_6 h_6 = \dot{m}_7 h_{7,rev} + \dot{W}_{ST,rev} \tag{6.228}$$

$$\eta_{ST} = \frac{\dot{W}_{ST}}{\dot{W}_{ST,rev}} \tag{6.229}$$

$$\dot{m}_6 s_6 + \dot{S}_{G,ST} = \dot{m}_7 s_7 \tag{6.230}$$

$$s_6 = s_{7,rev} \tag{6.231}$$

$$\dot{m}_6 ex_6 + \dot{W}_{ST} = \dot{m}_7 ex_7 + \dot{E}x_{D,ST} \tag{6.232}$$

Condenser

The exhaust from the steam turbine at state 7 is condensed to state 8 in an isobaric condenser.

$$\dot{m}_7 = \dot{m}_8 \tag{6.233}$$

$$\dot{m}_7 h_7 = \dot{m}_8 h_8 + \dot{Q}_{Cond} \tag{6.234}$$

$$\dot{m}_7 s_7 + \dot{S}_{G,Cond} = \dot{m}_8 s_8 + \frac{\dot{Q}_{Cond}}{T_{amb}} \tag{6.235}$$

$$\dot{m}_7 ex_7 = \dot{m}_8 ex_8 + \dot{E}x_{Q,Cond} + \dot{E}x_{D,Cond} \tag{6.236}$$

$$\dot{E}x_{Q,Cond} = \dot{Q}_{Cond}\left(1 - \frac{T_0}{T_{amb}}\right) \tag{6.237}$$

Condensate pump

A pump increases the pressure of the working fluid from state 8 to state 5 and circulates the condensate back to the boiler via a partially isentropic process.

$$\dot{m}_8 h_8 + \dot{W}_P = \dot{m}_5 h_5 \tag{6.238}$$

$$\dot{m}_8 h_8 + \dot{W}_{P,rev} = \dot{m}_5 h_{5,rev} \tag{6.239}$$

$$\eta_P = \frac{\dot{W}_{P,rev}}{\dot{W}_P} \tag{6.240}$$

$$PR = \frac{P_5}{P_8} \tag{6.241}$$

$$\dot{m}_8 s_8 + \dot{S}_{G,P} = \dot{m}_5 s_5 \tag{6.242}$$

$$s_8 = s_{5,rev} \tag{6.243}$$

$$\dot{m}_8 ex_8 + \dot{W}_P = \dot{m}_5 ex_5 + \dot{E}x_{D,P} \tag{6.244}$$

Generator

When there is demand for cooling, high-temperature HTF can be used to provide the necessary heat to the generator in an absorption refrigeration cycle.

$$\dot{m}_9 = \dot{m}_{10} \tag{6.245}$$

$$\dot{m}_{11} = \dot{m}_{12} + \dot{m}_{18} \tag{6.246}$$

$$\dot{m}_9 C_{P,HTF}\left(T_9 - T_{10}\right) + V_{HTF}\left(P_9 - P_{10}\right) + \dot{m}_{11} h_{11} = \dot{m}_{12} h_{12} + \dot{m}_{18} h_{18} \tag{6.247}$$

$$\dot{m}_9 C_{P,HTF} \ln\left(\frac{T_9}{T_{10}}\right) + \dot{m}_{11} s_{11} + \dot{S}_{G,Gen} = \dot{m}_{12} s_{12} + \dot{m}_{18} s_{18} \tag{6.248}$$

$$\dot{m}_9 ex_9 + \dot{m}_{11} ex_{11} = \dot{m}_{10} ex_{10} + \dot{m}_{12} ex_{12} + \dot{m}_{18} ex_{18} + \dot{E}x_{D,Gen} \tag{6.249}$$

Condenser

The NH_3-rich vapour at state 12 enters the condenser and exits at state 13 after rejecting heat to the high-temperature reservoir.

$$\dot{m}_{12} = \dot{m}_{13} \tag{6.250}$$

$$\dot{m}_{12} h_{12} = \dot{m}_{13} h_{13} + \dot{Q}_{Cond,ARC} \tag{6.251}$$

$$\dot{m}_{12} s_{12} + \dot{S}_{G,Cond,ARC} = \dot{m}_{13} s_{13} + \frac{\dot{Q}_{Cond,ARC}}{T_{amb}} \tag{6.252}$$

$$\dot{m}_{12} ex_{12} = \dot{m}_{13} ex_{13} + \dot{E}x_{Q,Cond,ARC} + \dot{E}x_{D,Cond,ARC} \tag{6.253}$$

$$\dot{E}x_{Q,Cond,ARC} = \dot{Q}_{Cond,ARC}\left(1 - \frac{T_0}{T_{amb}}\right) \tag{6.254}$$

Expansion valve 1

The NH_3-rich vapour at state 13 enters the expansion valve and undergoes an isenthalpic flash process that drops its pressure and temperature to state 14.

$$\dot{m}_{13} = \dot{m}_{14} \tag{6.255}$$

$$\dot{m}_{13} h_{13} = \dot{m}_{14} h_{14} \tag{6.256}$$

$$\dot{m}_{13} s_{13} + \dot{S}_{G,EV,1} = \dot{m}_{14} s_{14} \tag{6.257}$$

$$\dot{m}_{13} ex_{13} = \dot{m}_{14} ex_{14} + \dot{E}x_{D,EV,1} \tag{6.258}$$

Evaporator

The evaporator is where the working fluid absorbs heat from the low-temperature reservoir. The temperature of the working fluid therefore increases from state 14 to state 15.

$$\dot{m}_{14} = \dot{m}_{15} \tag{6.259}$$

$$\dot{m}_{14} h_{14} + \dot{Q}_{Evap} = \dot{m}_{15} h_{15} \tag{6.260}$$

$$\dot{m}_{14} s_{14} + \frac{\dot{Q}_{Evap}}{T_{Indoor}} + \dot{S}_{G,Evap} = \dot{m}_{15} s_{15} \tag{6.261}$$

$$\dot{m}_{14} ex_{14} + \dot{E}x_{Q,Evap} = \dot{m}_{15} ex_{15} + \dot{E}x_{D,Evap} \tag{6.262}$$

$$\dot{E}x_{Q,Evap} = \dot{Q}_{Evap}\left(1 - \frac{T_0}{T_{Indoor}}\right) \tag{6.263}$$

Absorber

The NH_3-rich vapour at state 15 dissolves and reacts with the weak NH_3-H_2O solution at state 20 in the absorber. This exothermic reaction yields a strong NH_3-H_2O solution at state 16.

$$\dot{m}_{15} + \dot{m}_{20} = \dot{m}_{16} \tag{6.264}$$

$$\dot{m}_{15} h_{15} + \dot{m}_{20} h_{20} = \dot{m}_{16} h_{16} + \dot{Q}_{Abs} \tag{6.265}$$

$$\dot{m}_{15} s_{15} + \dot{m}_{20} s_{20} + \dot{S}_{G,Abs} = \dot{m}_{16} s_{16} + \frac{\dot{Q}_{Abs}}{T_{lamb}} \tag{6.266}$$

$$\dot{m}_{15} ex_{15} + \dot{m}_{20} ex_{20} = \dot{m}_{16} ex_{16} + \dot{E}x_{Q,Abs} + \dot{E}x_{D,Abs} \tag{6.267}$$

$$\dot{E}x_{Q,Abs} = \dot{Q}_{Abs}\left(1 - \frac{T_0}{T_{amb}}\right) \tag{6.268}$$

Pump

The pump increases the pressure of the strong solution from state 16 to state 17 and feeds the solution to the regenerator via a partially isentropic process.

$$\dot{m}_{16} = \dot{m}_{17} \tag{6.269}$$

$$\dot{m}_{16} h_{16} + \dot{W}_{P,ARC} = \dot{m}_{17} h_{17} \tag{6.270}$$

$$\dot{m}_{16}h_{16} + \dot{W}_{P,ARC,rev} = \dot{m}_{17}h_{17,rev} \tag{6.271}$$

$$\eta_P = \frac{\dot{W}_{P,ARC,rev}}{\dot{W}_{P,ARC}} \tag{6.272}$$

$$\dot{m}_{16}s_{16} + \dot{S}_{G,P,ARC} = \dot{m}_{17}s_{17} \tag{6.273}$$

$$s_{16} = s_{17,rev} \tag{6.274}$$

$$\dot{m}_{16}ex_{16} + \dot{W}_{P,ARC} = \dot{m}_{17}ex_{17} + \dot{E}x_{D,P,ARC} \tag{6.275}$$

Regenerator

The regenerator enables heat transfer between the strong solution from the pump and the weak solution from the generator.

$$\dot{m}_{17} = \dot{m}_{11} \tag{6.276}$$

$$\dot{m}_{18} = \dot{m}_{19} \tag{6.277}$$

$$\dot{m}_{17}h_{17} + \dot{m}_{18}h_{18} = \dot{m}_{11}h_{11} + \dot{m}_{19}h_{19} \tag{6.278}$$

$$\dot{m}_{17}s_{17} + \dot{m}_{18}s_{18} + \dot{S}_{G,Reg} = \dot{m}_{11}s_{11} + \dot{m}_{19}s_{19} \tag{6.279}$$

$$\dot{m}_{17}ex_{17} + \dot{m}_{18}ex_{18} = \dot{m}_{11}ex_{11} + \dot{m}_{19}ex_{19} + \dot{E}x_{D,Reg} \tag{6.280}$$

Expansion valve 2

The weak NH_3-H_2O solution at state 19 enters the expansion valve and undergoes an isenthalpic flash process that drops its pressure and temperature to state 20.

$$\dot{m}_{19}h_{19} = \dot{m}_{20}h_{20} \tag{6.281}$$

$$\dot{m}_{19}s_{19} + \dot{S}_{G,EV,2} = \dot{m}_{20}s_{20} \tag{6.282}$$

$$\dot{m}_{19}ex_{19} = \dot{m}_{20}ex_{20} + \dot{E}x_{D,EV,2} \tag{6.283}$$

Efficiency

The system exergy efficiency (ψ) is the ratio of total exergy outputs to total exergy inputs. Therefore,

$$\psi = \frac{\dot{W}_{Load} + \dot{E}x_{Q,Evap} + \dot{E}x_{Q,SH} + \dot{m}_{In}^{HT}ex_{HT} + \dot{m}_{In}^{CT}ex_{CT}}{\dot{E}x_{Q,Solar} + \dot{E}x_{Wind} + \dot{m}_{Out}^{HT}ex_{HT} + \dot{m}_{Out}^{CT}ex_{CT} + \dot{m}_{MSW}ex_{MSW}} \tag{6.284}$$

where $\dot{W}_{Load}$ denotes the community electrical power demand, $\dot{E}x_{Q,Evap}$ the rate thermal exergy needs to be removed from community households, $\dot{E}x_{Q,SH}$ the thermal exergy

rate of space heating, $\dot{m}_{In}^{HT}$ the mass flow rate into the hot tank, ex_{HT} the specific physical exergy of high-temperature heat transfer fluid, $\dot{m}_{In}^{CT}$ the mass flow rate into the cold tank, and ex_{CT} the specific physical exergy of low-temperature heat transfer fluid.

Table 6.9: Modelling parameters that apply to the solar-thermal-wind-biomass system.

Parameter	Value	Reference
Absorbance factor	0.80	Romero-Alvarez and Zarza (2007)
Concentration ratio	30	Kreith and Kreider (2011)
Heat capacity of Therminol	2.3 kJ kg^{-1} K^{-1}	Romero-Alvarez and Zarza (2007)
Pressure of HTF in receiver	1000 kPa	Kreith and Kreider (2011)
Specific volume of Therminol	0.0012 m^3 kg^{-1}	Romero-Alvarez and Zarza (2007)
Temperature of cold tank	250°C	Kreith and Kreider (2011)
Temperature of hot tank	350°C	Kreith and Kreider (2011)

6.10 Geothermal-Biomass System

Enhanced geothermal systems are seen as a promising option to reduce the carbon intensity of base load power (Nathwani and Blackstock, 2012). Enhanced geothermal systems are not dependent on naturally-occurring geothermal reservoirs and can be engineered by hydraulic stimulation to enhance the permeability of the reservoir and create sufficient connectivity for a heat transfer fluid (Beckers et al., 2014). Another benefit is that enhanced geothermal systems do not require energy storage. The technology has not yet been commercialized but the size of the resource base and its widespread availability offers great potential (Tester et al., 2006).

6.10.1 System Description

A geothermal system that extracts heat from the earth as a source of energy is proposed to meet the energy needs of a 50-household community in Ontario. The geothermal system is integrated with district heating and an absorption refrigeration cycle (Figure 6.13) to ensure the community has a reliable supply of energy.

Geofluid is extracted at state 1 at a wellhead temperature and pressure of 200°C and 1600 kPa. The geofluid is then pumped to one of three separate subsystems – a flash

steam power plant and organic Rankine cycle, an absorption refrigeration cycle, or a district heating network.

To generate power, the geofluid is first pumped to an expansion valve, where it flashes and separates into vapour and liquid components. The vapour fraction of the geofluid enters a steam turbine at state 5, where it generates work and is then condensed and reinjected into the geothermal reservoir. The hot liquid fraction leaves the separation chamber at state 8 and enters the bottoming cycle of the flash-steam power plant. The liquid geofluid transfers heat to an organic working fluid (n-pentane) in the evaporator and leaves at state 9. It then combines with another stream at state 17 to be used in a district heating network.

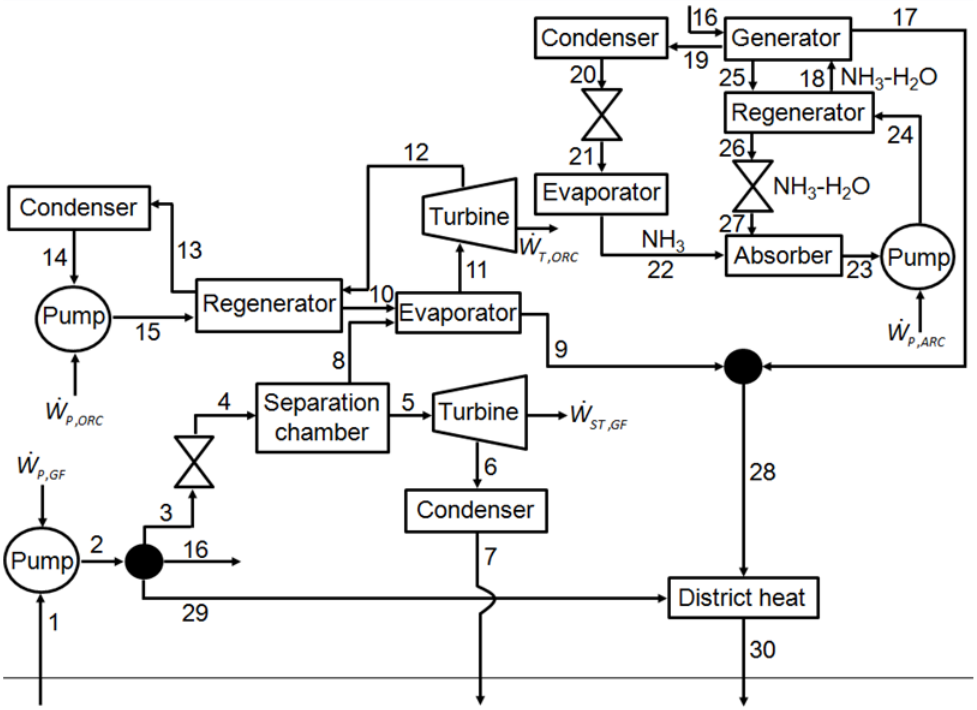

Figure 6.13: General layout of a geothermal system with district heating and an absorption refrigeration cycle.

The vaporized organic working fluid leaves the evaporator at state 11 and expands in a work-generating turbine. The working fluid then preheats the incoming stream at state 15 to state 16 and exits the regenerator to be condensed and recirculated through the cycle.

6.10.2 Analysis

A thermodynamic model of the system was developed using the EES software. The model was run for 365 days with four different input variables: 1) electricity demand per household (excluding air conditioning), 2) air conditioning demand per household, 3) domestic hot water demand, and 4) ambient temperature. The modelling parameters that specifically apply to the geothermal-biomass system are presented in Table 6.10. The following assumptions apply to the system:

- The wellhead temperature and pressure of the geofluid does not decrease over the life cycle of the system.
- On-demand supply of geofluid at wellhead conditions.
- Compressors, pumps, and turbines are modelled as partially isentropic devices.

Geofluid pump

A pump draws hot geofluid from the production well at state 1 and increases its pressure and temperature to state 2 via a partially isentropic process.

$$\dot{m}_1 = \dot{m}_2 \tag{6.285}$$

$$\dot{m}_1 h_1 + \dot{W}_{P,GF} = \dot{m}_2 h_2 \tag{6.286}$$

$$\dot{m}_1 h_1 + \dot{W}_{P,GF,rev} = \dot{m}_2 h_{2,rev} \tag{6.287}$$

$$\eta_P = \frac{\dot{W}_{P,GF,rev}}{\dot{W}_{P,GF}} \tag{6.288}$$

$$PR_{GF} = \frac{P_2}{P_1} \tag{6.289}$$

$$\dot{m}_1 s_1 + \dot{S}_{G,P,GF} = \dot{m}_2 s_2 \tag{6.290}$$

$$s_1 = s_{2,rev} \tag{6.291}$$

$$\dot{m}_1 ex_1 + \dot{W}_{P,GF} = \dot{m}_2 ex_2 + \dot{E}x_{D,P,GF} \tag{6.292}$$

Geofluid separation

The geofluid at state 2 is separated into three different streams. The stream at state 3 produces power in a flash-steam power plant and an organic Rankine cycle. The stream

at state 16 drives the absorption chiller, which provides cooling to the community. The stream at state 29 supplements the community's district heating system.

$$\dot{m}_2 = \dot{m}_3 + \dot{m}_{16} + \dot{m}_{29} \tag{6.293}$$

Expansion valve

The expansion valve is modelled as an isenthalpic process, where the geofluid is flashed to a liquid-vapour mixture.

$$\dot{m}_3 = \dot{m}_4 \tag{6.294}$$

$$\dot{m}_3 h_3 = \dot{m}_4 h_4 \tag{6.295}$$

$$\dot{m}_3 s_3 + \dot{S}_{G,EV,GF} = \dot{m}_4 s_4 \tag{6.296}$$

$$\dot{m}_3 ex_3 = \dot{m}_4 ex_4 + \dot{E}x_{D,EV,GF} \tag{6.297}$$

Separation chamber

The separation chamber separates the liquid geofluid from the vapour. The quality of geofluid at state 5 is zero (i.e., pure vapour) while the quality at state 8 is zero (i.e., pure liquid).

$$\dot{m}_4 = \dot{m}_5 + \dot{m}_8 \tag{6.298}$$

$$\dot{m}_4 h_4 = \dot{m}_5 h_5 + \dot{m}_8 h_8 \tag{6.299}$$

$$\dot{m}_4 s_4 + \dot{S}_{G,Sep,GF} = \dot{m}_5 s_5 + \dot{m}_8 s_8 \tag{6.300}$$

$$\dot{m}_4 ex_4 = \dot{m}_5 ex_5 + \dot{m}_8 ex_8 + \dot{E}x_{D,Sep,GF} \tag{6.301}$$

Steam turbine

A steam turbine generates work by expanding the vapour-phase geofluid from state 5 to state 6 via a partially isentropic process.

$$\dot{m}_5 = \dot{m}_6 \tag{6.302}$$

$$\dot{m}_5 h_5 = \dot{m}_6 h_6 + \dot{W}_{ST,GF} \tag{6.303}$$

$$\dot{m}_5 h_5 = \dot{m}_6 h_{6,rev} + \dot{W}_{ST,GF,rev} \tag{6.304}$$

$$\eta_{ST} = \frac{\dot{W}_{ST,GF}}{\dot{W}_{ST,GF,rev}} \tag{6.305}$$

$$\dot{m}_5 s_5 + \dot{S}_{G,ST,GF} = \dot{m}_6 s_6 \tag{6.306}$$

$$s_5 = s_{6,rev} \tag{6.307}$$

$$\dot{m}_5 ex_5 + \dot{W}_{ST,GF} = \dot{m}_6 ex_6 + \dot{E}x_{D,ST,GF} \tag{6.308}$$

Condenser

Geofluid at state 6 is condensed to state 7 in an isobaric condenser and reinjected back into the geothermal reservoir.

$$\dot{m}_6 = \dot{m}_7 \tag{6.309}$$

$$\dot{m}_6 h_6 = \dot{m}_7 h_7 + \dot{Q}_{Cond,GF} \tag{6.310}$$

$$\dot{m}_6 s_6 + \dot{S}_{G,Cond,GF} = \dot{m}_7 s_7 + \frac{\dot{Q}_{Cond,GF}}{T_{amb}} \tag{6.311}$$

$$\dot{m}_6 ex_6 = \dot{m}_7 ex_7 + \dot{E}x_{Q,Cond,GF} + \dot{E}x_{D,Cond,GF} \tag{6.312}$$

$$\dot{E}x_{Q,Cond,GF} = \dot{Q}_{Cond,GF}\left(1 - \frac{T_0}{T_{amb}}\right) \tag{6.313}$$

Evaporator

The liquid-phase geofluid at state 8 is cooled to state 9 in an isobaric evaporator, where it raises the temperature of an organic working fluid from state 10 to state 11.

$$\dot{m}_8 = \dot{m}_9 \tag{6.314}$$

$$\dot{m}_{10} = \dot{m}_{11} \tag{6.315}$$

$$\dot{m}_8 h_8 + \dot{m}_{10} h_{10} = \dot{m}_9 h_9 + \dot{m}_{11} h_{11} \tag{6.316}$$

$$\dot{m}_8 s_8 + \dot{m}_{10} s_{10} + \dot{S}_{G,Evap,ORC} = \dot{m}_9 s_9 + \dot{m}_{11} s_{11} \tag{6.317}$$

$$\dot{m}_8 ex_8 + \dot{m}_{10} ex_{10} = \dot{m}_9 ex_9 + \dot{m}_{11} ex_{11} + \dot{E}x_{D,Evap,ORC} \tag{6.318}$$

Turbine

A turbine generates work by expanding the organic working fluid from state 11 to state 12 via a partially isentropic process.

$$\dot{m}_{11} = \dot{m}_{12} \tag{6.319}$$

$$\dot{m}_{11} h_{11} = \dot{m}_{12} h_{12} + \dot{W}_{T,ORC} \tag{6.320}$$

$$\dot{m}_{11} h_{11} = \dot{m}_{12} h_{12,rev} + \dot{W}_{T,ORC,rev} \tag{6.321}$$

$$\eta_T = \frac{\dot{W}_{T,ORC}}{\dot{W}_{T,ORC,rev}} \tag{6.322}$$

$$\dot{m}_{11} s_{11} + \dot{S}_{G,T,ORC} = \dot{m}_{12} s_{12} \tag{6.323}$$

$$s_{11} = s_{12,rev} \tag{6.324}$$

$$\dot{m}_{11} ex_{11} + \dot{W}_{T,ORC} = \dot{m}_{12} ex_{12} + \dot{E}x_{D,T,ORC} \tag{6.325}$$

Regenerator

Hot organic working fluid enters the regenerator at state 12 and leaves at a lower temperature at state 13 while colder organic working fluid enters at state 15 and exits at a higher temperature at state 10.

$$\dot{m}_{12} = \dot{m}_{13} \tag{6.326}$$

$$\dot{m}_{15} = \dot{m}_{10} \tag{6.327}$$

$$\dot{m}_{12} h_{12} + \dot{m}_{15} h_{15} = \dot{m}_{13} h_{13} + \dot{m}_{10} h_{10} \tag{6.328}$$

$$\dot{m}_{12} s_{12} + \dot{m}_{15} s_{15} + \dot{S}_{G,Reg,ORC} = \dot{m}_{13} s_{13} + \dot{m}_{10} s_{10} \tag{6.329}$$

$$\dot{m}_{12} ex_{12} + \dot{m}_{15} ex_{15} = \dot{m}_{13} ex_{13} + \dot{m}_{10} ex_{10} + \dot{E}x_{D,Reg,ORC} \tag{6.330}$$

Condenser

Organic working fluid at state 13 is condensed to state 14 in an isobaric condenser.

$$\dot{m}_{13} = \dot{m}_{14} \tag{6.331}$$

$$\dot{m}_{13} h_{13} = \dot{m}_{14} h_{14} + \dot{Q}_{Cond,ORC} \tag{6.332}$$

$$\dot{m}_{13} s_{13} + \dot{S}_{G,Cond,ORC} = \dot{m}_{14} s_{14} + \frac{\dot{Q}_{Cond,ORC}}{T_{amb}} \tag{6.333}$$

$$\dot{m}_{13} ex_{13} = \dot{m}_{14} ex_{14} + \dot{E}x_{Q,Cond,ORC} + \dot{E}x_{D,Cond,ORC} \tag{6.334}$$

$$\dot{E}x_{Q,Cond,ORC} = \dot{Q}_{Cond,ORC}\left(1 - \frac{T_0}{T_{amb}}\right) \tag{6.335}$$

Condensate pump

The condensate of the organic Rankine cycle at state 14 is pumped to a higher pressure at state 15 via a partially isentropic process.

$$\dot{m}_{14} = \dot{m}_{15} \tag{6.336}$$

$$\dot{m}_{14}h_{14} + \dot{W}_{P,ORC} = \dot{m}_{15}h_{15} \tag{6.337}$$

$$\dot{m}_{14}h_{14} + \dot{W}_{P,ORC,rev} = \dot{m}_{15}h_{15,rev} \tag{6.338}$$

$$\eta_P = \frac{\dot{W}_{P,ORC,rev}}{\dot{W}_{P,ORC}} \tag{6.339}$$

$$\dot{m}_{14}s_{14} + \dot{S}_{G,P,ORC} = \dot{m}_{15}s_{15} \tag{6.340}$$

$$s_{14} = s_{15,rev} \tag{6.341}$$

$$\dot{m}_{14}ex_{14} + \dot{W}_{P,ORC} = \dot{m}_{15}ex_{15} + \dot{E}x_{D,P,ORC} \tag{6.342}$$

Generator

Hot geofluid enters the generator at state 16 and leaves at a lower temperature at state 17. A mixture of NH_3-H_2O enters the generator at state 18 and exits as an ammonia-rich vapour at state 19 and a weak NH_3-H_2O mixture at state 25.

$$\dot{m}_{16} = \dot{m}_{17} \tag{6.343}$$

$$\dot{m}_{18} = \dot{m}_{19} + \dot{m}_{25} \tag{6.344}$$

$$\dot{m}_{16}h_{16} + \dot{m}_{18}h_{18} = \dot{m}_{17}h_{17} + \dot{m}_{19}h_{19} + \dot{m}_{25}h_{25} \tag{6.345}$$

$$\dot{m}_{16}s_{16} + \dot{m}_{18}s_{18} + \dot{S}_{G,Gen} = \dot{m}_{17}s_{17} + \dot{m}_{19}s_{19} + \dot{m}_{25}s_{25} \tag{6.346}$$

$$\dot{m}_{16}ex_{16} + \dot{m}_{18}ex_{18} = \dot{m}_{17}ex_{17} + \dot{m}_{19}ex_{19} + \dot{m}_{25}ex_{25} + \dot{E}x_{D,Gen} \tag{6.347}$$

Condenser

Organic working fluid at state 13 is condensed to state 14 in an isobaric condenser.

$$\dot{m}_{13} = \dot{m}_{14} \tag{6.348}$$

$$\dot{m}_{13}h_{13} = \dot{m}_{14}h_{14} + \dot{Q}_{Cond,ORC} \tag{6.349}$$

$$\dot{m}_{13}s_{13} + \dot{S}_{G,Cond,ORC} = \dot{m}_{14}s_{14} + \frac{\dot{Q}_{Cond,ORC}}{T_{amb}} \tag{6.350}$$

$$\dot{m}_{13}ex_{13} = \dot{m}_{14}ex_{14} + \dot{E}x_{Q,Cond,ORC} + \dot{E}x_{D,Cond,ORC} \tag{6.351}$$

$$\dot{E}x_{Q,Cond,ORC} = \dot{Q}_{Cond,ORC}\left(1 - \frac{T_0}{T_{amb}}\right) \tag{6.352}$$

Table 6.10: Modelling parameters that apply to the geothermal-biomass system (DiPippo, 2008).

Parameter	Value
Geothermal gradient	30°C km^{-1}
Pressure of flash tank	500 kPa
Pressure ratio of geofluid pump	1.5
Wellhead pressure of geofluid	1600 kPa
Wellhead temperature of geofluid	200°C

6.11 Nuclear-Based System

The last case study is a nuclear-based system. Although nuclear energy is more commonly associated with base load, utility-scale power, there is growing interest in the benefits provided by small-to-medium sized nuclear reactors such as construction logistics, plant safety, operational flexibilities, and plant economics (Carelli et al., 2010; Ingersoll, 2009).

6.11.1 System Description

Nuclear power plants are similar to traditional thermal generating stations (e.g., coal-fired power plants) in that they produce electricity through steam-driven thermodynamic cycles. Unlike traditional fossil-fired power plants reliant on combustion, nuclear reactors produce steam through the heat released during fission (Michaelides, 2012).

There are many different types and configurations of nuclear reactors. This case study is of a light water reactor, which uses common water as the fuel moderator and coolant. A subset of light water reactors are pressurized water reactors, where the coolant always remains in the liquid phase (Michaelides, 2012). The coolant in the primary loop transfers energy via a steam generator to the working fluid in the secondary, power-generating loop. The exhaust steam from the secondary loop drives a district heating system that distributes heat to the community. The electricity generated drives a vapour-compression refrigeration cycle that delivers cooling services to the community. The design of the nuclear-based system is illustrated in Figure 6.14.

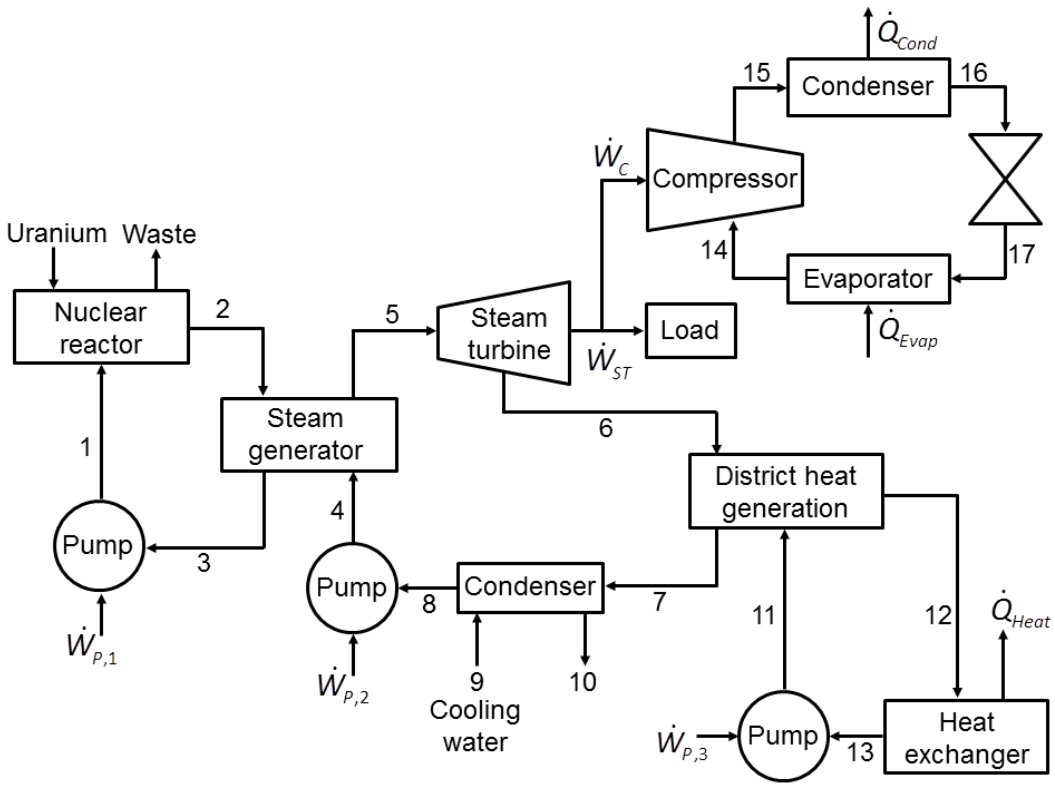

Figure 6.14: General layout of a nuclear-based system with district heating and a refrigeration cycle.

6.11.2 Analysis

A thermodynamic model of the system was developed using the EES software. The model was run for 365 days with four different input variables: 1) electricity demand per household (excluding air conditioning), 2) air conditioning demand per household, 3) domestic hot water demand, and 4) ambient temperature. The modelling parameters that specifically apply to the nuclear-based system are presented in Table 6.11. The following assumptions apply to the system:

- Nuclear reactor assumed to be a source of high-temperature heat.
- Compressors, pumps, and turbines are modelled as partially isentropic devices.
- Pressure drop across heat exchangers.

Nuclear reactor

Light water reactors use common water as the fuel moderator. In pressurized water reactors, high-pressure water enters the nuclear reactor at state 1 and leaves at a higher temperature at state 2.

$$\dot{m}_1 = \dot{m}_2 \tag{6.353}$$

$$\dot{m}_1 h_1 + \dot{Q}_{Nuclear} = \dot{m}_2 h_2 \tag{6.354}$$

$$\dot{m}_1 s_1 + \frac{\dot{Q}_{Nuclear}}{T_{Nuclear}} + \dot{S}_{G,Nuclear} = \dot{m}_2 s_2 \tag{6.355}$$

$$\dot{m}_1 ex_1 + \dot{E}x_{Q,Nuclear} = \dot{m}_2 ex_2 + \dot{E}x_{D,Nuclear} \tag{6.356}$$

$$\dot{E}x_{Q,Nuclear} = \dot{Q}_{Nuclear}\left(1 - \frac{T_0}{T_{Nuclear}}\right) \tag{6.357}$$

Steam generator

High-temperature pressurized water at state 2 enters a steam generator and exits at a lower temperature at state 3. The heat transferred converts saturated water at state 4 to steam at state 5.

$$\dot{m}_2 = \dot{m}_3 \tag{6.358}$$

$$\dot{m}_4 = \dot{m}_5 \tag{6.359}$$

$$\dot{m}_2 h_2 + \dot{m}_4 h_4 = \dot{m}_3 h_3 + \dot{m}_5 h_5 \tag{6.360}$$

$$\dot{m}_2 s_2 + \dot{m}_4 s_4 + \dot{S}_{G,SG} = \dot{m}_3 s_3 + \dot{m}_5 s_5 \tag{6.361}$$

$$\dot{m}_2 ex_2 + \dot{m}_4 ex_4 = \dot{m}_3 ex_3 + \dot{m}_5 ex_5 + \dot{E}x_{D,SG} \tag{6.362}$$

Coolant pump

Pressurized cooling water at state 3 is circulated from the steam generator to the nuclear reactor at state 1 by the coolant pump. The pump is modelled as a partially isentropic device.

$$\dot{m}_3 h_3 + \dot{W}_{P,1} = \dot{m}_1 h_1 \tag{6.363}$$

$$\dot{m}_3 h_3 + \dot{W}_{P,1,rev} = \dot{m}_1 h_{1,rev} \tag{6.364}$$

$$\eta_P = \frac{\dot{W}_{P,1,rev}}{\dot{W}_{P,1}} \tag{6.365}$$

$$\dot{m}_3 s_3 + \dot{S}_{G,P,1} = \dot{m}_1 s_1 \tag{6.366}$$

$$s_3 = s_{1,rev} \tag{6.367}$$

$$\dot{m}_3 ex_3 + \dot{W}_{P,1} = \dot{m}_1 ex_1 + \dot{E}x_{D,P,1} \tag{6.368}$$

Steam turbine

A steam turbine generates work by expanding the steam from state 5 to state 6 via a partially isentropic process.

$$\dot{m}_5 = \dot{m}_6 \tag{6.369}$$

$$\dot{m}_5 h_5 = \dot{m}_6 h_6 + \dot{W}_{ST} \tag{6.370}$$

$$\dot{m}_5 h_5 = \dot{m}_6 h_{6,rev} + \dot{W}_{ST,rev} \tag{6.371}$$

$$\eta_{ST} = \frac{\dot{W}_{ST}}{\dot{W}_{ST,rev}} \tag{6.372}$$

$$\dot{m}_5 s_5 + \dot{S}_{G,ST} = \dot{m}_6 s_6 \tag{6.373}$$

$$s_5 = s_{6,rev} \tag{6.374}$$

$$\dot{m}_5 ex_5 + \dot{W}_{ST} = \dot{m}_6 ex_6 + \dot{E}x_{D,ST} \tag{6.375}$$

District heat generation

Exhaust from the steam turbine at state 6 partially condenses in a heat exchanger to state 7 to generate hot water for the district heating system. Water at state 11 is heated to the distribution temperature at state 12.

$$\dot{m}_6 = \dot{m}_7 \tag{6.376}$$

$$\dot{m}_{11} = \dot{m}_{12} \tag{6.377}$$

$$\dot{m}_6 h_6 + \dot{m}_{11} h_{11} = \dot{m}_7 h_7 + \dot{m}_{12} h_{12} \tag{6.378}$$

$$\dot{m}_6 s_6 + \dot{m}_{11} s_{11} + \dot{S}_{G,DH} = \dot{m}_7 s_7 + \dot{m}_{12} s_{12} \tag{6.379}$$

$$\dot{m}_6 ex_6 + \dot{m}_{11} ex_{11} = \dot{m}_7 ex_7 + \dot{m}_{12} ex_{12} + \dot{E}x_{D,DH} \tag{6.380}$$

Condenser

After producing hot water for the district heating system, the exhaust steam at state 7 is condensed to a saturated liquid at state 8 in an isobaric condenser. Cooling water at state 9 exits the condenser at a slightly higher temperature at state 10.

$$\dot{m}_7 = \dot{m}_8 \tag{6.381}$$

$$\dot{m}_9 = \dot{m}_{10} \tag{6.382}$$

$$\dot{m}_7 h_7 + \dot{m}_9 h_9 = \dot{m}_8 h_8 + \dot{m}_{10} h_{10} \tag{6.383}$$

$$\dot{m}_7 s_7 + \dot{m}_9 s_9 + \dot{S}_{G,Cond} = \dot{m}_8 s_8 + \dot{m}_{10} s_{10} \tag{6.384}$$

$$\dot{m}_7 ex_7 + \dot{m}_9 ex_9 = \dot{m}_8 ex_8 + \dot{m}_{10} ex_{10} + \dot{E}x_{D,Cond} \tag{6.385}$$

Condensate pump

Condensate at state 8 is circulated back to the steam generator at state 4 by the condensate pump. The pump is modelled as a partially isentropic device.

$$\dot{m}_8 h_8 + \dot{W}_{P,2} = \dot{m}_4 h_4 \tag{6.386}$$

$$\dot{m}_8 h_8 + \dot{W}_{P,2,rev} = \dot{m}_4 h_{4,rev} \tag{6.387}$$

$$\eta_P = \frac{\dot{W}_{P,2,rev}}{\dot{W}_{P,2}} \tag{6.388}$$

$$\dot{m}_8 s_8 + \dot{S}_{G,P,2} = \dot{m}_4 s_4 \tag{6.389}$$

$$s_8 = s_{4,rev} \tag{6.390}$$

$$\dot{m}_8 ex_8 + \dot{W}_{P,2} = \dot{m}_4 ex_4 + \dot{E}x_{D,P,2} \tag{6.391}$$

Heat exchanger

Hot water at state 12 is circulated through the heat distribution grid to provide district heating to the community. The water leaves the distribution grid at state 13.

$$\dot{m}_{12} = \dot{m}_{13} \tag{6.392}$$

$$\dot{m}_{12} h_{12} = \dot{m}_{13} h_{13} + \dot{Q}_{Heating} \tag{6.393}$$

$$\dot{m}_{12} s_{12} + \dot{S}_{G,Heating} = \dot{m}_{13} s_{13} + \frac{\dot{Q}_{Heating}}{T_{DH}} \tag{6.394}$$

$$\dot{m}_{12} ex_{12} = \dot{m}_{13} ex_{13} + \dot{E}x_{Q,Heating} + \dot{E}x_{D,Heating} \tag{6.395}$$

$$\dot{E}x_{Q,Heating} = \dot{Q}_{Heating}\left(1 - \frac{T_0}{T_{DH}}\right) \tag{6.396}$$

District heating pump

Water at state 13 is circulated back to the steam generator at state 11 by the district heating pump. The pump is modelled as a partially isentropic device.

$$\dot{m}_{13} h_{13} + \dot{W}_{P,3} = \dot{m}_{11} h_{11} \tag{6.397}$$

$$\dot{m}_{13} h_{13} + \dot{W}_{P,3,rev} = \dot{m}_{11} h_{11,rev} \tag{6.398}$$

$$\eta_P = \frac{\dot{W}_{P,3,rev}}{\dot{W}_{P,3}} \tag{6.399}$$

$$\dot{m}_{13} s_{13} + \dot{S}_{G,P,3} = \dot{m}_{11} s_{11} \tag{6.400}$$

$$s_{13} = s_{11,rev} \tag{6.401}$$

$$\dot{m}_{13} ex_{13} + \dot{W}_{P,3} = \dot{m}_{11} ex_{11} + \dot{E}x_{D,P,3} \tag{6.402}$$

Table 6.11: Modelling parameters that apply to the nuclear-based system.

Parameter	Value	Reference
Heat generated by fission of natural uranium	160 GJ kg^{-1}	Touran (2008)
Nuclear exergy of natural uranium	584 GJ kg^{-1}	Szargut (2005)
Pressure of coolant	15 MPa	Buongiorno (2010)
Pressure of Rankine cycle working fluid	6.2 MPa	Buongiorno (2010)
Temperature of coolant entering reactor	275°C	Buongiorno (2010)
Temperature of coolant leaving reactor	315°C	Buongiorno (2010)
Temperature of water entering steam generator	220°C	Buongiorno (2010)

Chapter 7 : Results and Discussion

This chapter presents the results of analysis related to weighting factors and the aforementioned case studies. Also included is a discussion of the results.

7.1 Weighting Factors

The importance coefficients and trade-off factors of sub-indicators and category indicators are determined based on the approach described in Chapter 4. Scores are assigned to each sub-indicator on a scale of 1-5 ("very unimportant" to "very important") for time, space, and receptor criteria to evaluate relative importance. Trade-off factors are determined through pair-wise comparisons of sub-indicators based on the aforementioned scores.

7.1.1 ER

The ER category consists of energy- and exergy-related sub-indicators. The relative importance of each is presented in Table 7.1.

Table 7.1: Evaluation of the relative importance of the EnER and ExER sub-indicators within the ER category indicator.

Perspective	Criteria	EnER	ExER
Individualist	Time	-	3
	Space	-	3
	Receptor	-	4
	Sum	-	10
	Importance	**-**	**1.00**
Egalitarian	Time	-	5
	Space	-	3
	Receptor	-	3
	Sum	-	11
	Importance	**-**	**1.00**
Hierarchist	Time	-	4.0
	Space	-	3.0
	Receptor	-	3.5
	Sum	-	10.5
	Importance	**-**	**1.00**

The concept of exergy is based on the second law of thermodynamics, which considers both the quantity and quality of energy. Hence, the second-law measure of efficiency is utilized while first-law efficiencies are mentioned in the analysis but not implemented in actual sustainability assessments. Even though the ExER is the only sub-indicator considered, scores still need to be assigned to assist in calculating the contribution of the ER category to the overall sustainability of the system.

ExER measures the proximity of an energy system to its maximum thermodynamic efficiency. The ratio is important from a long-term perspective, when resource scarcity will necessitate more efficient methods of production. The individualist archetype has a short-term, local, and anthropocentric perspective but ExER is still relevant since technological efficiency improvements can lead to reduced costs and lower emissions, for example. This leads to a score of three for both the time and space criteria. In addition, exergy efficiency is linked to areas important to humans such as cost and resource use, which leads to a score of four for the receptor criterion.

The egalitarian archetype has a long-term, global, and ecocentric perspective. ExER is very important on a long time horizon, which implies a score of five for that criterion. The sub-indicator is relevant on a global scale since improvements in exergy efficiency may lead to emission reductions and better resource utilization. Although humans are the more sensitive receptors, ecosystems may also be affected.

7.1.2 EF

The EF category consists of two sub-indicators – AF and CV. The relative importance of each is presented in Table 7.2.

Both sub-indicators are judged to be very important from short-term, local, and anthropocentric perspectives central to the individualist worldview. The reverse is true from the egalitarian perspective. The AF is very unimportant over time as externalities such as resource depletion and environmental stress are internalized into cost assessments. CV is only slightly more important because on an extended time horizon because technological breakthroughs may unexpectedly occur.

Table 7.2: Evaluation of the relative importance of the AF and CV sub-indicators within the EF category indicator.

Perspective	Criteria	AF	CV
Individualist	Time	5	5
	Space	5	5
	Receptor	5	5
	Sum	15	15
	Importance	**0.50**	**0.50**
Egalitarian	Time	1	1
	Space	4	3
	Receptor	2	2
	Sum	7	6
	Importance	**0.54**	**0.46**
Hierarchist	Time	3.0	3.0
	Space	4.5	4.0
	Receptor	3.5	3.5
	Sum	11.0	10.5
	Importance	**0.51**	**0.49**

The intra-category trade-off factors of sub-indicators are determined through pair-wise comparisons. The results are compiled in a comparison matrix (Table 7.3), which is then used to construct an evaluation matrix (Table 7.4).

Table 7.3: Comparison matrix for the AF and CV sub-indicators within the EF category indicator.

Perspective	Indicator	AF	CV
Individualist	AF	1	1
	CV	1	1
	Sum	2	2
Egalitarian	AF	1	2
	CV	0.5	1
	Sum	1.5	3.0
Hierarchist	AF	1	2
	CV	0.5	1
	Sum	1.5	3.0

Table 7.4: Evaluation matrix for the AF and CV sub-indicators within the EF category indicator.

Perspective	Indicator	AF	CV	Trade-off factor
Individualist	AF	0.50	0.50	**0.50**
	CV	0.50	0.50	**0.50**
Egalitarian	AF	0.67	0.67	**0.67**
	CV	0.33	0.33	**0.33**
Hierarchist	AF	0.67	0.67	**0.67**
	CV	0.33	0.33	**0.33**

7.1.3 SF

The SF category consists of three sub-indicators – mass, area, and volume. The relative importance of each is presented in Table 7.5.

Table 7.5: Evaluation of the relative importance of mass, area, and volume sub-indicators within the SF category indicator.

Perspective	Criteria	Mass	Area	Volume
Individualist	Time	-	3	-
	Space	-	3	-
	Receptor	-	3	-
	Sum	-	9	-
	Importance	**-**	**1.00**	**-**
Egalitarian	Time	-	4	-
	Space	-	4	-
	Receptor	-	4	-
	Sum	-	12	-
	Importance	**-**	**1.00**	**-**
Hierarchist	Time	-	3.5	-
	Space	-	3.5	-
	Receptor	-	3.5	-
	Sum	-	10.5	-
	Importance	**-**	**1.00**	**-**

The relevant sub-indicator for the SF category depends on the application. The case studies assessed are all stationary energy systems where area is the dominant consideration. Mass and volume sub-indicators are therefore ignored in this analysis.

7.1.4 GEIP

The GEIP category consists of three sub-indicators – GWP, SODP, and ADP. The relative importance of each is presented in Table 7.6.

Table 7.6: Evaluation of the relative importance of the GWP, SODP, and ADP sub-indicators within the GEIP category indicator.

Perspective	Criteria	GWP	SODP	ADP
Individualist	Time	3	5	1
	Space	3	4	2
	Receptor	5	5	4
	Sum	10	14	7
	Importance	**0.32**	**0.45**	**0.23**
Egalitarian	Time	5	5	4
	Space	5	3	4
	Receptor	5	3	4
	Sum	15	11	12
	Importance	**0.39**	**0.29**	**0.32**
Hierarchist	Time	4.0	5.0	2.5
	Space	4.0	3.5	3.0
	Receptor	5.0	4.0	4.0
	Sum	13.0	12.5	9.5
	Importance	**0.37**	**0.36**	**0.27**

The GEIP category contains some of the most critical sustainability indicators. Global warming is a very important long-term concern but its short-term effect is considered to be neutral. However, if the incidence of extreme weather patterns can be more strongly linked to global warming this evaluation may change. On the other hand, stratospheric ozone depletion is very important on short- and long-term time horizons. Abiotic depletion is very unimportant as a near-term concern but gains in importance over time. The potential substitutability of scarce resources with more abundant alternatives through technological innovation suggests that abiotic depletion is “only” important over an extended time horizon.

The comparison and evaluation matrices for the GEIP intra-category trade-off factors are compiled in Tables 7.7 and 7.8, respectively.

Table 7.7: Comparison matrix for the GWP, SODP, and ADP sub-indicators within the GEIP category indicator.

Perspective	Indicator	GWP	SODP	ADP
Individualist	GWP	1	0.25	5
	SODP	4	1	8
	ADP	0.20	0.13	1
	Sum	5.2	1.4	14.0
Egalitarian	GWP	1	5	4
	SODP	0.20	1	4
	ADP	0.25	0.25	1
	Sum	1.5	6.3	9.0
Hierarchist	GWP	1	2	5
	SODP	0.50	1	4
	ADP	0.20	0.25	1
	Sum	1.7	3.3	10.0

Table 7.8: Evaluation matrix for the GWP, SODP, and ADP sub-indicators within the GEIP category indicator.

Perspective	Indicator	GWP	SODP	ADP	Trade-off factor
Individualist	GWP	0.19	0.18	0.36	**0.24**
	SODP	0.77	0.73	0.57	**0.69**
	ADP	0.04	0.09	0.07	**0.07**
Egalitarian	GWP	0.69	0.80	0.44	**0.65**
	SODP	0.14	0.16	0.44	**0.25**
	ADP	0.17	0.04	0.11	**0.11**
Hierarchist	GWP	0.59	0.62	0.50	**0.57**
	SODP	0.29	0.31	0.40	**0.33**
	ADP	0.12	0.08	0.10	**0.10**

7.1.5 APP

The APP category consists of seven sub-indicators – Fine Particulate Matter, Coarse Particulate Matter, Sulphur Dioxide, Carbon Monoxide, Nitrogen Dioxide, Ground-Level Ozone, and Lead. The relative importance of each is presented in Table 7.9.

Most of the sub-indicators are considered to be “very important” from an individualist perspective as air pollution tends to be more of a local, short-term concern that impacts humans. However, a contaminant such as lead has a negative effect on both human and ecosystem receptors and is more long-lived in the environment than other species. Lead

will therefore have a high score and carry more weight than other criteria air contaminants.

Table 7.9: Evaluation of the relative importance of the $PM_{2.5}$, PM_{10}, SO_2, CO, NO_2, O_3, and Pb sub-indicators within the APP category indicator.

Perspective	Criteria	$PM_{2.5}$	PM_{10}	SO_2	CO	NO_2	O_3	Pb
Individualist	Time	5	5	5	5	5	5	5
	Space	5	5	5	5	5	5	5
	Receptor	5	5	2	4	4	4	5
	Sum	15	15	12	14	14	14	15
	Importance	**0.15**	**0.15**	**0.12**	**0.14**	**0.14**	**0.14**	**0.15**
Egalitarian	Time	1	1	1	1	1	1	5
	Space	1	1	1	1	1	1	1
	Receptor	1	1	4	1	4	1	5
	Sum	3	3	6	3	6	3	11
	Importance	**0.09**	**0.09**	**0.17**	**0.09**	**0.17**	**0.09**	**0.31**
Hierarchist	Time	3.0	3.0	3.0	3.0	3.0	3.0	5.0
	Space	3.0	3.0	3.0	3.0	3.0	3.0	3.0
	Receptor	3.0	3.0	3.0	2.5	4.0	2.5	5.0
	Sum	9.0	9.0	9.0	8.5	10.0	8.5	13.0
	Importance	**0.13**	**0.13**	**0.13**	**0.13**	**0.15**	**0.13**	**0.19**

The egalitarian perspective is also concerned with the health and well-being of ecosystems. Molecules such as SO_2 and NO_2 that have a role to play in acid rain formation are also given higher scores for the receptor criterion from an egalitarian perspective. However, neither is as persistent in the environment as lead, which means they have shorter residence times.

The comparison and evaluation matrices for the APP intra-category trade-off factors are compiled in Tables 7.10 and 7.11, respectively.

7.1.6 WPP

The WPP category consists of three sub-indicators – EP, FAETP, and MAETP. The importance of water pollution somewhat depends on the location of the community. Proximity to aquatic ecosystems varies widely across the world. Nevertheless, even if a community is not directly affected by water pollution the interconnectedness of the

world suggests that everyone is affected in one way or another. The relative importance of each water pollution sub-indicator is presented in Table 7.12.

Table 7.10: Comparison matrix for the $PM_{2.5}$, PM_{10}, SO_2, CO, NO_2, O_3, and Pb sub-indicators within the APP category indicator.

Perspective	Indicator	$PM_{2.5}$	PM_{10}	SO_2	CO	NO_2	O_3	Pb
Individualist	$PM_{2.5}$	1	1	4	2	2	2	1
	PM_{10}	1	1	4	2	2	2	1
	SO_2	0.25	0.25	1	0.33	0.33	0.33	0.25
	CO	0.5	0.5	3	1	1	1	0.5
	NO_2	0.5	0.5	3	1	1	1	0.5
	O_3	0.5	0.5	3	1	1	1	0.5
	Pb	1	1	4	2	2	2	1
	Sum	4.8	4.8	22.0	9.3	9.3	9.3	4.8
Egalitarian	$PM_{2.5}$	1	1	0.25	1	0.25	1	0.11
	PM_{10}	1	1	0.25	1	0.25	1	0.11
	SO_2	4	4	1	4	1	4	0.17
	CO	1	1	0.25	1	0	1	0.11
	NO_2	4	4	1	4	1	4	0.17
	O_3	1	1	0.25	1	0.25	1	0.11
	Pb	9	9	6	9	6	9	1
	Sum	21.0	21.0	9.0	21.0	9.0	21.0	1.8
Hierarchist	$PM_{2.5}$	1	1	1	2	0.5	2	0.2
	PM_{10}	1	1	1	2	0.5	2	0.2
	SO_2	1	1	1	2	0.5	2	0.2
	CO	0.5	0.5	0.5	1	0.33	1	0.17
	NO_2	2	2	2	3	1	3	0.25
	O_3	0.5	0.5	0.5	1	0.33	1	0.17
	Pb	5	5	5	6	4	6	1
	Sum	11.0	11.0	11.0	17.0	7.2	17.0	2.2

Eutrophication can occur in freshwater or marine aquatic ecosystems. Although important, the direct impact on humans is not strongly felt unless a community is located near an aquatic ecosystem experiencing eutrophication. A score of one is assigned for the individualist receptor. However, a score of five is assigned to the egalitarian receptor because eutrophication consumes dissolved oxygen and can lead to anoxic zones in a body of water with very little aquatic life.

Table 7.11: Evaluation matrix for the $PM_{2.5}$, PM_{10}, SO_2, CO, NO_2, O_3, and Pb sub-indicators within the APP category indicator.

Perspective	Indicator	$PM_{2.5}$	PM_{10}	SO_2	CO	NO_2	O_3	Pb	Trade-off factor
Individualist	$PM_{2.5}$	0.21	0.21	0.18	0.21	0.21	0.21	0.21	**0.21**
	PM_{10}	0.21	0.21	0.18	0.21	0.21	0.21	0.21	**0.21**
	SO_2	0.05	0.05	0.05	0.04	0.04	0.04	0.05	**0.04**
	CO	0.11	0.11	0.14	0.11	0.11	0.11	0.11	**0.11**
	NO_2	0.11	0.11	0.14	0.11	0.11	0.11	0.11	**0.11**
	O_3	0.11	0.11	0.14	0.11	0.11	0.11	0.11	**0.11**
	Pb	0.21	0.21	0.18	0.21	0.21	0.21	0.21	**0.21**
Egalitarian	$PM_{2.5}$	0.05	0.05	0.03	0.05	0.03	0.05	0.06	**0.04**
	PM_{10}	0.05	0.05	0.03	0.05	0.03	0.05	0.06	**0.04**
	SO_2	0.19	0.19	0.11	0.19	0.11	0.19	0.09	**0.15**
	CO	0.05	0.05	0.03	0.05	0.03	0.05	0.06	**0.04**
	NO_2	0.19	0.19	0.11	0.19	0.11	0.19	0.09	**0.15**
	O_3	0.05	0.05	0.03	0.05	0.03	0.05	0.06	**0.04**
	Pb	0.43	0.43	0.67	0.43	0.67	0.43	0.56	**0.52**
Hierarchist	$PM_{2.5}$	0.09	0.09	0.09	0.12	0.07	0.12	0.09	**0.10**
	PM_{10}	0.09	0.09	0.09	0.12	0.07	0.12	0.09	**0.10**
	SO_2	0.09	0.09	0.09	0.12	0.07	0.12	0.09	**0.10**
	CO	0.05	0.05	0.05	0.06	0.05	0.06	0.08	**0.05**
	NO_2	0.18	0.18	0.18	0.18	0.14	0.18	0.11	**0.17**
	O_3	0.05	0.05	0.05	0.06	0.05	0.06	0.08	**0.05**
	Pb	0.45	0.45	0.45	0.35	0.56	0.35	0.46	**0.44**

The importance of freshwater compared to marine ecotoxicity depends on the local geography. In many cases freshwater systems are more of a local concern while marine systems are more of a global concern. However, both impact human and ecosystem receptors.

The comparison and evaluation matrices for the WPP intra-category trade-off factors are compiled in Tables 7.13 and 7.14, respectively.

Table 7.12: Evaluation of the relative importance of the EP, FAETP, and MAETP sub-indicators within the WPP category indicator.

Perspective	Criteria	EP	FAETP	MAETP
Individualist	Time	3	4	2
	Space	3	5	3
	Receptor	1	5	3
	Sum	7	14	8
	Importance	**0.24**	**0.48**	**0.28**
Egalitarian	Time	1	3	4
	Space	2	2	5
	Receptor	5	5	5
	Sum	8	10	14
	Importance	**0.25**	**0.31**	**0.44**
Hierarchist	Time	2.0	3.5	3.0
	Space	2.5	3.5	4.0
	Receptor	3.0	5.0	4.0
	Sum	7.5	12.0	11.0
	Importance	**0.25**	**0.39**	**0.36**

Table 7.13: Comparison matrix for the EP, FAETP, and MAETP sub-indicators within the WPP category indicator.

Perspective	Indicator	EP	FAETP	MAETP
Individualist	EP	1	0.13	0.5
	FAETP	8	1	7
	MAETP	2	0.14	1
	Sum	11.0	1.3	8.5
Egalitarian	EP	1	0.33	0.14
	FAETP	3	1	0.2
	MAETP	7	5	1
	Sum	11.0	6.3	1.3
Hierarchist	EP	1	0.17	0.2
	FAETP	6	1	2
	MAETP	5	0.5	1
	Sum	12.0	1.7	3.2

Table 7.14: Evaluation matrix for the EP, FAETP, and MAETP sub-indicators within the WPP category indicator.

Perspective	Indicator	EP	FAETP	MAETP	Trade-off factor
Individualist	EP	0.09	0.10	0.06	**0.08**
	FAETP	0.73	0.79	0.82	**0.78**
	MAETP	0.18	0.11	0.12	**0.14**
Egalitarian	EP	0.09	0.05	0.11	**0.08**
	FAETP	0.27	0.16	0.15	**0.19**
	MAETP	0.64	0.79	0.74	**0.72**
Hierarchist	EP	0.08	0.10	0.06	**0.08**
	FAETP	0.50	0.60	0.63	**0.58**
	MAETP	0.42	0.30	0.31	**0.34**

7.1.7 Category Weighting Factors

Inter-category weighting factors for each perspective are derived based on prior criteria scores. The relative importance of each inter-category indicator is presented in Table 7.15.

Table 7.15: Evaluation of the relative importance of the ER, EF, SF, GEIP, APP, and WPP category indicators.

Perspective	Criteria	ER	EF	SF	GEIP	APP	WPP
Individualist	Time	3.0	5.0	3.0	3.0	5.0	3.0
	Space	3.0	5.0	3.0	3.0	5.0	3.7
	Receptor	4.0	5.0	3.0	4.7	4.1	3.0
	Sum	10.0	15.0	9.0	10.7	14.1	9.7
	Importance	**0.15**	**0.22**	**0.13**	**0.16**	**0.21**	**0.14**
Egalitarian	Time	5.0	1.0	4.0	4.7	1.6	2.7
	Space	3.0	3.5	4.0	4.0	1.0	3.0
	Receptor	3.0	2.0	4.0	4.0	2.4	5.0
	Sum	11.0	6.5	12.0	12.7	5.0	10.7
	Importance	**0.19**	**0.11**	**0.21**	**0.22**	**0.09**	**0.18**
Hierarchist	Time	4.0	3.0	3.5	3.8	3.3	2.8
	Space	3.0	4.3	3.5	3.5	3.0	3.3
	Receptor	3.5	3.5	3.5	4.3	3.3	4.0
	Sum	10.5	10.8	10.5	11.7	9.6	10.2
	Importance	**0.17**	**0.17**	**0.17**	**0.18**	**0.15**	**0.16**

The comparison and evaluation matrices for the inter-category trade-off factors are compiled in Tables 7.16 and 7.17, respectively.

Table 7.16: Comparison matrix for the ER, EF, SF, GEIP, APP, and WPP category indicators.

Perspective	Indicator	ER	EF	SF	GEIP	APP	WPP
Individualist	ER	1	0.17	2	0.5	0.2	1
	EF	6	1	7	5	2	6
	SF	0.5	0.14	1	0.33	0.17	1
	GEIP	2	0.2	3	1	0.25	2
	APP	5	0.5	6	4	1	5
	WPP	1	0.17	2	0.5	0.2	1
	Sum	15.5	2.2	21.0	11.3	3.8	15.5
Egalitarian	ER	1	6	0.5	0.33	7	1
	EF	0.17	1	0.14	0.14	3	0.2
	SF	2	7	1	0.5	8	2
	GEIP	3	7	2	1	9	3
	APP	0.14	0.33	0.13	0.11	1	0.14
	WPP	1	5	0.5	0.33	7	1
	Sum	7.3	26.3	4.3	2.4	35.0	7.3
Hierarchist	ER	1	1	1	0.5	2	1
	EF	1	1	1	0.5	2	2
	SF	1	1	1	0.5	2	1
	GEIP	2	2	2	1	3	3
	APP	0.5	0.5	0.5	0.33	1	0.5
	WPP	1	0.5	1	0.33	2	1
	Sum	6.5	6.0	6.5	3.2	12.0	8.5

7.1.8 Questionnaire

One of the most common methods of eliciting weighting factors in multi-criteria decision analysis is the panel approach. A voluntary questionnaire distributed to participants of the 3rd World Sustainability Forum, an online conference held November 1-30, 2013, asked respondents to rate the importance of various sustainability indicators. Indicators were classified on a spectrum ranging from “very unimportant” to “very important.” An indicator selected as “very unimportant” was assigned a score of one while a “very important” indicator was assigned a score of five. The number of conference participants that responded to the online questionnaire was 50, although

only 37 actually completed the task. A summary of the results of the questionnaire for sustainability sub-indicators is provided in Table 7.18.

Table 7.17: Evaluation matrix for the ER, EF, SF, GEIP, APP, and WPP category indicators.

Perspective	Indicator	ER	EF	SF	GEIP	APP	WPP	Trade-off factor
Individualist	ER	0.06	0.08	0.10	0.04	0.05	0.06	**0.07**
	EF	0.39	0.46	0.33	0.44	0.52	0.39	**0.42**
	SF	0.03	0.07	0.05	0.03	0.04	0.03	**0.04**
	GEIP	0.13	0.09	0.14	0.09	0.07	0.13	**0.11**
	APP	0.32	0.23	0.29	0.35	0.26	0.32	**0.30**
	WPP	0.06	0.08	0.10	0.04	0.05	0.06	**0.07**
Egalitarian	ER	0.14	0.23	0.12	0.14	0.20	0.14	**0.16**
	EF	0.02	0.04	0.03	0.06	0.09	0.03	**0.04**
	SF	0.27	0.27	0.23	0.21	0.23	0.27	**0.25**
	GEIP	0.41	0.27	0.47	0.41	0.26	0.41	**0.37**
	APP	0.02	0.01	0.03	0.05	0.03	0.02	**0.03**
	WPP	0.14	0.19	0.12	0.14	0.20	0.14	**0.15**
Hierarchist	ER	0.15	0.17	0.15	0.16	0.17	0.12	**0.15**
	EF	0.15	0.17	0.15	0.16	0.17	0.24	**0.17**
	SF	0.15	0.17	0.15	0.16	0.17	0.12	**0.15**
	GEIP	0.31	0.33	0.31	0.32	0.25	0.35	**0.31**
	APP	0.08	0.08	0.08	0.11	0.08	0.06	**0.08**
	WPP	0.15	0.08	0.15	0.11	0.17	0.12	**0.13**

There is little variability in the importance of sustainability sub-indicators according to questionnaire respondents, which ranges from 4.1 (CV) to 4.8 (GWP). The lowest scores were assigned to the economic-based sub-indicators, which might be a reflection of the ecocentric views of participants in an online sustainability conference. Also of interest is that the panel assigned a higher score to the EnER compared to the ExER even though second-law-based measures of efficiency take both the quantity and quality of energy into account. Relevant to the discussion is that six respondents answered “Not sure” with respect to the importance of the ExER to sustainability compared to only two for the EnER. This suggests that there may have been a number of respondents who were not as familiar with the concept of exergy, which had a negative effect on its score relative to the more familiar concept of energy.

Table 7.18: Average importance scores, standard deviations, and coefficients of variation for sustainability sub-indicators based on responses to the questionnaire.

Sub-indicator	Mean	Standard deviation	Coefficient of variation (%)
EnER	4.7	0.50	11
ExER	4.4	0.49	11
AF	4.3	0.79	18
CV	4.1	0.93	23
GWP	4.8	0.42	9
SODP	4.5	0.70	15
ADP	4.5	0.64	14
Particulate Matter	4.7	0.47	10
SO_2	4.5	0.56	12
CO	4.7	0.64	14
NO_2	4.5	0.61	13
O_3	4.5	0.71	16
Pb	4.6	0.70	15
EP	4.5	0.50	11
FAETP	4.7	0.47	10

There is also little variability from questionnaire respondents as to the importance of individual sustainability sub-indicators. The coefficient of variation (i.e., ratio of standard deviation to the mean) ranges from 9% (GWP) to 23% (CV).

A comparison of the importance of sustainability sub-indicators based on the panel and time-space-receptor methods is presented in Figure 7.1. This figure demonstrates that importance scores of sustainability sub-indicators fluctuate depending on the elicitation method. For example, the range in scores is much greater when applying the time-space-receptor method. The challenge for a panel is that every indicator seems "important," which makes it difficult to differentiate between them.

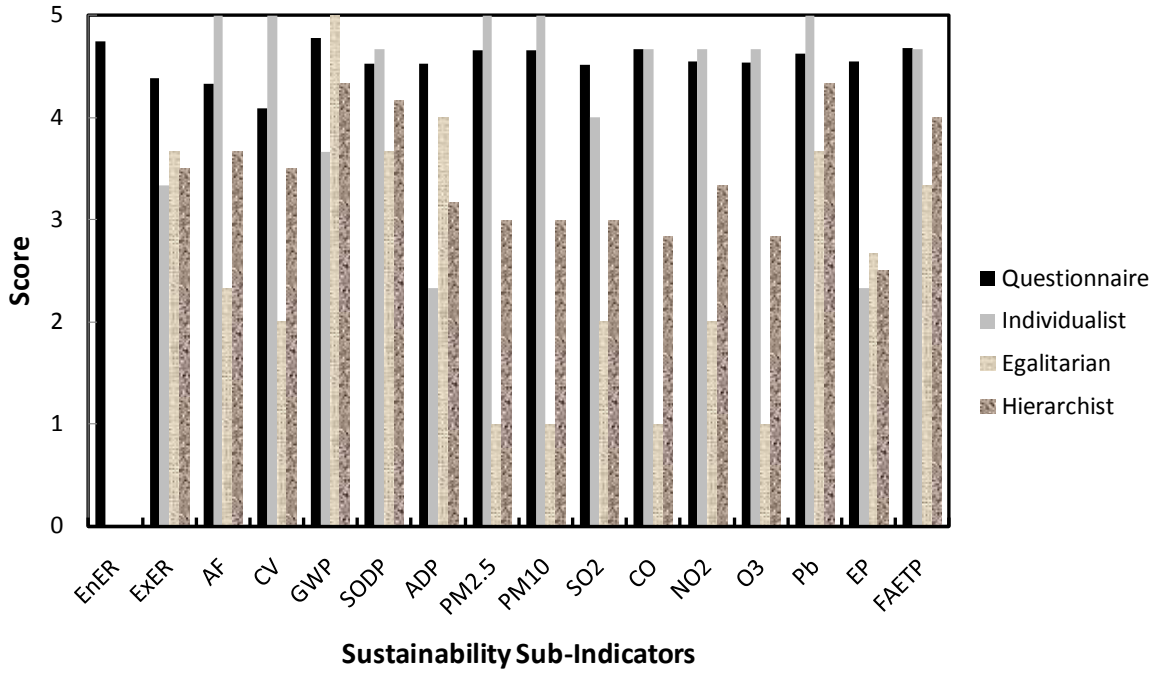

Figure 7.1: Importance scores of sustainability sub-indicators based on a questionnaire to a panel and time-space-receptor methods.

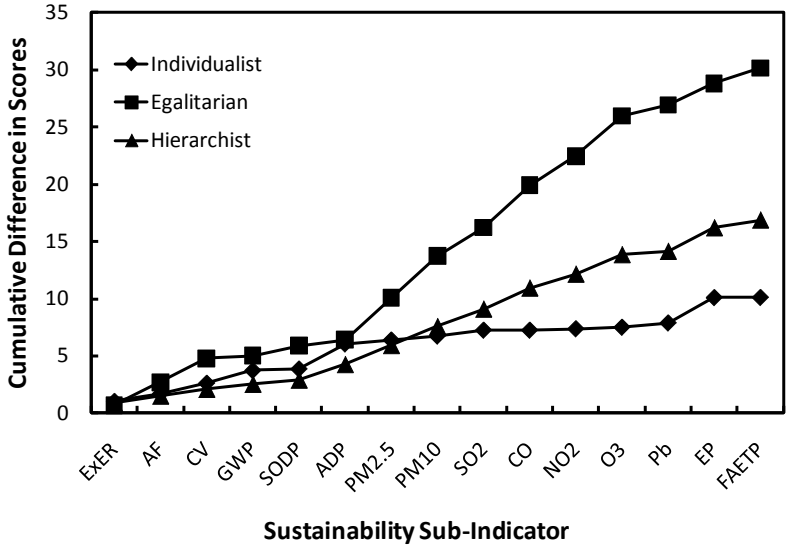

Figure 7.2: Cumulative difference in the importance of sustainability sub-indicators derived through the time-space-receptor method relative to the panel method.

The cumulative difference between the score of a sub-indicator based on the questionnaire and the score based on sustainability perspectives is shown in Figure 7.2. A larger number in Figure 7.2 equates to a larger cumulative difference relative to the

panel method. The perspective that most closely approximates questionnaire respondents is the individualist, which has a cumulative difference of 10. The cumulative difference of the egalitarian perspective is 30. Most of that cumulative difference is accumulated in the APP category, which is evaluated as much more important by questionnaire respondents than by the egalitarian perspective.

The questionnaire also asked conference participants to evaluate the importance of category indicators with respect to sustainability. A summary of the results of the questionnaire for category indicators is provided in Table 7.19.

Table 7.19: Average importance scores, standard deviations, and coefficients of variation for category indicators based on responses to the questionnaire.

Category	Mean	Standard deviation	Coefficient of variation (%)
ER	4.5	0.69	15
EF	4.1	0.86	21
SF	3.7	0.86	23
GEIP	4.8	0.42	9
APP	4.7	0.53	11
WPP	4.7	0.45	10

There is a greater range of importance scores for category indicators using the panel approach compared to the range for sub-indicators. The scores range from 3.7 (SF) to 4.8 (GEIP). Although SF exhibits the lowest score, the respondents assign the second-lowest score to the EF category (i.e., 4.1), which is consistent with earlier responses from the panel with respect to sustainability sub-indicators. However, it is important to recognize that the panel was selected from an online conference on sustainability and very likely has an ecocentric perspective.

A comparison of the importance of category indicators based on the panel and time-space-receptor methods is presented in Figure 7.3. This figure demonstrates that importance scores of category indicators fluctuate depending on the elicitation method.

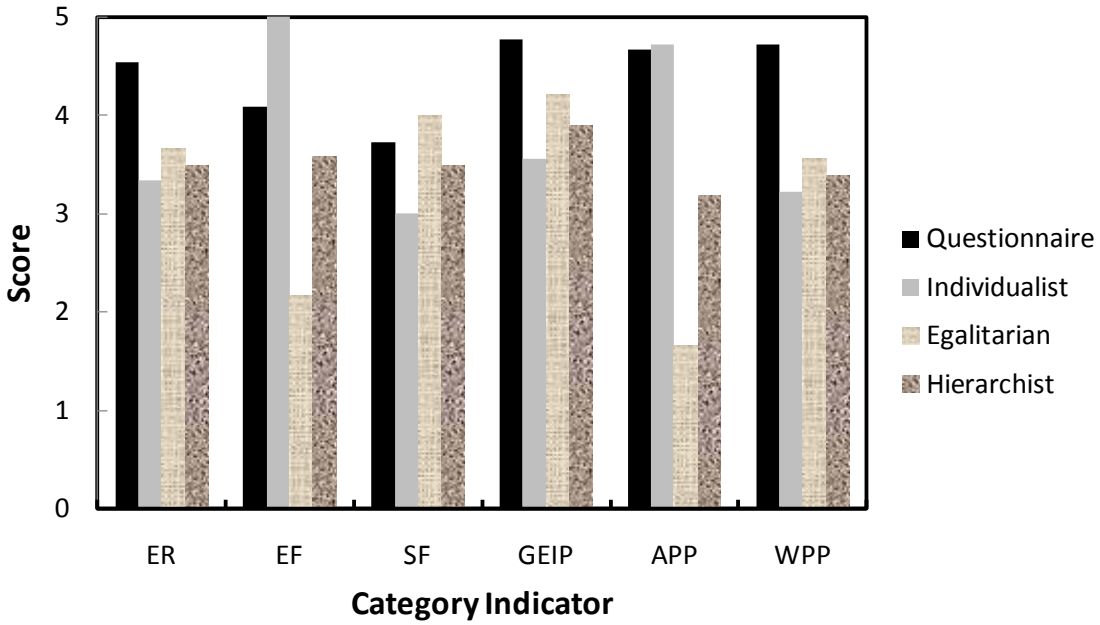

Figure 7.3: Importance scores of category indicators based on a questionnaire to a panel and time-space-receptor methods.

The cumulative difference in the importance of category indicators derived through the time-space-receptor method relative to the panel method is shown in Figure 7.4.

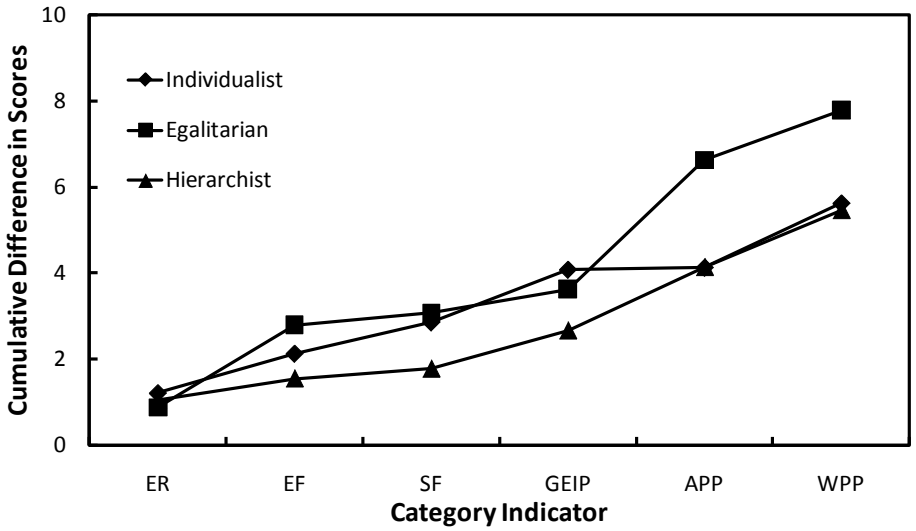

Figure 7.4: Cumulative difference in the importance of category indicators derived through the time-space-receptor method relative to the panel method.

The individualist and hierarchist perspectives equally approximate questionnaire respondents since both archetypes have a cumulative difference of 5.5. On the other

hand, the cumulative difference of the egalitarian perspective is 7.8. Figure 7.4 shows that the accumulated difference for the individualist and egalitarian perspectives is very similar until GEIP. However, the slope of the egalitarian function then increases steeply while the slope of the individualist function becomes zero. The slope of each function is then approximately equal from APP to WPP. The low importance of APP derived through the egalitarian time-space-receptor method significantly increases its cumulative difference.

7.2 Case Studies

The results of sustainability assessments for each of the case studies described in Chapter 6 are presented here. The life-cycle assessment software SimaPro was used to determine life-cycle emission factors for the GEIP, APP, and WPP categories.

7.2.1 Reference System

The reference system is a gas-fired power plant that provides heat, cold, and power to the community. The daily demand for natural gas fluctuates over the course of a year (Figure 7.5).

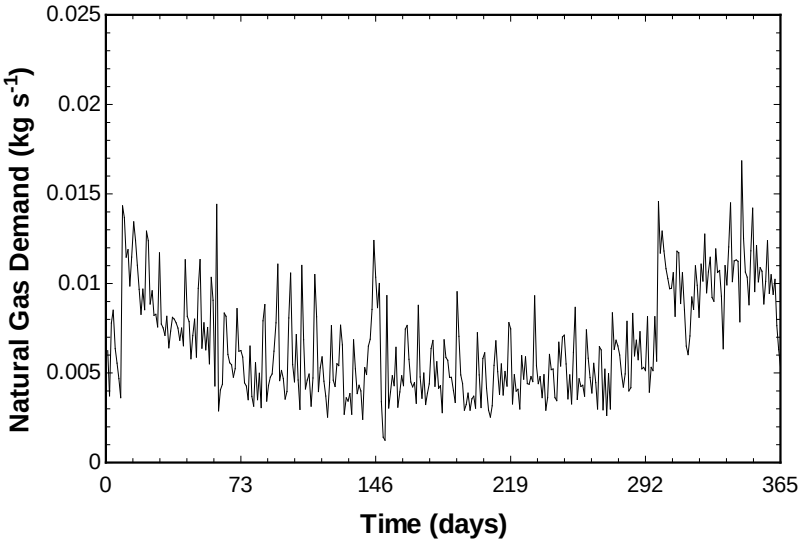

Figure 7.5: Natural gas consumption over one year for a 50-household community in Ontario (day "1" corresponds to August 1, 2009).

Natural gas use peaks during summer months to meet the demand for cooling. Overall gas use for the year is approximately 260,000 kg, which is equivalent to 5,200 kg per household. The average household in Ontario consumes approximately 1,700 kg of natural gas per year for heating (Statistics Canada, 2007).

Each component of the reference system is associated with a certain amount of exergy destruction. The annual exergy destruction for each subsystem over 365 days is presented in Figure 7.6.

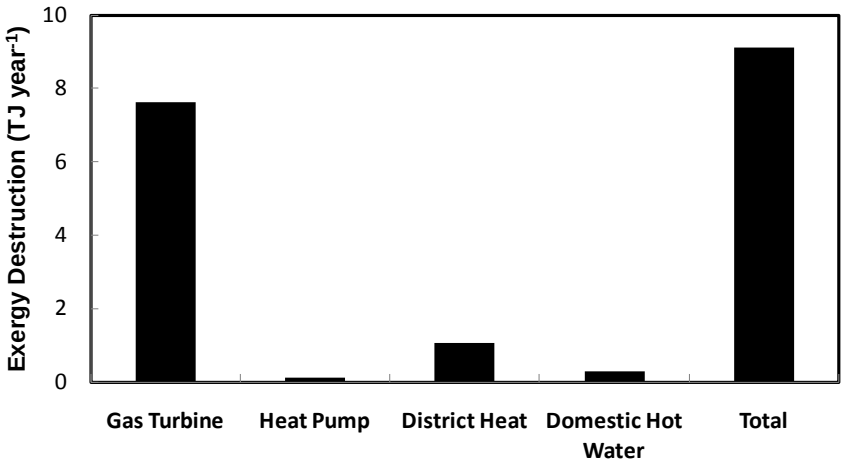

Figure 7.6: Annual exergy destruction of subsystems in the reference system over a one-year period.

The largest share of annual exergy destruction is attributed to the power-generating gas-turbine subsystem (7.6 TJ per year). Within the gas-turbine subsystem, the combustion chamber contributes 6.1 TJ per year, which is 67% of the total annual exergy destruction (9.1 TJ per year). The energy and exergy efficiencies of the system are 41% and 19%, respectively.

A thermodynamic analysis of the system is a precursor to sustainability assessment. Thermodynamic, cost, and life-cycle emission factors are combined with weighting factors for three different perspectives to yield the sustainability assessment results presented in Tables 7.20-7.22.

Table 7.20: Sustainability assessment results for the reference system from the individualist perspective.

Category	Sub-indicator	$B_{i,j}$	$W_{i,j}$	B_j	W_j	$B_j \times W_j$
ER	EnER	0.02	0.00	0.00	0.07	0.000
	ExER	0.70	1.00	0.70		0.046
EF	AF	1.00	0.50	0.50	0.42	0.211
	CV	1.00	0.50	0.50		0.211
SF	Mass	0.00	0.00	0.00	0.04	0.000
	Area	1.00	1.00	1.00		0.042
	Volume	0.00	0.00	0.00		0.000
GEIP	GWP	0.02	0.24	0.01	0.11	0.001
	SODP	0.03	0.69	0.02		0.003
	ADP	1.00	0.07	0.07		0.007
APP	$PM_{2.5}$	1.00	0.21	0.21	0.30	0.062
	PM_{10}	1.00	0.21	0.21		0.062
	SO_2	1.00	0.04	0.04		0.013
	CO	1.00	0.11	0.11		0.033
	NO_2	1.00	0.11	0.11		0.033
	O_3	1.00	0.11	0.11		0.033
	Pb	1.00	0.21	0.21		0.061
WPP	EP	1.00	0.08	0.08	0.07	0.005
	FAETP	0.80	0.78	0.62		0.041
	MAETP	0.06	0.14	0.01		0.001
ISI						**0.86**

The ISI of the reference system ranges from a low of 0.52 for the egalitarian perspective to a high of 0.86 for the individualist perspective. The GEIP of the system is the largest contributor to the ISI. The GHG emissions associated with fossil fuel combustion drive the system's GWP while the formation of N_2O that occurs in nitrogen-rich, high-temperature environments is significant for SODP. On the other hand, the system scores very well with respect to the EF and APP, which explains the high ISI from an individualist perspective.

Table 7.21: Sustainability assessment results for the reference system from the egalitarian perspective.

Category	Sub-indicator	$B_{i,j}$	$W_{i,j}$	B_j	W_j	$B_j \times W_j$
ER	EnER	0.02	0.00	0.00	0.16	0.000
	ExER	0.70	1.00	0.70		0.111
EF	AF	1.00	0.67	0.67	0.04	0.029
	CV	1.00	0.33	0.33		0.015
SF	Mass	0.00	0.00	0.00	0.25	0.000
	Area	1.00	1.00	1.00		0.247
	Volume	0.00	0.00	0.00		0.000
GEIP	GWP	0.02	0.65	0.02	0.37	0.006
	SODP	0.03	0.25	0.01		0.003
	ADP	1.00	0.11	0.11		0.040
APP	$PM_{2.5}$	1.00	0.04	0.04	0.03	0.001
	PM_{10}	1.00	0.04	0.04		0.001
	SO_2	1.00	0.15	0.15		0.004
	CO	1.00	0.04	0.04		0.001
	NO_2	1.00	0.15	0.15		0.004
	O_3	1.00	0.04	0.04		0.001
	Pb	1.00	0.52	0.52		0.013
WPP	EP	1.00	0.08	0.08	0.15	0.013
	FAETP	0.80	0.19	0.15		0.024
	MAETP	0.06	0.72	0.04		0.006
ISI						**0.52**

Sustainability sub-indicators in Tables 7.20-7.22 with a $B_{i,j}$ value equal to one have no negative effect on ISI. Sub-indicators with a $B_{i,j}$ value less than one will have a negative effect on ISI, which is a function of the actual $B_{i,j}$ value and its weight. The reduction on ISI of each sustainability sub-indicator is graphed in Figure 7.7.

Figure 7.7 indicates that the GWP sub-indicator has the strongest possible effect on the sustainability of the system as it can reduce ISI from 0.025 to 0.23 units. The potential reduction in ISI is a function of $B_{i,j}$ and the weight of the sub-indicator. The SODP and MAETP sub-indicators have lesser but still significant effects. The only other relevant sub-indicator for this system is the ExER.

Table 7.22: Sustainability assessment results for the reference system from the hierarchist perspective.

Category	Sub-indicator	$B_{i,j}$	$W_{i,j}$	B_j	W_j	$B_j \times W_j$
ER	EnER	0.02	0.00	0.00	0.15	0.000
	ExER	0.70	1.00	0.70		0.107
EF	AF	1.00	0.67	0.67	0.17	0.115
	CV	1.00	0.33	0.33		0.057
SF	Mass	0.00	0.00	0.00	0.15	0.000
	Area	1.00	1.00	1.00		0.153
	Volume	0.00	0.00	0.00		0.000
GEIP	GWP	0.02	0.57	0.01	0.31	0.004
	SODP	0.03	0.33	0.01		0.004
	ADP	1.00	0.10	0.10		0.030
APP	$PM_{2.5}$	1.00	0.10	0.10	0.08	0.008
	PM_{10}	1.00	0.10	0.10		0.008
	SO_2	1.00	0.10	0.10		0.008
	CO	1.00	0.05	0.05		0.004
	NO_2	1.00	0.17	0.17		0.013
	O_3	1.00	0.05	0.05		0.004
	Pb	1.00	0.44	0.44		0.036
WPP	EP	1.00	0.08	0.08	0.13	0.011
	FAETP	0.80	0.58	0.46		0.060
	MAETP	0.06	0.34	0.02		0.003
ISI						**0.62**

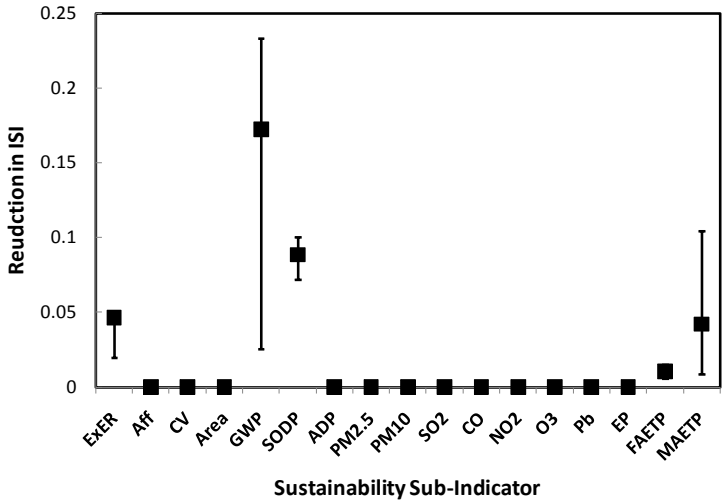

Figure 7.7: Reduction in ISI for each sustainability sub-indicator for the reference system.

The impact of this system on global warming and stratospheric ozone depletion is studied in more detail in Figures 7.8 and 7.9. The dashed horizontal line in Figure 7.8 represents actual annual per capita emissions from the gas-fired system while the solid-line function represents allowable emissions under IPCC scenario RCP2.6, where the global carbon budget is equally distributed amongst the population. The intersection of the two functions is the maximum allowable global population to stay within the international RCP2.6 carbon budget. For example, the allowable emissions curve intersects the horizontal gas-fired system line at a population of approximately 200 million people. If everyone in the world had an energy-demand profile as a typical Ontario household and met that demand through a gas-fired power plant, the planet would be constrained to 200 million people to stay within the confines of the RCP2.6 carbon budget. The intersection point can be shifted to the right by increasing the carbon budget or reducing per capita GHG emissions.

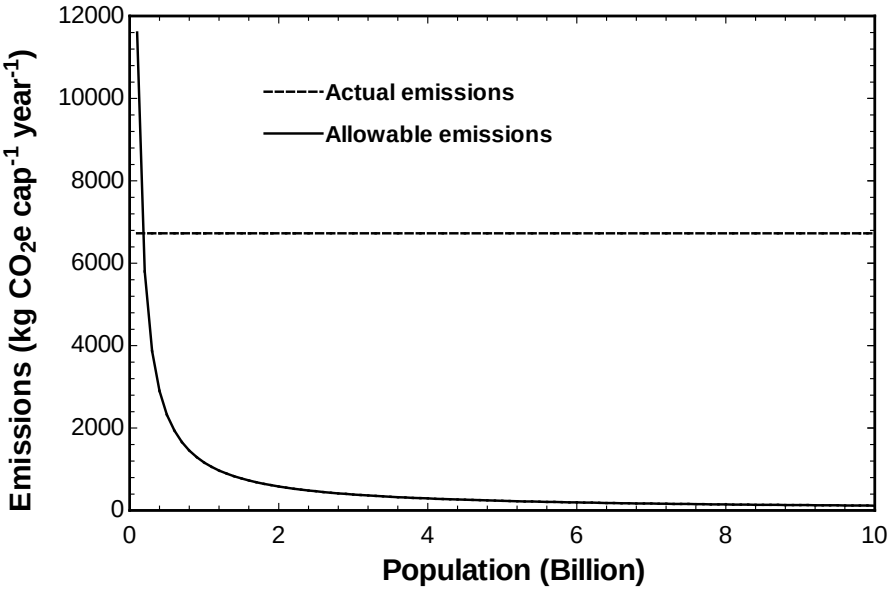

Figure 7.8: Actual and allowable annual per capita GHG emissions for the reference system based on the lower limit of the representative concentration pathway (RCP2.6) carbon budget.

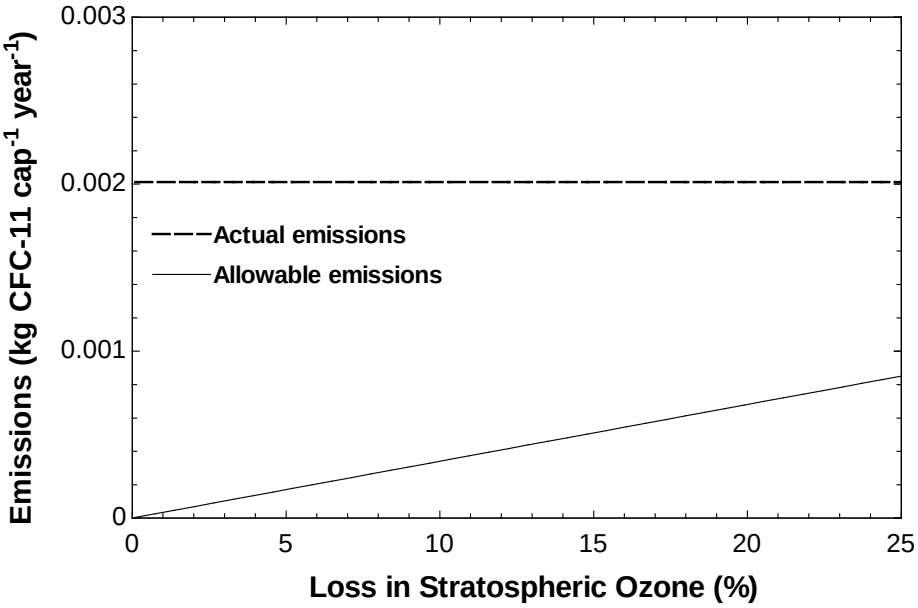

Figure 7.9: Actual and allowable annual per capita ozone-depleting substance emissions (including N_2O) for the reference system with respect to the percent loss in stratospheric ozone over the time scale for considering sustainability.

The graph in Figure 7.9 estimates the allowable amount of ozone-depleting substance emissions per capita per year as a function of the percent loss in stratospheric ozone over the time scale for considering sustainability. For example, a 2% loss in ozone over 50 years is equivalent to 0.04% per year. Actual annual per capita emissions from the reference system are approximately 0.002 kg CFC-11, most of which is due to the effect of N_2O. This corresponds to approximately 1% stratospheric ozone depletion per year, which is much higher than the 0.04% per year target value. Although the actual effect on the ozone layer is hard to determine due to the complexities associated with the photochemical reactions (Goedkoop and Spriensma, 2000) this is a useful approximation of potential impact.

The ISI of an energy system is a function of the time scale for considering sustainability. A longer time frame will in general make it harder to achieve sustainability due to challenges associated with global warming, stratospheric ozone depletion, and abiotic resource depletion. The effect of this parameter on ISI is illustrated in Figure 7.10.

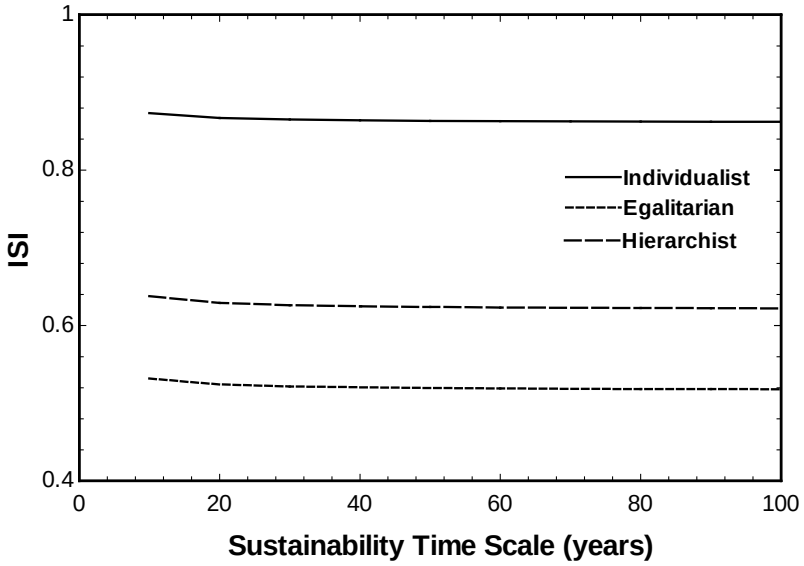

Figure 7.10: Variation of ISI with respect to the time scale for considering sustainability for the reference system.

Variations in the sustainability time horizon do not appear to have much of an effect on the sustainability of the system. The ISI of the reference system decreases very modestly for each perspective. The effect of weighting factor on the most critical sub-indicators is investigated in Figures 7.11 and 7.12.

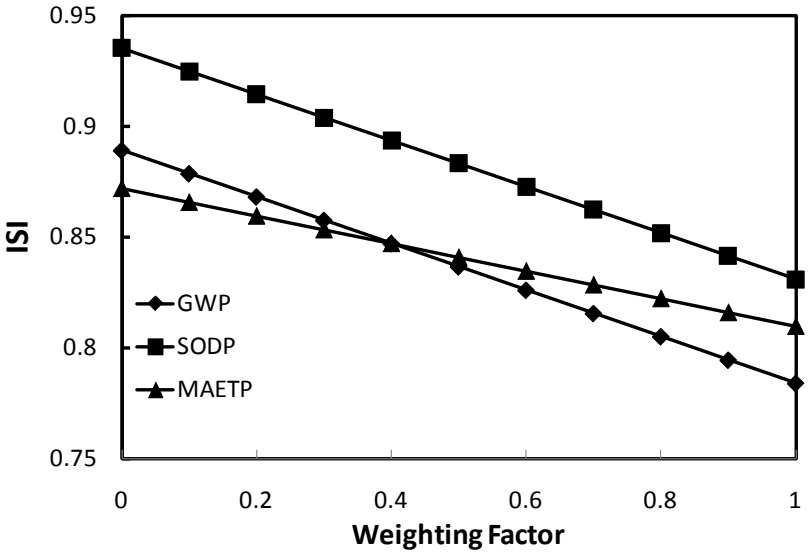

Figure 7.11: Variation of the individualist ISI with respect to weighting factor for the reference system.

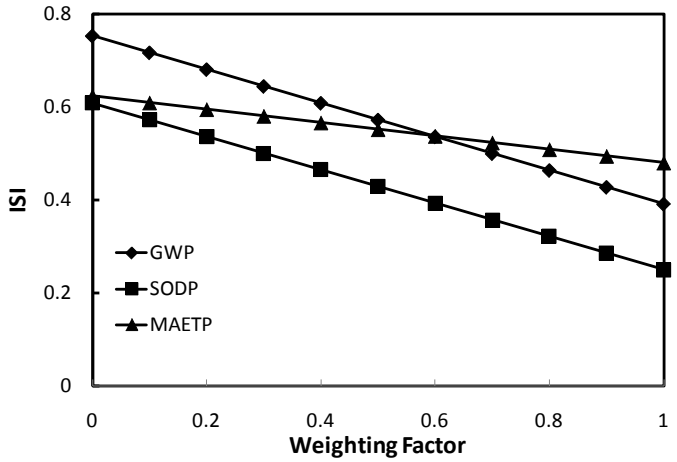

Figure 7.12: Variation of the egalitarian ISI with respect to weighting factor for the reference system.

The weighting factors associated with the SODP and GWP sub-indicators have the most significant effect. Excluding ozone layer depletion from consideration in the analysis increases the individualist ISI of the reference system from 0.86 (Table 7.20) to 0.94. Similarly, excluding climate change increases the egalitarian ISI from 0.52 (Table 7.21) to 0.75. Assignment of these weighting factors is critical in estimating the sustainability of the system.

The air-fuel ratio and pressure ratio of the gas-turbine subsystem are important parameters for the reference system. The impacts of these parameters on ISI are illustrated in Figures 7.13 and 7.14.

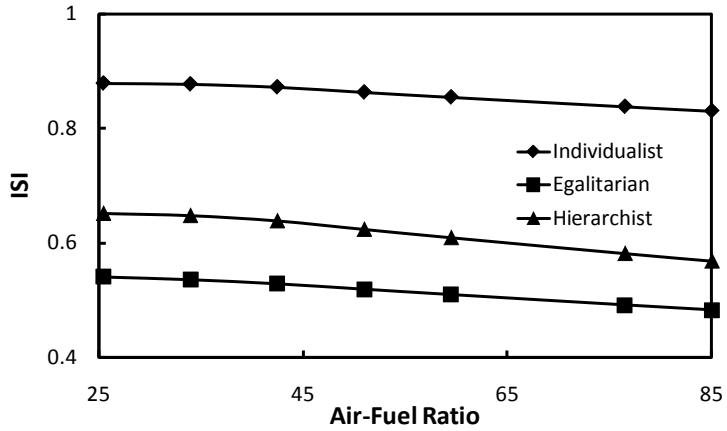

Figure 7.13: Variation of ISI with respect to air-fuel ratio for the reference system.

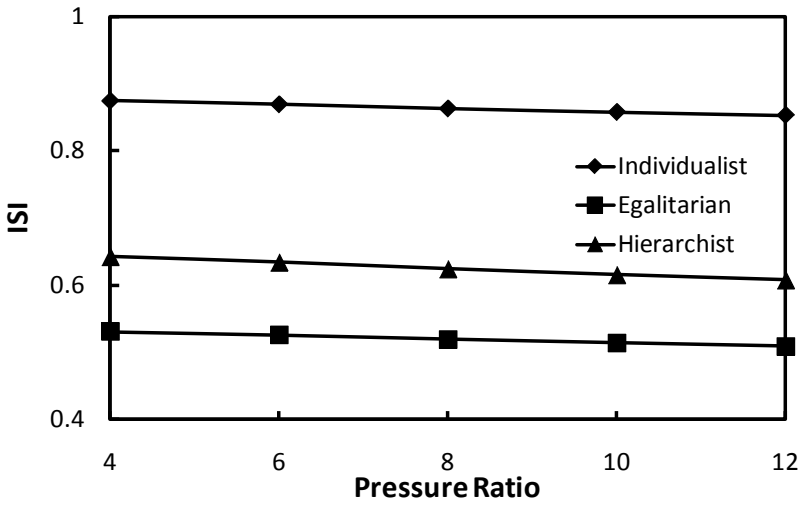

Figure 7.14: Variation of ISI with respect to pressure ratio for the reference system.

Increasing the air-fuel ratio has a negative impact on the ISI of the reference system. A lower air-fuel ratio implies that the working fluid is less diluted with air and reaches a higher post-combustion temperature. This increases the amount of power generated in the gas turbine and the overall sustainability of the system. However, the model does not account for the possibility that a higher temperature working fluid might require more advanced materials that could cost more and have higher life-cycle emissions. The effect of pressure ratio is modest compared to air-fuel ratio, where a pressure ratio of 8 results in a slightly better ISI compared to the alternatives.

7.2.2 Wind-Diesel System

The wind-diesel system utilizes a diesel generator when the available wind power is insufficient to meet the heat, cold, and electrical energy demands of the community. The daily demand for diesel fuel fluctuates over the course of a year (Figure 7.15).

The fluctuations in diesel fuel demand mirror the fluctuations in wind speed. Diesel fuel consumption over the course of one year is approximately 110,000 kg, which is less than half of the natural gas consumption for the reference system. This amount of diesel fuel consumption is specifically for a wind turbine with a rotor radius of 20 m and a rated wind speed and power of 15 m s^{-1} and 650 kW, respectively.

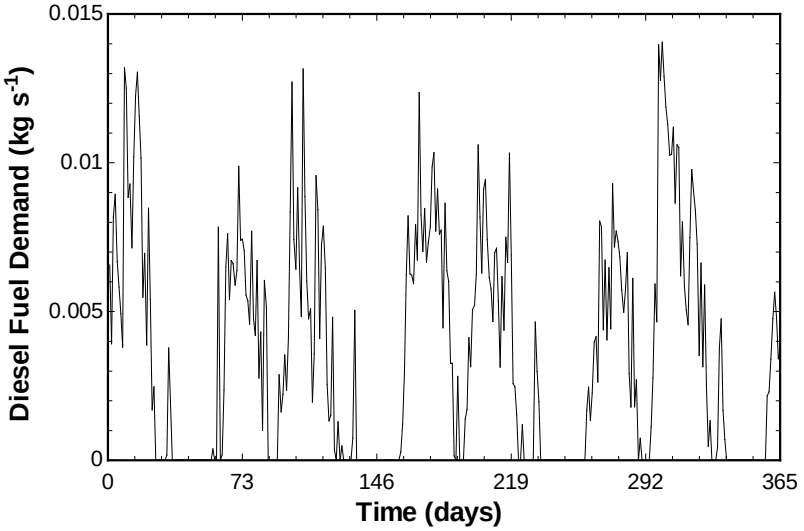

Figure 7.15: Diesel fuel demand over one year for a 50-household community in Ontario (day "1" corresponds to August 1, 2009).

Each component of the wind-diesel system is associated with a certain amount of exergy destruction. The annual exergy destruction for each subsystem over 365 days is presented in Figure 7.16.

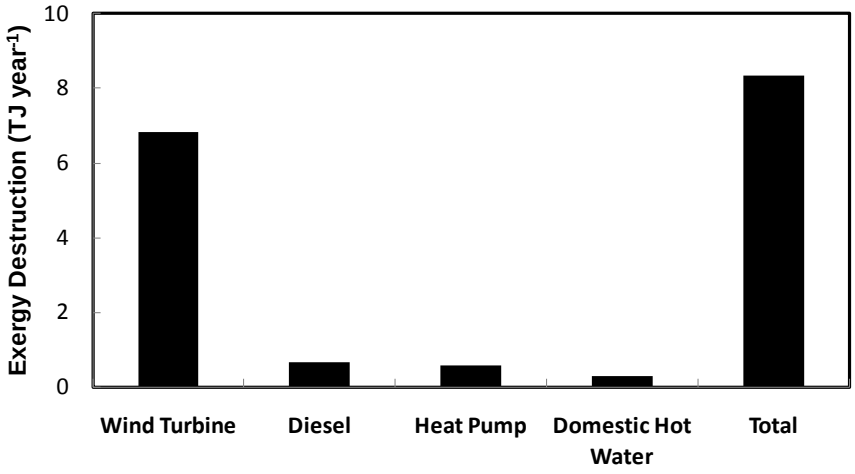

Figure 7.16: Annual exergy destruction of subsystems in the wind-diesel system over a one-year period.

The largest share of exergy destruction is attributed to the wind turbine subsystem (6.8 TJ per year) because only a fraction of the kinetic energy in wind is converted to

power. In addition, the cut-in wind speed curtails electricity production at wind speeds below 5 m s^{-1} (Berg, 2007), which also contributes to wind turbine exergy destruction. Since total exergy destruction is 8.4 TJ per year, the wind turbine subsystem is responsible for 82% of the total annual exergy destruction. The energy and exergy efficiencies of the system are 25% and 17%, respectively.

A thermodynamic analysis of the system is a precursor to sustainability assessment. Thermodynamic, cost, and life-cycle emission factors are combined with weighting factors for three different perspectives to yield the sustainability assessment results presented in Tables 7.23-7.25.

Table 7.23: Sustainability assessment results for the wind-diesel system from the individualist perspective.

Category	Sub-indicator	$B_{i,j}$	$W_{i,j}$	B_j	W_j	$B_j \times W_j$
ER	EnER	0.08	0.00	0.00	0.07	0.000
	ExER	0.55	1.00	0.55		0.037
EF	AF	1.00	0.50	0.50	0.42	0.211
	CV	1.00	0.50	0.50		0.211
SF	Mass	0.00	0.00	0.00	0.04	0.000
	Area	1.00	1.00	1.00		0.042
	Volume	0.00	0.00	0.00		0.000
GEIP	GWP	0.05	0.24	0.01	0.11	0.001
	SODP	0.02	0.69	0.01		0.001
	ADP	1.00	0.07	0.07		0.007
APP	$PM_{2.5}$	1.00	0.21	0.21	0.30	0.062
	PM_{10}	1.00	0.21	0.21		0.062
	SO_2	1.00	0.04	0.04		0.013
	CO	1.00	0.11	0.11		0.033
	NO_2	1.00	0.11	0.11		0.033
	O_3	1.00	0.11	0.11		0.033
	Pb	1.00	0.21	0.21		0.061
WPP	EP	1.00	0.08	0.08	0.07	0.005
	FAETP	1.00	0.78	0.78		0.051
	MAETP	0.17	0.14	0.02		0.002
ISI						**0.86**

Table 7.24: Sustainability assessment results for the wind-diesel system from the egalitarian perspective.

Category	Sub-indicator	$B_{i,j}$	$W_{i,j}$	B_j	W_j	$B_j \times W_j$
ER	EnER	0.08	0.00	0.00	0.16	0.000
	ExER	0.55	1.00	0.55		0.088
EF	AF	1.00	0.67	0.67	0.04	0.029
	CV	1.00	0.33	0.33		0.015
SF	Mass	0.00	0.00	0.00	0.25	0.000
	Area	1.00	1.00	1.00		0.247
	Volume	0.00	0.00	0.00		0.000
GEIP	GWP	0.05	0.65	0.03	0.37	0.011
	SODP	0.02	0.25	0.00		0.002
	ADP	1.00	0.11	0.11		0.040
APP	$PM_{2.5}$	1.00	0.04	0.04	0.03	0.001
	PM_{10}	1.00	0.04	0.04		0.001
	SO_2	1.00	0.15	0.15		0.004
	CO	1.00	0.04	0.04		0.001
	NO_2	1.00	0.15	0.15		0.004
	O_3	1.00	0.04	0.04		0.001
	Pb	1.00	0.52	0.52		0.013
WPP	EP	1.00	0.08	0.08	0.15	0.013
	FAETP	1.00	0.19	0.19		0.030
	MAETP	0.17	0.72	0.12		0.019
ISI						**0.52**

Much like the reference system, the wind-diesel system has a much better ISI from the individualist perspective compared to the egalitarian and hierarchist perspectives. Most fossil-fired energy systems are expected to produce high GHG and ozone-depleting substance (due to N_2O) emissions. This leads to a poor result for the GEIP, which is not weighted as heavily for the individualist perspective compared to others. A general observation noted from this case study and others is that the distance between the individualist and egalitarian ISI of fossil-fired systems is much larger than the distance for renewable-based systems. Moreover, the individualist ISI of a fossil-fired system is not always better than a renewable-based system and the egalitarian ISI of a renewable-based system is not always better than a fossil-fired system.

Table 7.25: Sustainability assessment results for the wind-diesel system from the hierarchist perspective.

Category	Sub-indicator	$B_{i,j}$	$W_{i,j}$	B_j	W_j	$B_j \times W_j$
ER	EnER	0.08	0.00	0.00	0.15	0.000
	ExER	0.55	1.00	0.55		0.085
EF	AF	1.00	0.67	0.67	0.17	0.115
	CV	1.00	0.33	0.33		0.057
SF	Mass	0.00	0.00	0.00	0.15	0.000
	Area	1.00	1.00	1.00		0.153
	Volume	0.00	0.00	0.00		0.000
GEIP	GWP	0.05	0.57	0.03	0.31	0.008
	SODP	0.02	0.33	0.01		0.002
	ADP	1.00	0.10	0.10		0.030
APP	$PM_{2.5}$	1.00	0.10	0.10	0.08	0.008
	PM_{10}	1.00	0.10	0.10		0.008
	SO_2	1.00	0.10	0.10		0.008
	CO	1.00	0.05	0.05		0.004
	NO_2	1.00	0.17	0.17		0.013
	O_3	1.00	0.05	0.05		0.004
	Pb	1.00	0.44	0.44		0.036
WPP	EP	1.00	0.08	0.08	0.13	0.011
	FAETP	1.00	0.58	0.58		0.075
	MAETP	0.17	0.34	0.06		0.008
ISI						**0.62**

Sustainability sub-indicators in Tables 7.23-7.25 with a $B_{i,j}$ value equal to one have no negative effect on ISI. Sub-indicators with a $B_{i,j}$ value less than one will have a negative effect on ISI, which is a function of the actual $B_{i,j}$ value and its weight. The reduction in ISI of each sustainability sub-indicator is graphed in Figure 7.17.

Once again, the GWP sub-indicator exhibits the greatest influence on the ISI. It has the potential to reduce ISI by 0.026 to 0.23 units. On the other hand, the SODP sub-indicator can only reduce ISI by 0.073 to 0.102 units. In addition, the ExER and MAETP sub-indicators can only reduce ISI by 0.029 to 0.071 and 0.007 to 0.092, respectively. This illustrates the critical shortcoming of fossil-fired energy systems as sources of GHG emissions.

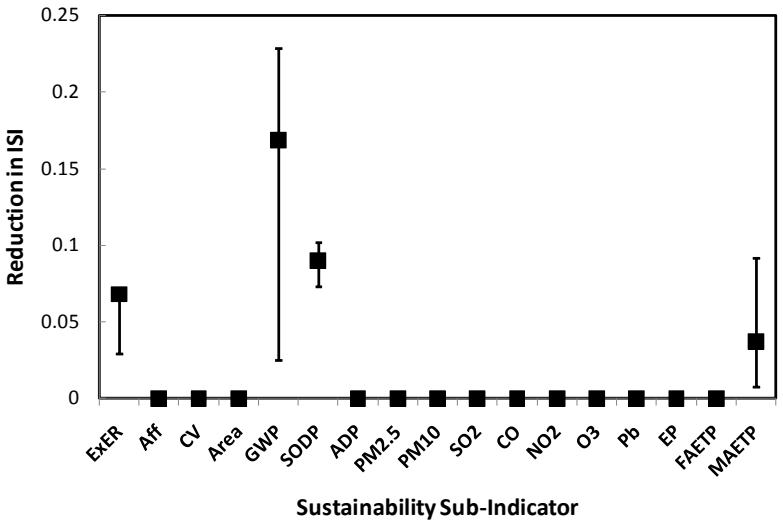

Figure 7.17: Reduction in ISI for each sustainability sub-indicator for the wind-diesel system.

The impact of this system on global warming and stratospheric ozone depletion is studied in more detail in Figures 7.18 and 7.19. The point of intersection in Figure 7.18 occurs at a population of approximately 300 million, which is higher than the reference system but still significantly short of the existing global population of 7 billion.

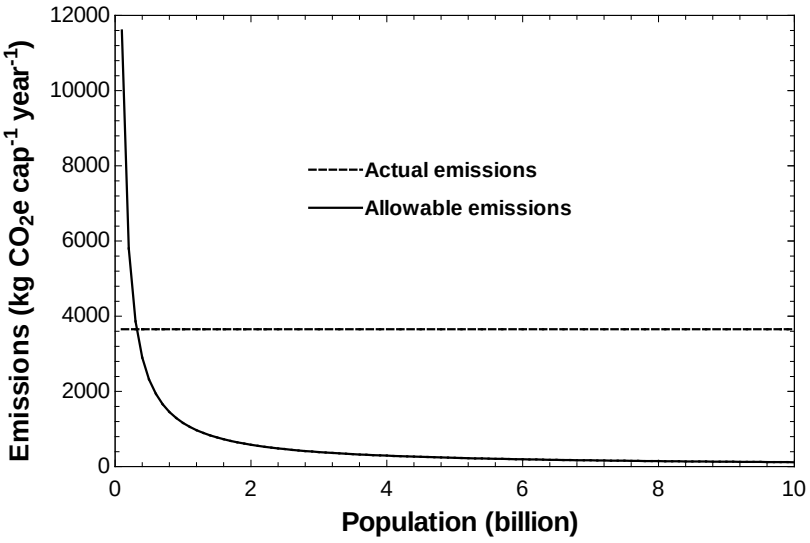

Figure 7.18: Actual and allowable annual per capita GHG emissions for the wind-diesel system based on the lower limit of the representative concentration pathway (RCP2.6) carbon budget.

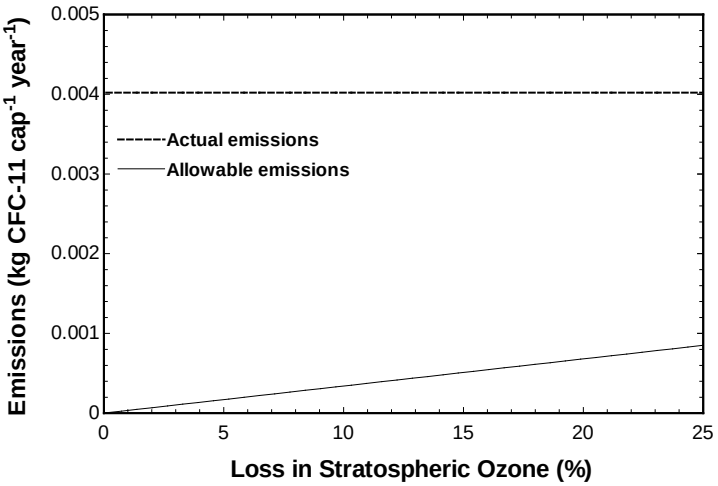

Figure 7.19: Actual and allowable annual per capita ozone-depleting substance emissions (including N_2O) for the wind-diesel system with respect to the percent loss in stratospheric ozone over the time scale for considering sustainability.

Ozone-depleting substance emissions are consistent with an annual loss in stratospheric ozone of approximately 1.2%, which is even higher than the reference system. It should be noted that diesel engines are notorious for producing high amounts of NO_X and N_2O (Koebel et al., 2000), the latter being an ozone-depleting substance.

The ISI of an energy system is a function of the time scale for considering sustainability. The effect of this parameter is illustrated in Figure 7.20.

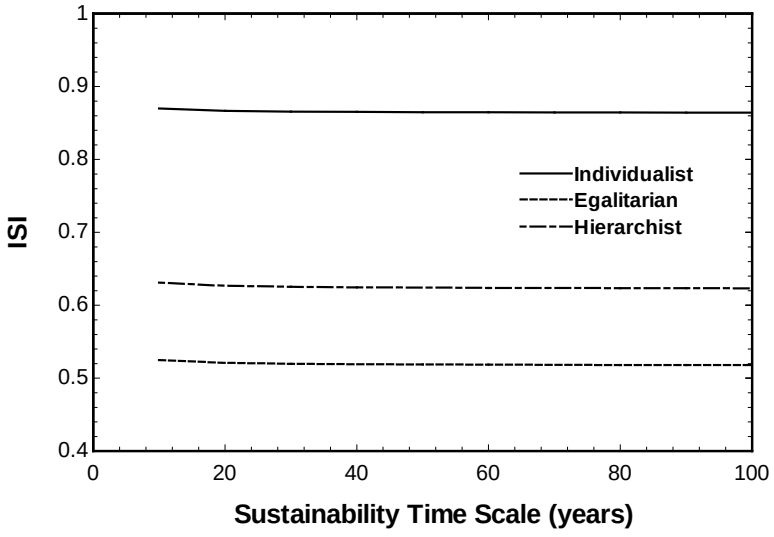

Figure 7.20: Variation of ISI with respect to the time scale for considering sustainability for the wind-diesel system.

Variations in the sustainability time scale do not have a noticeable effect as the ISI of the wind-diesel system decreases very modestly for each perspective.

Weighting factors can have a significant influence on the ISI of a system. The effect of weighting factor on the most critical sub-indicators is investigated in Figures 7.21 and 7.22.

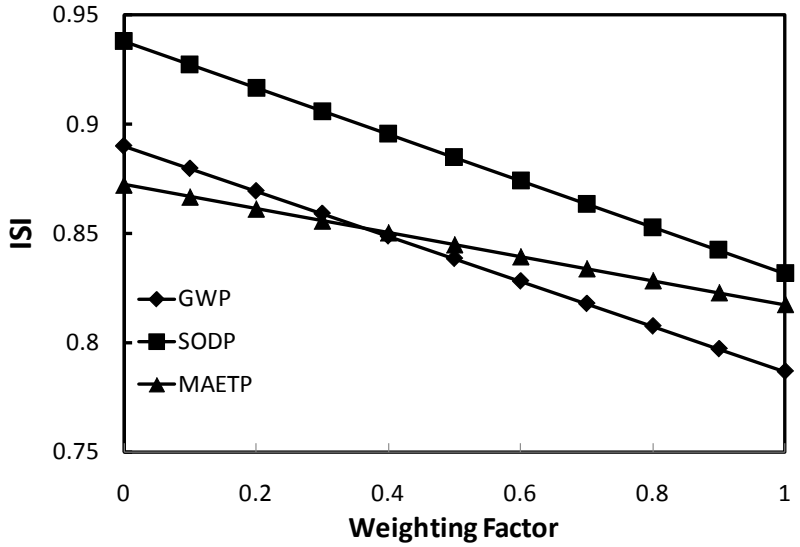

Figure 7.21: Variation of the individualist ISI with respect to weighting factor for the wind-diesel system.

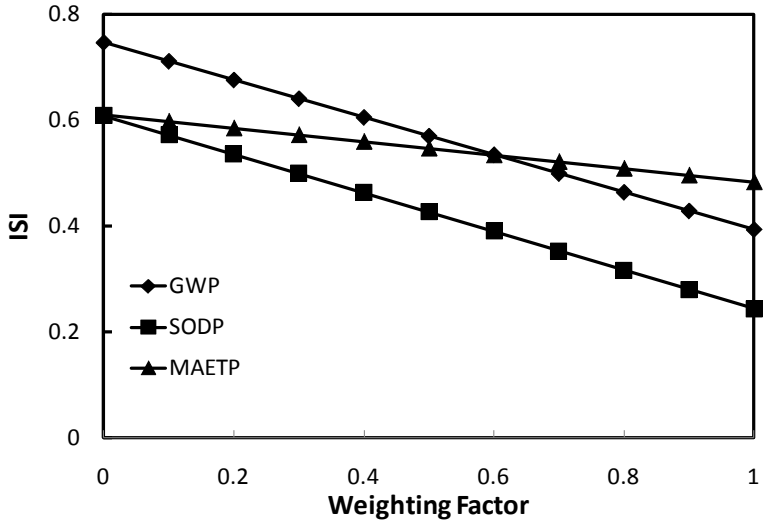

Figure 7.22: Variation of the egalitarian ISI with respect to weighting factor for the wind-diesel system.

The SODP and GWP weighting factors have the greatest impact. Excluding ozone layer depletion from consideration in the analysis increases the individualist ISI of the wind-diesel system from 0.86 (Table 7.23) to 0.94. Similarly, excluding climate change increases the egalitarian ISI from 0.52 (Table 7.24) to 0.75. Assignment of these weighting factors is critical in estimating the sustainability of the system. The weighting factor for MAETP is not as much of a factor.

The rotor radius of the wind turbine is an important parameter for the wind-diesel system. The size of the wind turbine is arbitrary for this system configuration due to the back-up diesel generator. The impact of the rotor radius on ISI is illustrated in Figure 7.23.

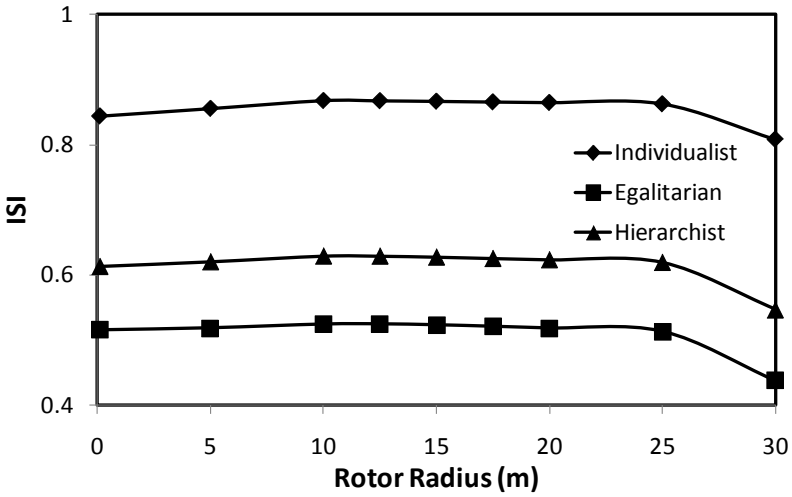

Figure 7.23: Variation of ISI with respect to wind turbine rotor radius for the wind-diesel system.

Increasing the size of the wind turbine allows for more wind-based generation, which can reduce demand on the back-up diesel generator. However, the size of the turbine is irrelevant on days when the wind speed is below the cut-in or above the cut-out speed. On these occasions the community is reliant on the back-up diesel subsystem.

Figure 7.23 shows that there is no benefit to the ISI when increasing the rotor radius beyond 12.5 m. In fact, there is steep decline in ISI when the rotor radius increases from

25 to 30 m. This occurs because a wind turbine with a 30 m rotor radius does not displace enough diesel fuel to offset the increase in cost and life-cycle emissions associated with a larger wind turbine.

The air-fuel ratio and pressure ratio of the diesel-fired subsystem are important parameters for the wind-diesel system. The impacts of these parameters on ISI are illustrated in Figures 7.24 and 7.25.

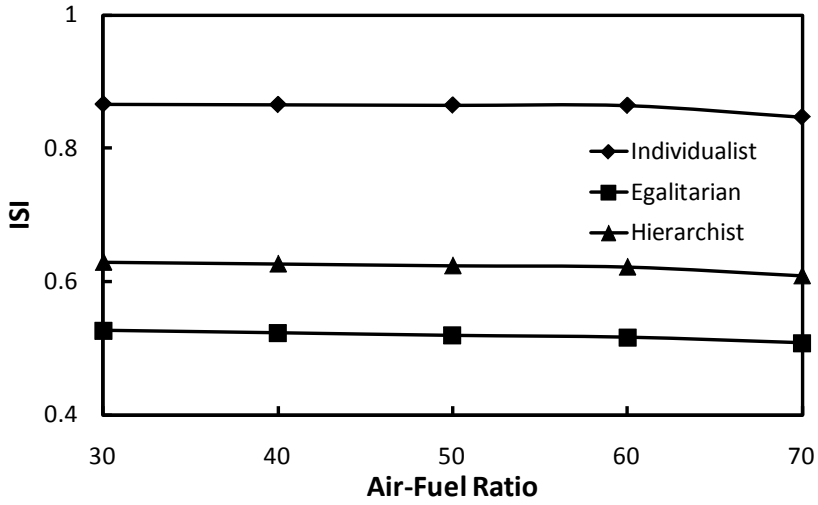

Figure 7.24: Variation of ISI with respect to air-fuel ratio for the wind-diesel system.

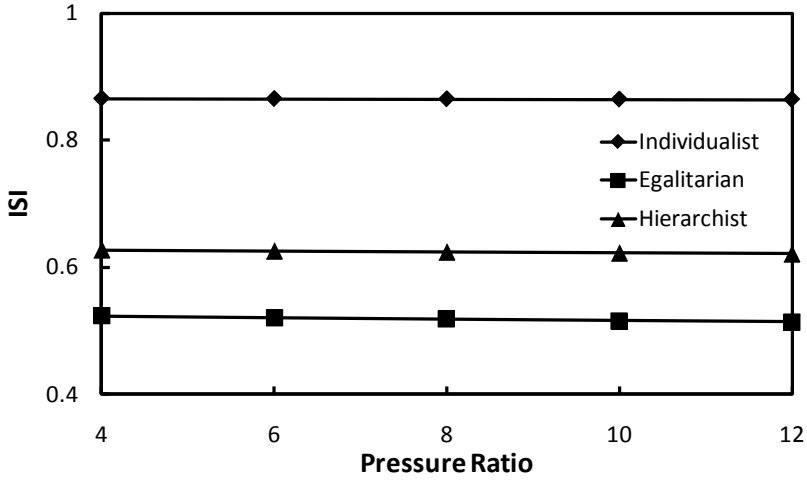

Figure 7.25: Variation of ISI with respect to pressure ratio for the wind-diesel system.

The impacts of air-fuel ratio and pressure ratio on ISI are similar to the impacts observed for the reference system. As was the case with the reference system, increasing the air-fuel ratio improves ISI although the model does not account for design changes due to a higher working fluid temperature. The effect of pressure ratio on ISI is negligible for the wind-diesel system.

7.2.3 Wind-Battery System

A wind turbine on its own is insufficient to ensure a reliable source of heat, cold, and power for a community and needs to be integrated with an energy storage device. Moreover, for a stand-alone energy system, the wind turbine needs to be large enough such that after a year of operation the net accumulation of energy in storage is positive. Figure 7.26 illustrates the behaviour of the lead-acid battery in the wind-battery system over the course of one year for a wind turbine with a rotor radius of 20 m.

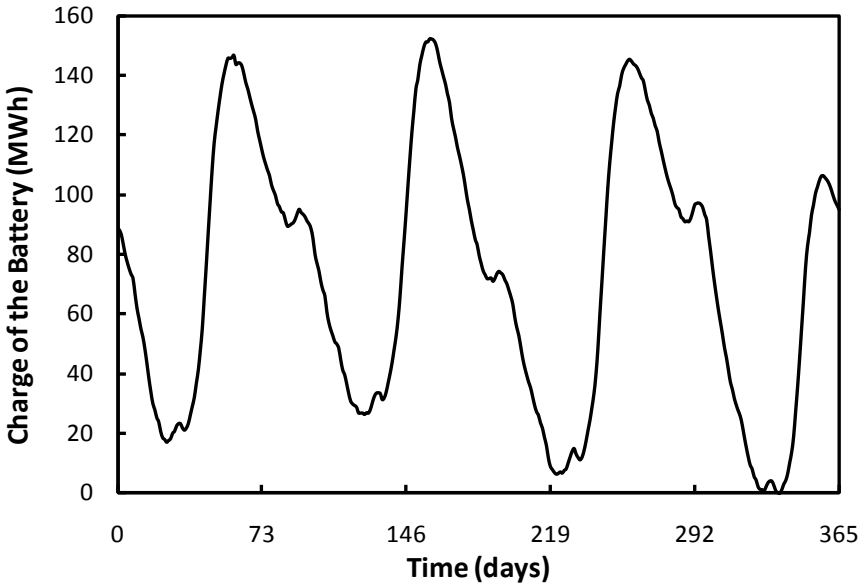

Figure 7.26: Variation in the charge of the battery over the course of one year for the wind-battery system (day "1" corresponds to August 1, 2009).

The battery discharges at the start of the year to compensate for low wind speeds but then enters a charging mode, where surplus electricity is generated due to higher wind

speeds. The battery cycles through charging and discharging modes until day 365, where the net accumulation of electrical energy is 4 MWh. The capacity of the battery to ensure a reliable supply of energy to the community needs to be at least 150 MWh.

Each component of the wind-battery system is associated with a certain amount of exergy destruction. The exergy destruction rates for each subsystem over 365 days are presented in Figure 7.27.

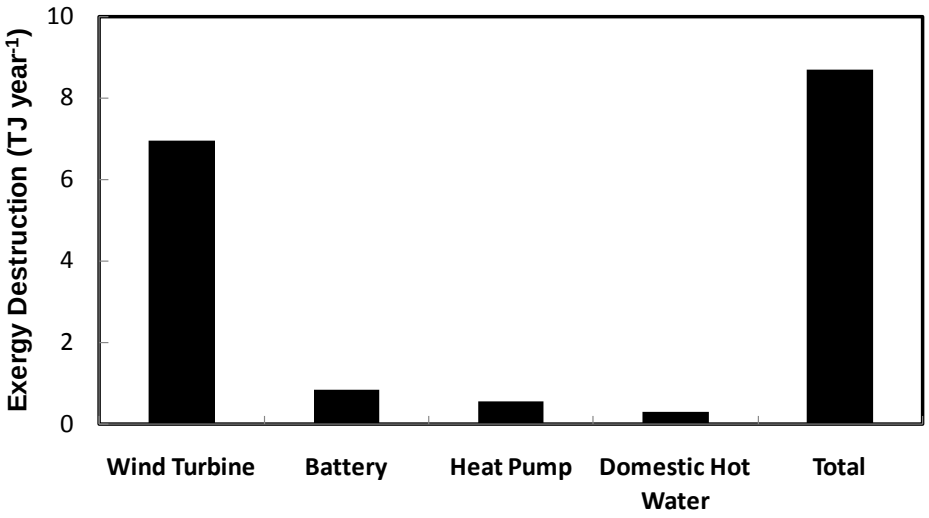

Figure 7.27: Annual exergy destruction of subsystems in the wind-battery system over a one-year period.

The largest share of exergy destruction is attributed to the wind turbine subsystem (7.0 TJ per year). Since total exergy destruction is 8.7 TJ per year, the wind turbine subsystem is responsible for 80% of the total exergy destruction. The lead-acid battery also makes a modest contribution to exergy destruction (0.85 TJ per year or 10% of the total).

A thermodynamic analysis of the system is a precursor to sustainability assessment. Thermodynamic, cost, and life-cycle emission factors are combined with weighting factors for three different perspectives to yield the sustainability assessment results presented in Tables 7.26-7.28.

Table 7.26: Sustainability assessment results for the wind-battery system from the individualist perspective.

Category	Sub-indicator	$B_{i,j}$	$W_{i,j}$	B_j	W_j	$B_j \times W_j$
ER	EnER	0.14	0.00	0.00	0.07	0.000
	ExER	0.37	1.00	0.37		0.024
EF	AF	0.09	0.50	0.05	0.42	0.019
	CV	1.00	0.50	0.50		0.211
SF	Mass	0.00	0.00	0.00	0.04	0.000
	Area	1.00	1.00	1.00		0.042
	Volume	0.00	0.00	0.00		0.000
GEIP	GWP	0.10	0.24	0.02	0.11	0.003
	SODP	0.07	0.69	0.05		0.005
	ADP	1.00	0.07	0.07		0.007
APP	$PM_{2.5}$	1.00	0.21	0.21	0.30	0.062
	PM_{10}	1.00	0.21	0.21		0.062
	SO_2	1.00	0.04	0.04		0.013
	CO	1.00	0.11	0.11		0.033
	NO_2	1.00	0.11	0.11		0.033
	O_3	1.00	0.11	0.11		0.033
	Pb	1.00	0.21	0.21		0.061
WPP	EP	0.66	0.08	0.05	0.07	0.004
	FAETP	0.25	0.78	0.20		0.013
	MAETP	0.02	0.14	0.00		0.000
ISI						**0.62**

The ISI of the wind-battery system ranges from 0.44 to 0.62, where the primary determinant of the score depends on the perspective. The EF category, specifically the AF sub-indicator, is the largest contributor to the score for the individualist perspective. The expected annual cost of a stand-alone wind-battery system to a household is approximately $76,000 whereas the median after-tax income of a household in Ontario is $69,300 (Statistics Canada, 2012), of which no more than 10% should be allocated to energy needs (Fankhauser and Tepic, 2007).

The GEIP, especially the GWP sub-indicator, is the largest contributor to the ISI score for both the egalitarian and hierarchist perspectives. Both perspectives weigh the category quite heavily but per capita annual life-cycle GHG emissions are 1700 kg CO_2e for the wind-battery system whereas the international carbon budget dictated by

RCP2.6 is 166 kg CO_2e, assuming that 20% of emissions are allocated to household energy services (OEE, 2013).

Table 7.27: Sustainability assessment results for the wind-battery system from the egalitarian perspective.

Category	Sub-indicator	$B_{i,j}$	$W_{i,j}$	B_j	W_j	$B_j \times W_j$
ER	EnER	0.14	0.00	0.00	0.16	0.000
	ExER	0.37	1.00	0.37		0.059
EF	AF	0.09	0.67	0.06	0.04	0.003
	CV	1.00	0.33	0.33		0.015
SF	Mass	0.00	0.00	0.00	0.25	0.000
	Area	1.00	1.00	1.00		0.247
	Volume	0.00	0.00	0.00		0.000
GEIP	GWP	0.10	0.65	0.06	0.37	0.023
	SODP	0.07	0.25	0.02		0.006
	ADP	1.00	0.11	0.11		0.040
APP	$PM_{2.5}$	1.00	0.04	0.04	0.03	0.001
	PM_{10}	1.00	0.04	0.04		0.001
	SO_2	1.00	0.15	0.15		0.004
	CO	1.00	0.04	0.04		0.001
	NO_2	1.00	0.15	0.15		0.004
	O_3	1.00	0.04	0.04		0.001
	Pb	1.00	0.52	0.52		0.013
WPP	EP	0.66	0.08	0.05	0.15	0.008
	FAETP	0.25	0.19	0.05		0.007
	MAETP	0.02	0.72	0.02		0.003
ISI						**0.44**

Sustainability sub-indicators in Tables 7.26-7.28 with a $B_{i,j}$ value equal to one have no negative effect on ISI. Sub-indicators with a $B_{i,j}$ value less than one will have a negative effect on ISI, which is a function of the actual $B_{i,j}$ value and its weight. The reduction in ISI of each sustainability sub-indicator is graphed in Figure 7.28. This is the first case study based entirely on renewable energy and storage, which leads to different results compared to the reference case and the wind-diesel system.

Table 7.28: Sustainability assessment results for the wind-battery system from the hierarchist perspective.

Category	Sub-indicator	$B_{i,j}$	$W_{i,j}$	B_j	W_j	$B_j \times W_j$
ER	EnER	0.14	0.00	0.00	0.15	0.000
	ExER	0.37	1.00	0.37		0.057
EF	AF	0.09	0.67	0.06	0.17	0.010
	CV	1.00	0.33	0.33		0.057
SF	Mass	0.00	0.00	0.00	0.15	0.000
	Area	1.00	1.00	1.00		0.153
	Volume	0.00	0.00	0.00		0.000
GEIP	GWP	0.10	0.57	0.05	0.31	0.017
	SODP	0.07	0.33	0.02		0.007
	ADP	1.00	0.10	0.10		0.030
APP	$PM_{2.5}$	1.00	0.10	0.10	0.08	0.008
	PM_{10}	1.00	0.10	0.10		0.008
	SO_2	1.00	0.10	0.10		0.008
	CO	1.00	0.05	0.05		0.004
	NO_2	1.00	0.17	0.17		0.013
	O_3	1.00	0.05	0.05		0.004
	Pb	1.00	0.44	0.44		0.036
WPP	EP	0.66	0.08	0.05	0.13	0.007
	FAETP	0.25	0.58	0.14		0.019
	MAETP	0.02	0.34	0.01		0.001
ISI						**0.44**

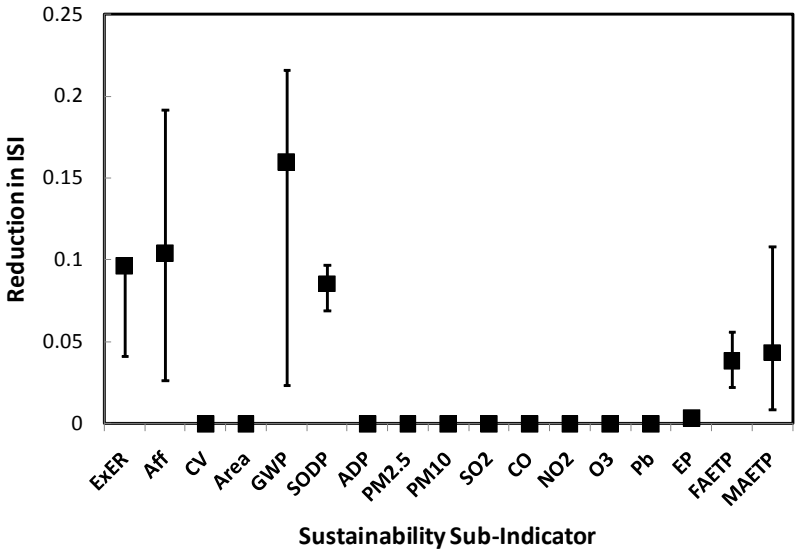

Figure 7.28: Reduction in ISI for each sustainability sub-indicator for the wind-battery system.

The GWP sub-indicator once again exhibits a substantial influence on the ISI of the system while the SODP and ExER are still relevant. However, AF is also a significant factor due to the substantial cost associated with a large lead-acid battery essential for ensuring a reliable supply of energy to the community. The impact of this system on global warming and stratospheric ozone depletion is studied in more detail in Figures 7.29 and 7.30.

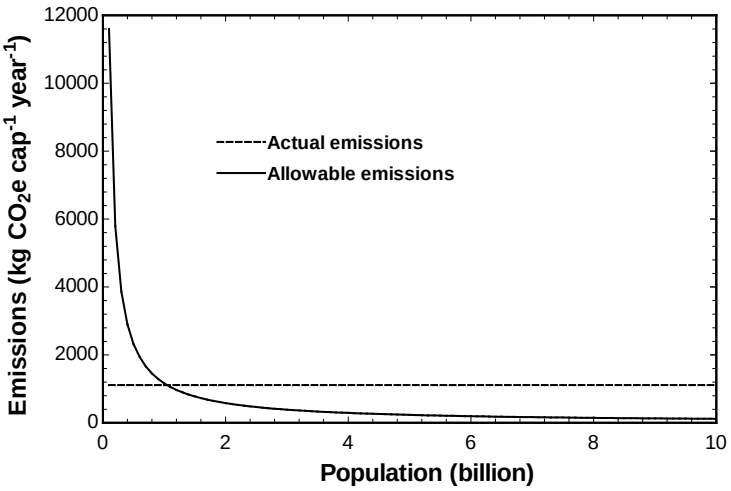

Figure 7.29: Actual and allowable annual per capita GHG emissions for the wind-diesel system based on the lower limit of the representative concentration pathway (RCP2.6) carbon budget.

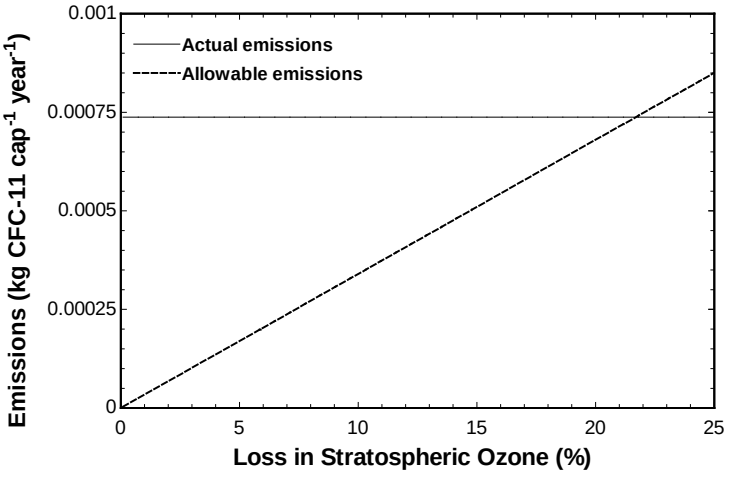

Figure 7.30: Actual and allowable annual per capita ozone-depleting substance emissions (including N_2O) with respect to the percent loss in stratospheric ozone over the time scale for considering sustainability.

The point of intersection in Figure 7.29 occurs at a population of approximately 1 billion, which is much higher than the previously considered fossil-fired systems but still significantly short of the existing global population of 7 billion. Similarly, emissions of ozone-depleting substances are consistent with an annual loss in stratospheric ozone of approximately 0.2%, which is also much less than the anticipated stratospheric ozone depletion for fossil-fired systems.

The sustainability time scale has a more pronounced effect on the ISI of the wind-battery system compared to both the reference and wind-diesel systems (Figure 7.31).

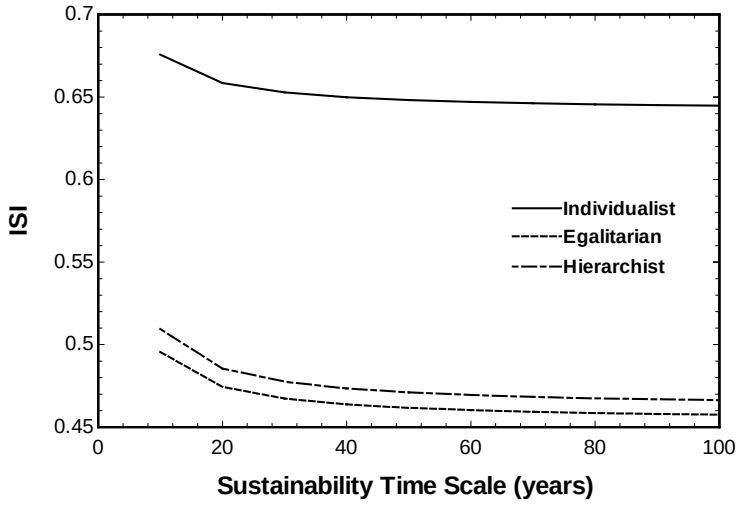

Figure 7.31: Variation of ISI with respect to the time scale for considering sustainability for the wind-battery system.

The effect of the time scale for considering sustainability on the ISI can best be described by an example. For example, the SODP of both the reference and wind-diesel systems is very low (i.e., $B_{GEIP,SODP} \approx 0$). The shape of the non-dimensional sub-indicator function (Figure 4.1) shows that an increase in $A_{i,j}$ when $B_{i,j}$ is already close to its minimum has little to no effect. This model of sustainability implies that a highly unsustainable situation does not substantially improve or deteriorate without larger changes. The opposite is true at the other end of the curve, where perturbations have a larger effect on the ISI of the system. The B-value of the SODP of the wind-battery

system is low (0.092) but still better than the fossil-fired systems, which makes it more sensitive to the time scale for considering sustainability.

The effect of weighting factor on the most critical sub-indicators is investigated in Figures 7.32 and 7.33.

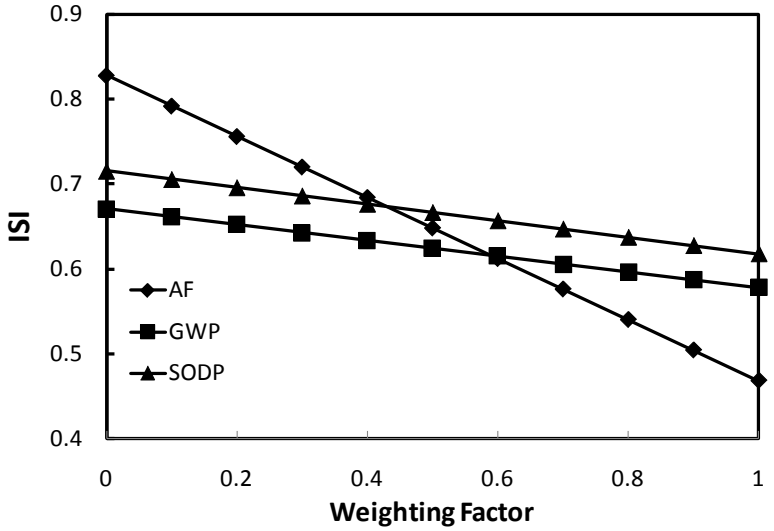

Figure 7.32: Variation of the individualist ISI with respect to weighting factor for the wind-battery system.

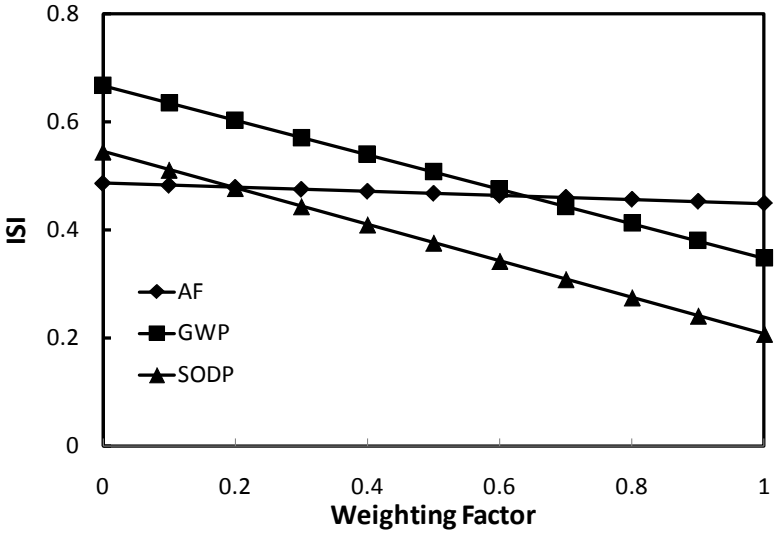

Figure 7.33: Variation of the egalitarian ISI with respect to weighting factor for the wind-battery system.

Figure 7.32 demonstrates that the individualist ISI is highly sensitive to the weighting factor attached to the AF sub-indicator. The individualist ISI ranges from 0.47 to 0.83 depending on the AF weighting factor. By comparison, the effect of GWP and SODP are minor.

The opposite is true for Figure 7.33, where the egalitarian ISI is very insensitive to the AF weighting factor and much more dependent on the GWP and SODP. For example, by excluding climate change from the analysis, the egalitarian ISI increases from 0.46 (Table 7.27) to 0.67.

The size of the wind turbine for a wind-battery system is not arbitrary as was the case for a wind-diesel system. There is a minimum rotor radius for a given set of demand criteria and operating conditions to meet the community's needs and ensure reliable energy supply.

Parameters that can have an effect on the ISI of the wind-battery system are the mechanical efficiency of the wind turbine and the charging efficiency of the battery. The impact wind turbine mechanical efficiency and battery charging efficiency appear in Figures 7.34 and 7.35, respectively.

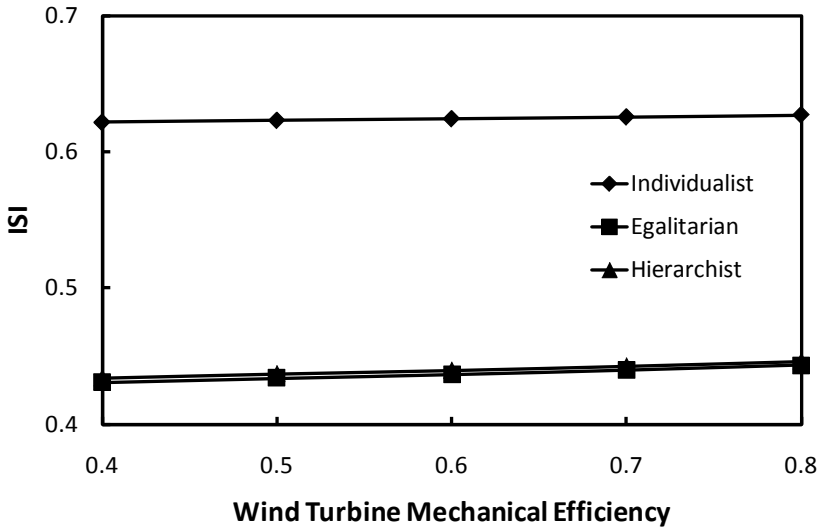

Figure 7.34: Variation of ISI with respect to wind turbine mechanical efficiency for the wind-diesel system.

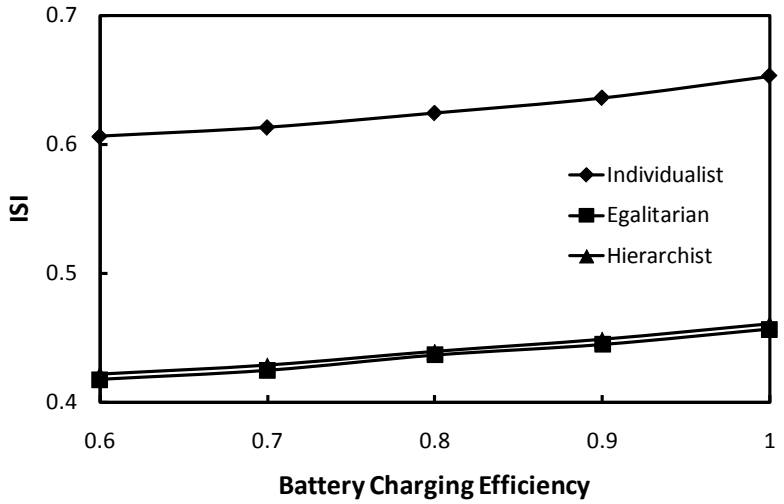

Figure 7.35: Variation of ISI with respect to wind turbine mechanical efficiency for the wind-diesel system.

Increasing the wind turbine and the battery charging efficiencies have modest but positive effects on ISI. More efficient energy conversion devices can reduce the size of the system and its life-cycle emissions. However, more advanced devices might also incur greater costs, which can have a negative effect on ISI.

7.2.4 Wind-Hydrogen System

Another option for storage is to integrate a wind turbine with hydrogen storage. Figure 7.36 illustrates the behaviour of the hydrogen storage subsystem over the course of one year for a wind turbine with a rotor radius of 28 m.

The hydrogen storage tanks are discharged at the start of the year to compensate for low wind speeds but are then charged when surplus electricity is generated due to higher wind speeds. The storage tanks cycle through stages of charging and discharging until day 365, when the net accumulation of hydrogen is 120 kg. According to Figure 7.36, the total capacity of the hydrogen storage tanks to ensure a reliable supply of energy to the community needs to be at least 8550 kg.

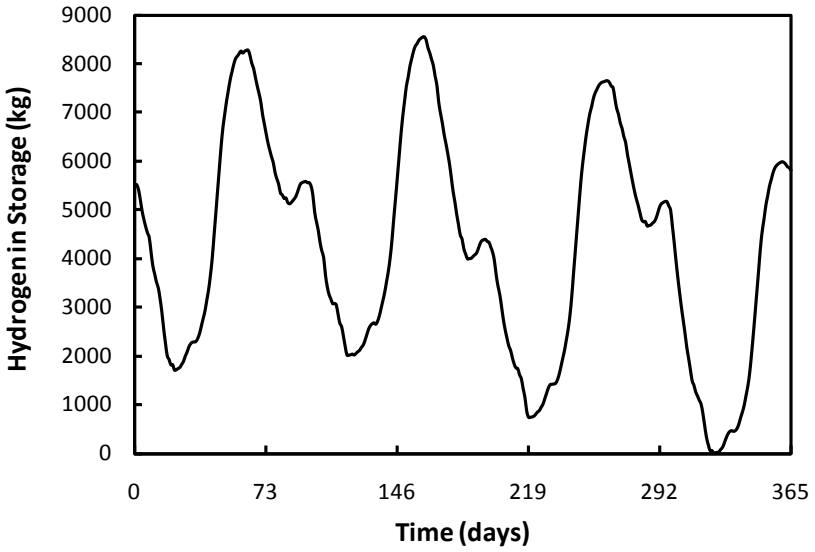

Figure 7.36: Variation in the amount of hydrogen in the storage tanks over the course of one year for the wind-hydrogen system (day "1" corresponds to August 1, 2009).

Each component of the wind-hydrogen system is associated with a certain amount of exergy destruction. The exergy destruction rates for each subsystem over 365 days are presented in Figure 7.37.

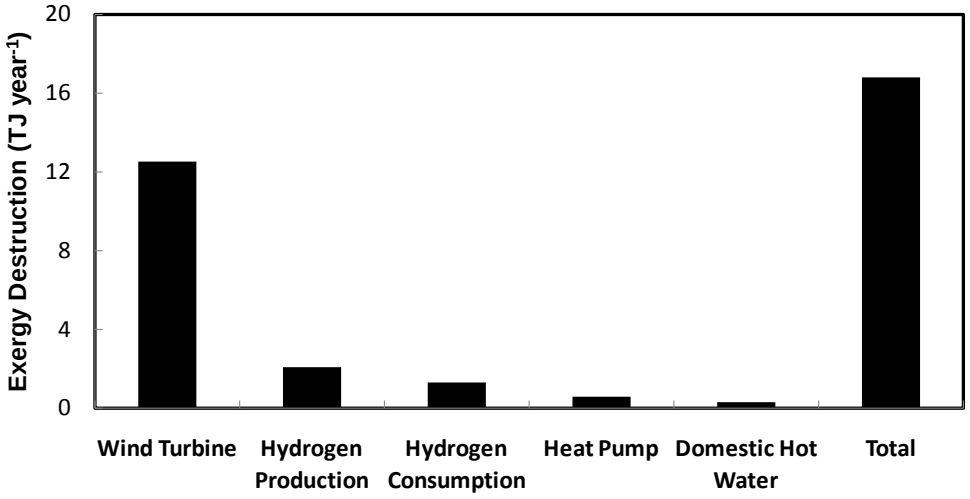

Figure 7.37: Annual exergy destruction of subsystems in the wind-hydrogen system over a one-year period.

The largest share of annual exergy destruction is attributed to the wind turbine subsystem (13 TJ per year). Since total exergy destruction is 18 TJ per year, the wind turbine subsystem is responsible for 72% of the total annual exergy destruction. The energy and exergy efficiencies of the system are 18% and 15%, respectively

A thermodynamic analysis of the system is a precursor to sustainability assessment. Thermodynamic, cost, and life-cycle emission factors are combined with weighting factors for three different perspectives to yield the sustainability assessment results presented in Tables 7.29-7.31.

Table 7.29: Sustainability assessment results for the wind-hydrogen system from the individualist perspective.

Category	Sub-indicator	$B_{i,j}$	$W_{i,j}$	B_j	W_j	$B_j \times W_j$
ER	EnER	0.58	0.00	0.00	0.07	0.000
	ExER	0.67	1.00	0.67		0.044
EF	AF	0.86	0.50	0.43	0.42	0.180
	CV	1.00	0.50	0.50		0.211
SF	Mass	0.00	0.00	0.00	0.04	0.000
	Area	0.91	1.00	0.91		0.038
	Volume	0.00	0.00	0.00		0.000
GEIP	GWP	0.23	0.24	0.06	0.11	0.006
	SODP	0.14	0.69	0.10		0.010
	ADP	1.00	0.07	0.07		0.007
APP	$PM_{2.5}$	1.00	0.21	0.21	0.30	0.062
	PM_{10}	1.00	0.21	0.21		0.062
	SO_2	1.00	0.04	0.04		0.013
	CO	1.00	0.11	0.11		0.033
	NO_2	1.00	0.11	0.11		0.033
	O_3	1.00	0.11	0.11		0.033
	Pb	1.00	0.21	0.21		0.061
WPP	EP	1.00	0.08	0.08	0.07	0.005
	FAETP	0.87	0.78	0.68		0.045
	MAETP	0.14	0.14	0.02		0.001
ISI						**0.84**

Table 7.30: Sustainability assessment results for the wind-hydrogen system from the egalitarian perspective.

Category	Sub-indicator	$B_{i,j}$	$W_{i,j}$	B_j	W_j	$B_j \times W_j$
ER	EnER	0.58	0.00	0.00	0.16	0.000
	ExER	0.67	1.00	0.67		0.106
EF	AF	0.86	0.67	0.57	0.04	0.025
	CV	1.00	0.33	0.33		0.015
SF	Mass	0.00	0.00	0.00	0.25	0.000
	Area	0.91	1.00	0.91		0.224
	Volume	0.00	0.00	0.00		0.000
GEIP	GWP	0.23	0.65	0.15	0.37	0.056
	SODP	0.14	0.25	0.03		0.013
	ADP	1.00	0.11	0.11		0.040
APP	$PM_{2.5}$	1.00	0.04	0.04	0.03	0.001
	PM_{10}	1.00	0.04	0.04		0.001
	SO_2	1.00	0.15	0.15		0.004
	CO	1.00	0.04	0.04		0.001
	NO_2	1.00	0.15	0.15		0.004
	O_3	1.00	0.04	0.04		0.001
	Pb	1.00	0.52	0.52		0.013
WPP	EP	1.00	0.08	0.08	0.15	0.013
	FAETP	0.87	0.19	0.17		0.026
	MAETP	0.14	0.72	0.10		0.016
ISI						**0.56**

The ISI for the wind-hydrogen system ranges from 0.55 to 0.83, where the primary determinant of the score depends on the perspective. There are several sub-indicators that have a modest contribution to the ISI for the individualist perspective, such as ExER, AF, GWP, and SODP. The same is true for the egalitarian and hierarchist perspectives.

Sustainability sub-indicators in Tables 7.29-7.31 with a $B_{i,j}$ value equal to one have no negative effect on ISI. Sub-indicators with a $B_{i,j}$ value less than one will have a negative effect on ISI, which is a function of the actual $B_{i,j}$ value and its weight. The range of the negative effect of each sustainability sub-indicator on ISI is graphed in Figure 7.38.

Table 7.31: Sustainability assessment results for the wind-hydrogen system from the hierarchist perspective.

Category	Sub-indicator	$B_{i,j}$	$W_{i,j}$	B_j	W_j	$B_j \times W_j$
ER	EnER	0.58	0.00	0.00	0.15	0.000
	ExER	0.67	1.00	0.67		0.102
EF	AF	0.86	0.67	0.57	0.17	0.098
	CV	1.00	0.33	0.33		0.057
SF	Mass	0.00	0.00	0.00	0.15	0.000
	Area	0.91	1.00	0.91		0.139
	Volume	0.00	0.00	0.00		0.000
GEIP	GWP	0.23	0.57	0.13	0.31	0.041
	SODP	0.14	0.33	0.05		0.014
	ADP	1.00	0.10	0.10		0.030
APP	$PM_{2.5}$	1.00	0.10	0.10	0.08	0.008
	PM_{10}	1.00	0.10	0.10		0.008
	SO_2	1.00	0.10	0.10		0.008
	CO	1.00	0.05	0.05		0.004
	NO_2	1.00	0.17	0.17		0.013
	O_3	1.00	0.05	0.05		0.004
	Pb	1.00	0.44	0.44		0.036
WPP	EP	1.00	0.08	0.08	0.13	0.011
	FAETP	0.87	0.58	0.50		0.065
	MAETP	0.14	0.34	0.05		0.006
ISI						**0.65**

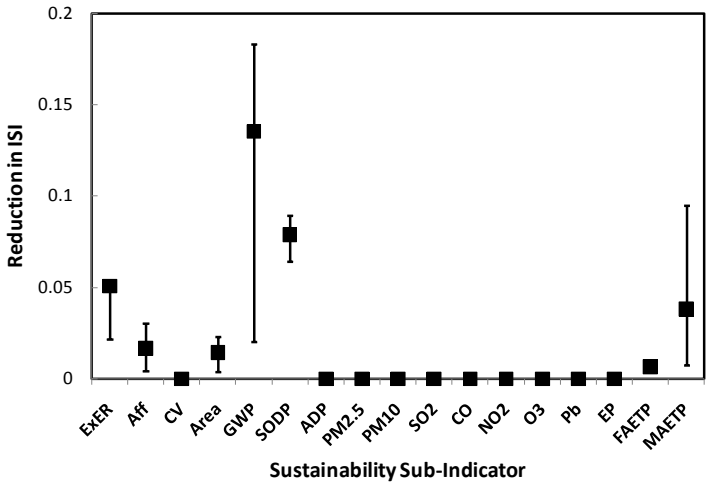

Figure 7.38: Reduction in ISI for each sustainability sub-indicator for the wind-hydrogen system.

Unlike the previous case studies, the Area sub-indicator is relevant to the sustainability of the system. The high exergy destruction rate of the hydrogen storage subsystem necessitates the installation of a larger wind turbine with greater land area requirements to meet the energy needs of the community.

In addition, the GWP and SODP are also very relevant to the sustainability assessment. These two sub-indicators are studied in more detail in Figures 7.39 and 7.40.

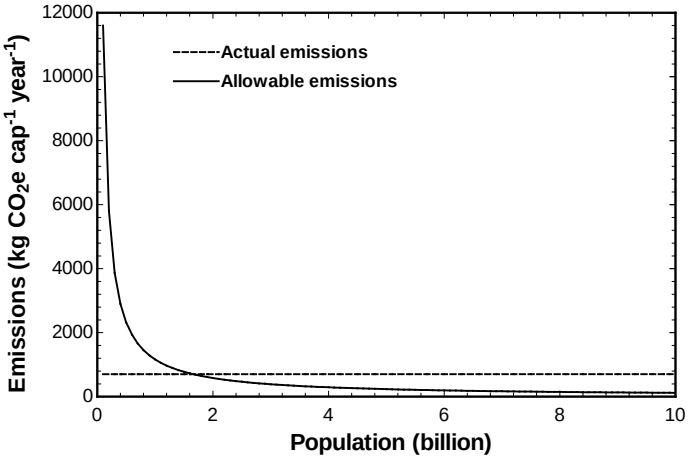

Figure 7.39: Actual and allowable annual per capita GHG emissions for the wind-hydrogen system based on the lower limit of the representative concentration pathway (RCP2.6) carbon budget.

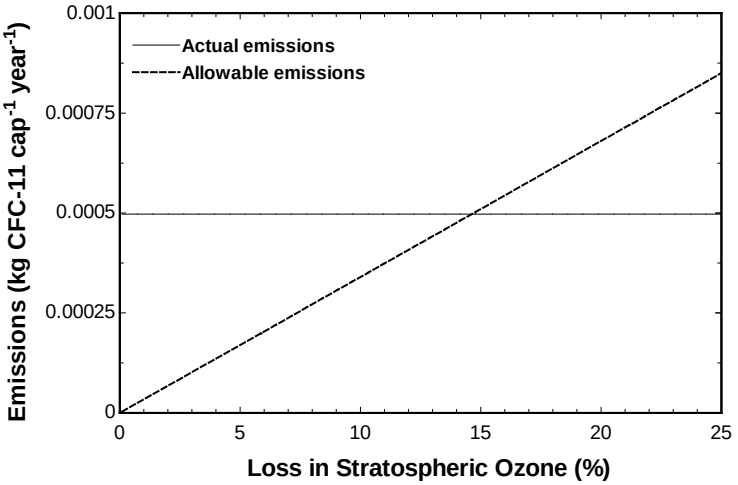

Figure 7.40: Actual and allowable annual per capita ozone-depleting substance emissions (including N_2O) with respect to the percent loss in stratospheric ozone over the time scale for considering sustainability.

The point of intersection in Figure 7.39 occurs at a population of approximately 1.8 billion, which is a further improvement on the wind-battery system but still significantly short of the existing global population of 7 billion. Similarly, emissions of ozone-depleting substances are consistent with a loss in stratospheric ozone of approximately 14%, which is also an improvement but still excessive.

The effect of the length of the sustainability horizon on the ISI (Figure 7.41) is similar to the effect on the wind-battery system. Since the SODP is not approaching zero, there is an observable impact on the ISI for the wind-hydrogen system. Although the time scale for considering sustainability also affects the ADP sub-indicator, its impact is insufficient to have any meaningful effect.

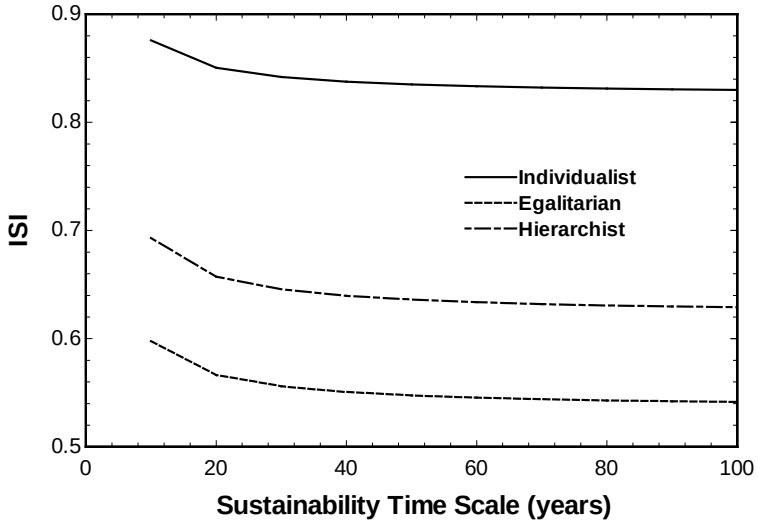

Figure 7.41: Variation of ISI with respect to the time scale for considering sustainability for the wind-hydrogen system.

The effect of weighting factor on the most critical sub-indicators is investigated in Figures 7.42 and 7.43.

The ISI from the individualist perspective (Figure 7.42) is less sensitive to the weighting factor attached to any single sub-indicator but a composite of relevant sub-indicators. This is not the case for the egalitarian perspective (Figure 7.43), where the weighting factors associated with the GWP and SODP are the most significant.

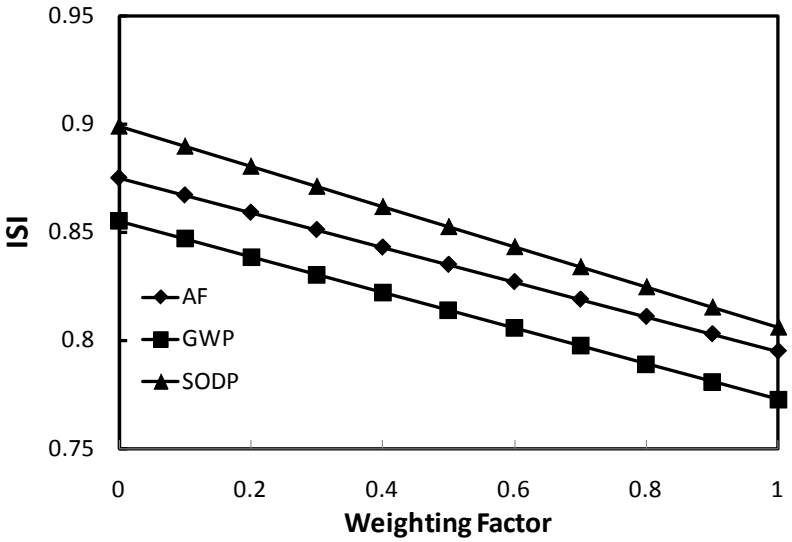

Figure 7.42: Variation of the individualist ISI with respect to weighting factor for the wind-hydrogen system.

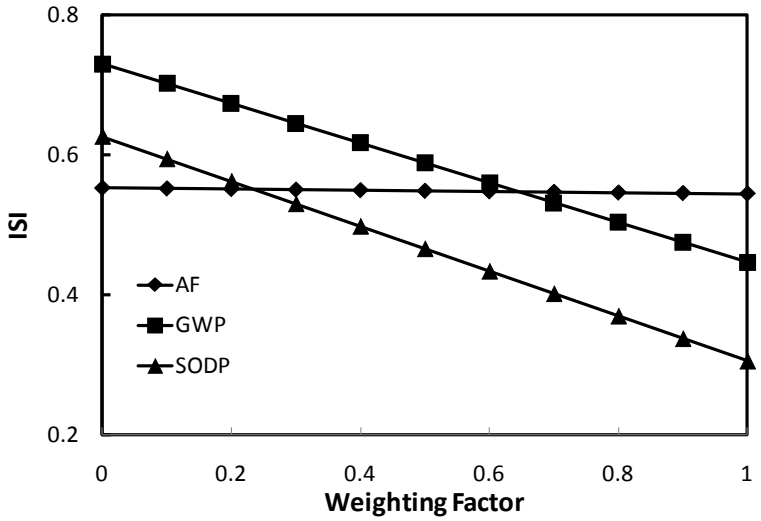

Figure 7.43: Variation of the egalitarian ISI with respect to weighting factor for the wind-hydrogen system.

Increasing the wind turbine mechanical efficiency has a modest but positive effect on the ISI of the system (Figure 7.44). More efficient energy conversion devices can reduce the size of the system and its life-cycle emissions. However, more advanced devices might also incur greater costs, which can have a negative effect on ISI.

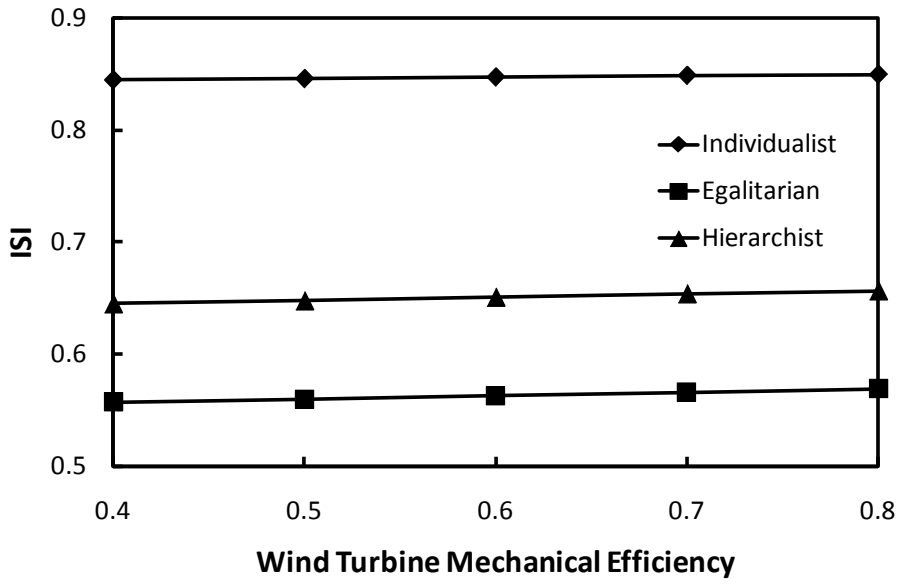

Figure 7.44: Variation of ISI with respect to wind turbine mechanical efficiency for the wind-hydrogen system.

7.2.5 Solar-PV-Battery System

An alternative to a wind turbine is a power-generating solar-PV system integrated with storage. Figure 7.45 illustrates the behaviour of the lead-acid battery in the solar-PV-battery system over the course of one year for a panel area of 3,500 m^2.

The battery is continuously discharged after day 80 as the availability of solar energy declines throughout the winter months. The battery is then continuously charged after day 220, when the solar irradiance begins to increase in intensity. The net charge of the battery after one year is 0.8 MWh. The capacity of the battery to ensure a reliable supply of energy to the community needs to be at least 130 MWh.

Each component of the solar-PV-battery system is associated with a certain amount of exergy destruction. The annual exergy destruction for each subsystem over 365 days is presented in Figure 7.46.

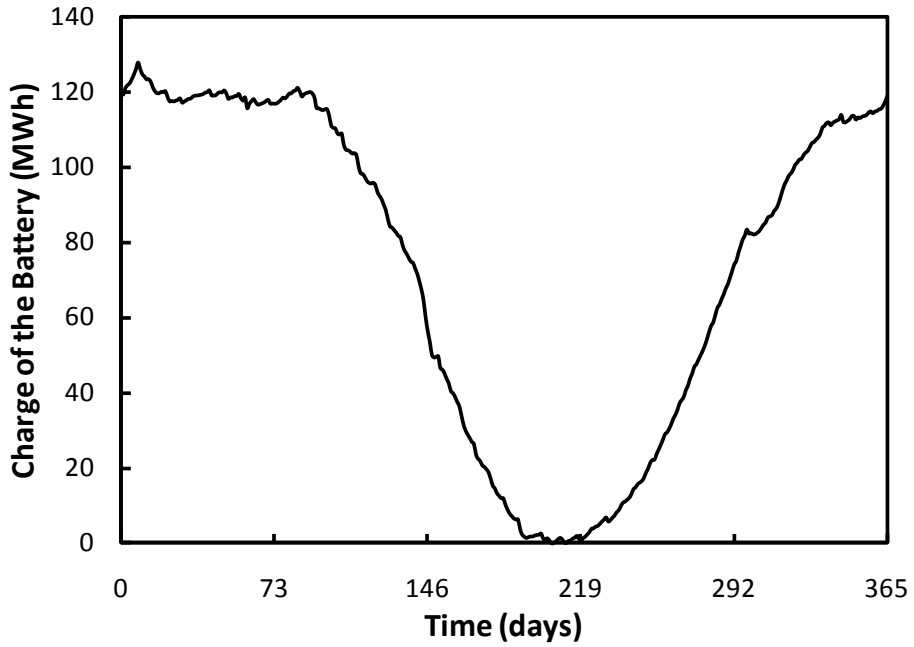

Figure 7.45: Variation in the charge of the battery over the course of one year for the solar-PV-battery system (day "1" corresponds to August 1, 2009).

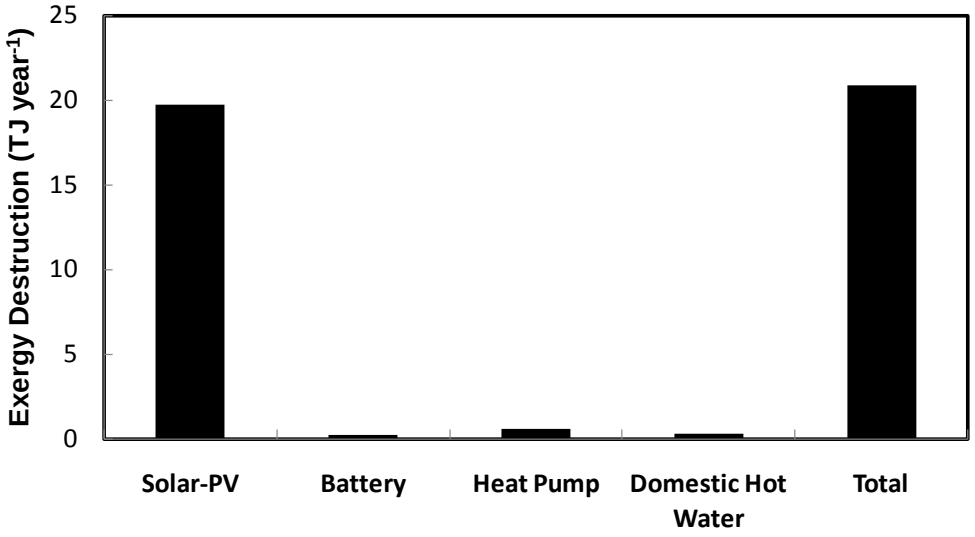

Figure 7.46: Annual exergy destruction of subsystems in the solar-PV-battery system over a one-year period.

The largest share of exergy destruction is attributed to the solar-PV subsystem (21 TJ per year) because the electric conversion efficiency of a PV panel is only 15%. Since the total exergy destruction is 22 TJ per year, the solar-PV subsystem is responsible for 95%

of total exergy destruction. The energy and exergy efficiencies of the system are 24% and 12%, respectively.

A thermodynamic analysis of the system is a precursor to sustainability assessment. Thermodynamic, cost, and life-cycle emission factors are combined with weighting factors for three different perspectives to yield the sustainability assessment results presented in Tables 7.32-7.34.

Table 7.32: Sustainability assessment results for the solar-PV-battery system from the individualist perspective.

Category	Sub-indicator	$B_{i,j}$	$W_{i,j}$	B_j	W_j	$B_j \times W_j$
ER	EnER	0.63	0.00	0.00	0.07	0.000
	ExER	0.84	1.00	0.84		0.056
EF	AF	0.11	0.50	0.05	0.42	0.023
	CV	1.00	0.50	0.50		0.211
SF	Mass	0.00	0.00	0.00	0.04	0.000
	Area	1.00	1.00	1.00		0.042
	Volume	0.00	0.00	0.00		0.000
GEIP	GWP	0.11	0.24	0.03	0.11	0.003
	SODP	0.07	0.69	0.05		0.005
	ADP	1.00	0.07	0.07		0.007
APP	$PM_{2.5}$	1.00	0.21	0.21	0.30	0.062
	PM_{10}	1.00	0.21	0.21		0.062
	SO_2	1.00	0.04	0.04		0.013
	CO	1.00	0.11	0.11		0.033
	NO_2	1.00	0.11	0.11		0.033
	O_3	1.00	0.11	0.11		0.033
	Pb	1.00	0.21	0.21		0.061
WPP	EP	0.74	0.08	0.06	0.07	0.004
	FAETP	0.30	0.78	0.23		0.015
	MAETP	0.03	0.14	0.00		0.000
ISI						**0.66**

Table 7.33: Sustainability assessment results for the solar-PV-battery system from the egalitarian perspective.

Category	Sub-indicator	$B_{i,j}$	$W_{i,j}$	B_j	W_j	$B_j \times W_j$
ER	EnER	0.63	0.00	0.00	0.16	0.000
	ExER	0.84	1.00	0.84		0.134
EF	AF	0.11	0.67	0.07	0.04	0.003
	CV	1.00	0.33	0.33		0.015
SF	Mass	0.00	0.00	0.00	0.25	0.000
	Area	1.00	1.00	1.00		0.247
	Volume	0.00	0.00	0.00		0.000
GEIP	GWP	0.11	0.65	0.07	0.37	0.025
	SODP	0.07	0.25	0.02		0.007
	ADP	1.00	0.11	0.11		0.040
APP	$PM_{2.5}$	1.00	0.04	0.04	0.03	0.001
	PM_{10}	1.00	0.04	0.04		0.001
	SO_2	1.00	0.15	0.15		0.004
	CO	1.00	0.04	0.04		0.001
	NO_2	1.00	0.15	0.15		0.004
	O_3	1.00	0.04	0.04		0.001
	Pb	1.00	0.52	0.52		0.013
WPP	EP	0.74	0.08	0.06	0.15	0.009
	FAETP	0.30	0.19	0.06		0.009
	MAETP	0.03	0.72	0.02		0.003
ISI						**0.52**

The ISI for the solar-PV-battery system ranges from 0.52 to 0.66, where the primary determinant of the score depends on the perspective. The EF category, specifically the AF sub-indicator, is the largest contributor to the score for the individualist perspective. The expected annual cost of a stand-alone solar-PV-battery system to a household is approximately $64,000 whereas the median after-tax income of a household in Ontario is $69,300 (Statistics Canada, 2012), of which no more than 10% should be allocated to energy needs (Fankhauser and Tepic, 2007).

Sustainability sub-indicators in Tables 7.32-7.34 with a $B_{i,j}$ value equal to one have no negative effect on ISI. Sub-indicators with a $B_{i,j}$ value less than one will have a negative effect on ISI, which is a function of the actual $B_{i,j}$ value and its weight. The range of the negative effect of each sustainability sub-indicator on ISI is graphed in Figure 7.47.

Table 7.34: Sustainability assessment results for the solar-PV-battery system from the hierarchist perspective.

Category	Sub-indicator	$B_{i,j}$	$W_{i,j}$	B_j	W_j	$B_j \times W_j$
ER	EnER	0.63	0.00	0.00	0.15	0.000
	ExER	0.84	1.00	0.84		0.129
EF	AF	0.11	0.67	0.07	0.17	0.012
	CV	1.00	0.33	0.33		0.057
SF	Mass	0.00	0.00	0.00	0.15	0.000
	Area	1.00	1.00	1.00		0.153
	Volume	0.00	0.00	0.00		0.000
GEIP	GWP	0.11	0.57	0.06	0.31	0.019
	SODP	0.07	0.33	0.02		0.007
	ADP	1.00	0.10	0.10		0.030
APP	$PM_{2.5}$	1.00	0.10	0.10	0.08	0.008
	PM_{10}	1.00	0.10	0.10		0.008
	SO_2	1.00	0.10	0.10		0.008
	CO	1.00	0.05	0.05		0.004
	NO_2	1.00	0.17	0.17		0.013
	O_3	1.00	0.05	0.05		0.004
	Pb	1.00	0.44	0.44		0.036
WPP	EP	0.74	0.08	0.06	0.13	0.008
	FAETP	0.30	0.58	0.17		0.022
	MAETP	0.03	0.34	0.01		0.001
ISI						**0.52**

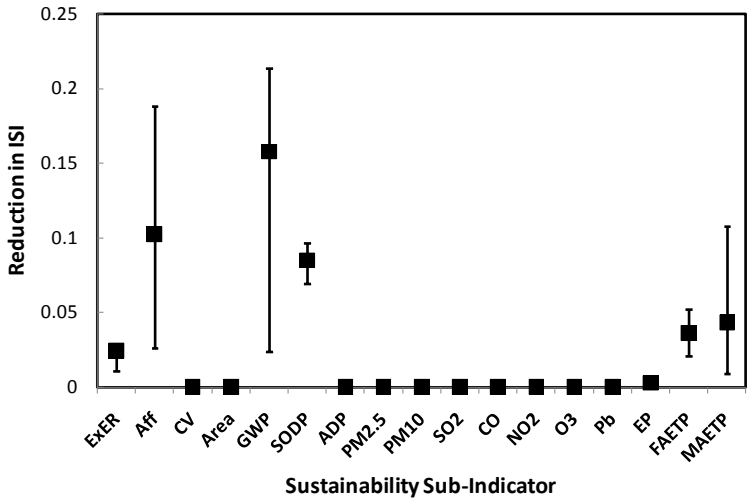

Figure 7.47: Reduction in ISI for each sustainability sub-indicator for the solar-PV-battery system.

The impact of other parameters on global warming and stratospheric ozone depletion is studied in more detail in Figures 7.48 and 7.49.

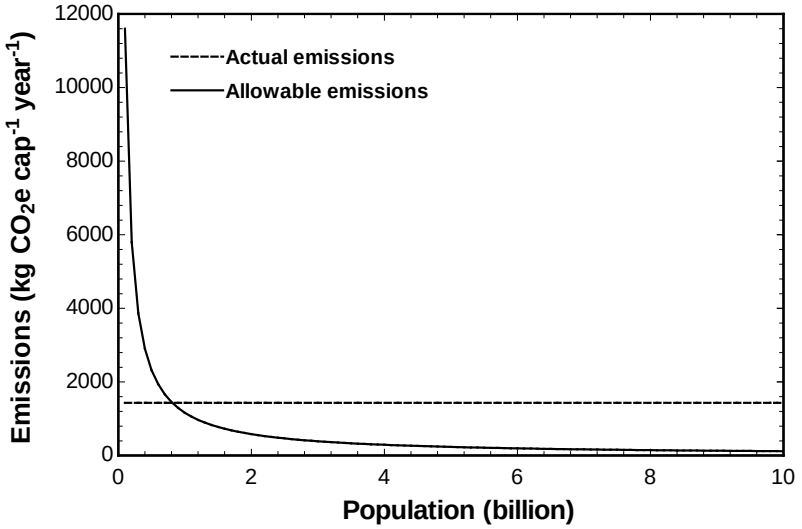

Figure 7.48: Actual and allowable annual per capita GHG emissions for the solar-PV-battery system based on the lower limit of the representative concentration pathway (RCP2.6) carbon budget.

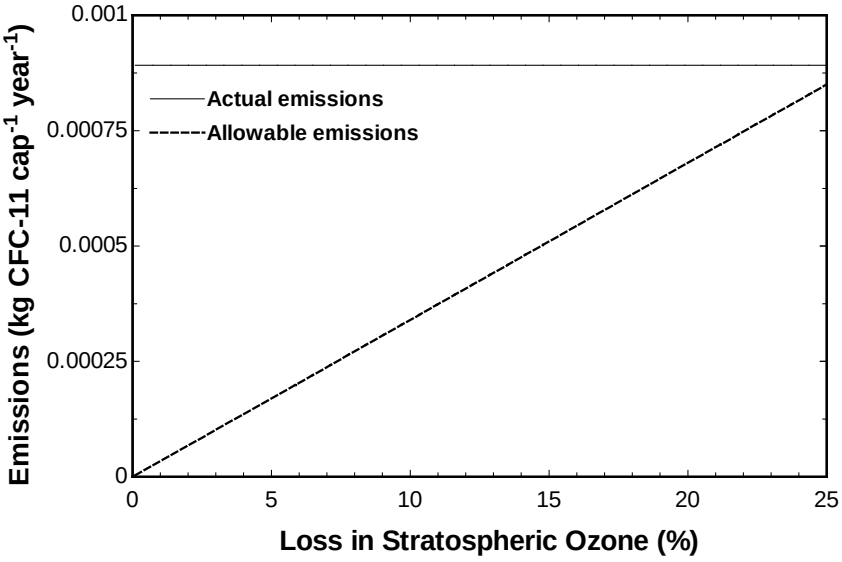

Figure 7.49: Actual and allowable annual per capita ozone-depleting substance emissions (including N_2O) with respect to the percent loss in stratospheric ozone over the time scale for considering sustainability.

The point of intersection in Figure 7.48 occurs at a population of approximately 400 million, which is much less than half of the population for the wind-battery system. Similarly, emissions of ozone-depleting substances are consistent with a loss in stratospheric ozone of approximately 26%, which is higher than the anticipated stratospheric ozone depletion for the wind-battery system (20%).

The sustainability time scale affects the ISI of the solar-PV-battery system in a similar manner as the wind-battery and wind-hydrogen systems (Figure 7.50). Since the SODP is not approaching zero, there is an observable impact on the ISI for the solar-PV-battery system. Although the time scale for considering sustainability also affects the ADP sub-indicator, its impact is insufficient to have any meaningful effect.

The effect of weighting factor on the most critical sub-indicators is investigated in Figures 7.51 and 7.52.

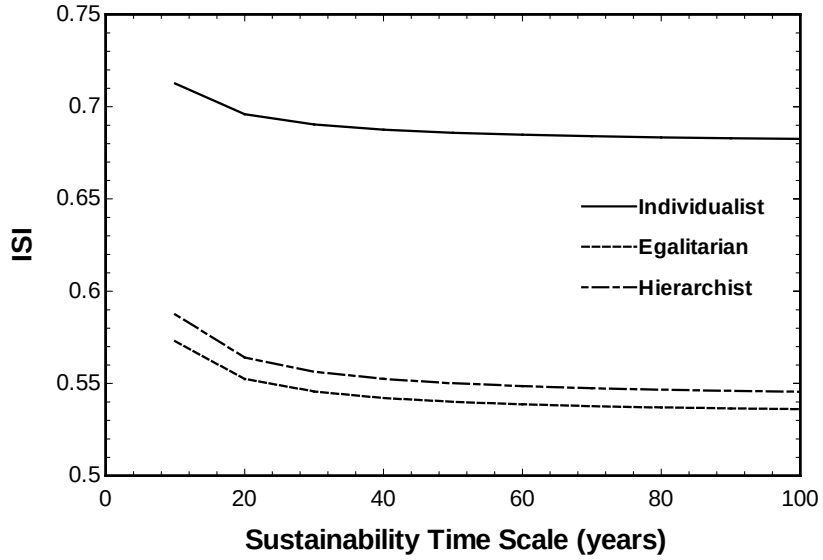

Figure 7.50: Variation of ISI with respect to the time scale for considering sustainability for the solar-PV-battery system.

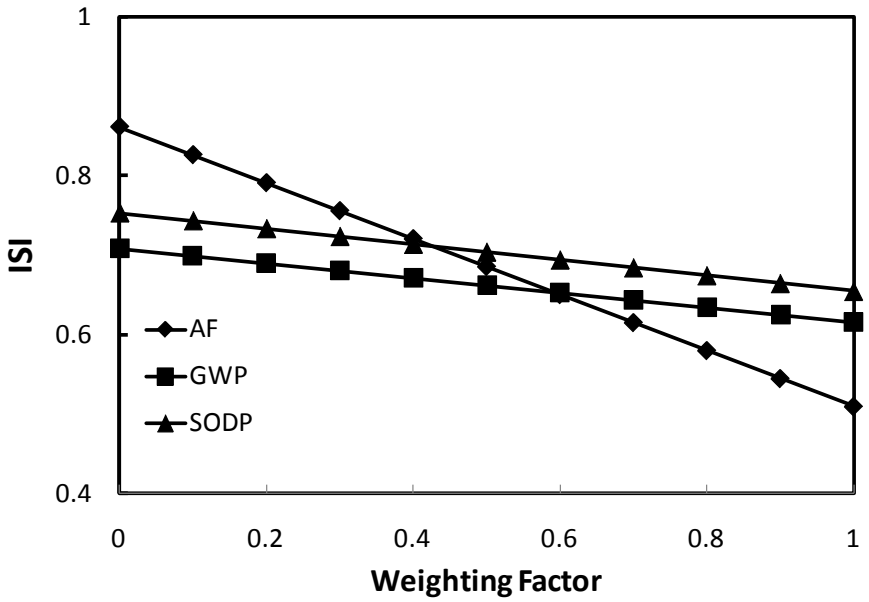

Figure 7.51: Variation of the individualist ISI with respect to weighting factor for the solar-PV-battery system.

Figure 7.51 demonstrates that the ISI from the individualist perspective is highly sensitive to the weighting factor attached to the AF sub-indicator. The opposite is true from an egalitarian perspective (Figure 7.52), where several sub-indicators are relevant.

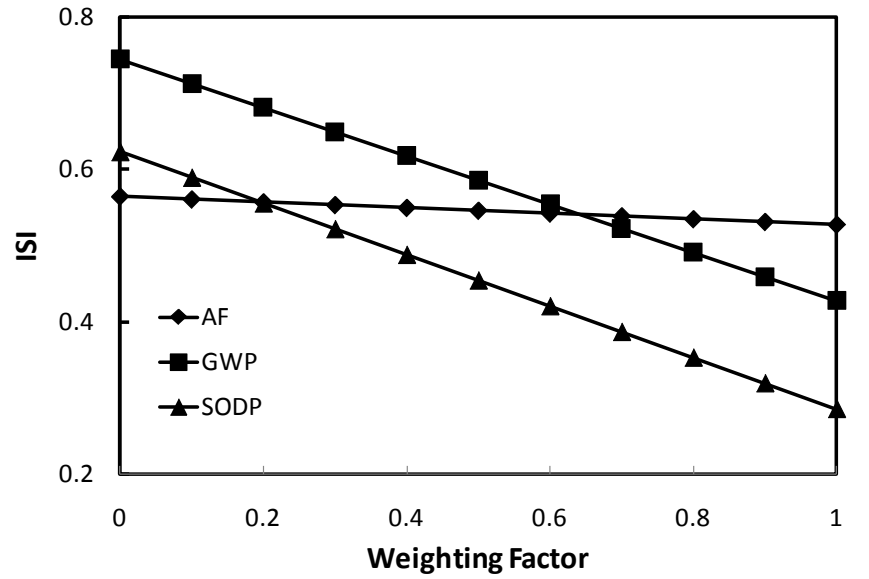

Figure 7.52: Variation of the egalitarian ISI with respect to weighting factor for the solar-PV-battery system.

The photovoltaic efficiency and battery charging efficiency are important parameters for the solar-PV-battery system. The impacts of these parameters on ISI are illustrated in Figures 7.53 and 7.54. At higher efficiencies, both of these parameters have a modest but positive effect on ISI. However, there may potentially be higher costs associated with more advanced batteries, which could have a negative effect on ISI.

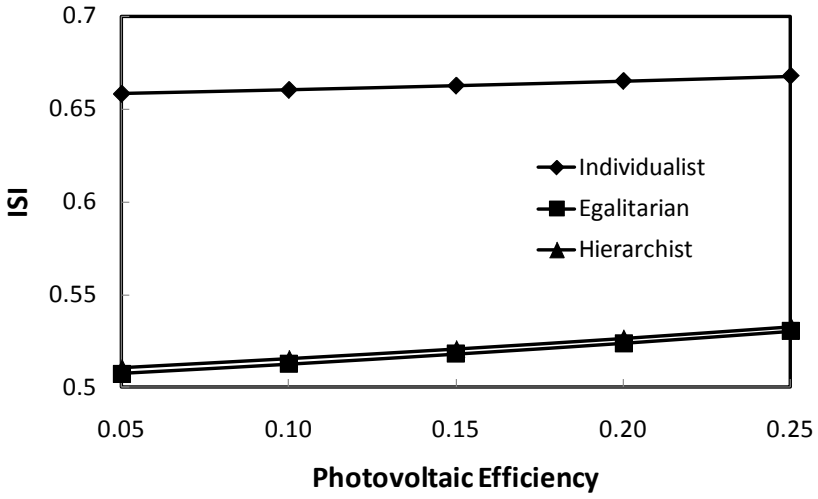

Figure 7.53: Variation of ISI with respect to photovoltaic efficiency for the solar-PV-battery system.

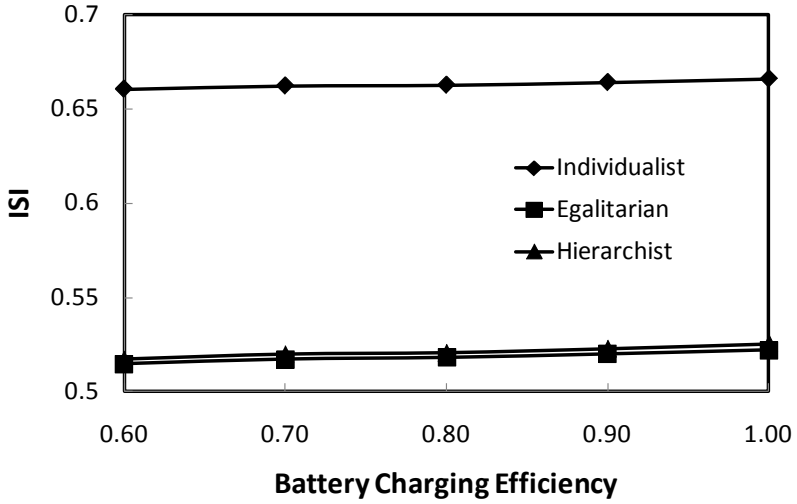

Figure 7.54: Variation of ISI with respect to battery charging efficiency for the solar-PV-battery system.

7.2.6 Solar-PV-Hydrogen System

An alternative to battery storage is hydrogen. Figure 7.55 illustrates the behaviour of the hydrogen storage subsystem in the solar-PV-hydrogen system over the course of one year for a panel area of 4200 m^2.

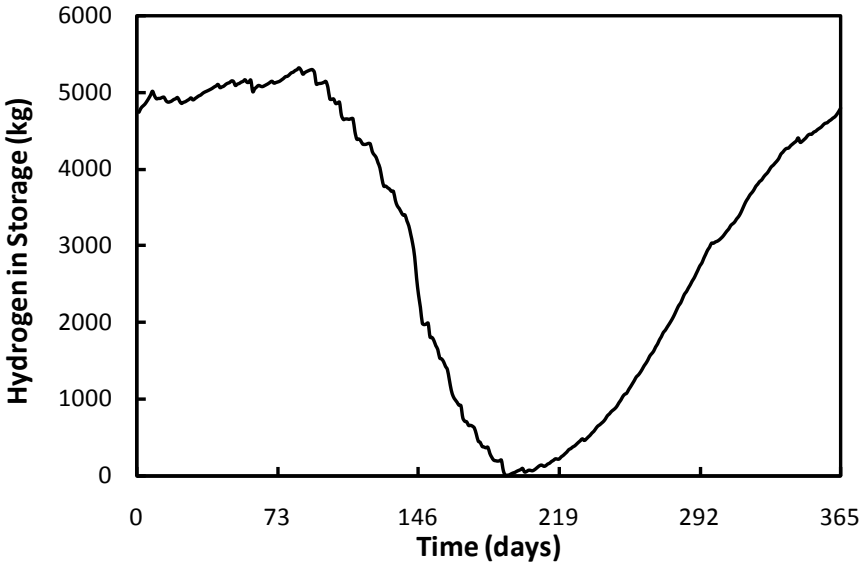

Figure 7.55: Variation in the amount of hydrogen in the storage tanks over the course of one year for the solar-PV-hydrogen system (day "1" corresponds to August 1, 2009).

The hydrogen storage tanks are continuously discharged after day 80 as the availability of solar energy declines throughout the winter months. The storage tanks are then continuously charged after day 193, when the solar irradiance begins to increase in intensity. The net accumulation of hydrogen after one year is 90 kg. The total capacity of the hydrogen storage tanks to ensure a reliable supply of energy to the community needs to be at least 5300 kg. As a comparison, the total capacity of the hydrogen storage tanks for the wind-hydrogen system has to be at least 8550 kg, which is approximately 60% larger. Also recall that the capacity of the lead-acid battery for the wind-battery system is approximately 20% larger than the required capacity for the solar-PV-battery system. Higher energy storage requirements for wind-based systems are an important factor as to why solar-based systems have better ISI scores.

Each component of the solar-PV-hydrogen system is associated with a certain amount of exergy destruction. The exergy destruction rates for each subsystem over 365 days are presented in Figure 7.56.

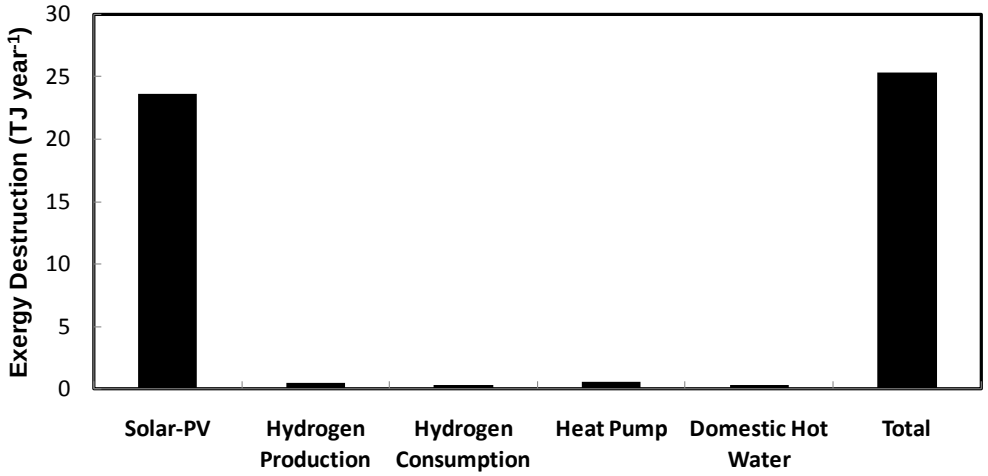

Figure 7.56: Annual exergy destruction of subsystems in the solar-PV-hydrogen system over a one-year period.

The largest share of exergy destruction is attributed to the solar-PV subsystem (24 TJ per year) because the electric conversion efficiency of a PV panel is only 15%. Unlike the wind-hydrogen system, where the hydrogen storage subsystem is responsible for a sizable proportion of exergy destruction, the extent of exergy destruction by the solar-PV subsystem overwhelms all other sources. Since the total annual exergy destruction is 25 TJ per year, the solar-PV subsystem is responsible for 96% of exergy destruction. The energy and exergy efficiencies of the system are 21% and 11%, respectively.

A thermodynamic analysis of the system is a precursor to sustainability assessment. Thermodynamic, cost, and life-cycle emission factors are combined with weighting factors for three different perspectives to yield the sustainability assessment results presented in Tables 7.35-7.37.

Table 7.35: Sustainability assessment results for the solar-PV-hydrogen system from the individualist perspective.

Category	Sub-indicator	$B_{i,j}$	$W_{i,j}$	B_j	W_j	$B_j \times W_j$
ER	EnER	0.69	0.00	0.00	0.07	0.000
	ExER	0.85	1.00	0.85		0.056
EF	AF	1.00	0.50	0.50	0.42	0.211
	CV	1.00	0.50	0.50		0.211
SF	Mass	0.00	0.00	0.00	0.04	0.000
	Area	1.00	1.00	1.00		0.042
	Volume	0.00	0.00	0.00		0.000
GEIP	GWP	0.32	0.24	0.08	0.11	0.009
	SODP	0.15	0.69	0.11		0.011
	ADP	1.00	0.07	0.07		0.007
APP	$PM_{2.5}$	1.00	0.21	0.21	0.30	0.062
	PM_{10}	1.00	0.21	0.21		0.062
	SO_2	1.00	0.04	0.04		0.013
	CO	1.00	0.11	0.11		0.033
	NO_2	1.00	0.11	0.11		0.033
	O_3	1.00	0.11	0.11		0.033
	Pb	1.00	0.21	0.21		0.061
WPP	EP	1.00	0.08	0.08	0.07	0.005
	FAETP	1.00	0.78	0.78		0.051
	MAETP	0.20	0.14	0.03		0.002
ISI						**0.90**

The ISI for the solar-PV-hydrogen system ranges from 0.65 to 0.90, where the primary determinant of the score depends on the perspective. Unlike previous solar- and wind-based systems, the AF sub-indicator has no effect on the ISI for all perspectives. In fact, the solar-PV-hydrogen system has the highest ISI of all the case studies except for the geothermal-biomass system, which is an exception (see Section 7.2.9).

The solar-PV-hydrogen system may have the best ISI but that does not mean it can be classified as "sustainable," which is how this approach differs from other sustainability assessments. The GWP and SODP sub-indicators should be of concern as they are both above their target values. Improvements related to efficiency, materials, and manufacturing can improve these scores but reducing energy demand at the community-level may have even greater impact.

Table 7.36: Sustainability assessment results for the solar-PV-hydrogen system from the egalitarian perspective.

Category	Sub-indicator	$B_{i,j}$	$W_{i,j}$	B_j	W_j	$B_j \times W_j$
ER	EnER	0.69	0.00	0.00	0.16	0.000
	ExER	0.85	1.00	0.85		0.136
EF	AF	1.00	0.67	0.67	0.04	0.029
	CV	1.00	0.33	0.33		0.015
SF	Mass	0.00	0.00	0.00	0.25	0.000
	Area	1.00	1.00	1.00		0.247
	Volume	0.00	0.00	0.00		0.000
GEIP	GWP	0.32	0.65	0.21	0.37	0.078
	SODP	0.15	0.25	0.04		0.014
	ADP	1.00	0.11	0.11		0.040
APP	$PM_{2.5}$	1.00	0.04	0.04	0.03	0.001
	PM_{10}	1.00	0.04	0.04		0.001
	SO_2	1.00	0.15	0.15		0.004
	CO	1.00	0.04	0.04		0.001
	NO_2	1.00	0.15	0.15		0.004
	O_3	1.00	0.04	0.04		0.001
	Pb	1.00	0.52	0.52		0.013
WPP	EP	1.00	0.08	0.08	0.15	0.013
	FAETP	1.00	0.19	0.19		0.030
	MAETP	0.20	0.72	0.14		0.022
ISI						**0.65**

Sustainability sub-indicators in Tables 7.35-7.37 with a $B_{i,j}$ value equal to one have no negative effect on ISI. Sub-indicators with a $B_{i,j}$ value less than one will have a negative effect on ISI, which is a function of the actual $B_{i,j}$ value and its weight. The range of the negative effect of each sustainability sub-indicator on ISI is graphed in Figure 7.57.

The GWP sub-indicator once again exhibits a great influence on the ISI of the system with lesser but still significant contributions from the SODP and MAETP sub-indicators.

The impact of other parameters on global warming and stratospheric ozone depletion is studied in more detail in Figures 7.58 and 7.59.

Table 7.37: Sustainability assessment results for the solar-PV-hydrogen system from the hierarchist perspective.

Category	Sub-indicator	$B_{i,j}$	$W_{i,j}$	B_j	W_j	$B_j \times W_j$
ER	EnER	0.69	0.00	0.00	0.15	0.000
	ExER	0.85	1.00	0.85		0.131
EF	AF	1.00	0.67	0.67	0.17	0.115
	CV	1.00	0.33	0.33		0.057
SF	Mass	0.00	0.00	0.00	0.15	0.000
	Area	1.00	1.00	1.00		0.153
	Volume	0.00	0.00	0.00		0.000
GEIP	GWP	0.32	0.57	0.18	0.31	0.057
	SODP	0.15	0.33	0.05		0.016
	ADP	1.00	0.10	0.10		0.030
APP	$PM_{2.5}$	1.00	0.10	0.10	0.08	0.008
	PM_{10}	1.00	0.10	0.10		0.008
	SO_2	1.00	0.10	0.10		0.008
	CO	1.00	0.05	0.05		0.004
	NO_2	1.00	0.17	0.17		0.013
	O_3	1.00	0.05	0.05		0.004
	Pb	1.00	0.44	0.44		0.036
WPP	EP	1.00	0.08	0.08	0.13	0.011
	FAETP	1.00	0.58	0.58		0.075
	MAETP	0.20	0.34	0.07		0.009
ISI						**0.73**

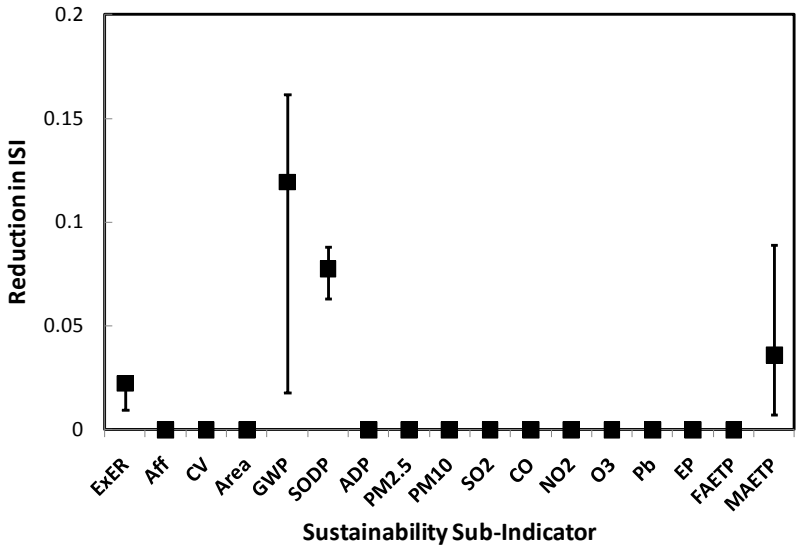

Figure 7.57: Reduction in ISI for each sustainability sub-indicator for the solar-PV-hydrogen system.

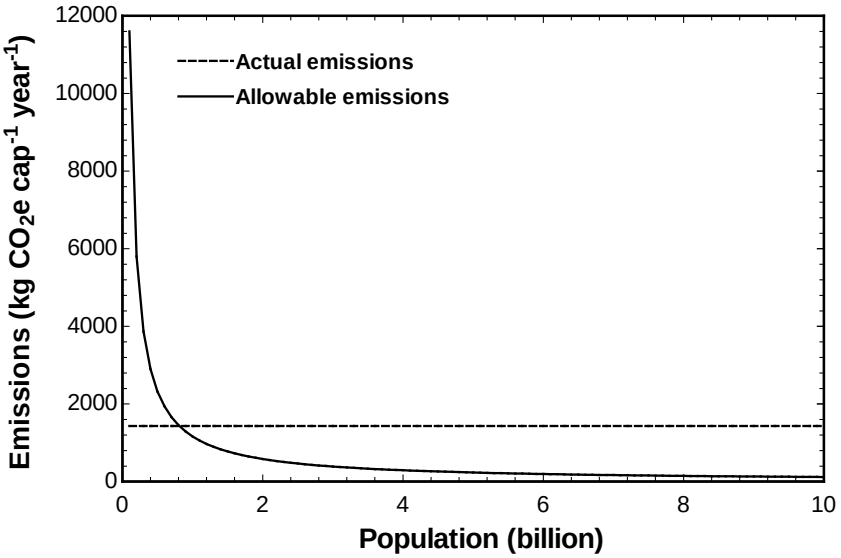

Figure 7.58: Actual and allowable annual per capita GHG emissions for the solar-PV-hydrogen system based on the lower limit of the representative concentration pathway (RCP2.6) carbon budget.

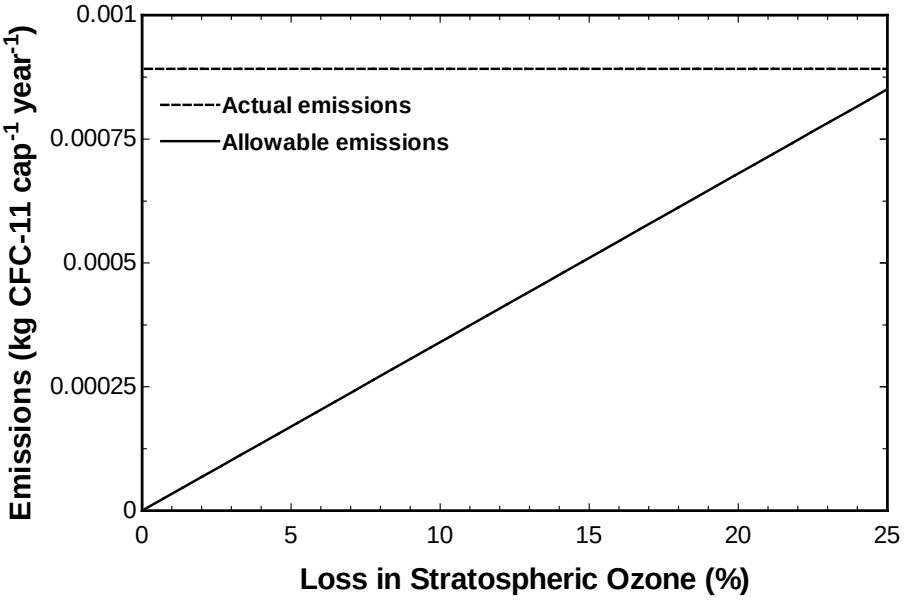

Figure 7.59: Actual and allowable annual per capita ozone-depleting substance emissions (including N_2O) with respect to the percent loss in stratospheric ozone over the time scale for considering sustainability.

The point of intersection in Figure 7.58 occurs at a population of approximately 2.4 billion, which is higher than other wind- and solar-based systems considered here.

Similarly, emissions of ozone-depleting substances are consistent with a loss in stratospheric ozone of approximately 14% over 50 years, which is also an improvement.

The sustainability time scale affects the ISI of the solar-PV-hydrogen system in a similar manner as the wind-battery, wind-hydrogen, and solar-PV-battery systems (Figure 7.60). Since the SODP is not approaching zero, there is an observable impact on the ISI over various time scales. As noted earlier, distributing a fixed amount of stratospheric ozone depletion over a longer time scale makes the threshold value more stringent, which reduces ISI. Although the time scale for considering sustainability also affects the ADP sub-indicator, its impact is insufficient to have any meaningful effect.

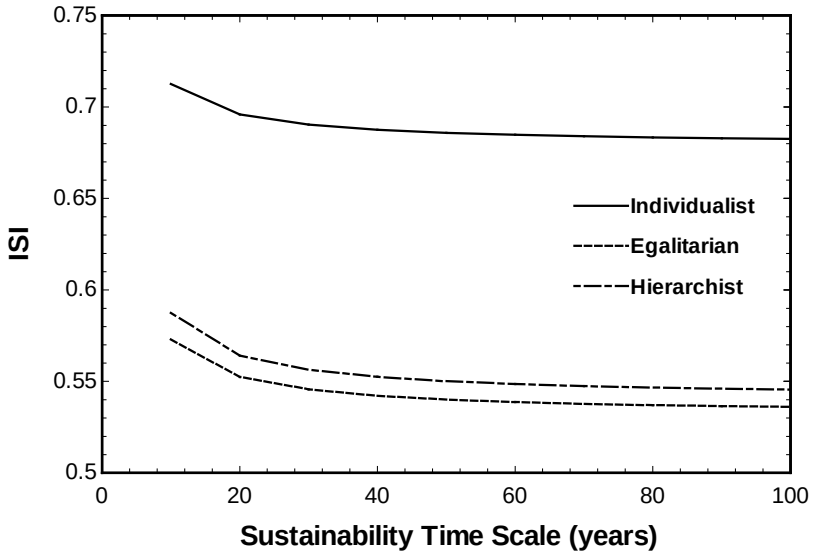

Figure 7.60: Variation of ISI with respect to the time scale for considering sustainability for the solar-PV-hydrogen system.

The effect of weighting factor on the most critical sub-indicators is investigated in Figures 7.61 and 7.62. Unlike other renewable-based systems, the ISI of the solar-PV-hydrogen system is not affected by AF. Consequently, the weighting factor associated with AF does not need to be considered.

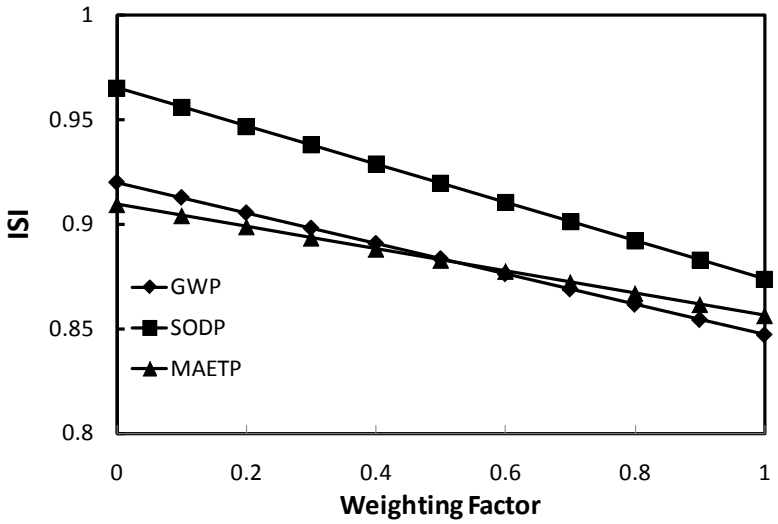

Figure 7.61: Variation of the individualist ISI with respect to weighting factor for the solar-PV-hydrogen system.

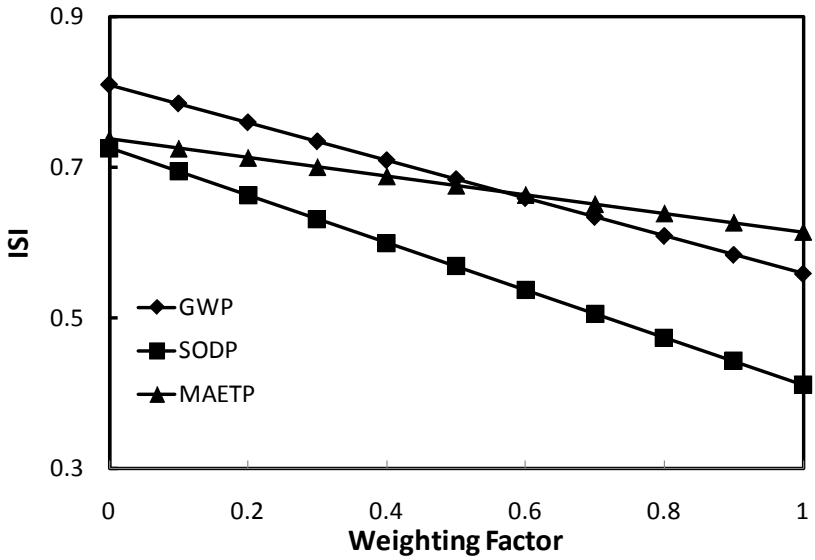

Figure 7.62: Variation of the egalitarian ISI with respect to weighting factor for the solar-PV-hydrogen system.

Figures 7.61 and 7.62 demonstrate that the ISI from both the individualist and egalitarian perspectives is most sensitive to the weighting factors attached to the GWP and SODP sub-indicators. The effects are especially substantial for the egalitarian ISI, which can decrease from 0.81 to 0.56 or 0.73 to 0.41 as the weighting factors for GWP or SODP increase from 0 to 1, respectively.

7.2.7 Solar-PV-Wind-Biomass System

A stand-alone solar-PV-wind-biomass system needs to deliver a continuous and reliable supply of heat, cold, and electrical energy to meet the needs of the community. A sufficiently large hydrogen storage system that generates a net amount of chemical energy after a year of operation is therefore required. Figure 7.63 illustrates the behaviour of the hydrogen production/consumption subsystem in the solar-PV-wind-biomass system over the course of one year for a panel area of 2000 m^2 and a wind turbine with a rotor radius of 16 m.

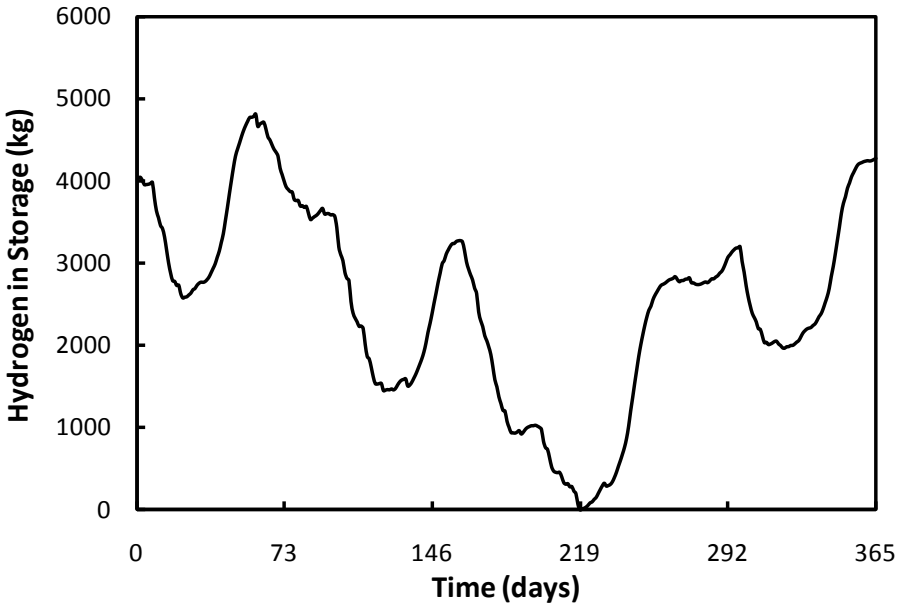

Figure 7.63: Variation in the amount of hydrogen in the storage tanks over the course of one year for the solar-PV-wind-biomass system (day "1" corresponds to August 1, 2009).

The hydrogen storage tanks cycle through charging and discharging modes until the net accumulation of hydrogen after one year is 245 kg. The total capacity of the hydrogen storage tanks to ensure a reliable supply of energy to the community needs to be at least 4800 kg. As a comparison, the required storage capacities for the wind-hydrogen and solar-PV-hydrogen systems are 8550 and 5300 kg, respectively. This illustrates the effect of hybridization on renewable energy storage requirements.

Each component of the solar-PV-wind-biomass system is associated with a certain amount of exergy destruction. The annual exergy destruction for each subsystem over 365 days is presented in Figure 7.66.

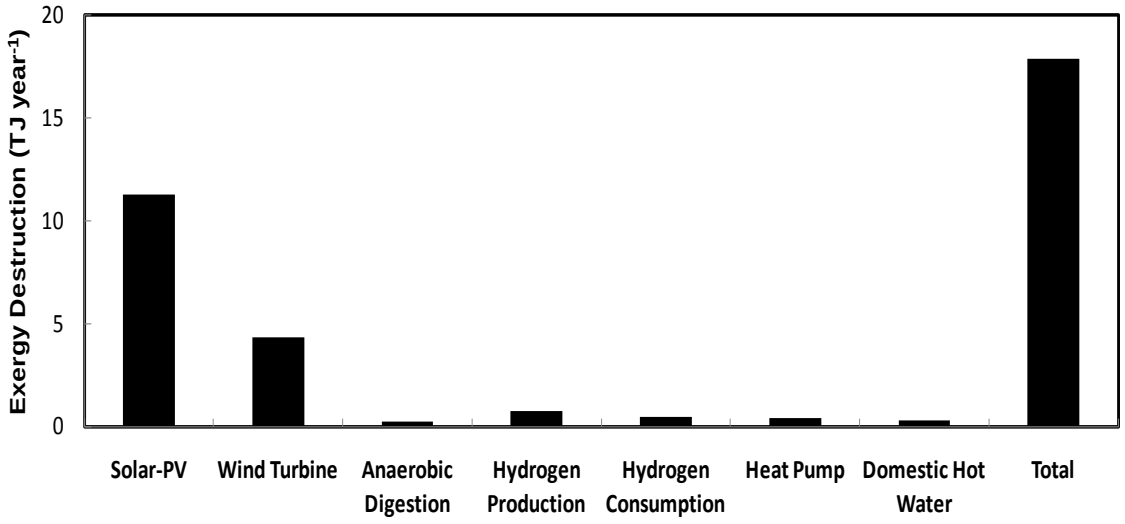

Figure 7.64: Annual exergy destruction of subsystems in the solar-PV-wind-biomass system over a one-year period.

The largest shares of exergy destruction are attributed to the solar-PV (11 TJ per year) and wind turbine (4.4 TJ per year) subsystems. Since total annual exergy destruction is 18 TJ, the solar-PV and wind turbine subsystems account for 61% and 24% of total exergy destruction, respectively. As a comparison, the total exergy destruction associated with the wind-hydrogen and solar-PV-hydrogen systems are 17 and 25 TJ per year, respectively. The energy and exergy efficiencies of the system are 22% and 13%, respectively.

A thermodynamic analysis of the system is a precursor to sustainability assessment. Thermodynamic, cost, and life-cycle emission factors are combined with weighting factors for three different perspectives to yield the sustainability assessment results presented in Tables 7.38-7.40.

Table 7.38: Sustainability assessment results for the solar-PV-wind-biomass system from the individualist perspective.

Category	Sub-indicator	$B_{i,j}$	$W_{i,j}$	B_j	W_j	$B_j \times W_j$
ER	EnER	0.61	0.00	0.00	0.07	0.000
	ExER	0.64	1.00	0.64		0.042
EF	AF	1.00	0.50	0.50	0.42	0.211
	CV	1.00	0.50	0.50		0.211
SF	Mass	0.00	0.00	0.00	0.04	0.000
	Area	1.00	1.00	1.00		0.042
	Volume	0.00	0.00	0.00		0.000
GEIP	GWP	0.32	0.24	0.08	0.11	0.008
	SODP	0.13	0.69	0.09		0.009
	ADP	1.00	0.07	0.07		0.007
APP	$PM_{2.5}$	1.00	0.21	0.21	0.30	0.062
	PM_{10}	1.00	0.21	0.21		0.062
	SO_2	1.00	0.04	0.04		0.013
	CO	1.00	0.11	0.11		0.033
	NO_2	1.00	0.11	0.11		0.033
	O_3	1.00	0.11	0.11		0.033
	Pb	1.00	0.21	0.21		0.061
WPP	EP	1.00	0.08	0.08	0.07	0.005
	FAETP	1.00	0.78	0.78		0.051
	MAETP	0.21	0.14	0.03		0.002
ISI						**0.89**

The ISI for the solar-PV-wind-biomass system ranges from 0.61 to 0.89, where the primary determinant of the score depends on the perspective. Unlike previous solar- and wind-based systems, the AF sub-indicator has no effect on the ISI for all perspectives.

Sustainability sub-indicators in Tables 7.38-7.40 with a $B_{i,j}$ value equal to one have no negative effect on ISI. Sub-indicators with a $B_{i,j}$ value less than one will have a negative effect on ISI, which is a function of the actual $B_{i,j}$ value and its weight. The range of the negative effect of each sustainability sub-indicator on ISI is graphed in Figure 7.65.

Table 7.39: Sustainability assessment results for the solar-PV-wind-biomass system from the egalitarian perspective.

Category	Sub-indicator	$B_{i,j}$	$W_{i,j}$	B_j	W_j	$B_j \times W_j$
ER	EnER	0.61	0.00	0.00	0.16	0.000
	ExER	0.64	1.00	0.64		0.102
EF	AF	1.00	0.67	0.67	0.04	0.029
	CV	1.00	0.33	0.33		0.015
SF	Mass	0.00	0.00	0.00	0.25	0.000
	Area	1.00	1.00	1.00		0.247
	Volume	0.00	0.00	0.00		0.000
GEIP	GWP	0.32	0.65	0.21	0.37	0.077
	SODP	0.13	0.25	0.03		0.012
	ADP	1.00	0.11	0.11		0.040
APP	$PM_{2.5}$	1.00	0.04	0.04	0.03	0.001
	PM_{10}	1.00	0.04	0.04		0.001
	SO_2	1.00	0.15	0.15		0.004
	CO	1.00	0.04	0.04		0.001
	NO_2	1.00	0.15	0.15		0.004
	O_3	1.00	0.04	0.04		0.001
	Pb	1.00	0.52	0.52		0.013
WPP	EP	1.00	0.08	0.08	0.15	0.013
	FAETP	1.00	0.19	0.19		0.030
	MAETP	0.21	0.72	0.15		0.023
ISI						**0.61**

GWP again exhibits a great influence on the ISI of the system with lesser but still significant contributions from the ExER, SODP, and MAETP sub-indicators.

The impact of other parameters on global warming and stratospheric ozone depletion is studied in more detail in Figures 7.66 and 7.67. The point of intersection in Figure 7.66 occurs at a population of approximately 2.3 billion, which is higher than other wind- and solar-based systems considered here. Similarly, emissions of ozone-depleting substances are consistent with a loss in stratospheric ozone of approximately 14% over 50 years, which is also an improvement but still excessive.

Table 7.40: Sustainability assessment results for the solar-PV-wind-biomass system from the hierarchist perspective.

Category	Sub-indicator	$B_{i,j}$	$W_{i,j}$	B_j	W_j	$B_j \times W_j$
ER	EnER	0.61	0.00	0.00	0.15	0.000
	ExER	0.64	1.00	0.64		0.098
EF	AF	1.00	0.67	0.67	0.17	0.115
	CV	1.00	0.33	0.33		0.057
SF	Mass	0.00	0.00	0.00	0.15	0.000
	Area	1.00	1.00	1.00		0.153
	Volume	0.00	0.00	0.00		0.000
GEIP	GWP	0.32	0.57	0.18	0.31	0.057
	SODP	0.13	0.33	0.04		0.013
	ADP	1.00	0.10	0.10		0.030
APP	$PM_{2.5}$	1.00	0.10	0.10	0.08	0.008
	PM_{10}	1.00	0.10	0.10		0.008
	SO_2	1.00	0.10	0.10		0.008
	CO	1.00	0.05	0.05		0.004
	NO_2	1.00	0.17	0.17		0.013
	O_3	1.00	0.05	0.05		0.004
	Pb	1.00	0.44	0.44		0.036
WPP	EP	1.00	0.08	0.08	0.13	0.011
	FAETP	1.00	0.58	0.58		0.075
	MAETP	0.21	0.34	0.07		0.009
ISI						**0.70**

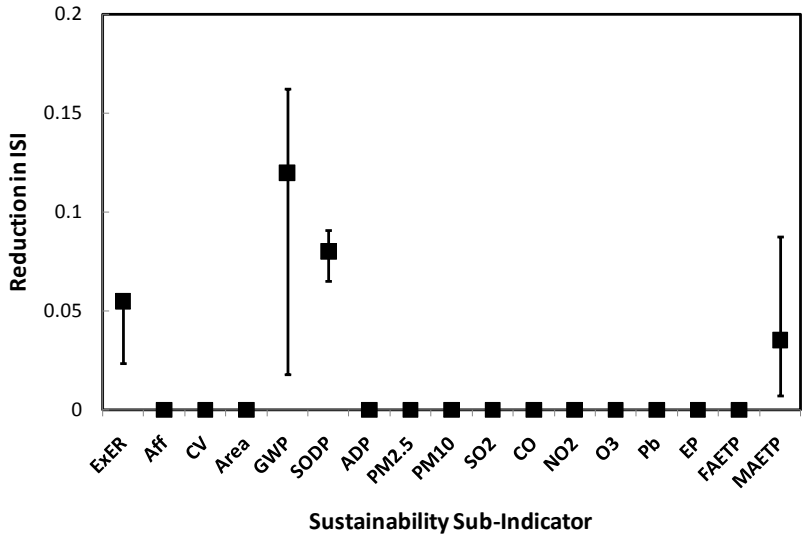

Figure 7.65: Reduction in ISI for each sustainability sub-indicator for the solar-PV-wind-biomass system.

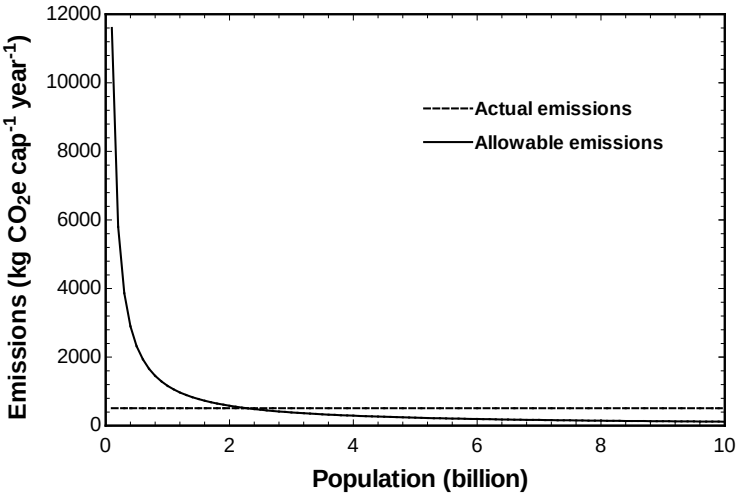

Figure 7.66: Actual and allowable annual per capita GHG emissions for the solar-PV-wind-biomass system based on the lower limit of the representative concentration pathway (RCP2.6) carbon budget.

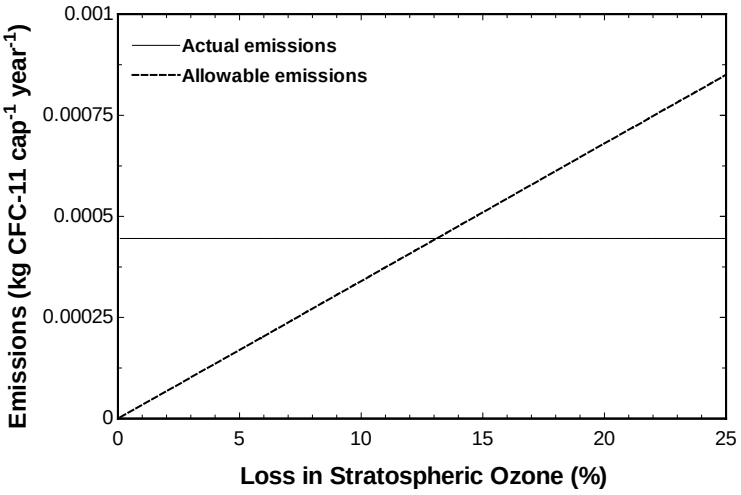

Figure 7.67: Actual and allowable annual per capita ozone-depleting substance emissions (including N_2O) with respect to the percent loss in stratospheric ozone over the time scale for considering sustainability.

A longer sustainability time scale decreases the ISI of the solar-PV-wind-biomass system primarily by distributing the acceptable amount of stratospheric ozone layer depletion over a longer period of time (Figure 7.68). This reduces the threshold emissions of ozone-depleting substances per capita per year.

The effects of weighting factor on the most critical sub-indicators are investigated in Figures 7.69 and 7.70.

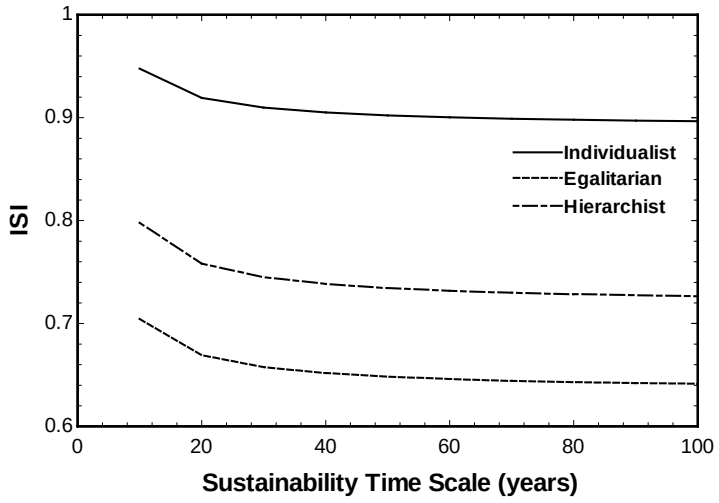

Figure 7.68: Variation of ISI with respect to the time scale for considering sustainability for the solar-PV-wind-biomass system.

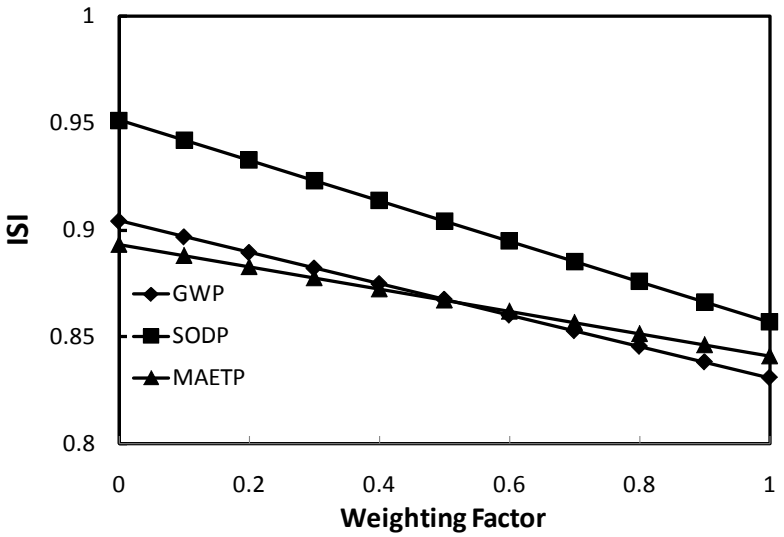

Figure 7.69: Variation of the individualist ISI with respect to weighting factor for the solar-PV-wind-biomass system.

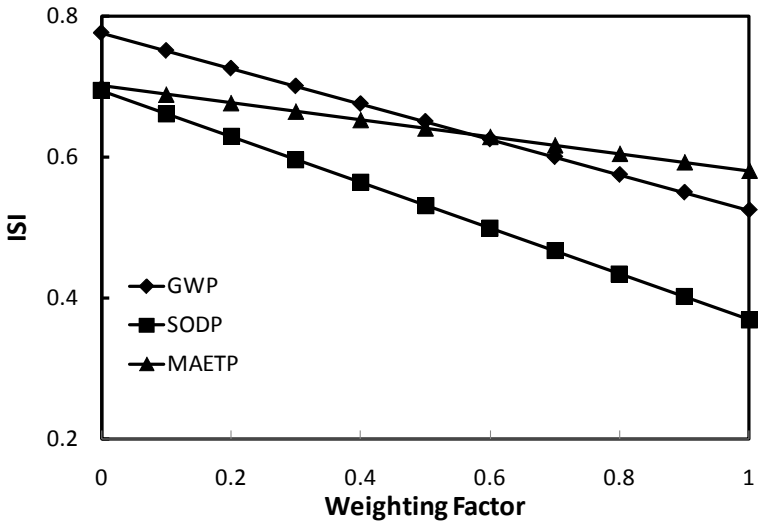

Figure 7.70: Variation of the egalitarian ISI with respect to weighting factor for the solar-PV-wind-biomass system.

Figures 7.69 and 7.70 demonstrate that the ISI from both the individualist and egalitarian perspectives is most sensitive to the weighting factor attached to the GWP and SODP sub-indicators. The effects are especially substantial for the egalitarian ISI, which can decrease from 0.78 to 0.52 or 0.69 to 0.37 as the weighting factors for GWP or SODP increase from 0 to 1, respectively.

7.2.8 Solar-Thermal-Wind-Biomass System

A stand-alone solar-thermal-wind-biomass system needs to deliver a continuous and reliable supply of heat, cold, and electrical energy to meet the needs of the community. A sufficiently large thermal energy storage and battery-electric system is therefore required. Figure 7.71 illustrates the dynamics of the hot thermal energy storage tank for a solar-thermal-wind-biomass system with a parabolic trough collector area of 2000 m^2 and a wind turbine rotor radius of 16 m.

Near the beginning of the year heat transfer fluid is mostly discharged from the hot tank to the cold tank. The hot tank then goes through cycles of charging and discharging until the end of the year, where the net accumulation is 1000 m^3. The required hot fluid storage capacity to ensure a reliable supply of energy to the community is 7500 m^3.

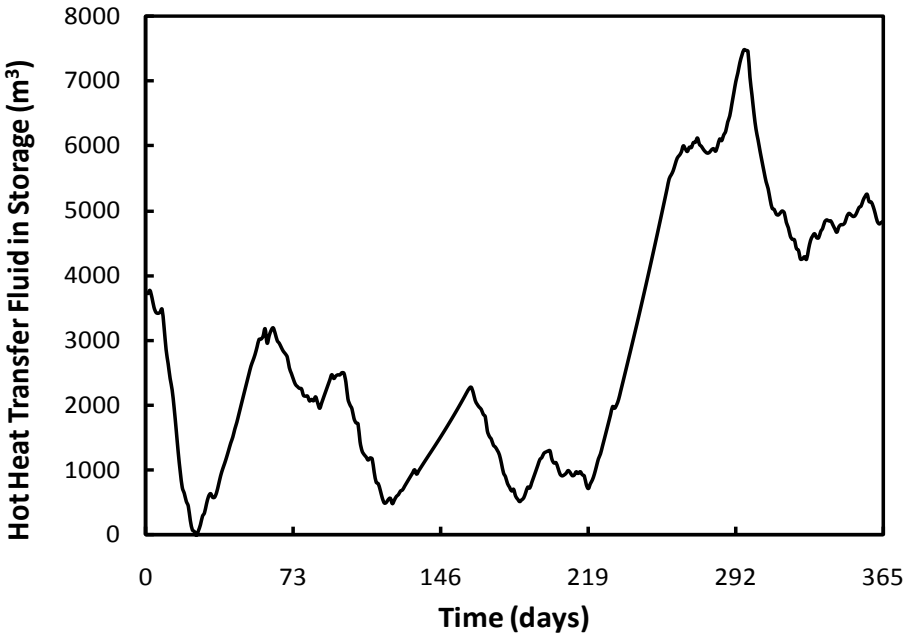

Figure 7.71: Variation in the amount of hot heat transfer fluid in storage over the course of one year for the solar-thermal-wind-biomass system (day "1" corresponds to August 1, 2009).

Figure 7.72 illustrates the behaviour of the battery subsystem over the course of one year. The lead-acid battery goes through several charge/discharge cycles until the net charge after one year is 3 MWh. The capacity of the battery to ensure a reliable supply of energy to the community needs to be at least 110 MWh.

Each component of the solar-thermal-wind-biomass system is associated with a certain amount of exergy destruction. The annual exergy destruction for each subsystem over 365 days is presented in Figure 7.73.

The largest shares of exergy destruction are attributed to the solar-thermal (5.8 TJ per year) and wind turbine (4.4 TJ per year) subsystems. The power-generating Rankine cycle subsystem is also responsible for a large share of exergy destruction (2.8 TJ per year). Total annual exergy destruction is 16 TJ. Consequently, the solar-thermal, wind turbine, and Rankine cycle subsystems are responsible for 36%, 27%, and 18% of total exergy destruction, respectively. As a comparison, the total exergy destruction of the solar-PV-wind-biomass system is 18 TJ per year, which is not that much higher than the

solar-thermal-wind-biomass system. The energy and exergy efficiencies of the system are 31% and 22%, respectively.

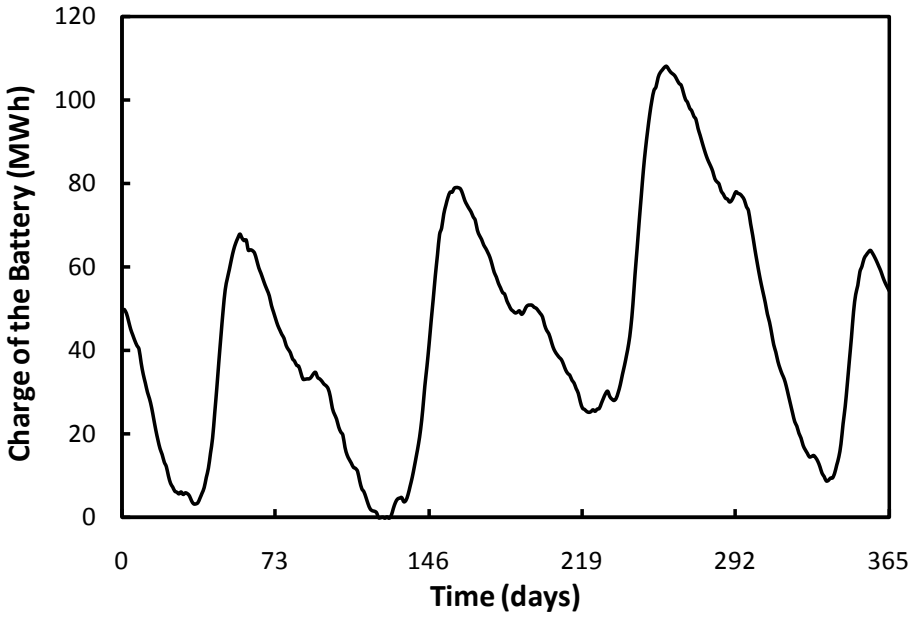

Figure 7.72: Variation in the charge of the battery over the course of one year for the solar-thermal-wind-biomass system (day "1" corresponds to August 1, 2009).

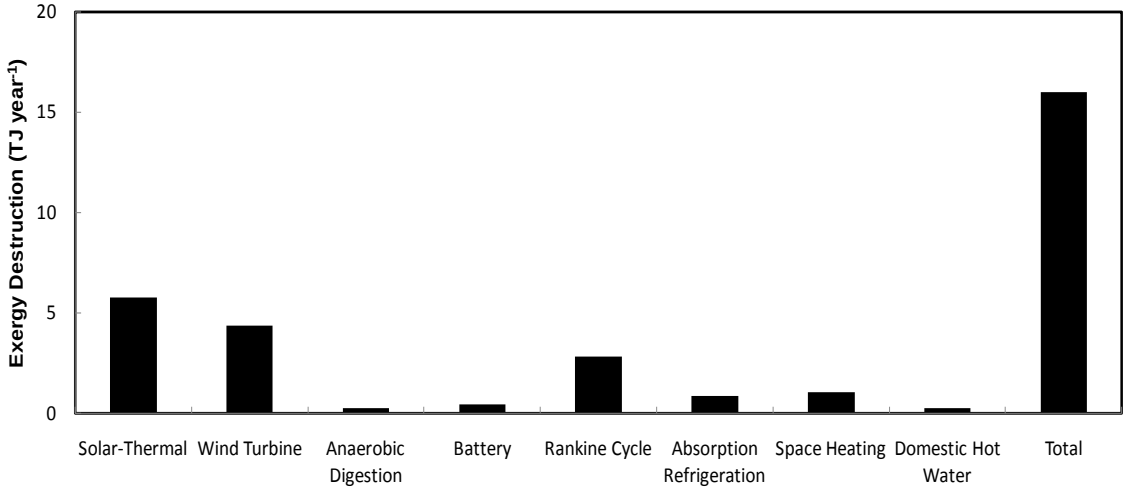

Figure 7.73: Annual exergy destruction of subsystems in the solar-thermal-wind-biomass system over a one-year period.

A thermodynamic analysis of the system is a precursor to sustainability assessment. Thermodynamic, cost, and life-cycle emission factors are combined with weighting factors for three different perspectives to yield the sustainability assessment results presented in Tables 7.41-7.43.

Table 7.41: Sustainability assessment results for the solar-thermal-wind-biomass system from the individualist perspective.

Category	Sub-indicator	$B_{i,j}$	$W_{i,j}$	B_j	W_j	$B_j \times W_j$
ER	EnER	0.53	0.00	0.00	0.07	0.000
	ExER	0.48	1.00	0.48		0.032
EF	AF	0.06	0.50	0.03	0.42	0.012
	CV	1.00	0.50	0.50		0.211
SF	Mass	0.00	0.00	0.00	0.04	0.000
	Area	1.00	1.00	1.00		0.042
	Volume	0.00	0.00	0.00		0.000
GEIP	GWP	0.10	0.24	0.03	0.11	0.003
	SODP	0.08	0.69	0.05		0.006
	ADP	1.00	0.07	0.07		0.007
APP	$PM_{2.5}$	1.00	0.21	0.21	0.30	0.062
	PM_{10}	1.00	0.21	0.21		0.062
	SO_2	1.00	0.04	0.04		0.013
	CO	1.00	0.11	0.11		0.033
	NO_2	1.00	0.11	0.11		0.033
	O_3	1.00	0.11	0.11		0.033
	Pb	1.00	0.21	0.21		0.061
WPP	EP	0.82	0.08	0.07	0.07	0.005
	FAETP	0.28	0.78	0.22		0.015
	MAETP	0.03	0.14	0.00		0.000
ISI						**0.63**

The ISI for the solar-thermal-wind-biomass system ranges from 0.46 to 0.63, where the primary determinant of the score depends on the perspective. Both the AF and GWP sub-indicators are critical to the ISI of the system.

Table 7.42: Sustainability assessment results for the solar-thermal-wind-biomass system from the egalitarian perspective.

Category	Sub-indicator	$B_{i,j}$	$W_{i,j}$	B_j	W_j	$B_j \times W_j$
ER	EnER	0.53	0.00	0.00	0.16	0.000
	ExER	0.48	1.00	0.48		0.076
EF	AF	0.06	0.67	0.04	0.04	0.002
	CV	1.00	0.33	0.33		0.015
SF	Mass	0.00	0.00	0.00	0.25	0.000
	Area	1.00	1.00	1.00		0.247
	Volume	0.00	0.00	0.00		0.000
GEIP	GWP	0.10	0.65	0.07	0.37	0.025
	SODP	0.08	0.25	0.02		0.007
	ADP	1.00	0.11	0.11		0.040
APP	$PM_{2.5}$	1.00	0.04	0.04	0.03	0.001
	PM_{10}	1.00	0.04	0.04		0.001
	SO_2	1.00	0.15	0.15		0.004
	CO	1.00	0.04	0.04		0.001
	NO_2	1.00	0.15	0.15		0.004
	O_3	1.00	0.04	0.04		0.001
	Pb	1.00	0.52	0.52		0.013
WPP	EP	0.82	0.08	0.07	0.15	0.010
	FAETP	0.28	0.19	0.05		0.008
	MAETP	0.03	0.72	0.02		0.003
ISI						**0.46**

The cost of the solar-thermal-wind-biomass system is a concern. The annual cost to a household is $120,000 whereas the median after-tax income of a household is $69,300 (Statistics Canada, 2012). A significant portion of that cost is due to the high cost associated with large thermal and electrical energy storage systems. Also important from a sustainability perspective are the ExER, GWP, SODP, and MAETP sub-indicators.

Sustainability sub-indicators in Tables 7.41-7.43 with a $B_{i,j}$ value equal to one have no negative effect on ISI. Sub-indicators with a $B_{i,j}$ value less than one will have a negative effect on ISI, which is a function of the actual $B_{i,j}$ value and its weight. The range of the negative effect of each sustainability sub-indicator on ISI is graphed in Figure 7.76.

Table 7.43: Sustainability assessment results for the solar-thermal-wind-biomass system from the hierarchist perspective.

Category	Sub-indicator	$B_{i,j}$	$W_{i,j}$	B_j	W_j	$B_j \times W_j$
ER	EnER	0.53	0.00	0.00	0.15	0.000
	ExER	0.48	1.00	0.48		0.073
EF	AF	0.06	0.67	0.04	0.17	0.006
	CV	1.00	0.33	0.33		0.057
SF	Mass	0.00	0.00	0.00	0.15	0.000
	Area	1.00	1.00	1.00		0.153
	Volume	0.00	0.00	0.00		0.000
GEIP	GWP	0.10	0.57	0.06	0.31	0.018
	SODP	0.08	0.33	0.03		0.008
	ADP	1.00	0.10	0.10		0.030
APP	$PM_{2.5}$	1.00	0.10	0.10	0.08	0.008
	PM_{10}	1.00	0.10	0.10		0.008
	SO_2	1.00	0.10	0.10		0.008
	CO	1.00	0.05	0.05		0.004
	NO_2	1.00	0.17	0.17		0.013
	O_3	1.00	0.05	0.05		0.004
	Pb	1.00	0.44	0.44		0.036
WPP	EP	0.82	0.08	0.07	0.13	0.009
	FAETP	0.28	0.58	0.16		0.021
	MAETP	0.03	0.34	0.01		0.001
ISI						**0.46**

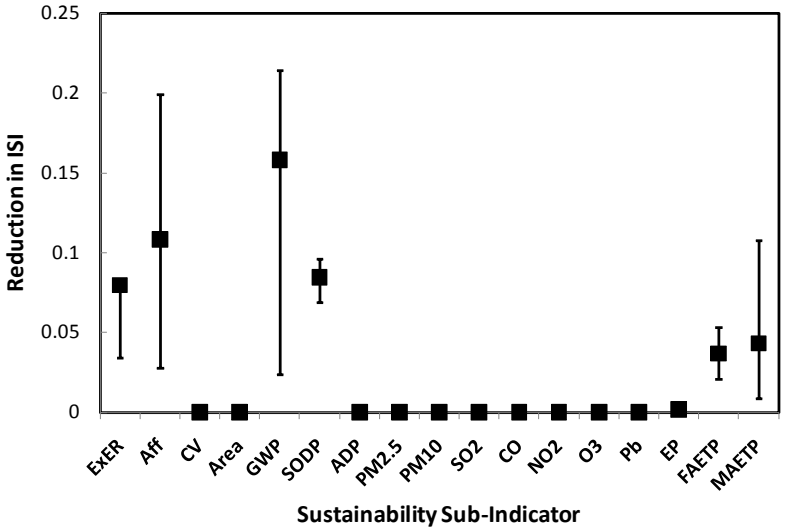

Figure 7.74: Reduction in ISI for each sustainability sub-indicator for the solar-thermal-wind-biomass system.

Several sub-indicators have a range of negative effects on ISI including GWP, AF, MAETP, ExER, and SODP.

The impact of other parameters on global warming and stratospheric ozone depletion is studied in more detail in Figures 7.75 and 7.76.

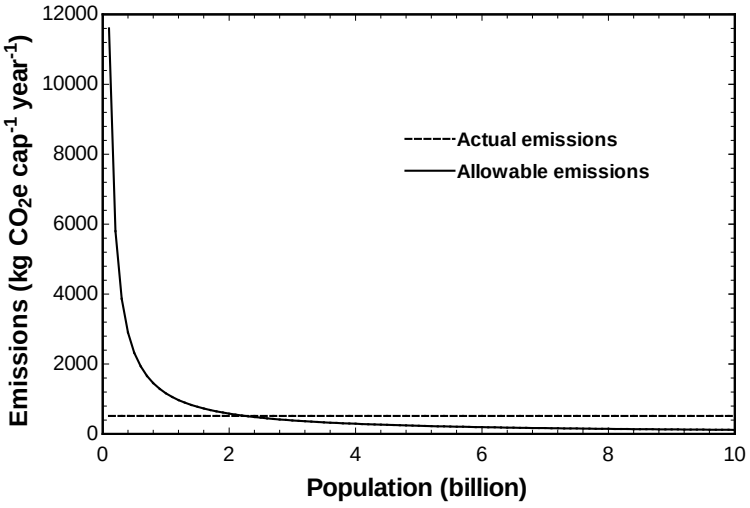

Figure 7.75: Actual and allowable annual per capita GHG emissions for the solar-thermal-wind-biomass system based on the lower limit of the representative concentration pathway (RCP2.6) carbon budget.

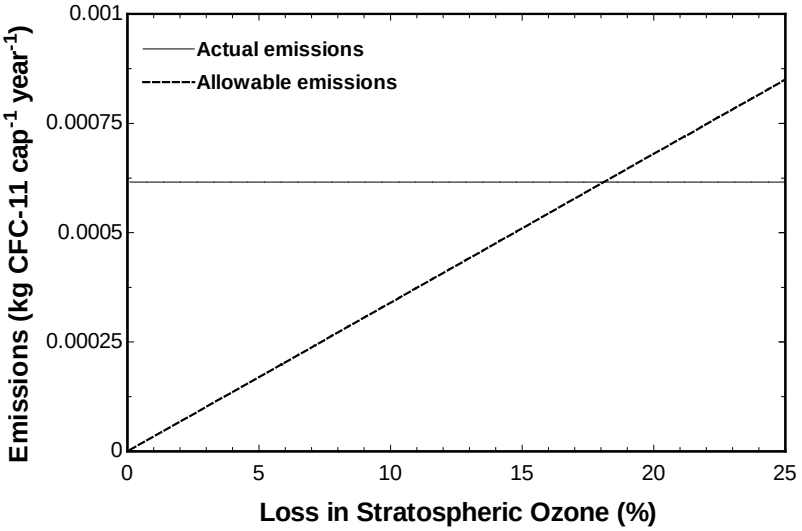

Figure 7.76: Actual and allowable annual per capita ozone-depleting substance emissions (including N_2O) with respect to the percent loss in stratospheric ozone over the time scale for considering sustainability.

The point of intersection in Figure 7.75 occurs at a population of approximately 1.2 billion, which is higher than other wind- and solar-based systems considered here. Similarly, emissions of ozone-depleting substances are consistent with a loss in stratospheric ozone of approximately 18% over 50 years, which is still an excessive amount of stratospheric ozone depletion.

A longer sustainability time scale decreases the ISI of the solar-thermal-wind-biomass system primarily by distributing the acceptable amount of stratospheric ozone layer depletion over a longer period of time (Figure 7.77). This reduces the threshold emissions of ozone-depleting substances per capita per year.

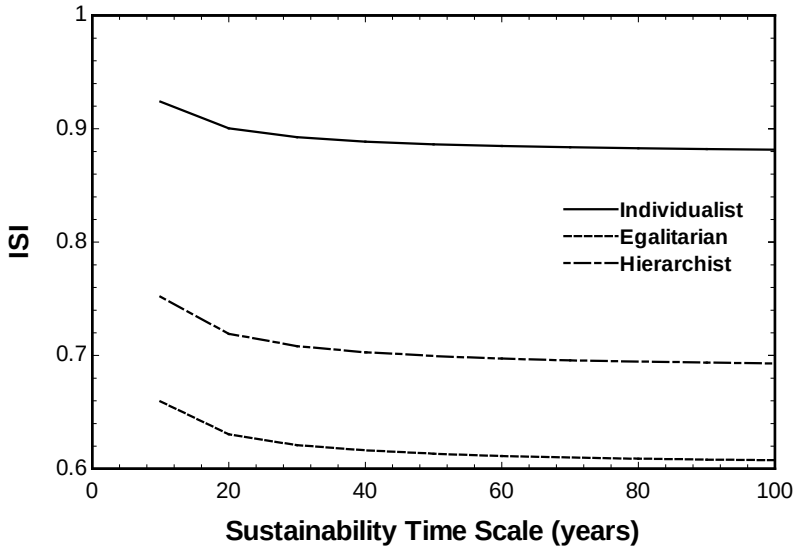

Figure 7.77: Variation of ISI with respect to the time scale for considering sustainability for the solar-thermal-wind-biomass system.

The effect of weighting factor on the most critical sub-indicators is investigated in Figures 7.78 and 7.79.

Figure 7.78 indicates that the weighting factor attached to the AF sub-indicator has the most significant effect on ISI for the individualist perspective. In fact, the ISI decreases from 0.84 to 0.46 as the weighting factor for the AF sub-indicator increases from 0 to 1.

The impact of AF on the egalitarian ISI is much more subdued. The egalitarian ISI only decreases from 0.52 to 0.48 as the AF weighting factor increases from 0 to 1. However, Figure 7.79 indicates that the egalitarian ISI is much more sensitive to GEIP sub-indicators. For example, the egalitarian ISI decreases from 0.69 to 0.38 and 0.57 and 0.24 as the weighting factors for GWP and SODP increase from 0 to 1, respectively.

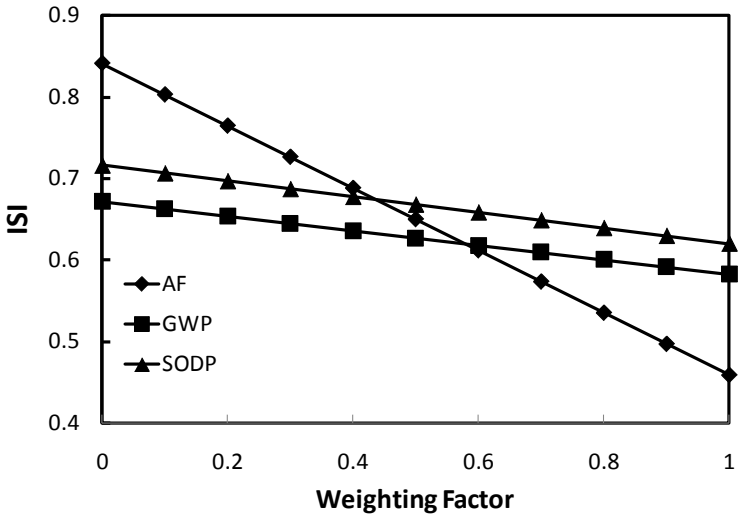

Figure 7.78: Variation of the individualist ISI with respect to weighting factor for the solar-thermal-wind-biomass system.

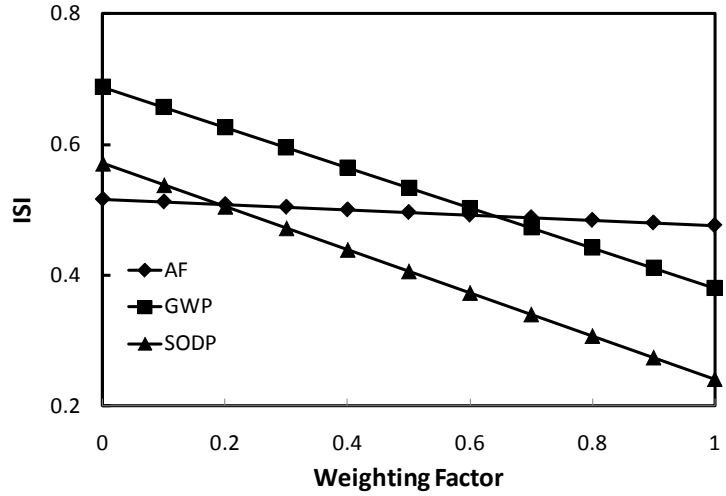

Figure 7.79: Variation of the egalitarian ISI with respect to weighting factor for the solar-thermal-wind-biomass system.

7.2.9 Geothermal-Biomass System

An enhanced geothermal system is a promising technology that has not yet been commercialized. The SimaPro life-cycle assessment software, which is used to estimate environmental emissions, does not include enhanced geothermal systems. The results that follow therefore represent a limited sustainability assessment of a geothermal-biomass system.

Enhanced geothermal systems are assumed to not require any storage and are expected to produce hot geofluid on demand. The fluctuation in the demand for hot geofluid from the underground geothermal reservoir is presented in Figure 7.80.

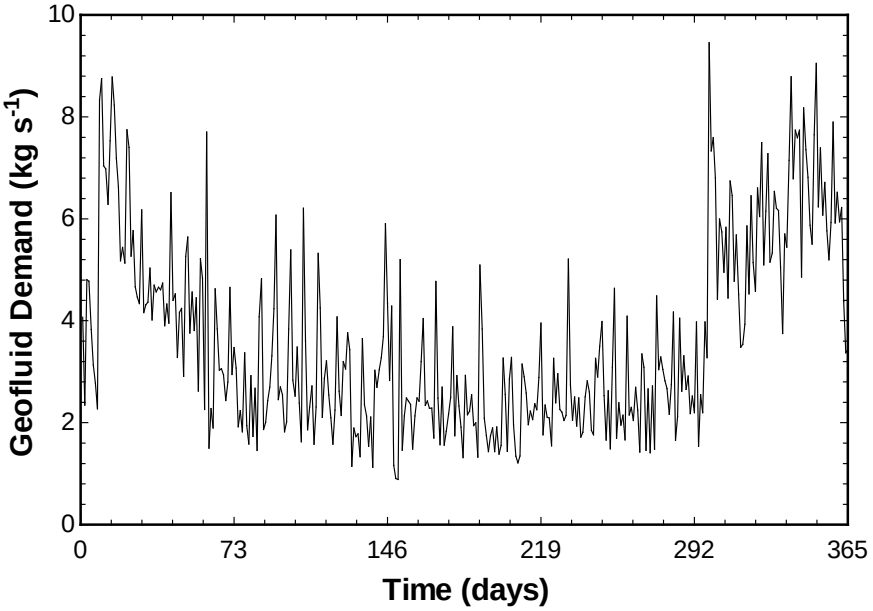

Figure 7.80: Geofluid demand over one year for a 50-household community in Ontario (day "1" corresponds to August 1, 2009).

The demand for geofluid peaks during the summer when electricity demand is at its highest. Demand gradually declines during the winter and picks back up again during the summer.

Each component of the geothermal-biomass system is associated with a certain amount of exergy destruction. The annual exergy destruction for each subsystem over 365 days is presented in Figure 7.81.

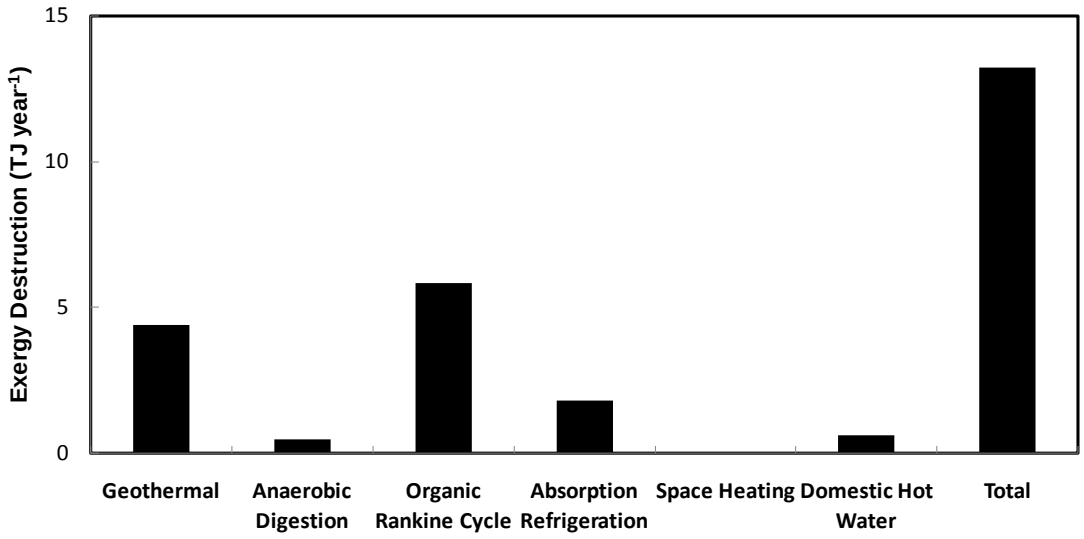

Figure 7.81: Annual exergy destruction of subsystems in the geothermal-biomass system over a one-year period.

The largest shares of exergy destruction are attributed to the organic Rankine cycle (5.8 TJ per year) and geothermal (4.4 TJ per year) subsystems. Since the annual total exergy destruction is 13 TJ per year, the organic Rankine cycle and geothermal subsystems are responsible for 45% and 34% of exergy destruction, respectively. As a comparison to the other hybrid energy systems, the total exergy destruction of the solar-PV-wind-biomass and solar-thermal-wind-biomass system is 18 and 16 TJ per year, respectively. The energy and exergy efficiencies of the system are 23% and 46%, respectively.

A thermodynamic analysis of the system is a precursor to sustainability assessment. Thermodynamic, cost, and life-cycle emission factors are combined with weighting factors for three different perspectives to yield the sustainability assessment results presented in Tables 7.44-7.46.

Table 7.44: Sustainability assessment results for the geothermal-biomass system from the individualist perspective.

Category	Sub-indicator	$B_{i,j}$	$W_{i,j}$	B_j	W_j	$B_j \times W_j$
ER	En	0.95	0.00	0.00	0.07	0.000
	Ex	0.85	1.00	0.85		0.056
EF	AF	0.78	0.50	0.39	0.42	0.165
	CV	0.50	0.50	0.25		0.106
SF	Mass	0.00	0.00	0.00	0.04	0.000
	Area	1.00	1.00	1.00		0.042
	Volume	0.00	0.00	0.00		0.000
GEIP	GWP	1.00	0.24	0.24	0.11	0.026
	SODP	1.00	0.69	0.69		0.074
	ADP	1.00	0.07	0.07		0.007
APP	$PM_{2.5}$	1.00	0.21	0.21	0.30	0.062
	PM_{10}	1.00	0.21	0.21		0.062
	SO_2	1.00	0.04	0.04		0.013
	CO	1.00	0.11	0.11		0.033
	NO_2	1.00	0.11	0.11		0.033
	O_3	1.00	0.11	0.11		0.033
	Pb	1.00	0.21	0.21		0.061
WPP	EP	1.00	0.08	0.08	0.07	0.005
	FAETP	1.00	0.78	0.78		0.051
	MAETP	1.00	0.14	0.14		0.009
ISI						**0.84**

The geothermal-biomass system is associated with less exergy destruction and better ISI values compared to the other hybrid energy systems. The ISI ranges from 0.84 to 0.96 for the individualist and egalitarian perspectives, respectively. In fact, the geothermal-biomass system is unique in that it is the only case study where the lowest ISI occurs from the individualist perspective. This is the case because the individualist perspective puts greater weight on the EF category indicator, which does not score as well for the geothermal-biomass system relative to other impact categories. However, as was mentioned earlier, the full life-cycle impact of an enhanced geothermal system is unknown and its emissions are more than likely underestimated.

Table 7.45: Sustainability assessment results for the geothermal-biomass system from the egalitarian perspective.

Category	Sub-indicator	$B_{i,j}$	$W_{i,j}$	B_j	W_j	$B_j \times W_j$
ER	En	0.95	0.00	0.00	0.16	0.000
	Ex	0.85	1.00	0.85		0.134
EF	AF	0.78	0.67	0.52	0.04	0.023
	CV	0.50	0.33	0.17		0.007
SF	Mass	0.00	0.00	0.00	0.25	0.000
	Area	1.00	1.00	1.00		0.247
	Volume	0.00	0.00	0.00		0.000
GEIP	GWP	1.00	0.65	0.65	0.37	0.239
	SODP	1.00	0.25	0.25		0.092
	ADP	1.00	0.11	0.11		0.040
APP	$PM_{2.5}$	1.00	0.04	0.04	0.03	0.001
	PM_{10}	1.00	0.04	0.04		0.001
	SO_2	1.00	0.15	0.15		0.004
	CO	1.00	0.04	0.04		0.001
	NO_2	1.00	0.15	0.15		0.004
	O_3	1.00	0.04	0.04		0.001
	Pb	1.00	0.52	0.52		0.013
WPP	EP	1.00	0.08	0.08	0.15	0.013
	FAETP	1.00	0.19	0.19		0.030
	MAETP	1.00	0.72	0.72		0.111
ISI						**0.96**

Sustainability sub-indicators in Tables 7.44-7.46 with a $B_{i,j}$ value equal to one have no negative effect on ISI. Sub-indicators with a $B_{i,j}$ value less than one will have a negative effect on ISI, which is a function of the actual $B_{i,j}$ value and its weight. The range of the negative effect of each sustainability sub-indicator on ISI is graphed in Figure 7.82.

The CV sub-indicator exhibits the greatest influence on the ISI of the system by far. Although they are not important from a geothermal-biomass sustainability perspective, the impact of this system on global warming and stratospheric ozone depletion is presented in Figures 7.83 and 7.84.

Table 7.46: Sustainability assessment results for the geothermal-biomass system from the hierarchist perspective.

Category	Sub-indicator	$B_{i,j}$	$W_{i,j}$	B_j	W_j	$B_j \times W_j$
ER	En	0.95	0.00	0.00	0.15	0.000
	Ex	0.85	1.00	0.85		0.129
EF	AF	0.78	0.67	0.52	0.17	0.090
	CV	0.50	0.33	0.17		0.029
SF	Mass	0.00	0.00	0.00	0.15	0.000
	Area	1.00	1.00	1.00		0.153
	Volume	0.00	0.00	0.00		0.000
GEIP	GWP	1.00	0.57	0.57	0.31	0.177
	SODP	1.00	0.33	0.33		0.104
	ADP	1.00	0.10	0.10		0.030
APP	$PM_{2.5}$	1.00	0.10	0.10	0.08	0.008
	PM_{10}	1.00	0.10	0.10		0.008
	SO_2	1.00	0.10	0.10		0.008
	CO	1.00	0.05	0.05		0.004
	NO_2	1.00	0.17	0.17		0.013
	O_3	1.00	0.05	0.05		0.004
	Pb	1.00	0.44	0.44		0.036
WPP	EP	1.00	0.08	0.08	0.13	0.011
	FAETP	1.00	0.58	0.58		0.075
	MAETP	1.00	0.34	0.34		0.045
ISI						**0.92**

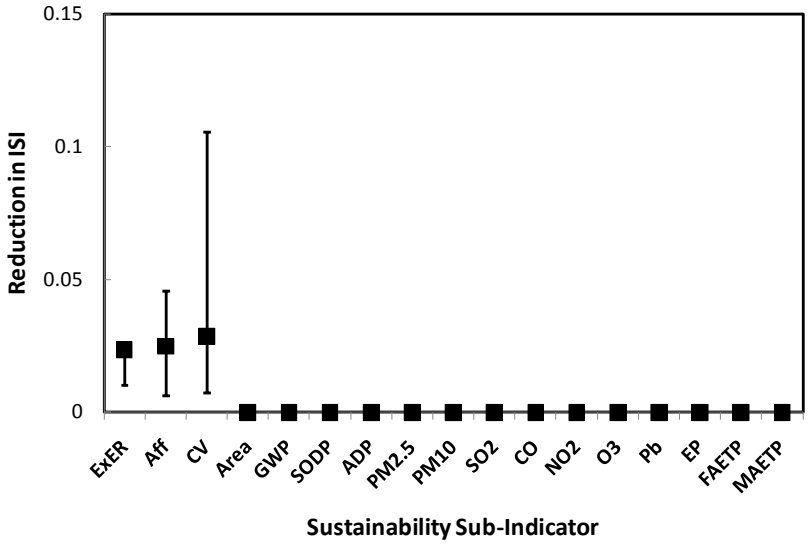

Figure 7.82: Reduction in ISI for each sustainability sub-indicator for the geothermal-biomass system.

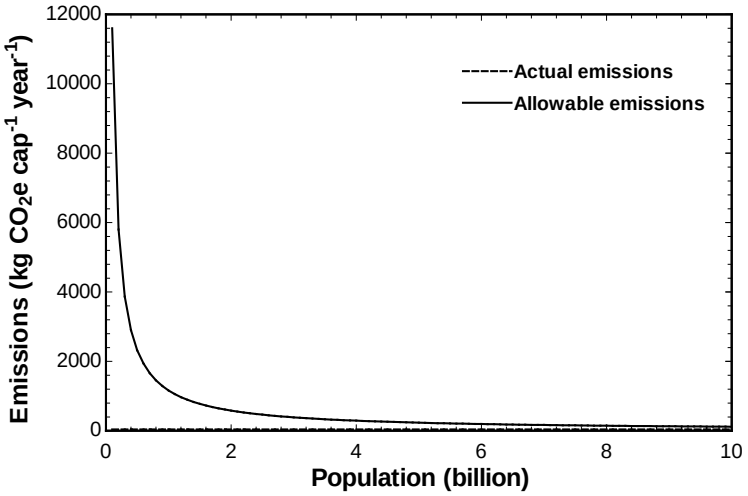

Figure 7.83: Actual and allowable annual per capita GHG emissions for the geothermal-biomass system based on the lower limit of the representative concentration pathway (RCP2.6) carbon budget.

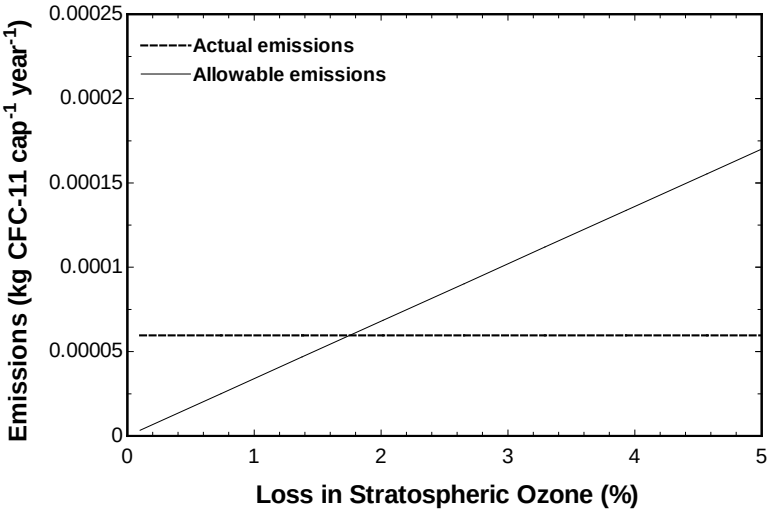

Figure 7.84: Actual and allowable annual per capita ozone-depleting substance emissions (including N_2O) with respect to the percent loss in stratospheric ozone over the time scale for considering sustainability.

There is no point of intersection in Figure 7.83 before and including 10 billion people. Unfortunately the incomplete life-cycle data on the enhanced geothermal system limit the applicability of these results. Conversely, the emissions of ozone-depleting substances fall below the 2% loss of stratospheric ozone, which is considered the

threshold in the sustainability assessment. However, this result is also limited by incomplete data.

The effect of weighting factor on the most critical sub-indicators is investigated in Figures 7.85 and 7.86. These figures reinforce the idea that CV is a critical sub-indicator in the limited sustainability assessment.

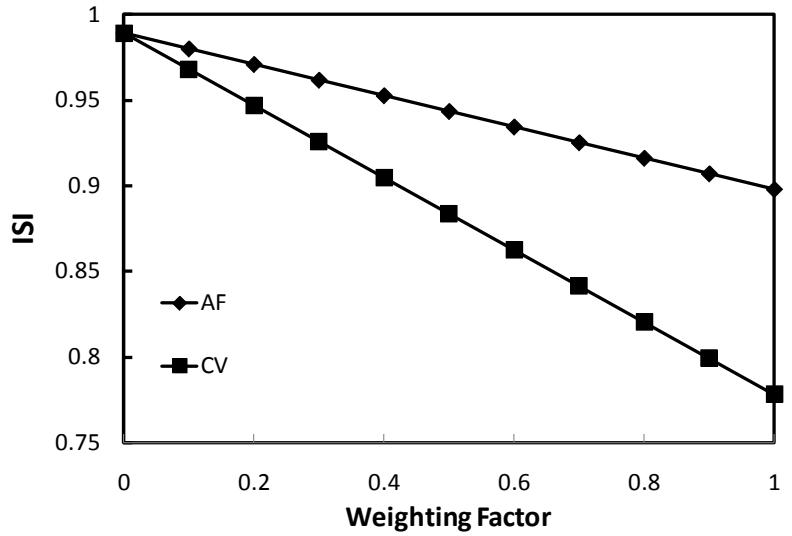

Figure 7.85: Variation of the individualist ISI with respect to weighting factor for the geothermal-biomass system.

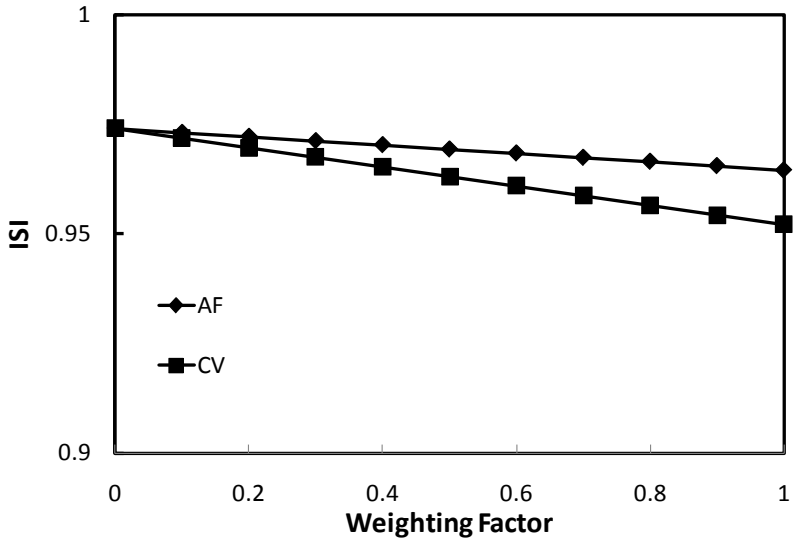

Figure 7.86: Variation of the egalitarian ISI with respect to weighting factor for the geothermal-biomass system.

Figure 7.85 demonstrates that the CV sub-indicator has the most significant effect on the individualist ISI. Increasing the CV weighting factor from 0 to 1 can decrease the individualist ISI from 0.99 to 0.78. The effect of the AF sub-indicator is not nearly as important.

The effect of both AF and CV on the egalitarian ISI is much more subdued (Figure 7.86). EF sub-indicators are not weighted very heavily from the egalitarian perspective, which explains the weak relationship that exists between the sub-indicators and the egalitarian ISI.

7.2.10 Nuclear-Based System

The last case study to be examined is a nuclear-based system. The energy requirements of the nuclear-based system are estimated based on natural uranium. The daily demand of natural uranium is presented in Figure 7.87.

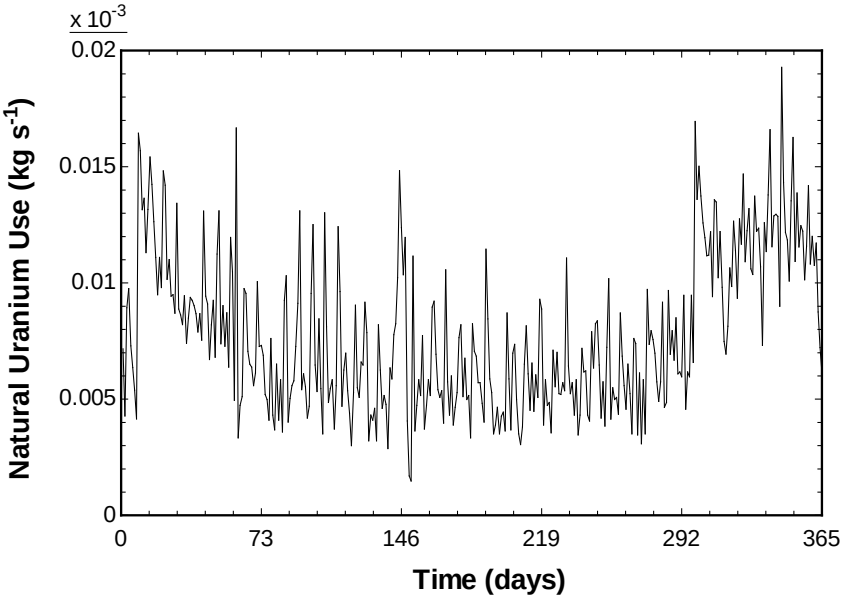

Figure 7.87: Natural uranium consumption over one year for a 50-household community in Ontario (day "1" corresponds to August 1, 2009).

Natural uranium requirements peak during summer months to meet the demand for cooling. In total, 247 kg of natural uranium is required per year, which is equivalent to

1.2 kg per person per year. Similarly, 2.5 kg of nuclear waste is generated per year, which is equivalent to 0.013 kg per person per year.

Each component of the nuclear-based system is associated with a certain amount of exergy destruction. The annual exergy destruction for each subsystem over 365 days is presented in Figure 7.88.

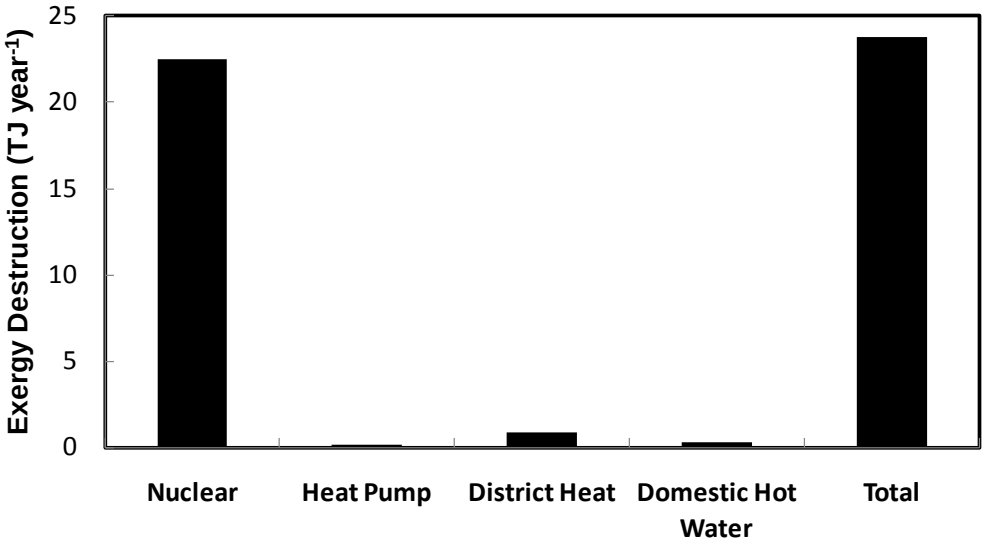

Figure 7.88: Annual exergy destruction of subsystems in the nuclear-based system over a one-year period.

The largest share of exergy destruction is attributed to the power-generating nuclear subsystem (22 TJ per year). Since total exergy destruction is 24 TJ per year, the nuclear subsystem accounts for 92% of the total.

A thermodynamic analysis of the system is a precursor to a sustainability assessment. Thermodynamic, cost, and life-cycle emissions factors are combined with weighting factors for three different perspectives to yield the sustainability assessment results presented in Tables 7.47-7.49.

Table 7.47: Sustainability assessment results for the nuclear-based system from the individualist perspective.

Category	Sub-indicator	$B_{i,j}$	$W_{i,j}$	B_j	W_j	$B_j \times W_j$
ER	En	0.60	0.00	0.00	0.07	0.000
	Ex	0.51	1.00	0.51		0.034
EF	AF	0.10	0.50	0.05	0.42	0.021
	CV	1.00	0.50	0.50		0.211
SF	Mass	1.00	0.00	0.00	0.04	0.000
	Area	0.03	1.00	0.03		0.001
	Volume	0.00	0.00	0.00		0.000
GEIP	GWP	1.00	0.24	0.24	0.11	0.026
	SODP	0.52	0.69	0.36		0.039
	ADP	1.00	0.07	0.07		0.007
APP	$PM_{2.5}$	1.00	0.21	0.21	0.30	0.062
	PM_{10}	1.00	0.21	0.21		0.062
	SO_2	1.00	0.04	0.04		0.013
	CO	1.00	0.11	0.11		0.033
	NO_2	1.00	0.11	0.11		0.033
	O_3	1.00	0.11	0.11		0.033
	Pb	1.00	0.21	0.21		0.061
WPP	EP	1.00	0.08	0.08	0.07	0.005
	FAETP	1.00	0.78	0.78		0.051
	MAETP	0.87	0.14	0.12		0.008
ISI						**0.70**

The ISI of the nuclear-based system ranges from a low of 0.60 for the egalitarian perspective to a high of 0.70 for the individualist perspective. The system does not score well with respect to the AF and Area sub-indicators. On the other hand, the system scores very well for environment-based categories such as GEIP, APP, and WPP. It is important to note that the potential environmental impact of long-term nuclear waste storage and disposal is not considered.

Sustainability sub-indicators in Tables 7.47-7.49 with a $B_{i,j}$ value equal to one have no negative effect on ISI. Sub-indicators with a $B_{i,j}$ value less than one will have a negative effect on ISI, which is a function of the actual $B_{i,j}$ value and its weight. The range of the negative effect of each sustainability sub-indicator on ISI is graphed in Figure 7.89.

Table 7.48: Sustainability assessment results for the nuclear-based system from the egalitarian perspective.

Category	Sub-indicator	$B_{i,j}$	$W_{i,j}$	B_j	W_j	$B_j \times W_j$
ER	En	0.60	0.00	0.00	0.16	0.000
	Ex	0.51	1.00	0.51		0.081
EF	AF	0.10	0.67	0.07	0.04	0.003
	CV	1.00	0.33	0.33		0.015
SF	Mass	1.00	0.00	0.00	0.25	0.000
	Area	0.03	1.00	0.03		0.008
	Volume	0.00	0.00	0.00		0.000
GEIP	GWP	1.00	0.65	0.65	0.37	0.239
	SODP	0.52	0.25	0.13		0.048
	ADP	1.00	0.11	0.11		0.040
APP	$PM_{2.5}$	1.00	0.04	0.04	0.03	0.001
	PM_{10}	1.00	0.04	0.04		0.001
	SO_2	1.00	0.15	0.15		0.004
	CO	1.00	0.04	0.04		0.001
	NO_2	1.00	0.15	0.15		0.004
	O_3	1.00	0.04	0.04		0.001
	Pb	1.00	0.52	0.52		0.013
WPP	EP	1.00	0.08	0.08	0.15	0.013
	FAETP	1.00	0.19	0.19		0.030
	MAETP	0.87	0.72	0.63		0.096
ISI						**0.60**

The sub-indicators that have potential negative effects on the ISI of a nuclear-based system are different than in previous case studies. The two most obvious ones are the Area and GWP sub-indicators. Sustainability assessment results for previous case studies did not identify land area as a potential concern. However, Figure 7.89 demonstrates that Area has the largest range of potential negative effect on ISI. The other case studies were much more likely to identify climate change as an area of concern. This is clearly not the case for a nuclear-based system, which is not negatively affected by the GWP sub-indicator.

Table 7.49: Sustainability assessment results for the nuclear-based system from the hierarchist perspective.

Category	Sub-indicator	$B_{i,j}$	$W_{i,j}$	B_j	W_j	$B_j \times W_j$
ER	En	0.60	0.00	0.00	0.15	0.000
	Ex	0.51	1.00	0.51		0.078
EF	AF	0.10	0.67	0.07	0.17	0.011
	CV	1.00	0.33	0.33		0.057
SF	Mass	1.00	0.00	0.00	0.15	0.000
	Area	0.03	1.00	0.03		0.005
	Volume	0.00	0.00	0.00		0.000
GEIP	GWP	1.00	0.57	0.57	0.31	0.177
	SODP	0.52	0.33	0.17		0.054
	ADP	1.00	0.10	0.10		0.030
APP	$PM_{2.5}$	1.00	0.10	0.10	0.08	0.008
	PM_{10}	1.00	0.10	0.10		0.008
	SO_2	1.00	0.10	0.10		0.008
	CO	1.00	0.05	0.05		0.004
	NO_2	1.00	0.17	0.17		0.013
	O_3	1.00	0.05	0.05		0.004
	Pb	1.00	0.44	0.44		0.036
WPP	EP	1.00	0.08	0.08	0.13	0.011
	FAETP	1.00	0.58	0.58		0.075
	MAETP	0.87	0.34	0.30		0.039
ISI						**0.62**

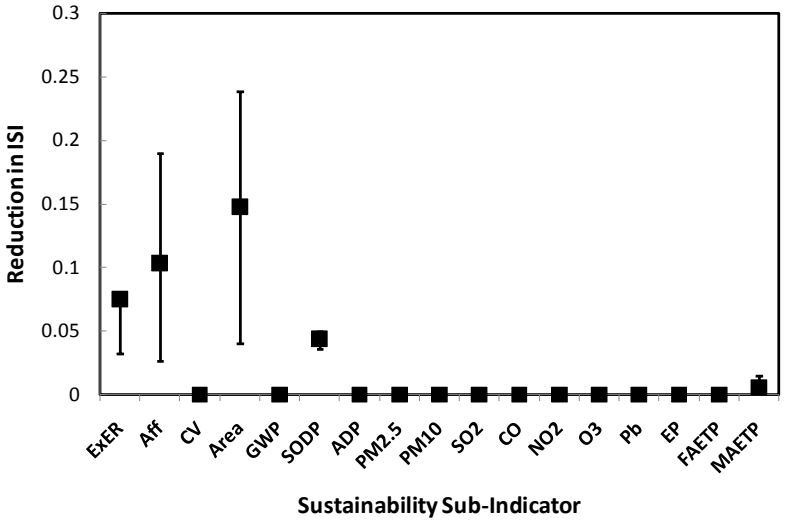

Figure 7.89: Reduction in ISI for each sustainability sub-indicator for the nuclear-based system.

Weighting factors can have a significant influence on the ISI of a system. The effect of weighting factor on the most critical sub-indicators is investigated in Figures 7.90 and 7.91.

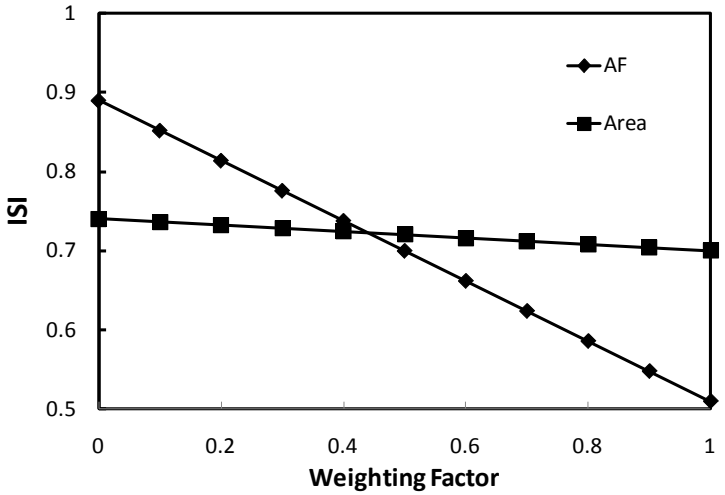

Figure 7.90: Variation of the individualist ISI with respect to weighting factor for the nuclear-based system.

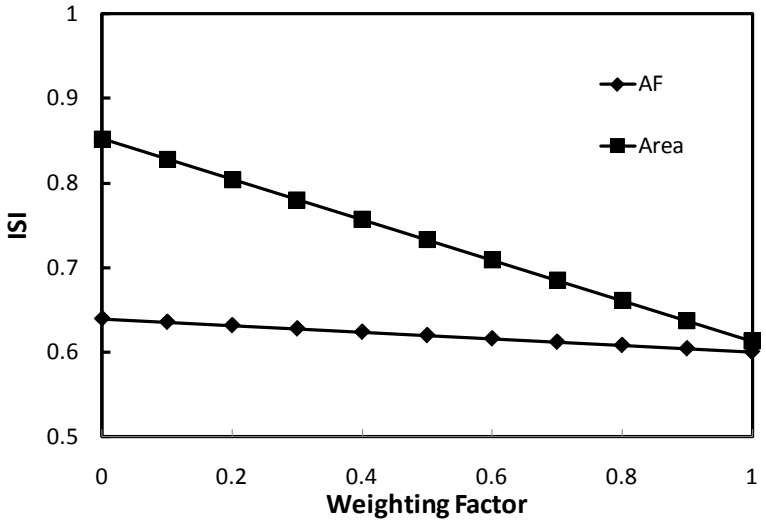

Figure 7.91: Variation of the egalitarian ISI with respect to weighting factor for the nuclear-based system.

Figure 7.90 demonstrates that the weighting factor associated with the AF sub-indicator has the most significant impact on the individualist ISI. Increase the weighting factor from 0 to 1 decreases the individualist ISI from 0.89 to 0.51. A similar change in the weighting factor of the Area sub-indicator has very little effect.

The roles are reversed in Figure 7.91, where the Area sub-indicator has the most significant effect. Increasing the weighting factor associated with the Area sub-indicator decreases the egalitarian ISI from 0.85 to 0.61. The corresponding impact of AF is much more subdued.

There are unique challenges associated with nuclear-based systems that need to be considered in a sustainability assessment. As is the case with the dioxin-emitting waste incineration plant described in Section 5.3, custom indicators need to be designed to produce a more comprehensive assessment of the nuclear-based system. For example, below are two areas of concern related to nuclear-based systems that require special indicators that were not included in the sustainability assessment.

The first area of concern is disposal of radioactive waste. The nuclear fuel cycle produces low-, intermediate-, and high-level radioactive waste along with spent fuel that needs to be safely disposed of (Adamantiades and Kessides, 2009). Beyond the technical challenges of disposal of radioactive waste are the political challenges of finding a suitable site (Kraft, 2013). The difficulty associated with finding and getting approval for an appropriate long-term storage site in the US has led to storage of high-level radioactive waste and spent nuclear fuel at 129 sites in 39 states (Sanders, 2013). A sustainability indicator related to disposal of radioactive waste would have to somehow identify a sustainable level of waste production as a threshold value. This is a significant challenge based on the technical, social, political, and environmental concerns surrounding nuclear waste production and disposal.

The second area of concern is cooling water availability. Nuclear plants require large volumes of cooling water for once-through or closed-loop cooling systems (McMahon and Price, 2011). Consequently, nuclear-based systems need adequate supplies of cooling water for safety and other purposes. Moreover, given the risk and safety

concerns associated with nuclear power (Adamantiades and Kessides, 2009), cooling water availability is more likely to be a non-negotiable indicator (see Section 7.6).

7.3 Comparative Assessment

A comparison of the ISI of all the different case studies for each of the perspectives is presented in Figure 7.92. Excluding the geothermal-biomass system, the solar-PV-hydrogen system has the best ISI for all three perspectives. Energy systems integrated with hydrogen-based storage have a superior ISI relative to battery-based systems. A stand-alone system driven by an intermittent energy source requires significant storage capacity. The analysis demonstrates that the required size of a lead-acid battery to meet the heat, cold, and electrical energy storage needs is very large and the associated costs and emissions significantly affects overall sustainability. Moreover, solar-PV-based systems have a better ISI relative to wind-based systems, all else being equal.

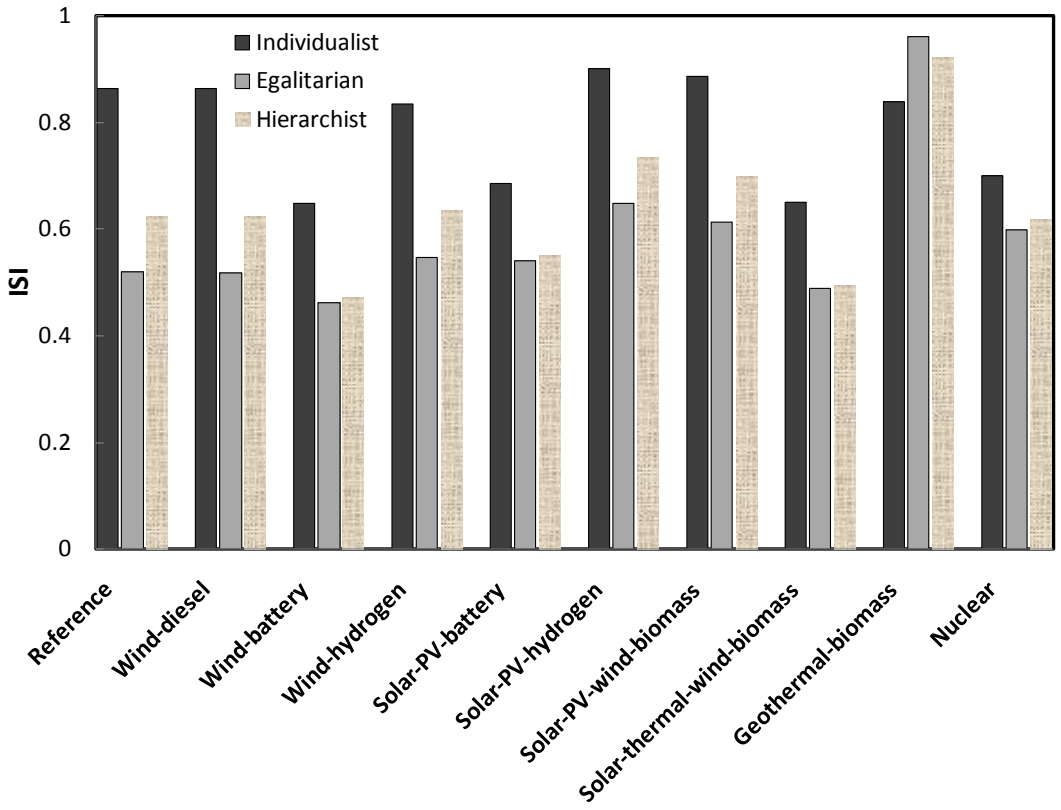

Figure 7.92: ISI of each case study from each perspective.

The ISI of each case study relative to the reference case is presented in Figure 7.93 to illustrate the potential improvement in sustainability by switching to renewable-based energy sources. An ISI ratio greater than one indicates that the system is more sustainable than the reference case and vice-versa.

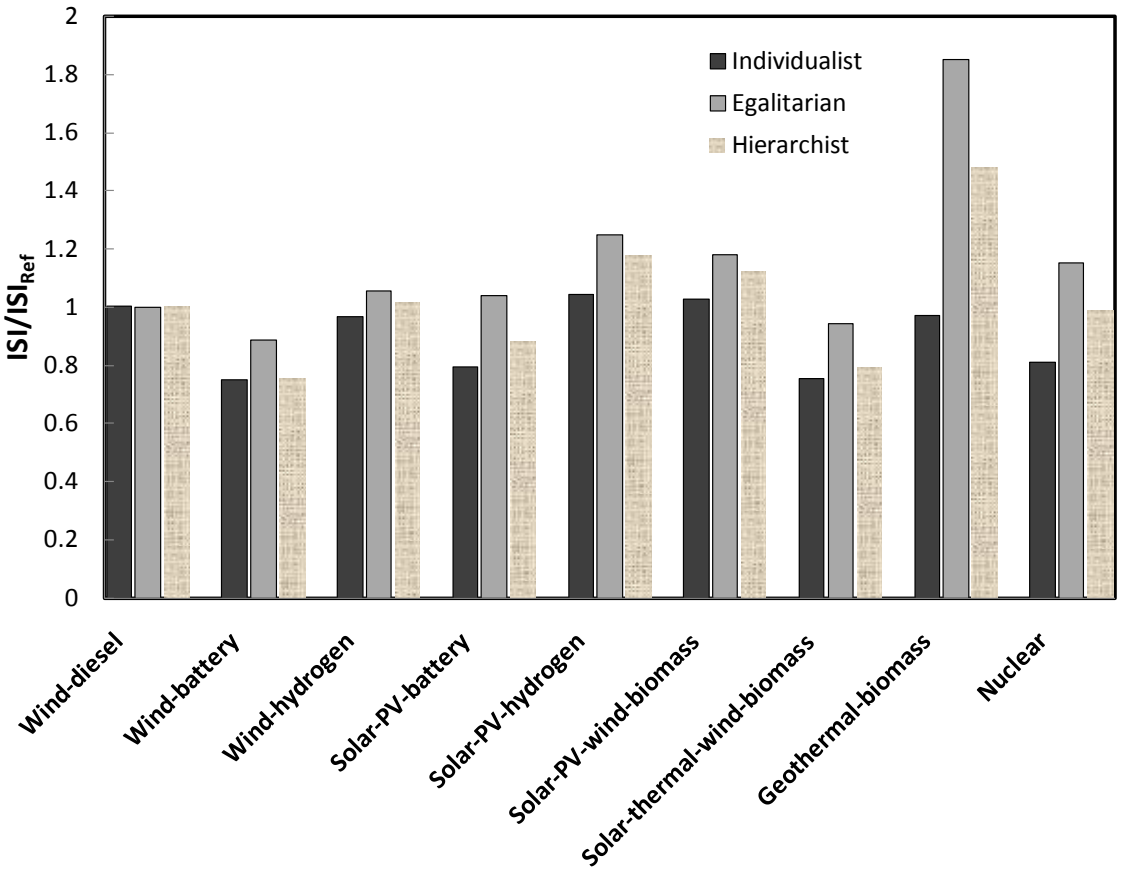

Figure 7.93: ISI of each case study relative to the ISI for the reference case from each perspective.

Each case study that includes battery-based storage is less sustainable than the reference case from an individualist perspective. The sustainability assessments demonstrate that lead-acid batteries are very expensive as a means of storing the large amounts of energy required for a stand-alone system to operate without any fossil-fired back-up system. Moreover, the individualist perspective puts significant weight on the EF category, which is negatively affected by battery-based storage systems. Only the

solar-PV-hydrogen and solar-PV-wind-biomass systems have ISI ratios greater than one for this perspective.

The egalitarian perspective is less concerned with economic criteria and more oriented towards long-term, global environmental impacts. The expectation that renewable-based energy systems will have better ISI scores from this perspective is only partially true. Once again, battery-based case studies have worse ISI scores relative to the reference case for the egalitarian perspective but the differences are minor. The life-cycle emissions associated with large lead-acid batteries are significant even though they occur in the construction phase of the life cycle.

The ADP sub-indicator did not have a detrimental effect on the case studies. Even energy systems that directly utilize fossil fuels during operation did not exceed the threshold for resource depletion. This is due in part to the selection of the time scale for considering sustainability (i.e., 50 years), which is too short to lead to the exhaustion of a resource. Figure 7.94 projects the implications of the sustainability horizon on three systems with the highest ADP.

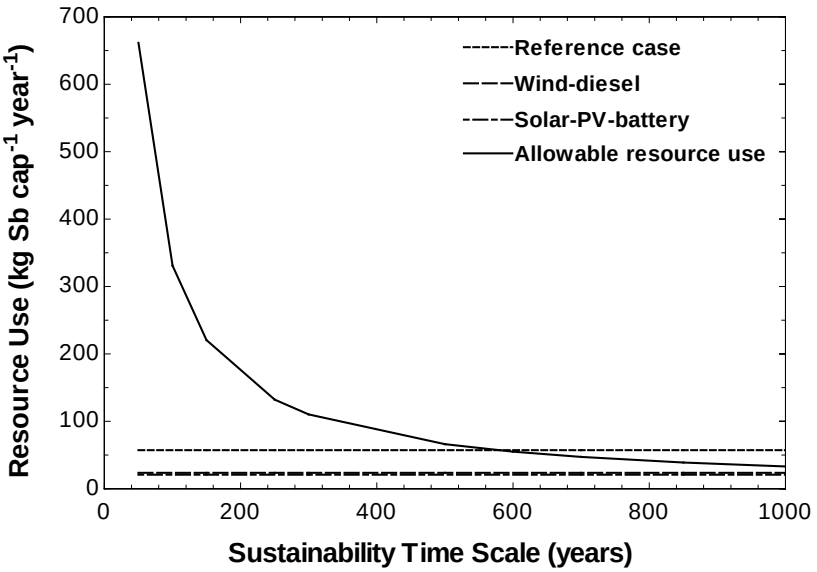

Figure 7.94: Allowable resource use relative to the time scale for considering sustainability for different energy systems.

Increasing the time scale for considering sustainability predictably decreases the tolerable amount of resource use. However, it takes a horizon of approximately 600 years for the allowable resource use curve to intersect with the ADP of the reference gas-turbine system. Moreover, the wind-diesel and solar-PV-battery lines intersect with the curve well past a 1000-year sustainability horizon.

The sustainability assessments revealed that the GWP and SODP sub-indicators were often important contributors to the ISI of each system. Table 7.50 compares various systems based on three results of the sustainability assessment: a) the sustainable global population based on an equally distributed global carbon budget, b) the stratospheric ozone loss over the time scale for considering sustainability, and c) the required storage capacity. The geothermal-biomass system is excluded because of the lack of life-cycle emission data on enhanced geothermal systems.

Table 7.50: The sustainable global population based on an equally distributed global carbon budget, stratospheric ozone loss over 50 years, and required storage capacity associated with each system.

System	Population (billion)	Stratospheric ozone loss	Required storage capacity
1. Reference	0.2	59%	N/A
2. Wind-diesel	0.3	74%	N/A
3. Wind-battery	1.0	22%	150 MWh
4. Wind-hydrogen	1.8	14%	8550 kg
5. Solar-PV-battery	0.4	26%	130 MWh
6. Solar-PV-hydrogen	2.4	14%	5330 kg
7. Solar-PV-wind-biomass	2.3	14%	4810 kg
8. Solar-thermal-wind-biomass	1.2	18%	110 MWh

The solar-PV-hydrogen system is projected to be capable of meeting the needs of 2.4 billion people while staying within the RCP2.6 international carbon budget. This assumes that every household in the world has a demand profile similar to the residential energy use of a typical Ontario household. Unfortunately this is well below the global population of 7 billion but the demand profile of a typical household can change significantly depending on climatic conditions and technological end-use efficiency. The global population that can be sustained using fossil-fired technology is substantially less.

Sustainable development demands global improvements in quality of life within the resource and restorative capacity of the environment. The carbon budget analysis demonstrates that meeting stringent GHG emission targets that limit global warming to less than 2°C and improving standards of living through higher rates of energy use might be possible if low-carbon energy sources are utilized.

The loss of stratospheric ozone over the time scale for considering sustainability (i.e., 50 years) is at least 14% (0.28% per year). It is very difficult to say whether this level of depletion is "sustainable" because the Montreal Protocol mandates reducing ozone-depleting substance emissions to zero. However, the ozone layer is a complex web of interactions capable of self-repair and recovery.

Sustainability assessments of the case studies suggest that the AF, GWP, and SODP sub-indicators are the most relevant. Moreover, the weighting factors associated with each of these sub-indicators have a substantial effect on the overall results of the assessment. There is a real concern that a sustainability assessment utilizing this approach can be made to appear appealing or unappealing based solely on the selection of these weighting factors.

The sustainability assessments of energy systems throughout this thesis and their findings can provide valuable insight on criteria that should be considered when designing community energy systems. The considerations are listed in Table 7.51.

Technical criteria such as energy availability and the community's demand profile are important considerations that may dictate the energy conversion and storage technologies. Economic criteria provide insight on the level of investment a community is capable of making in supporting a decentralized energy system. The assessments showed that stand-alone systems can be affordable or expensive. Communities with a lower standard of living and higher rate of unemployment may be better served by energy systems that offer greater job-creation potential.

Table 7.51: Design considerations for community energy systems.

Criteria	Consideration
Technical	1. Energy availability 2. Demand profile
Economic	1. Income distribution 2. Job-creation potential 3. Proximity to industry
Social	1. Population density 2. Proximity to sensitive receptors 3. Political environment
Environmental	1. Background air quality 2. Meteorological conditions 3. Geographic conditions

Social criteria such as population density and the local political environment may have a strong influence on the type of energy system that gets built. A higher population density could justify more capital-intensive projects such as enhanced geothermal systems while the local political environment may support one technology over another. A strong political will could even create opportunities for government grants and subsidies. The proximity to sensitive receptors could affect where an energy system is sited if air dispersion modelling indicates that sensitive receptors may be vulnerable to unsafe levels of air pollutants.

Environmental criteria are important especially when it comes to emissions. A community with existing air quality issues is less likely to support an energy system with potential air emission concerns. Moreover, meteorological conditions can affect how sensitive receptors are impacted by emissions. Local geographic conditions will impact the fate of pollutants and concentration in various environmental compartments.

These are just a sample of some of the criteria that should be considered when designing a community energy system.

7.4 Optimization

Optimization procedures can be applied to the case study sustainability assessments to determine the optimal value of parameters that maximize the Integrated

Sustainability Index. The wind-diesel system, which combines renewable and non-renewable energy sources, is used as a demonstration of optimization.

The size of the wind turbine in a wind-diesel system is arbitrary because any shortfall in supply can be met by the back-up diesel-based subsystem. Other variables to consider as part of the optimization are the air-fuel ratio and pressure ratio of the diesel-fired gas-turbine subsystem. The following constraints were applied to each of the independent variables: a) rotor radius (5-15 m), b) pressure ratio (4-12), and c) air-fuel ratio (45-80). The three ISI perspectives served as objective functions and were separately optimized. The wind-diesel system is studied for typical winter and summer cases and the results of the optimization procedure are presented in Table 7.52.

Table 7.52: Optimization of the wind-diesel system ISI from three different perspectives using three independent variables.

Case	Perspective	Air-fuel ratio	Pressure ratio	Rotor radius (m)	ISI
Winter	Individualist	45	8	15	0.55
	Egalitarian	45	8	15	0.53
	Hierarchist	45	8	15	0.54
Summer	Individualist	45	8	15	0.68
	Egalitarian	45	8	15	0.56
	Hierarchist	45	8	15	0.62

A built-in genetic algorithm in EES is used for the optimization procedure. The analysis suggests that the objective function for all three perspectives is maximized when the air-fuel ratio is at its minimum value, the pressure ratio is equal to 8, and the rotor radius is at its maximum value. The stoichiometric air-fuel ratio of diesel fuel is approximately 14.5 but much higher ratios are required to ensure complete combustion (Obert, 1973). The wind-diesel model does not take this into account and assumes complete combustion of the fuel. Consequently, the lowest possible value of the air-fuel ratio, which maximizes the temperature of the working fluid, is always selected by the optimization algorithm as the optimal air-fuel ratio to maximize ISI.

Although the maximum ISI occurs at the maximum wind turbine rotor radius this may not be true in all scenarios. For example, an optimization procedure can be

implemented to determine the capital cost at which a larger wind turbine is less attractive than a diesel-fired gas-turbine generator from a sustainability perspective. The relationship between the maximum ISI and the capital cost of a wind turbine is illustrated in Figures 7.95 and 7.96 for the winter and summer cases, respectively.

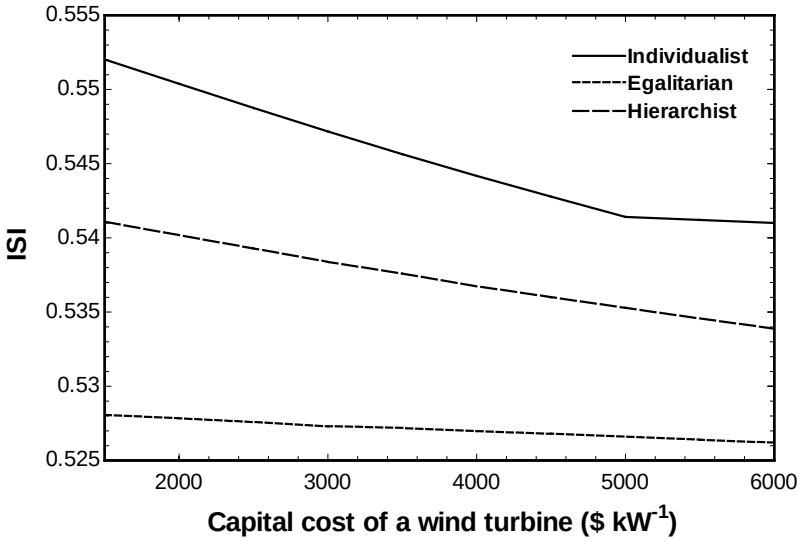

Figure 7.95: Variation in the maximum ISI with respect to the capital cost of a wind turbine for the winter case of a wind-diesel system.

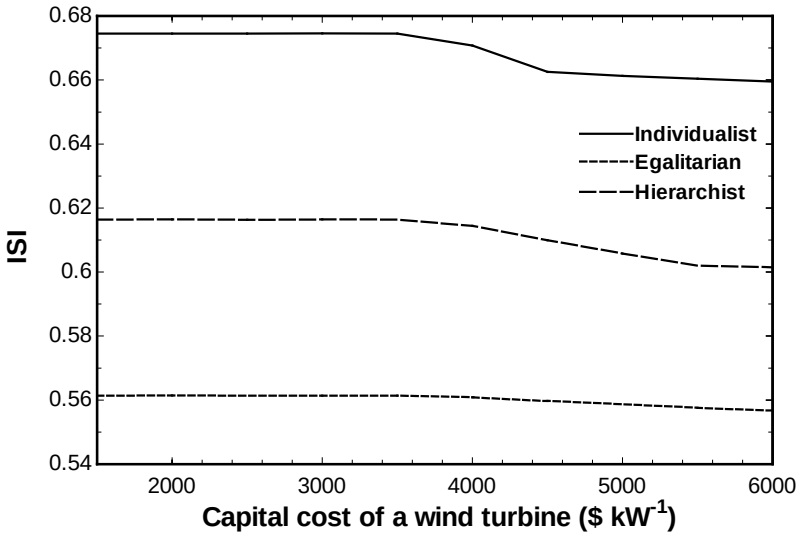

Figure 7.96: Variation in the maximum ISI with respect to the capital cost of a wind turbine for the summer case of a wind-diesel system.

The ISI for each perspective decreases as the capital cost of the wind turbine increases. For the winter case (Figure 7.95), the decrease in maximum ISI for the egalitarian and hierarchist perspectives is fairly constant over the range of capital costs. The decline in maximum ISI for the individualist perspective is fairly constant until \$5000 kW^{-1}, at which point the slope of the line changes and decreases at a slower rate. This is the crossover point where the benefits of a wind turbine no longer outweigh the costs and the optimal rotor radius decreases below 15 m (Figure 7.97). As a comparison, the capital cost of an onshore wind turbine is approximately \$2000 kW^{-1} (EIA, 2013; EPA, 2012).

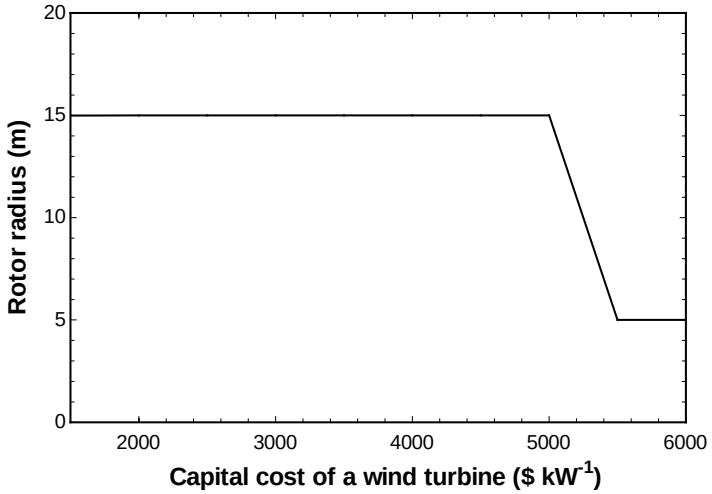

Figure 7.97: The change in the optimal value of the rotor radius that maximizes the individualist ISI as a function of wind turbine capital cost for the winter case of a wind-diesel system.

A similar pattern occurs for the summer case (Figure 7.96) except the individualist crossover point is at \$4500 kW^{-1} (Figure 7.98). Moreover, there is also a capital cost at which a 15 m rotor radius is no longer desirable from a hierarchist perspective. That crossover point is at \$5500 kW^{-1}.

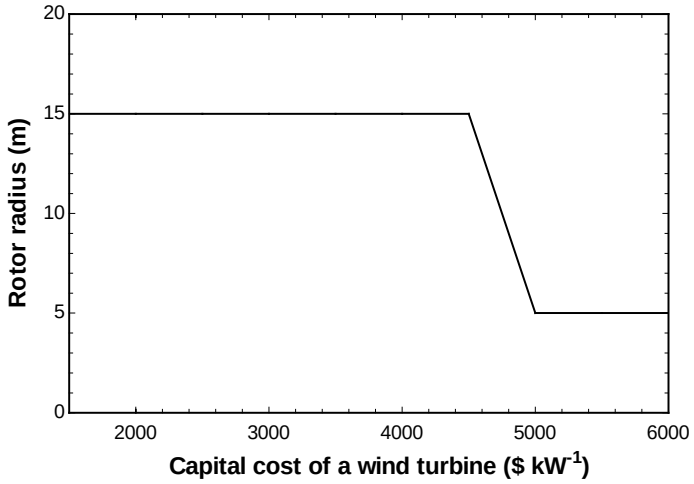

Figure 7.98: The change in the optimal value of the rotor radius that maximizes the individualist ISI as a function of wind turbine capital cost for the summer case of a wind-diesel system.

It should be noted that there are no crossover points for the egalitarian perspective over the range of wind turbine capital costs in Figures 7.95 and 7.96. This perspective puts less weight on the cost and affordability of energy systems, which leads to a maximum ISI that is less sensitive to changes in the capital cost of a wind turbine.

In addition to optimization, artificial neural networks are another class of mathematical approaches that could be used to gain a better understanding of the sustainability of energy systems. An artificial neural network is a modelling mechanism that identifies the rules that govern the optimal solutions to nonlinear problems (Buscema, 2002). The network consists of nodes and weighted connections between those nodes that form a complex, interconnected system similar to biological neural networks (Kriesel, 2007). These networks can discover the underlying rules that connect various sets of data and can learn by adjusting those rules as new data becomes available (Buscema, 2002).

The structure of an artificial neural network has similarities to the structure of the developed sustainability assessment approach, where input data and variables are converted to outputs through weighted connections. For a given case study with a specific set of inputs, artificial neural networks can identify the sets of weighting factors

that yield the optimal results. This provides the analyst with useful information on the strengths and weaknesses of an energy system from a sustainability perspective.

Although useful, artificial neural networks should not be a substitute for independently deriving weighting factors using the approaches outlined in Chapter 4. Sustainability is a multidimensional concept and weighting factors represent the importance and substitutability of criteria according to the analyst, stakeholders, and decision makers. The generally held view in the literature on sustainability assessment is that weighting factors should be independent of alternatives (Rowley et al., 2012).

7.5 Model Validation

The results of the sustainability assessment model can be validated through a comparison to existing assessments in the literature. Afgan (2010) compared natural gas combined cycle, wind, and solar-PV power plants on the basis of efficiency, cost, GHG emissions, and land area. Comparisons were conducted based on two cases. The first case assigned the highest priority to efficiency and equal weights to the remaining criteria. The second case assigned the highest priority to GHG emissions and cost and equal weights to the remaining criteria. In both cases, the natural gas combined cycle power plant had the highest ranking while the wind and solar-PV power plants ranked second and third, respectively.

All three systems were assessed using the ISI approach for validation purposes. The natural gas combined cycle is presented in Figure 7.99. The ISI of each system for both cases utilizing the same weighting factors as in the study by Afgan (2010) is reported in Table 7.53.

Both methods rank the natural gas combined cycle power plant as the most sustainable system for both case 1 and case 2. However, Afgan (2010) ranks the wind turbine as more sustainable compared to the ISI approach, which prefers the solar-PV system. This example demonstrates that a sustainability assessment based on the ISI is consistent with at least one other approach in the literature although more validation is needed.

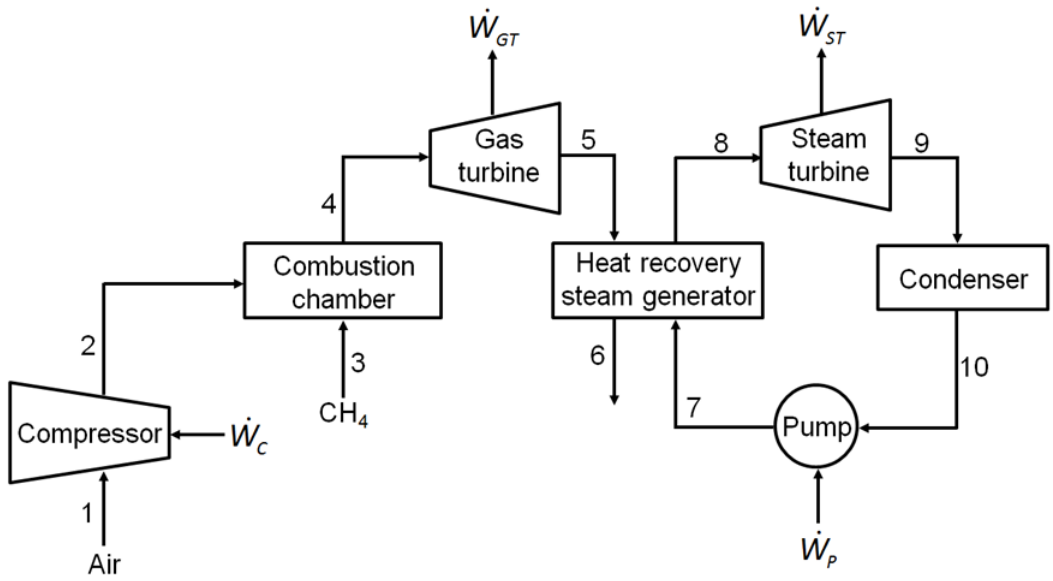

Figure 7.99: General layout of a natural gas combined cycle power plant.

Table 7.53: Energy system rankings according to Afgan (2010) and the ISI.

System	ISI		ISI ranking		Afgan (2010)	
	Case 1	Case 2	Case 1	Case 2	Case 1	Case 2
Natural gas combined cycle	0.78	0.67	1	1	1	1
Wind turbine	0.67	0.55	3	3	2	2
Solar-photovoltaic	0.77	0.61	2	2	3	3

Comparing the effectiveness of different approaches is a challenge for sustainability assessment models. Sustainability is not something that can be directly measured, which limits our ability to gauge the performance of sustainability assessment tools. Nevertheless, there are some general guidelines that can be helpful.

First, approaches that utilize a life-cycle perspective are preferable. Second, target values should be based on sustainability-based threshold values. Third, approaches that contain a range of indicators that span technical, economic, social, and environmental criteria are more likely to provide a better overall assessment. Fourth, a sustainability index that is tailored to the specific system under investigation (e.g., a dioxin indicator for a waste incineration plant) is desirable.

There is a fine line between a sustainability assessment index based on a range of multi-criteria indicators and an index that is watered down by too many. Every additional indicator with a non-zero weighting factor will dilute the weighting factors associated with other indicators within the same category. This is a challenge that faces the sustainability analyst with no clear-cut answer.

7.6 Hybrid Sustainability Assessment

Evaluating the sustainability of a system often involves trade-offs. In a compensatory sustainability assessment a deficit in one area can be compensated by improvements in other areas. However, there may be some limits that are non-negotiable and an interest in setting a minimum standard on the part of the sustainability analyst, decision maker, and potential stakeholders. A hybrid sustainability assessment that incorporates a preliminary screening phase prior to the actual assessment is one way of combining a compensatory approach with non-negotiable hard targets. A flow chart of the hybrid approach is presented in Figure 7.100.

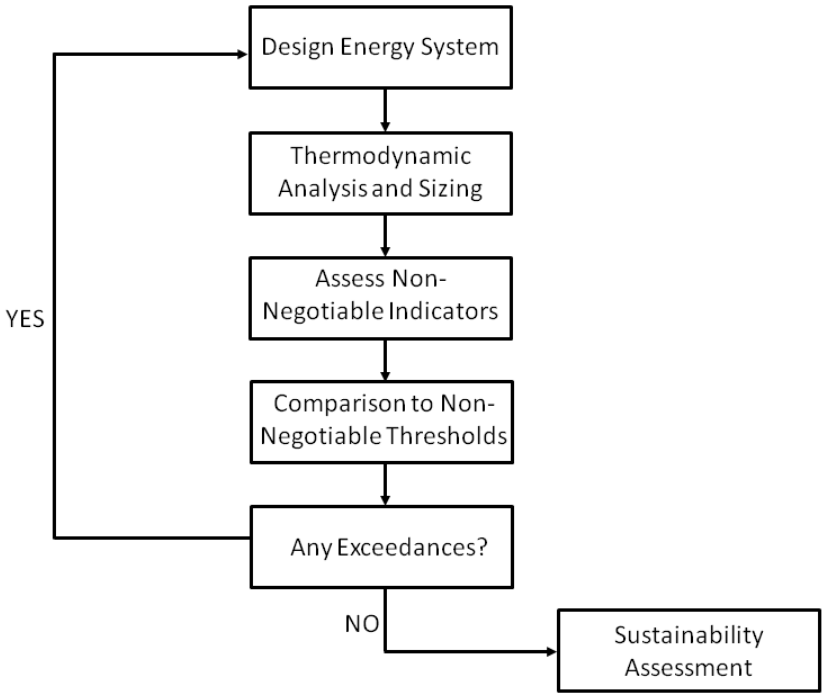

Figure 7.100: Flow chart of a hybrid sustainability assessment of an energy system.

The flow chart stipulates that non-negotiable indicators must first be calculated and compared to non-negotiable thresholds before proceeding to the actual sustainability assessment. If the non-negotiable indicator exceeds the threshold, then the energy system must be redesigned. For example, suppose that GWP is a non-negotiable indicator but that the threshold in the preliminary screening is not as stringent as the threshold in the actual sustainability assessment. In other words, the non-negotiable threshold could be the upper emission limit of RCP2.6 as opposed to the lower, more stringent emission limit. If the candidate energy system meets the upper emission limit of RCP2.6 it may then proceed to the actual assessment, where the lower emission limit of RCP2.6 becomes the new threshold value. However, if the candidate system fails to meet the less stringent but non-negotiable threshold, then it does not proceed to the next stage of the assessment and must be redesigned. Indicators related to safety issues are also good candidates as non-negotiable thresholds.

7.7 Application of Methodology to Canada

The proposed sustainability assessment approach can provide valuable insight on important sustainability-related criteria for energy systems. An interesting idea is to apply the approach beyond energy system assessment. A potential application of the approach is to assess sustainable development in Canada.

Modern capitalist economies are dependent on economic growth to ensure their own economic stability (Homer-Dixon, 2007). Economic growth is also perceived to offer sustained improvements in human welfare (Jackson, 1996). Even the well-known Human Development Index uses economic output (i.e., GDP) per capita as a proxy for the development of a nation-state, in addition to education and life expectancy metrics (Morse, 2013). Some of the criticisms of this approach are that intra-country income inequality is not represented and environmental issues are excluded from the index. Despite its ubiquity, GDP per capita is an ineffective measure of economic development (Jackson, 1996), let alone sustainable development.

Many of the sustainability indicators presented in Section 5.1 can be applied to assess sustainable development in Canada. Once the proper indicators are selected, the current status needs to be assessed. Ideally, there will also be a historical record of the indicators to track progress over time. The historical and current status of indicators then needs to be compared to sustainability-based target values, as described in Chapters 4 and 5.

Indicators such as GHG emissions, ozone-depleting substance emissions, and abiotic resource depletion can be evaluated at a national level. On the other hand, it is more appropriate to monitor air quality at the local and municipal level. Similar to air quality, there are many different chemical species that can affect water quality. One possibility is to sample environmental DNA directly to determine the health of an aquatic ecosystem (Jones, 2013).

There are limitations in the extent to which the proposed sustainability assessment approach can assess sustainable development in Canada. Other indicators related to intragenerational equity, infrastructure, and power density can provide valuable insight on the progress of sustainable development.

Intragenerational equity is an important aspect of sustainable development. Indicators need to be developed at the local level across Canada that measure household income, cost of living, unemployment, and poverty. This is especially true for Canada's Aboriginal peoples, who suffer from a sizable income gap relative to the rest of the population and high costs of living for those in isolated reserve communities (Wilson and Macdonald, 2010).

Infrastructure can guide behaviour and decision-making in a society, which makes it a key component of sustainable development. Long-lived capital stock and infrastructure locks in patterns of energy use for decades into the future (National Academy of Sciences et al., 2010). Fossil-fired power plants commit to burning fossil fuels. Low-density suburban communities increase car dependency and require new road infrastructure. Extensive road and highway networks can also be thought of as encouraging the development of low-density suburban communities.

Infrastructure can also have a positive impact on sustainable development. Smart grids that allow bidirectional electron flows facilitate integration of distributed energy into the electricity-supply network (Coll-Mayor et al., 2007). Cycling arteries that prioritize cyclists over motorists ("bike boulevards") or provide a high degree of separation from motor vehicle traffic are likely to promote active transportation (Russell, 2010). Tracking the type of infrastructure projects undertaken can provide deep insight on sustainable development in Canada.

An economy that can be sustained over the long term is expected to exploit renewable resources and limit the use of non-renewable resources (Daly, 2005). Although renewable resources are abundant, the power densities of renewable energy flows are orders of magnitude less than the power densities of fossil fuels (Smil, 2007). A comparison of electric power densities for different sources is presented in Table 7.54.

Table 7.54: Electric power densities of energy sources (adapted from Smil (2007)).

Source	Electric power density (W m^{-2})	
	Low	High
Natural gas	200	2000
Coal	100	1000
Solar (photovoltaic)	4	9
Wind	0.5	1.5
Biomass	0.5	0.6

Solar energy converted to electricity through a photovoltaic cell has the highest power density of the renewable energy flows but is still significantly less than the power density from fossil-fired generating stations. The challenge is that there is a mismatch between renewable energy flows and the high power density needs of existing infrastructure, which is 10-1000 W m^{-2} (Smil, 2007). A useful metric to assess sustainable development is to track the power density requirements of communities across the country and assess the ability of renewable energy flows to meet that demand.

Sustainable development is a significant multidimensional challenge that can be approached in many different ways. Some of the indicators discussed in this thesis are applicable in assessing sustainable development but they need to be combined with

other indicators to offer a more comprehensive assessment. A few additional indicators are proposed but, as is often the case with sustainability-related issues, there are many others that can be developed.

Chapter 8 : Conclusions and Recommendations

This chapter presents the concluding remarks of this study and offers recommendations for future work.

8.1 Conclusions

The goal to achieve a sustainable society that will endure over the long term is desirable but a standard and universally accepted sustainability assessment index does not yet exist. This thesis develops a general framework for determining the ISI of a system based on a three-step process of normalization, weighting, and aggregation. The originality of this new index is that it incorporates fundamental thermodynamic, economic, and environmental constraints to combine indicators from multiple dimensions into a single-score evaluation of sustainability. The framework is then implemented to develop a novel, multidimensional assessment of the sustainability of community energy systems. The ISI is evaluated for several different case studies and the results are interpreted and translated into findings and conclusions. The specific concluding remarks of this thesis are stated as follows:

- The solar-PV-hydrogen system has the highest ISI (0.65-0.90) from all three sustainability perspectives although variations in weighting factors can decrease ISI down to 0.41.
- The wind-battery system has the lowest ISI (0.44-0.62) from all three sustainability perspectives although variations in weighting factors can increase ISI up to 0.83.
- The wind-battery system requires the largest battery (150 MWh), which is responsible for 95% of the total cost of the system.
- The GWP of the solar-PV-hydrogen system suggests that 2.4 billion people can have a similar electricity-demand profile as a typical Ontario household while staying within RCP2.6 international carbon budget. The corresponding population for the reference gas-fired system is only 0.2 billion.

- Stratospheric ozone depletion due to the wind-hydrogen, solar-PV-hydrogen, and solar-PV-wind-biomass system is estimated to be approximately 14% over 50 years, which is much higher than the 2% target value. However, determining a tolerable level of ozone layer depletion is a challenge.
- Stratospheric ozone depletion due to the wind-diesel system is estimated to be approximately 74%, which is due to the high amount of N_2O produced by a diesel engine.
- Increasing the sustainability time scale noticeably deceases the ISI of the solar- and wind-based systems but has very little effect on fossil-fired systems that already have very low scores for environmental indicators.
- The sustainability time scale has to be at least 600 years before overall resource depletion becomes a concern. Depletion of specific resources could occur on shorter time scales but needs to be individually considered in the assessment.
- An optimization analysis shows that when the capital cost of a wind turbine reaches approximately \$5000 kW^{-1} the ISI of a wind-diesel system is maximized when the size of the wind turbine is minimized.
- Respondents to a questionnaire on the importance of sustainability indicators assigned the highest importance to GWP with very low variability. Economy-based indicators (i.e., AF and CV) received the lowest scores but with higher variability.

8.2 Recommendations

The following recommendations for future work are suggested:

- This study developed indicators for several sustainability criteria but this is only a starting point. Future assessments should include indicators specific to that case study, such as natural gas depletion or radioactive waste production.

- Social indicators such as local job creation potential, health, and public acceptance should be considered while still avoiding double-counting problems.
- The effect of applying a geometric aggregation procedure as opposed to a linear approach on the ISI of systems should be considered.
- Changing the location of the assessment should be considered as this will affect input variables (e.g., solar irradiance, wind speed, energy demand) and other parameters (e.g., background air quality, available land area), all of which will impact the ISI of a system.
- The potential improvement in ISI as a result of multi-generation (e.g., transportation fuels, desalinated water) systems should be studied.

The practical applications of this research are:

- Multi-criteria assessment of energy systems that indicates the performance of a system with respect to several sustainability-related parameters.
- Fostering an improved understanding of energy systems from a holistic, systems perspective. Unlike other sustainability assessments, this approach puts indicators and criteria into context by comparing to actual limits imposed by thermodynamic, economic, and environmental constraints.
- A high-level tool to assist decision makers in developing evidence-based policy by providing a holistic view of energy systems.

References

Adamantiades, A., Kessides, I., 2009. Nuclear power for sustainable development: current status and future prospects. Energy Policy. 37:5149-5166.

Afgan, N.H., 2010. Sustainability paradigm: intelligent energy system. Sustainability. 2:3812–3830.

Afgan, N.H., Carvalho, M.G., Hovanov, N.V., 2000. Energy system assessment with sustainability indicators. Energy Policy. 28:603–612.

Afgan, N.H., Carvalho, M.G., 2002. Multi-criteria assessment of new and renewable energy power plants. Energy. 27:739–755.

Ahlroth, S., Nilsson, M., Finnveden, G., Hjelm, O., Hochschorner, E., 2011. Weighting and valuation in selected environmental systems analysis tools – suggestions for further developments. Journal of Cleaner Production. 19:145-156.

Ay, M., Midilli, A., Dincer, I., 2006. Thermodynamic modeling of a proton exchange membrane fuel cell. International Journal of Exergy. 6:16-44.

Ayres, R.U., 2007. On the practical limits to substitution. Ecological Economics. 61:115-128.

Azapagic, A., 2007. Life cycle assessment as an environmental sustainability tool, in: Dewulf, J., Langenhove, H.V. (Eds.), Renewables-Based Technology: Sustainability Assessment. John Wiley & Sons, Ltd, Chichester, UK.

Badescu, V., 2008. Exact and approximate statistical approaches for the exergy of blackbody radiation. Central European Journal of Physics. 6:344-350.

Bare, J., Gloria, T., Norris, G., 2006. Development of the method and US normalization database for life cycle impact assessment and sustainability metrics. Environmental Science & Technology. 40:5108–5115.

Beckers, K.F., Lukawski, M.Z., Anderson, B.J., Moore, M.C., Tester, J.W., 2014. Levelized costs of electricity and direct-use heat from Enhanced Geothermal Systems. Journal of Renewable and Sustainable Energy. 6:013141.

Bekele, G., Palm, B., 2010. Feasibility study for a standalone solar-wind-based hybrid energy system for application in Ethiopia. Applied Energy. 87:487-495.

Bell, S., Morse, S., 2008. Sustainability Indicators: Measuring the Immeasurable? Earthscan, London, UK.

Berg, D.E., 2007. Wind energy conversion, in: Kreith, F., Goswami, D.Y. (Eds.), Handbook of Energy Efficiency and Renewable Energy. CRC Press, Boca Raton, USA.

Bernal-Agustín, J.L., R. Dufo-López, and D.M. Rivas-Ascaso, 2006. Design of isolated hybrid systems minimizing costs and pollutant emissions. Renewable Energy. 31:2227-2244.

Blanc, I., Friot, D., Margni, M., Jolliet, O., 2008. Towards a new index for environmental sustainability based on a DALY weighting approach. Sustainable Development. 16:251-260.

Böhringer, C., Jochem, P.E.P., 2007. Measuring the immeasurable – a survey of sustainability indices. Ecological Economics. 63:1-8.

Bossel, H., 2001. Assessing viability and sustainability: a systems-based approach for deriving comprehensive indicator sets. Conservation Ecology. 5:12.

Brent, A.C., Rogers, D.E., 2010. Renewable rural electrification: sustainability assessment of mini-hybrid off-grid technological systems in the African context. Renewable Energy. 35:257-265.

Buongiorno, J., 2010. Pressurized water reactor description. Engineering of Nuclear Systems, MIT OpenCourseWare.

Buscema, M., 2002. A brief overview and introduction to artificial neural networks. Substance Use & Misuse. 37:1093-1148.

Carelli, M.D., Garrone, P., Locatelli, G., Mancini, M., Mycoff, C., et al., 2010. Economic features of integral, modular, small-to-medium size reactors. Progress in Nuclear Energy. 52:403-414.

Carifio, J., Perla, R.J., 2007. Ten common misunderstandings, misconceptions, persistent myths and urban legends about Likert scales and Likert response formats and their antidotes. Journal of Social Sciences. 3:106-116.

Carrera, D.G., Mack, A., 2010. Sustainability assessment of energy technologies via social indicators: results of a survey among European energy experts. Energy Policy. 38:1030-1039.

Carta, J.A., González, J., 2001. Self-sufficient energy supply for isolated systems: wind-diesel systems in the Canary Islands. The Energy Journal. 22:115-145.

Cengel, Y.A, Boles, M.A., 2010. Thermodynamics: an Engineering Approach, 7th Edition. McGraw-Hill Education, Columbus, USA.

Chicco, G., Mancarella, P., 2009. Distributed multi-generation: a comprehensive view. Renewable and Sustainable Energy Reviews. 13:535-551.

Coll-Mayor, D., Paget, M., Lightner, E., 2007. Future intelligent power grids: analysis of the vision in the European Union and the United States. Energy Policy. 35:2453-2465.

Coscieme, L., Pulselli, F.M., Jørgensen, S.E., Bastianoni, S., Marchettini, N., 2013. Thermodynamics-based categorization of ecosystems in a socio-ecological context. Ecological Modelling. 258:1-8.

Critchley, J., 2011. Draft Environmental Code of Practice for Elimination of Fluorocarbon Emissions from Refrigeration and Air Conditioning Systems. Environment Canada, Gatineau, Canada.

Daly, H.E., 1990. Toward some operational principles of sustainable development. Ecological Economics. 2:1-6.

Daly, H.E., 2005. Economics in a full world. Scientific American. 293:100-107.

Daly, H.E., 2008. A Steady-State Economy. Report to the Sustainable Development Commission, UK.

Dewulf, H., Van Langenhove, H., Mulder, J., van den Berg, M.M.D., van der Kooi, H.J., de Swaan Arons, J., 2000. Illustrations towards quantifying the sustainability of technology. Green Chemistry. 2:108-114.

Dincer, I., Rosen, M.A., 2013. Exergy: Energy, Environment and Sustainable Development, 2nd ed. Elsevier, Oxford, UK.

Dincer, I., Zamfirescu, C., 2012. Potential options to greenize energy systems. Energy. 46:5-15.

DiPippo, R., 2008. Geothermal Power Plants: Principles, Applications, Case Studies and Environmental Impact. Elsevier, Oxford, UK.

Ehrenfeld, J.R., 2004. Can industrial ecology be the "science of sustainability"? Journal of Industrial Ecology. 8:1-3.

EIA, 2013. Updated Capital Cost Estimates for Utility Scale Electricity Generating Plants. US Department of Energy, Washington, D.C.

Environment Canada, 2013. NAPS Data Products. Gatineau, QC. Available online: http://maps-cartes.ec.gc.ca/rnspa-naps/data.aspx?lang=en (accessed on July 3, 2014).

EPA, 2011. National Ambient Air Quality Standards. Washington, D.C. Available online: http://www.epa.gov/air/criteria (accessed on March 13, 2014).

EPA, 2012. Benzene. Washington, D.C. Available online: http://www.epa.gov/ttn/atw/hlthef/benzene.html (accessed on July 3, 2014).

EPA, 2013. Renewable Energy Cost Database. Washington, D.C. Available online: http://www.epa.gov/cleanenergy/energy-resources/renewabledatabase.html (accessed on August 21, 2014).

Evans, R.L., 2007. Fueling Our Future: an introduction to sustainable energy. Cambridge University Press, New York, USA.

Evans, A., Strezov, V., Evans, T.J., 2009. Assessment of sustainability indicators for renewable energy technologies. Renewable and Sustainable Energy Reviews. 13:1082-1088.

Evans, J.S., Wolff, S.K., Phonboon, K., Levy, J.I., Smith, K.R., 2002. Exposure efficiency: an idea whose time has come? Chemosphere. 49:1075-1091.

Fankhauser, S., Tepic, S., 2007. Can poor consumers pay for energy and water? An affordability analysis for transition countries. Energy Policy. 35:1038–1049.

Ferrari, S., Genoud, S., Lesourd, J., 2001. Thermodynamics and economics: towards exergy-based indicators of sustainable development. Swiss Journal of Economics and Statistics. 137:319–336.

Frangopoulos, C.A., Keramioti, D.E., 2010. Multi-criteria evaluation of energy systems with sustainability considerations. Entropy. 12:1006–1020.

Gasparatos, A., El-Haram, M., and M. Horner, 2008. A critical review of reductionist approaches for assessing the progress towards sustainability. Environmental Impact Assessment Review. 28:286-311.

Genoud, S., Lesourd, J., 2009. Characterization of sustainable development indicators for various power generation technologies. International Journal of Green Energy. 6:257-267.

Gnanapragasam, N.V., Reddy, B.V., Rosen, M.A., 2010. A methodology for assessing the sustainability of hydrogen production from solid fuels. Sustainability. 2:1472–1491.

Goedkoop, M., Spriensma, R., 2000. The Eco-Indicator 99: A damage oriented method for life cycle impact assessment. PRe Consultants, Amersfoort, Netherlands.

Graedel, T.E., Allenby, B.R., 2010. Industrial Ecology and Sustainable Engineering. Prentice Hall, Upper Saddle River, New Jersey, USA.

Gruber, P.W., Medina, P.A., Keoleian, G.A., Kesler, S.E., Everson, M.P., Wallington, T.J., 2011. Global lithium availability: a constraint for electric vehicles? Journal of Industrial Ecology. 15:760-775.

Guinée, J.B., 2002. Handbook on Life Cycle Assessment: Operation Guide to the ISO Standards. Kluwer Academic Publishers, New York, USA.

Hacatoglu, K., Dincer, I., Rosen, M.A., 2011. Exergy analysis of a hybrid solar hydrogen system with activated carbon storage. International Journal of Hydrogen Energy. 36:3273-3282.

Hacatoglu, K., Dincer, I., Rosen, M.A., 2013a. Exergy analysis of a hybrid solar-wind-biomass system with thermal and electrical energy storage for a community. Proceedings of the Sixth International Exergy, Energy and Environment Symposium (IEEES-6), Rize, Turkey, July 1-4, 2013.

Hacatoglu, K., Dincer, I., Rosen, M.A., 2014. A new model to assess the environmental impact and sustainability of energy systems, Journal of Cleaner Production. DOI: 10.1016/j.jclepro.2014.06.050.

Hacatoglu, K., Rosen, M.A., Dincer, I., 2012. Comparative life cycle assessment of hydrogen and other selected fuels. International Journal of Hydrogen Energy. 37:9933-9940.

Hacatoglu, K., Rosen, M.A., Dincer, I., 2013b. An approach to assessment of sustainability of energy systems, in: Dincer, I., Colpan, C.O., Kadioglu, F. (Eds.), Causes, Impacts and Solutions to Global Warming. Springer, New York, USA.

Harrison, K., Levene, J.I., 2008. Electrolysis of water, in: Rajeshwar, K., McConnell, R., Licht, S. (Eds.), Solar Hydrogen Generation. Springer, New York, USA.

Hart, M., 1999. Guide to Sustainable Community Indicators. Hart Environmental Data, North Andover, Massachusetts, USA.

Homer-Dixon, T., 2007. The Upside of Down: Catastrophe, Creativity and the Renewal of Civilization. Random House of Canada Limited, Toronto, Canada.

IAEA, 2005. Energy indicators for sustainable development: guidelines and methodologies. Vienna, Austria.

Ingersoll, D.T., 2009. Deliberately small reactors and the second nuclear era. Progress in Nuclear Energy. 51:589-603.

IPCC, 2005. Safeguarding the Ozone Layer and the Global Climate System. Cambridge University Press, Cambridge, UK.

IPCC, 2013. Summary for Policymakers, in: Stocker, T.F., Qin, D., Plattner, G.K., Tignor, M., Allen, S.K., et al. (Eds.), Climate Change 2013: The Physical Science Basis. Contribution of Working Group I to the Fifth Assessment Report of the Intergovernmental Panel on Climate Change. Cambridge University Press, Cambridge, UK.

Isherwood, W., Smith, J.R., Aceves, S.M., Berry, G., Clark, W., et al., 2000. Remote power systems with advanced storage technologies for Alaskan villages. Energy. 25:1005-1020.

Jackson J., 1999. Resources – Not Garbage: Municipal Solid Waste in Ontario. Prepared for the Environmental Agenda for Ontario Project.

Jackson, T., 1996. Material Concerns: Pollution, Profit, and Quality of Life. Routledge, London, UK.

Jones, M., 2013. Environmental DNA: genetics steps forward when traditional ecological surveys falls short. Fisheries. 38:332-333.

Jørgensen, S.E., 2010. Ecosystem services, sustainability and thermodynamic indicators. Ecological Complexity. 7:311-313.

Jørgensen, S.E., Ludovisi, A., Nielsen, S.N., 2010. The free energy and information embodied in the amino acid chains of organisms. Ecological Modelling. 221:2388-2392.

Juwana, I., Muttil, N., Perera, B.J.C., 2012. Indicator-based water sustainability assessment – a review. Science of the Total Environment. 438:357-371.

Kates, R.W., Parris, T.M., Leiserowitz, A.A., 2005. What is sustainable development? Environment. 47:8–21.

Kayhanian, M., Tchobanoglous, G., Brown, R.C., 2007. Biomass conversion processes for energy recovery, in: Kreith, F., Goswami, D.Y. (Eds.), Handbook of Energy Efficiency and Renewable Energy. CRC Press, Boca Raton, USA.

Kemp, D.D., 2004. Exploring Environmental Issues. Routledge, London, UK.

Khan, M.J., Iqbal, M.T., 2005. Dynamic modeling and simulation of a small wind-fuel cell hybrid energy system. Renewable Energy. 30:421-439.

Kim, Y., Yang, Y., Bae, J., Suh, S., 2012. The importance of normalization references in interpreting life cycle assessment results. Journal of Industrial Ecology. 17:385–395.

Kitz, K., 2007. Geothermal power generation, in: Kreith, F., Goswami, D.Y. (Eds), Handbook of Energy Efficiency and Renewable Energy. CRC Press, Boca Raton, USA.

Koebel, M., Elsener, M., Kleeman, M., 2000. Urea-SCR: a promising technique to reduce NO_X emissions from automotive engines. Catalysis Today. 59:335-345.

Kraft, M.E., 2013. Nuclear power and the challenge of high-level waste disposal in the United States. Polity. 45:265-280.

Kreith, F., Kreider, J.F., 2011. Principles of Sustainable Energy. CRC Press, Boca Raton, USA.

Kriesel, D., 2007. A Brief Introduction to Neural Networks. Available online: http://www.dkriesel.com (accessed on August 18, 2014).

Kushnir, D., Sandén, B.A., 2012. The time dimension and lithium resource constraints for electric vehicles. Resources Policy. 37:93-103.

Lenzen, M., 2008. Double-counting in life cycle calculations. Journal of Industrial Ecology. 12:583-599.

McKay, G., 2002. Dioxin characterisation, formation and minimisation during municipal solid waste (MSW) incineration: review. Chemical Engineering Journal. 86:343-368.

McMahon, J.E., Price, S.K., 2011. Water and energy interactions. Annual Review of Environment and Resources. 36:163-191.

Michaelides, E.E., 2012. Alternative Energy Sources. Springer-Verlag, Berlin, Germany.

Midilli, A., Dincer, I., 2009. Development of some exergetic parameters for PEM fuel cells for measuring environmental impact and sustainability. International Journal of Hydrogen Energy. 34:3858-3872.

Ministry of Labour, 2012. A Guide to the Occupational Health and Safety Act. Available online: http://www.labour.gov.on.ca/english/hs/pubs/ohsa/index.php (accessed on August 26, 2014).

Ministry of the Environment, 2011. Proposal to Amend Ontario Regulation 419/05: Air Pollution – Local Air Quality, under the Environmental Protection Act to include an Ontario Air Standard for Benzene. EBR Registry Number: 010-7186.

Morris D.R., Szargut J., 1986. Standard chemical exergy of some elements and compounds on the planet Earth. Energy. 11:733-755.

Morse, S., 2013. Bottom rail on top: the shifting sands of sustainable development indicators as tools to assess progress. Sustainability. 5:2421-2441.

Morse, S., Fraser, E.D.G., 2005. Making 'dirty' nations look clean? The nation state and the problem of selecting and weighting indices as tools for measuring progress towards sustainability. Geoforum. 36:625-640.

Nardo, M., Saisana, M., Saltelli, A., Tarantola, S., Hoffmann, A., Giovannini, E., 2008. Handbook on Constructing Composite Indicators. Organisation for Economic Co-operation and Development, Paris, France.

Nathwani, J., Blackstock, J., 2012. Equinox Blueprint: Energy 2030. Waterloo Global Science Initiative, Waterloo, Canada.

National Academy of Sciences, National Academy of Engineering, National Research Council, 2010. Real Prospects for Energy Efficiency in the United States. National Academies Press, Washington, D.C., USA.

Ness, B., Urbel-Piirsalu, E., Anderberg, S., Olsson, L., 2007. Categorising tools for sustainability assessment. Ecological Economics 60:498-508.

Neto, M.R.B, Carvalho, P.C.M., Carioca, J.O.B., Canafístula, F.J.F., 2010. Biogas/photovoltaic hybrid power system for decentralizing energy supply of rural areas. Energy Policy. 38:4497-4506.

Neuman, W.L., 2010. Social Research Methods: Qualitative and Quantitative Approaches. Pearson PLC, London, UK.

Neves, A.R., Leal, V., 2010. Energy sustainability indicators for local energy planning: review of current practices and derivation of a new framework. Renewable and Sustainable Energy Reviews. 14:2723-2735.

Niisoe, T., Nakamura, E., Harada, K., Ishikawa, H., Hitomi, T., Watanabe, T., Wang, Z., Koizumi, A., 2010. A global transport model of lead in the atmosphere. Atmospheric Environment. 44:1806–1814.

NRC, 1999. Our Common Journey: A Transition Toward Sustainability. National Academy Press, Washington, D.C., USA.

Obert, E.F., 1973. Internal Combustion Engines and Air Pollution. Intext Educational Publishers, New York, USA.

OEE, 2013. Energy Use Data Handbook, 1990 to 2010. Natural Resources Canada: Ottawa, Canada.

Østergaard, P.O., Mathiesen, B.V., Möller, B., Lund, H., 2010. A renewable energy scenario for Aalborg Municipality based on low-temperature geothermal heat, wind power and biomass. Energy. 35:4892-4901.

Parris, T.M., Kates, R.W., 2003. Characterizing and measuring sustainable development. Annual Review of Environment and Resources. 28:559-586.

Pepermans, G., Driesen, J., Haeseldonckx, D., Belmans, R., D'haeseleer, W., 2005. Distributed generation: definition, benefits and issues. Energy Policy. 33:787-798.

Pérez-Navarro, A., Alfonso, D., Álvarez, C., Ibáñez, F., Sánchez, C., Segura, I., 2010. Hybrid biomass-wind power plant for reliable energy generation. Renewable Energy. 35:1436-1443.

Perrino, C., 2010. Atmospheric particulate matter. Proceedings of a CISB Minisymposium. Rome, Italy.

Ravishankara, A.R., Daniel, J.S., Portmann, R.W., 2009. Nitrous oxide (N_2O): the dominant ozone-depleting substance emitted in the 21st century. Science. 326:123–125.

Reddy, T.A., Battisti, R., Schweiger, H., Weiss, W., Morehouse, J.H., et al., 2007. Solar thermal energy conversion, in: Kreith, F., Goswami, D.Y. (Eds.), Handbook of Energy Efficiency and Renewable Energy. CRC Press, Boca Raton, USA.

Reed, M.S., Fraser, E.D.G., Morse, S., Dougill, A.J., 2005. Integrating methods for developing sustainability indicators to facilitate learning and action. Ecology and Society. 10:6.

Rennings, K., Wiggering, H., 1997. Steps towards indicators of sustainable development: linking economic and ecological concepts. Ecological Economics. 20:25-36.

River-Austrui, J., Borrajo, M.A., Martinez, K., Adrados, M.A., Abalos, M., et al., 2011. Assessment of polychlorinated dibenzo-p-dioxin and dibenzofuran emissions from a hazardous waste incineration plant using long-term sampling equipment. Chemosphere. 82:1343-1349.

Romero-Alvarez M., Zarza E., 2007. Concentrating solar thermal power, in: Kreith, F., Goswami, D.Y. (Eds.), Handbook of Energy Efficiency and Renewable Energy. CRC Press, Boca Raton, USA.

Rosen, M.A., 2009. Energy sustainability: a pragmatic approach and illustrations. Sustainability. 1:55-80.

Rosen M.A., Dincer I., 1997. On exergy and environmental impact. International Journal of Energy Resources. 21:643-654.

Rosen, M.A., Dincer, I., Kanoglu, M., 2008. Role of exergy in increasing efficiency and sustainability and reducing environmental impact. Energy Policy. 36:128-137.

Rowley, H.V., Peters, G.M., Lundie, S., Moore, S.J., 2012. Aggregating sustainability indicators: beyond the weighted sum. Journal of Environmental Management. 111:24-33.

Russell, A.C., 2010. Building Better Cycling Arteries in Cities: a Lesson for Toronto. Clear Air Partnership, Toronto, Canada.

Saldanha, N., Beausoleil-Morrison, I., 2012. Measured end-use electric load profiles for 12 Canadian houses at high temporal resolution. Energy and Buildings. 49:519-530.

Sanders, C.E., 2013. Review of the development of the transportation, aging, and disposal (TAD) waste disposal system for the proposed Yucca Mountain geologic repository. Progress in Nuclear Energy. 62:8-15.

Sandler, S.I., 1999. Chemical and Engineering Thermodynamics, 3rd Edition. John-Wiley & Sons, Inc., New York, USA.

Schiermeier, Q., Tollefson, J., Scully, T., Witze, A., Morton, O., 2008. Electricity without carbon. Nature. 454:816-823.

Sciubba, E., Zullo, F., 2011. Is sustainability a thermodynamic concept? International Journal of Exergy. 8:68-85.

Shakya, B.D., Aye, L., Musgrave, P., 2005. Technical feasibility and financial analysis of hybrid wind-photovoltaic system with hydrogen storage for Cooma. International Journal of Hydrogen Energy. 30:9-20.

Singh, R.K., Murty, H.R., Gupta, S.K., Dikshit, A.K., 2009. An overview of sustainability assessment methodologies. Ecological Indicators. 9:189-212.

Smil, V., 2003. Energy at the Crossroads: Global Perspectives and Uncertainties. The MIT Press, Cambridge, USA.

Smil, V., 2007. Energy in Nature and Society: General Energetics of Complex Systems. The MIT Press, Cambridge, USA.

Soloveichik, G.L., 2011. Battery technologies for large-scale energy storage. Annual Review of Chemical and Biomolecular Engineering. 2:503-527.

Sørensen, B., 2011. Life-Cycle Analysis of Energy Systems: From Methodology to Applications. Royal Society of Chemistry, Cambridge, UK.

Statistics Canada, 2007. Household energy use, by fuel type and by province. Households and the Environment Survey: Energy Use. Ottawa, Canada.

Statistics Canada, 2012. Median after-tax income, by economic family type, 2010 constant dollars, annual (CANSIM Table 202-0605). Ottawa, Canada.

Steinfeld, H., Gerber, P., Wassenaar, T., Castel, V., Rosales, M., et al., 2006. Livestock's Long Shadow: Environmental Issues and Options. Food and Agriculture Organization of the United Nations, Rome, Italy.

Stranddorf, H.K., Hoffmann, L., Schmidt, A., 2005. Impact categories, normalisation and weighting in LCA. Environmental News No. 78. Danish Ministry of the Environment, Environmental Protection Agency, Copenhagen, Denmark.

Szargut, J., 2005. Exergy Method: Technical and Ecological Applications. WIT Press, Southampton, UK.

Tainter, J.A., 1988. The collapse of complex societies. Cambridge University Press, Cambridge, UK.

Tester, J.W., Anderson, B.J., Batchelor, A.S., Blackwell, D.D., DiPippo, R., et al., 2006. The Future of Geothermal Energy. Idaho National Laboratory, Idaho Falls, USA.

Touran, N., 2014. What is nuclear waste? Available online: http://www.whatisnuclear.com/articles/waste.html (accessed on August 26, 2014).

vanLoon, G.W., Duffy, S.J., 2003. Environmental Chemistry: a Global Perpsective. Oxford University Press, Oxford, UK.

Vera, I., Langlois, L., 2007. Energy indicators for sustainable development. Energy. 32:875-882.

WCED, 1987. Our Common Future. Oxford University Press, New York, USA.

Weather Network, 2014. Statistics: Toronto, Ontario, Canada. Available online: http://past.theweathernetwork.com/statistics/CL6158350 (accessed on September 10, 2014).

Wilson, D., Macdonald, D., 2010. The Income Gap Between Aboriginal Peoples and the Rest of Canada. Canadian Centre for Policy Alernatives, Ottawa, Canada.

Zini, G., Marazzi, R., Pedrazzi, S., Tartarini, P., 2010. A solar hydrogen hybrid system with activated carbon storage. International Journal of Hydrogen Energy. 35:4909-4917.

Zini, G., Tartarini, P., 2010. Wind-hydrogen energy stand-alone system with carbon storage: modeling and simulation. Renewable Energy. 35:2461-2467.

Zoulias, E.I., Lymberopoulos, N., 2007. Techno-economic analysis of the integration of hydrogen energy technologies in renewable energy-based stand-alone power systems. Renewable Energy. 32:680-696.

Zvolinschi, A., Kjelstrup, S., Bolland, O., van der Kooi, H.J., 2007. Exergy sustainability indicators as a tool in industrial ecology. Journal of Industrial Ecology. 11:85–98.